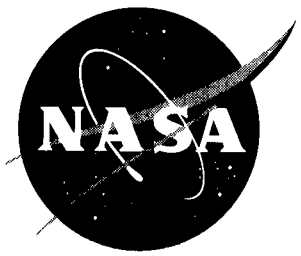

NASA Contractor Report 4744

New Instrumentation Technologies for Testing the Bonding of Sensors to Solid Materials

H.M. Hashemian, C.S. Shell, and C.N. Jones

Contract NAS8–40165
Prepared for Marshall Space Flight Center

May 1996

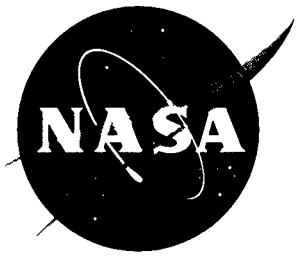

NASA Contractor Report 4744

New Instrumentation Technologies for Testing the Bonding of Sensors to Solid Materials

H.M. Hashemian, C.S. Shell, and C.N. Jones
Analysis and Measurement Services Corporation
Knoxville, Tennessee 37923

National Aeronautics and Space Administration
Marshall Space Flight Center • MSFC, Alabama 35812

Prepared for Marshall Space Flight Center
under Contract NAS8–40165

May 1996

ISBN: 1-882148-05-3

PROJECT SUMMARY
NASA SBIR PHASE II FINAL REPORT

PROJECT NO.: N/A **CONTRACT NO.:** NAS 8-40165 **NASA CENTER:** MSFC

PROJECT TITLE: New Instrumentation Technologies For Testing The Bonding of Sensors To Solid Materials

COMPANY: Analysis and Measurement Services Corporation

ADDRESS: AMS 9111 Cross Park Drive, Knoxville, Tennessee 37923
Phone: (423) 691-1756 / Fax: (423) 691-9344 / E-Mail: info@ams-corp.com

---

SUMMARY: 1. THE INNOVATION; 2. RESEARCH OBJECTIVES; 3. RESEARCH RESULTS; 4. WERE RESEARCH OBJECTIVES MET? 5. IS PHASE III JUSTIFIED? 6. POTENTIAL NASA PHASE III APPLICATIONS; 7. COMMERCIAL APPLICATIONS POTENTIAL.

New techniques were successfully developed and validated for testing the bonding of thermocouples, RTDs, and strain gages to solid materials. Testing the bonding of thermocouples has applications in the SRM nozzle development programs, and testing the bonding of RTDs and strain gages has applications in the space shuttle program.

In development of improved materials for SRM nozzle liners, thermocouples are embedded in the material for transient temperature measurements. These measurements are made to validate the theoretical models that have been developed to describe the behavior of the material under firing conditions involving very high temperatures. If thermocouples are not in good contact with the material, transient temperature measurements will have large lags and would not be useful for model validation. Up to now, a reliable method was not available for passive testing of embedded thermocouple installation. The technology that was developed here will help verify the degree of bonding between an embedded thermocouple and the host material and thereby minimize model validation errors.

In space shuttle main engines (SSMEs), surface-mounted RTDs are used on fuel and oxidizer lines as a means of detecting leaking values. Under the harsh operating conditions of an engine, the RTDs may become loose or detached from the piping and preclude timely leak detection. The technology that was developed in this project will help verify the bonding of RTDs and enable NASA to identify leaking values in space shuttles in a timely manner.

The existing Loop Current Step Response method was used to develop most of the technologies described in this report. This method is based on applying an electrical current to the sensor through its normal leads. The current creates Joule heating in the sensor, the amount of which depends on the sensor's ability to dissipate the heat. The transient output of the sensor during the heating or cooling (after the current is cut off) is recorded and analyzed to determine the degree of bonding between the sensor and the material on which it is installed. In addition, the LCSR method was proven to be useful in thermocouple circuit diagnostics. The method successfully detected secondary junctions and reverse-connected thermocouples during field measurements which helped NASA and its contractor avoid difficulties that would have been encountered if these problems were not identified.

In addition to thermocouples and RTDs, the LCSR method can be used to test the installation of strain gages. Testing the installation of strain gages has many aerospace applications, especially in testing the performance of space shuttle main engines. In fact, strain gages, as installed on test bed SSMEs, were successfully tested during field measurements performed in this project.

In addition to meeting NASA's needs, the technologies that were developed in this project have applications not only in other aerospace facilities, but also in all industrial and scientific processes that require transient temperature and strain measurements in solid materials.

SUBMITTED H. M. Hashemian DATE 2/9/96

TABLE OF CONTENTS

TABLE OF CONTENTS
(Continued)

LIST OF FIGURES

LIST OF FIGURES
(Continued)

LIST OF FIGURES
(Continued)

LIST OF FIGURES
(Continued)

LIST OF FIGURES
(Continued)

LIST OF FIGURES
(Continued)

LIST OF FIGURES
(Continued)

LIST OF TABLES

LIST OF ABBREVIATIONS

A/D	Analog to Digital Convertor
AFL	Antiflood Line
AMS	Analysis and Measurement Services Corporation
CIP	Cured-In-Place
CLTS	Cryogenic Linear Temperature Sensors
C-P	Carbon-Phenolic
EMTA	Erosion Monitoring Thermocouple Array
FFT	Fast Fourier Transform
GIT	Gallium-Indium-Tin
IR	Insulation Resistance
LCSR	Loop Current Step Response
MFV	Main Fuel Valve
M-M	Micro-Measurements
MSFC	Marshall Space Flight Center
NAS	Nozzle Ablative Simulation
NASA	National Aeronautics and Space Administration
NTC	Negative Temperature Coefficient
OD	Outside Diameter
OPOV	Oxidizer Preburner Oxidizer Valve
PRT	Platinum Resistance Thermometer
PSD	Power Spectral Density
PTC	Positive Temperature Coefficient
R&D	Research and Development

LIST OF ABBREVIATIONS
(Continued)

RSRM	Redesigned Solid Rocket Motor
RTD	Resistance Temperature Detector
SBIR	Small Business Innovation Research
SHI	Self Heating Index
SPIP	Solid Propulsion Integrity Program
SRI	Southern Research Institute
SRM	Solid Rocket Motor
SSME	Space Shuttle Main Engine
TJC	Thermal Joint Compound
TTB	Technology Test Bed

1. INTRODUCTION

The accuracy and reliability of transient temperature, pressure, and other measurements depend on the dynamic response of sensors that are used to make the measurements.

The dynamic response of a sensor is comprised of an internal and an external component. The internal component depends on the sensor materials and dimensions and the external component depends on the contact between the sensor and the medium in which the sensor is used. If the contact is poor, then the sensor may take a long time to indicate a change in the parameter being measured. On the other hand, if the contact between the sensor and the host medium is good, the sensor output will follow the process closely.

For sensors that are attached to a solid surface or embedded in a solid material, the dynamic response depends strongly on the bonding between the sensor and the material. Therefore, it is important for the sensor to be in intimate contact with the material. This report presents new technology for verifying the bonding of sensors to solid materials by in-situ measurement of dynamic response of the sensor in the solid material. This technology has applications in most processes which involve measurement or monitoring of transient conditions. In this project, the technology was implemented in the following applications for NASA:

1. Testing the attachment of thermocouples that are used in testing the performance of composite materials for SRM nozzles.

2. Testing of thermocouples embedded in solid materials used for the lining of blast tubes in solid rocket boosters in space shuttles and other aerospace vehicles.

3. Verifying the bonding of skin-mount RTDs that are used on the fuel and oxidizer lines of space shuttles for detecting leaks from the valves in the lines.

4. Determining the attachment of strain gages that are used for load and vibration measurements in SSMEs.

The LCSR method was used in developing the new technology described in this report. This method was originally developed in the mid 1970s for in-situ response time testing of RTDs and thermocouples in nuclear power plants.[1] Subsequently, the method was adapted in the mid 1980s to response time testing of thermocouples in jet engine test facilities for the U.S. Air Force.[2,3] The advantage of the LCSR method is that it can be used for remote measurement of response time of sensors as installed in operating processes. The results of the LCSR test provides dynamic information not only about the sensor but also about the sensor-to-process coupling. The latter capability of the LCSR method is used to characterize the bonding of installed sensors to their host material.

The LCSR test is based on internal heating of the sensor by applying an electrical current to the sensor's extension leads. This creates Joule heating in the sensor. The amount of heating depends on the applied current (I) and the sensor resistance (R). Joule heating is also referred to as I^2R heating.

For LCSR testing of RTDs and strain gages, a DC current is used in a Wheatstone bridge arrangement to heat the sensor a few degrees above the ambient temperature. The bridge current is suddenly increased from about 1 or 2 mA to about 20 to 40 mA (for thin-film RTDs and strain gages; and 40 to 80 mA for regular industrial RTDs) while the bridge output is recorded for a few seconds to a few minutes depending on the sensor and the conditions in which the sensor is tested. The bridge output is an exponential transient that can be analyzed to yield the dynamic response of the sensor under the actual installation and operating conditions tested. The response time value obtained in this manner is meaningful only for RTDs that are tested in

liquids and gaseous process media. In these cases, the response time that is obtained from the LCSR test is the same as the response time that would be obtained for the RTD if the process temperature experienced a step change.

For RTDs that are installed on solid surfaces, the LCSR test is not usually intended for response time measurements per se. Rather, the test is performed to identify a dynamic response that is indicative of how well the RTD is attached or bonded to the solid material. As such, the results of LCSR tests of RTDs on solid surfaces are often not referred to as response time. Rather, they are referred to as installation index. Similarly, for strain gages that are installed on solid surfaces, the LCSR test is used to provide a quantitative estimate of the strain gage bonding as opposed to yielding a response time value.

The LCSR procedure for testing the dynamic response of thermocouples is much different than RTDs and strain gages and involves different equipment and procedures. For thermocouples, the LCSR test is performed using an AC current to heat the thermocouple. For small diameter thermocouples, 50 to 200 mA of AC current is usually adequate, while for large diameter thermocouples up to 3 amps may be necessary. Higher heating currents are necessary for thermocouples because the resistance of thermocouples is distributed along the thermocouple wire as well as the sensing junction, while the resistance of RTDs and strain gages are concentrated mainly in the sensing element. Consequently, a small current can heat an RTD or a strain gage sufficiently to produce a useful LCSR test transient, while thermocouples require a much larger heating current for adequate Joule heating and a successful LCSR test.

For LCSR testing, the thermocouple is first heated for a few seconds and its output is monitored after the heating current is switched off. This provides an exponential transient that

results from cooling of the thermocouple junction. The cooling rate or the rate of the exponential decay depends on how fast the thermocouple junction returns to the ambient temperature. If the thermocouple junction is in good thermal contact with its surroundings, then it will cool faster and if it is in poor contact, it will cool slower. Hence, the LCSR method can reveal the quality of bonding between a thermocouple and a solid material and show if a group of thermocouples that are installed on a solid surface or embedded in a solid material have the same bonding quality. As in the case of RTDs and strain gages, for the applications discussed in this report, the dynamic response of thermocouples in solid materials is expressed in terms of an installation index as opposed to a response time value or a time constant.

The exponential transients that result from LCSR testing of RTDs or thermocouples are analyzed by fitting the LCSR data to a model. This model is used to transform the internal heating information to obtain the dynamic response of the sensor to an external temperature change. The LCSR model was developed in the mid 1970s based on a detailed heat transfer analysis of typical thermocouples and RTDs. A paper is attached in Appendix A that describes the fundamentals of temperature sensor response time testing including a detailed discussion of how the LCSR models were derived from a lumped-parameter analysis of a sensor.

2. PROJECT OBJECTIVES

The goal of this project was to adapt the existing LCSR method for testing the bonding of sensors to solid material not only for aerospace applications and to meet NASA's needs, but also for other industrial and scientific applications which involve transient temperature and strain measurements on solid surfaces or inside solid materials.

Although the technology developed in this project has applications beyond NASA, this report is concentrated on the NASA applications that are described below.

2.1 Testing of Composite Materials

A number of research projects have been underway in the aerospace industry to improve the understanding of the thermostructural behavior of composite materials used in SRM nozzles, turbine engines, hot structures, etc. Fundamental to this effort is accurate and timely temperature measurements made with thermocouples attached to a solid surface or embedded in a solid material.

In order to interpret the internal thermal data obtained under transient test conditions, one must have an estimate of the dynamic response of thermocouples to verify that the thermocouples are in good contact with the material under study. Since the dynamic response of a thermocouple in a solid material is strongly dependent on its installation (i.e., bonding) as well as the properties of the sensor and the material, an in-situ test technique was developed in this project to meet the following objectives:

1. Determine if, in spite of the hostile conditions imposed during firing tests, the thermocouple remains properly embedded in the material.

2. Determine if redundant thermocouples used in a material have comparable installation and their bonding to the material is consistent.

2.2 Validation of Theoretical Models

Analytical modeling techniques are routinely used to predict the thermostructural behavior of carbon-carbon, carbon-phenolic, and other composite materials used in aerospace applications. Hot firing tests with instrumented structures are used to validate the analytical models. These tests involve short run times, high heat fluxes, and consequently, rapid temperature transients. Temperature measurements made to date have often shown significant time lags with respect to the model predictions and unacceptable discrepancies between redundant temperature sensors. If it can be verified that thermocouples are in good contact with the solid material, and an estimate of their relative dynamic responses can be made, then the measured temperature data can be interpreted more accurately in validating the analytical models.

Up to now, a reliable method has not been available to evaluate the quality of a thermocouple installation in a solid material, or provide an estimate for the dynamic response of the thermocouple in the material. Consequently, it has not been possible to determine how well the output of a bonded or embedded thermocouple actually represents the temperature of the surrounding material under transient conditions. Neither was it possible to determine the extent to which the transient outputs of separate thermocouples are different due to actual material temperature differences as opposed to differences in the integrity of the installations. As a result, theoretical models that have been developed for the study of thermophysical properties of

composites could not be easily validated with experimental temperature data. Model validation involves comparing model predictions with actual temperature distributions in the composite material so that the models can be tuned under controlled conditions and later used as a general tool for evaluating the temperature response of other composites, and for the design of improved composites.

2.3 Testing the Thermal Performance of Blast Tube Liners

The inside wall of blast tubes in reusable SRMs are covered with a layer of material that must withstand the high temperatures experienced after the SRM is fired. As a part of this project, Type K thermocouples as installed in the blast tube liner materials for SRMs were tested in the laboratory. The purpose of these tests was to verify the operability and installation integrity of thermocouples before and after curing in SRM liner material.

2.4 Testing the Bonding of Surface Mounted RTDs and Strain Gages

In addition to thermocouples, the objective of this project was to develop an in-situ method that can be used for testing the attachment of RTDs and strain gages to solid materials. A method to verify the attachment of strain gages has applications in testing of SSMEs and a method to test the attachment of RTDs has applications in identifying leaking valves on the fuel lines of the space shuttle. The laboratory and field measurements described later in this report showed that the LCSR method is very successful in meeting these needs.

2.5 Cooperation with NASA and NASA Contractors

Most of the thermocouple work performed in this project involved samples provided by NASA contractors; Hercules Aerospace Company and Thiokol Corporation, and almost all the RTD and strain gage work was performed in cooperation with NASA at MSFC.

During this project, AMS was able to contribute to the Solid Propulsion Integrity Program (SPIP) and the space shuttle program in the following areas:

1. Laboratory tested thermocouples in composite samples made by NASA contractors to be fired at SRI and MSFC. These tests verified the consistency of thermocouple installations and helped identify the thermocouples that were improperly installed.

2. Field tested thermocouples prior to firing tests and identified problems such as secondary junctions in thermocouples, reverse-connected thermocouples, and thermocouples with inconsistent installations.

3. Laboratory and field tested skin-mount RTDs used for detection of leaking valves in SSME fuel lines. These tests were important to verify that the RTDs are securely attached to the lines as opposed to being loose, detached, or floating in the air.

A report written by the Boeing Aerospace Company and provided to NASA through Hercules has acknowledged the AMS contributions in support of NASA and its contractors.[4]

The conclusions of the Boeing report are reproduced verbatim in Table 2.1. The Boeing report also listed the thermocouple problems that have been or may be experienced in the SRM nozzle development program. The list is reproduced verbatim in Table 2.2.

2.6 Development of LCSR Test Equipment for NASA/MSFC

A set of LCSR hardware, software, and procedures was developed and delivered to NASA at the conclusion of this Phase II project in late January 1996. This equipment will provide NASA with independent in-house capability to perform LCSR measurements to characterize the installation quality of thermocouples in solid material. The equipment was successfully demonstrated to NASA/MSFC personnel who visited AMS in January 1996 for factory acceptance of the equipment prior to shipment.

TABLE 2.1

1993 ANALOG TESTING CONCLUSIONS

(Copied from Boeing Report - Reference 4, Page 53)

1. The Delta-M, sheathed thermocouple configuration provides higher temperature capability and a more consistent/repeatable response than the unsheathed configuration.

2. Air gaps around the thermocouple or between the plug and installation hole are detrimental to the response of the installation and should be eliminated or at least minimized.

3. Filler around the thermocouples enhances their response by providing more uniform thermal contact between the thermocouple and the Carbon-Phenolic. However, there is very little added benefit in using Graphite powder over the Boron Nitride slurry, in terms of thermocouple response, and the Boron Nitride is easier to control during the installation process.

4. Precision machining of the plug and installation hole is required to insure good thermal contact at the plug to hole interface.

5. The in-depth plug configuration is the best compromise of the three installations. The face thermocouple configuration almost inherently results in an air gap around the thermocouple, between the plug and installation hole, and the through plug configuration presents structural concerns due to the plug extending all the way through the flame surface which could initiate and/or increase erosion around the thermal probe installation.

6. The Delta-M manufacturing process must be improved to insure a thermocouple product which has adequate isolation to ground, a more robust transition joint and sheath integrity which prevents moisture absorption. Due to moisture absorption, many of the 1993 Delta-M thermocouples had to be baked at 145 °F for 3 hours. Simply baking out absorbed moisture was not an acceptable solution. Delta-M improved their processing and materials based on feedback from SPIP testing and the 1994 testing had fewer problems. Only the transition joint remained sensitive to handling damage.

7. The Loop Current Step Response system, while not able to provide an absolute measure of the time constant of the installation, is a valuable tool in defining the integrity of the installation in terms of secondary junctions within the thermocouple assembly, reversed leadwires, and nominal response, i.e., no large air gaps around the thermocouple.

8. We do not have any kind of an accuracy statement for the thermal probe installation due to lack of a reference/standard in the 1993 analog testing.

9. The MSFC Plasma Torch test facility is not a controlled enough test with such boundary conditions as well defined torch impact points to support code validation quality work. It is quite good for concept screening, however, several of these lessons learned items have subsequently been addressed/resolved in the 1994 testing.

TABLE 2.2

THERMOCOUPLE USAGE HISTORY SUMMARY

(Copied from Boeing Report - Reference #4, Page 5, Figure 3.0-1)

THERMOCOUPLE CHARACTERISTICS	TYPES USED/PROBLEM AREAS								
	WIRE-TYPE			SHEATHED			BECKMAN PROBE	PLUG	ERODING THERMOCOUPLE
	Polyimide	Glass	Bare	.010"	.020"	.040"			
RESPONSE TIME					X	X	X		
THERMAL LAG						X			
SECONDARY JUNCTIONS	X	X	X				X	X	X
MELT DOWN							X	X	
NOISE	X	X	X				X	X	
LEAKAGE/SEALS	X	X	X				X	X	
LOCATION OF JUNCTION	X	X	X	X	X	X	X	X	X

X = AREA OF REPORTED DIFFICULTY

3. HISTORICAL BACKGROUND

3.1 SRM Problems

The performance of SRMs depends on the quality of the composite materials used for the lining of the SRM nozzles. The material must withstand high temperatures (up to about 4000°F) and tolerate the hostile environments that exist during the firing of SRMs.

Due to a significant number of SRM anomalies and failures experienced by the Department of Defense (DoD) and NASA in the early 1980's, a committee headed by Dr. J. W. Littles of MSFC was formed in 1984 to identify the causes and provide resolutions to the persistent SRM problems. The Littles Committee was comprised of specialists from NASA, DoD, and the aerospace industry, and its mission was to assess the state-of-the-art of SRM nozzle design, manufacturing, and acceptance testing.

The Littles Committee concluded that a comprehensive R&D effort should be pursued to understand the behavior of the composite materials under SRM firing conditions and use the information to produce better composites and improve the performance of SRMs. In response, NASA initiated a multidisciplinary R&D program known as the Solid Propulsion Integrity Program (SPIP) to address all aspects of SRM nozzle design and performance. An important part of this program is the development and validation of analytical models to predict the behavior of such composites as carbon-carbon and carbon-phenolic materials used in the construction of SRM nozzles. The models are developed theoretically from the laws of heat transfer and validated under simulated or actual SRM firing conditions. The model validation task requires a variety of instrumentation to determine temperature, pressure, strain, stress, heat flux, and other parameters

that can describe the internal and surface responses of the composites when exposed to high temperatures.

The importance of good instrumentation and accurate measurement techniques was recognized by the Littles Committee when the SRM nozzle integrity program was established. Thus, the Littles plan recommended that R&D efforts be carried out to provide improved sensors and new instrumentation techniques to test the thermal and structural performance of SRMs.

3.2 Space Shuttle Needs

The major components of a space shuttle include the main engines, the solid rocket boosters, and the external fuel tank. Each shuttle has three main engines, two solid rocket boosters, and one external tank. These components are shown in Figure 3.1 and described individually in Tables 3.1 through 3.3.

The LCSR test was found to have two applications in the space shuttle program. These applications are described below.

Space shuttles use skin-mounted RTDs on their main engine fuel and oxidizer lines downstream of isolation valves to monitor for fuel (H_2) and oxidizer (LOX) leaks through the valves. Normally, the line should be at the ambient temperature when the isolation valves are closed. If there is any leak, the lines will become cold and the RTDs will reveal the leak, provided, of course, that the RTDs are properly bonded to the lines.

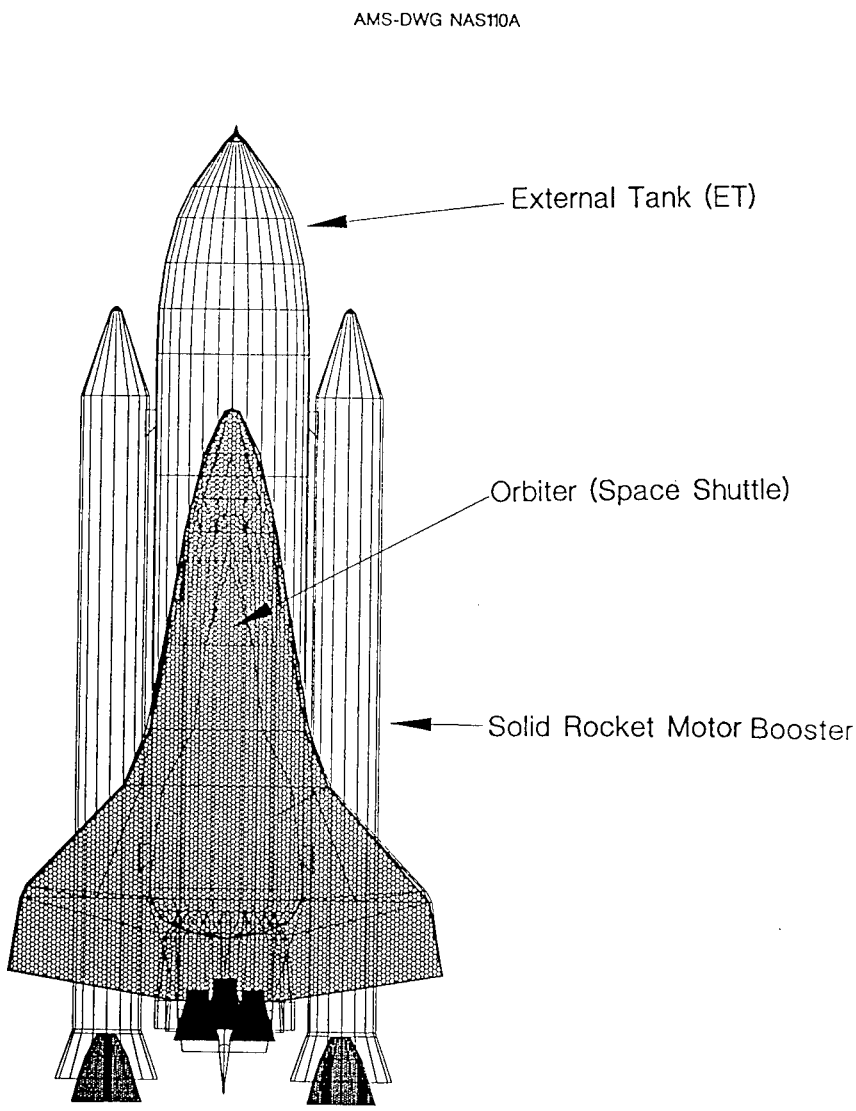

Figure 3.1 A Simplified Schematic of a Space Shuttle

TABLE 3.1

DESCRIPTION OF SPACE SHUTTLE MAIN ENGINE

The Space Shuttle main engine is an advanced liquid-fueled rocket engine. Its main features are variable thrust, high performance, reusability, redundancy, and a fully integrated controller.

Three identical main engines are mounted on the orbiter aft fuselage in a triangular pattern. The engines are spaced so that they are moveable during flight and, in conjunction with the two solid rocket boosters, are used to steer the Shuttle during flights as well as provide thrust for launch.

Fuel for the engines, liquid hydrogen and liquid oxygen, is contained in the external tank, the largest element of the Shuttle.

The main engines use a staged combustion cycle in which all propellants entering the engines are used to produce thrust. In the staged combustion cycle, propellants are burned partially at high pressure and relatively low temperature, and then burned completely at high temperature and high pressure in the main combustion chamber. The rapid mixing of the propellants under these conditions is so complete that a combustion efficiency of about 99 percent is attainable.

The Shuttle main engine uses a built-in electronic digital controller. The controller will accept commands from the orbiter for engine start, shutdown and change in throttle setting, and also will monitor engine operation. In the event of a failure, the controller takes action automatically to correct the problem or shutdown the engine safely.

TABLE 3.2

DESCRIPTION OF SOLID ROCKET BOOSTERS

Prior to launch, the entire weight of the Space Shuttle is supported on the launch pad by two solid rocket boosters. Each booster is attached to the pad by four large bolts.

The heart of each booster is the motor. It is made of four factory prepared segments filled with propellant at the manufacturer's facility and assembled at the launch site. The segmented design permits ease of fabrication, transportation and handling.

The exhaust nozzle in the aft segment of each motor, in conjunction with the orbiter main engines, steers the Shuttle during flight. It can be moved up to eight degrees by the booster thrust vector control system which is controlled by the orbiter guidance and control computer.

At burnout, the two solid rocket boosters are separated from the external tank by pyrotechnic (explosive) devices and moved away from the Shuttle vehicle by eight separation motors - four housed in the forward compartment and four mounted on the aft skirt. The separation motors are fired by a command from the orbiter. The recovery system, in the forward section of the booster, consists of parachutes and a homing device. Following separation - at about 5.8 kilometers (19,000 feet) - the booster is slowed by a drogue parachute and finally by three main parachutes to impact water at a speed of about 25 meters/second (85 feet/sec), aft end first. By entering the water this way, the air in the empty booster is trapped and compressed, causing the booster to float with the forward end out of the water. After divers insert a nozzle closure and force the water from the booster using air pumps, the booster is towed to shore.

After recovery, the booster is disassembled and refurbished. The motor segments are shipped to the manufacturer for reload for another Shuttle flight. The other systems are refurbished either at the launch site or at the respective manufactures' locations.

The two solid rocket boosters are each 149.1 feet (45.4 meters) high and 12.2 feet (3.7 meters) in diameter. Each weighs 1,300,000 pounds (589,670 kilograms). Their solid propellant consists of a mixture of aluminum powder, aluminum perchlorate powder, and a dash of iron oxide catalyst, held together with a polymer binder. They produce about 3.1 million pounds (13.8 million newtons) thrust each for the first few seconds after ignition, before gradually declining for the remainder of a two-minute burn. Together with the three main engines on the orbiter, this provides a total thrust of over 7.3 million pounds (32.5 million newtons) at liftoff.

TABLE 3.3

DESCRIPTION OF SPACE SHUTTLE EXTERNAL TANK

The Space Shuttle external tank (ET) is the largest single element and the only major non-reusable component of the Shuttle system. The ET is 154 feet (47 meters) long and 27.6 feet (8.4 meters) in diameter and carries more than 528,600 gallons (2 million liters) of cryogenic propellants that are fed to the orbiter's three main engines during powered flight.

The ET is the structural backbone of the Shuttle system and absorbs the thrust loads generated by the orbiter's three main engines and two solid rocket boosters.

The ET is actually three components in one: a liquid oxygen tank located in the forward position; a liquid hydrogen tank located aft; and an intertank assembly that connects the two propellant tanks and houses the forward solid rocket booster attachment points. The ET weighs approximately 1,655,600 pounds (751,000 kilograms) when filled with propellants and 66,000 ponds (29,900 kilograms) when empty.

The ET is covered with a multilayered thermal protective coating approximately 1 inch (2.5 centimeters) thick. The insulation allows the tank to withstand the extreme internal and external temperatures generated during prelaunch, launch, and flight. The exact materials, thicknesses, and methods of application vary at different locations on the tank.

The tank's design has been modified to reduce its weight and thus increase the shuttle's payload capability. The first lightweight ET flew on the sixth shuttle mission in April 1983, and weighed over 10,000 pounds (4,500 kilograms) less than the ET used on the first shuttle flight.

At launch, propellants are pressure fed at a combined rate of 1,035 gallons (3,900 liters) per second through 17-inch (43.2 centimeter) diameter feedlines to the orbiter's three main engines. Eight and one-half minutes into flight, when the orbiter and ET have reached an altitude of about 71 miles (114 kilometers), the main engines are cut off and the tank is jettisoned. Residual gaseous oxygen is used to initiate a slow tumble away from the orbiter, prevent the ET from skipping off the atmosphere, and assist in its break-up and descent into a remote ocean area.

The external fuel tank falls toward Earth following its jettisoning from the Space Shuttle during the first ten minutes of the flight.

Surface-mounted RTDs in space shuttles can become loose or detached from the fuel or oxidizer lines due to vibration and other harsh conditions during a shuttle flight. Thus, it is important to test the bonding of the RTDs on a periodic basis, especially after a shuttle flight or before a next flight to ensure that the RTDs are still attached. One of the objectives of this project, which has been successfully met, was to prove that the LCSR method is a reliable means for testing the skin-mount RTDs in the space shuttle's main engines.

4. DESCRIPTION OF LCSR TEST FOR THERMOCOUPLES

4.1 LCSR Test Principle

LCSR testing of thermocouples is based on internal heating of the thermocouple by applying an electrical current to its extension leads. The current is applied for a few seconds and then turned off. This heats the thermocouple junction several degrees above the ambient temperature. When the current is stopped, the thermocouple output is monitored as the junction cools to the ambient temperature. The rate of this cooling depends on the response time of the thermocouple and how well the thermocouple is attached to the material whose temperature is being monitored.

Extensive work with thermocouples in liquids and gases has shown that an analysis of the thermocouple cooling transient can provide the actual response time of the thermocouple under the installation and process conditions tested.[1,2,3] Details are provided in Appendix A.

Figure 4.1 shows a simplified schematic of the LCSR test equipment for thermocouples. An AC power supply is used to heat the thermocouple with a current about 50 mA to 1 amp depending on the thermocouple wire and sheath (if any) diameter. The heating current is applied for 2 to 10 seconds depending on the heat transfer conditions in which the thermocouple is tested. Following this heating period, the AC current is switched off and the thermocouple output is recorded until it reaches steady-state indicating that the thermocouple junction has returned to the ambient temperature.

Figure 4.2 illustrates the principle of the LCSR test and Figure 4.3 shows an actual LCSR transient for a thermocouple that was tested in the laboratory. Usually, the LCSR test is repeated

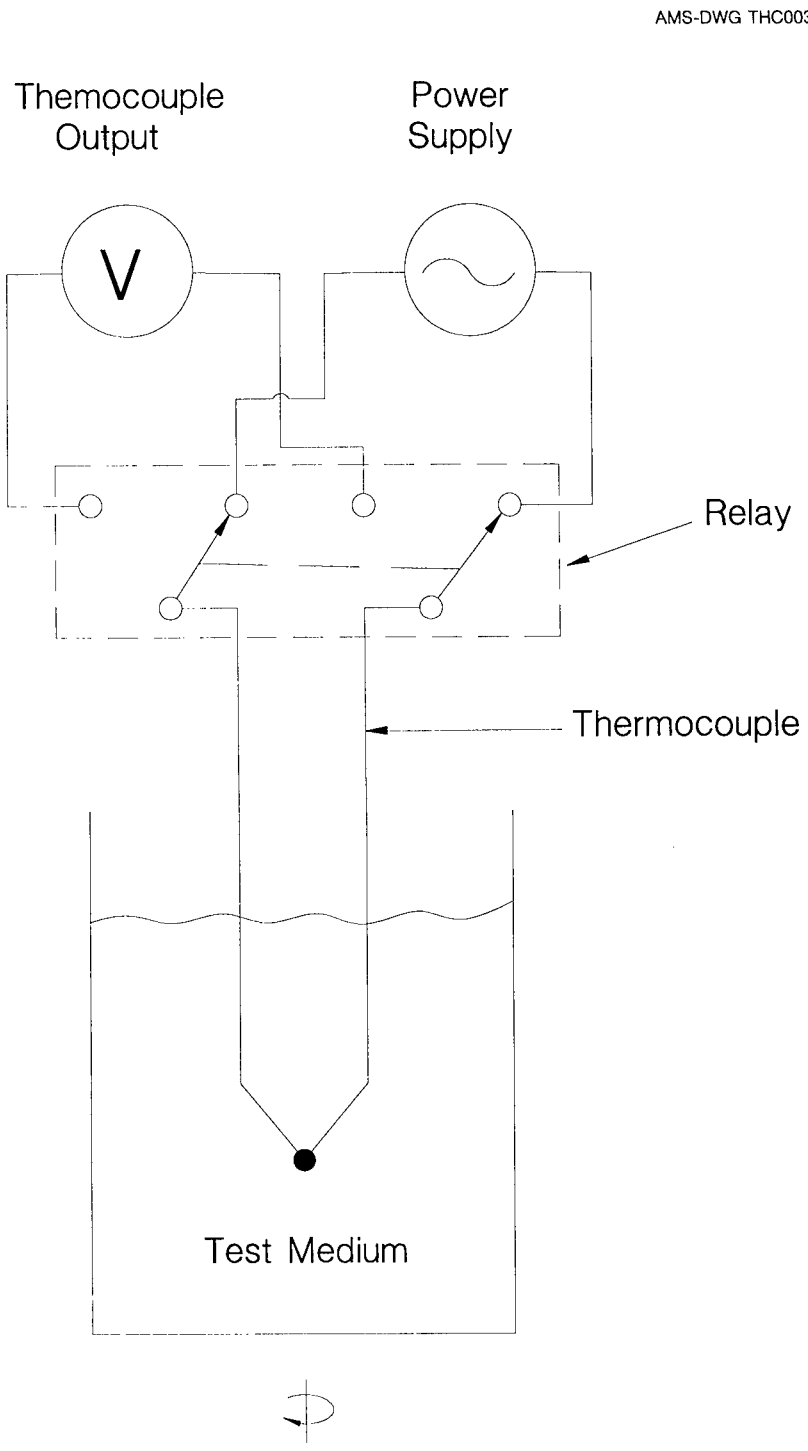

Figure 4.1 Simplified Schematic of Equipment for LCSR Testing of Thermocouples

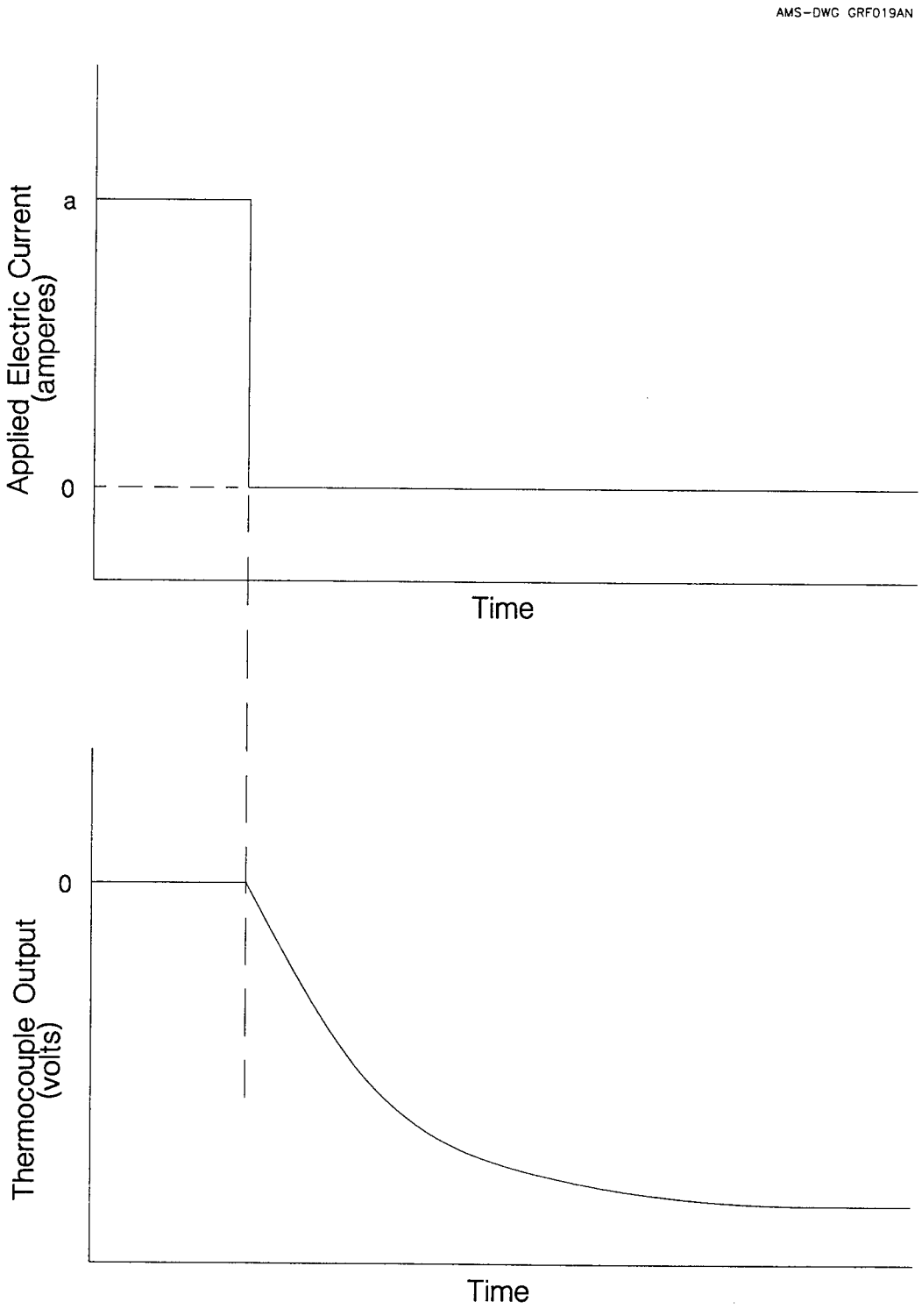

Figure 4.2 Illustration of Principle of LCSR Test for Thermocouples

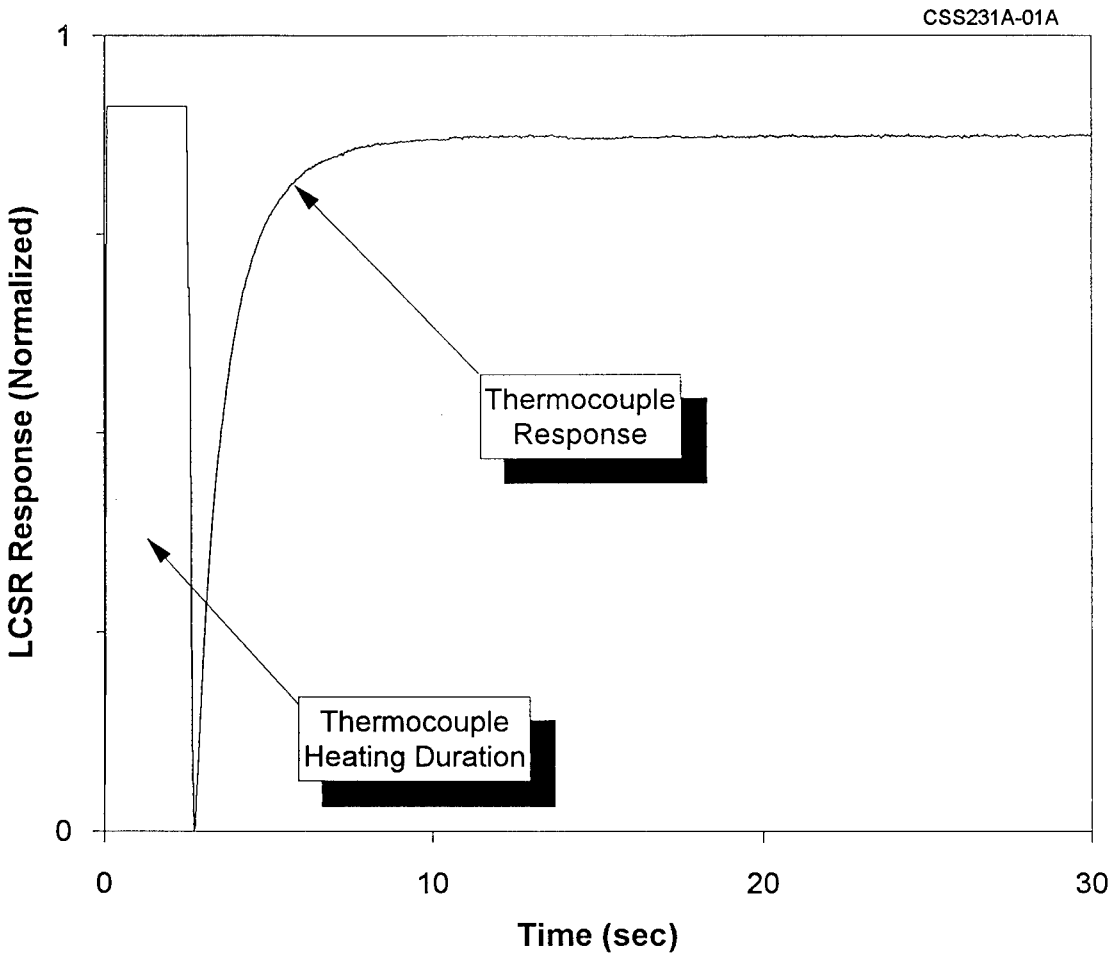

Figure 4.3 Actual LCSR Transient for a Thermocouple

5 to 20 times on each thermocouple and the resulting LCSR transients are averaged to provide a smooth LCSR transient to facilitate the analysis.

4.2 LCSR Data Analysis

The analysis of LCSR data involves an exponential peeling process to identify the poles of the thermocouple transfer function that are then used to give the in-situ response time of the thermocouple.

In this project, the interest in testing thermocouples was not as much in determining a response time as it was in verifying the thermocouple installation. As such, most of the analysis performed here involved comparing raw data plots of LCSR tests. Figure 4.4 shows LCSR data for two identical thermocouples as bonded to a solid material. The thermocouples do not exhibit comparable LCSR transients indicating that the bonding of the two thermocouples are different. To quantify the difference, the LCSR data can be analyzed to give an estimate of the dynamic response of the thermocouple. If a thermocouple is used in a liquid or gas, then it is customary and appropriate to express the LCSR results in terms of a single response time value or a time constant. However, when a thermocouple is installed on a solid surface or embedded in a solid material, it is appropriate to express the results of the LCSR test not in terms of a time constant or response time, but in terms of an installation index. In this report, the words installation index, response time, and LCSR results are used interchangeably to express the degree of bonding between a sensor and a solid material.

4.3 LCSR Test Equipment Supplied to NASA

The contract with NASA for the work reported herein called for a thermocouple LCSR test system to be constructed by AMS during the project and delivered to NASA at the conclusion

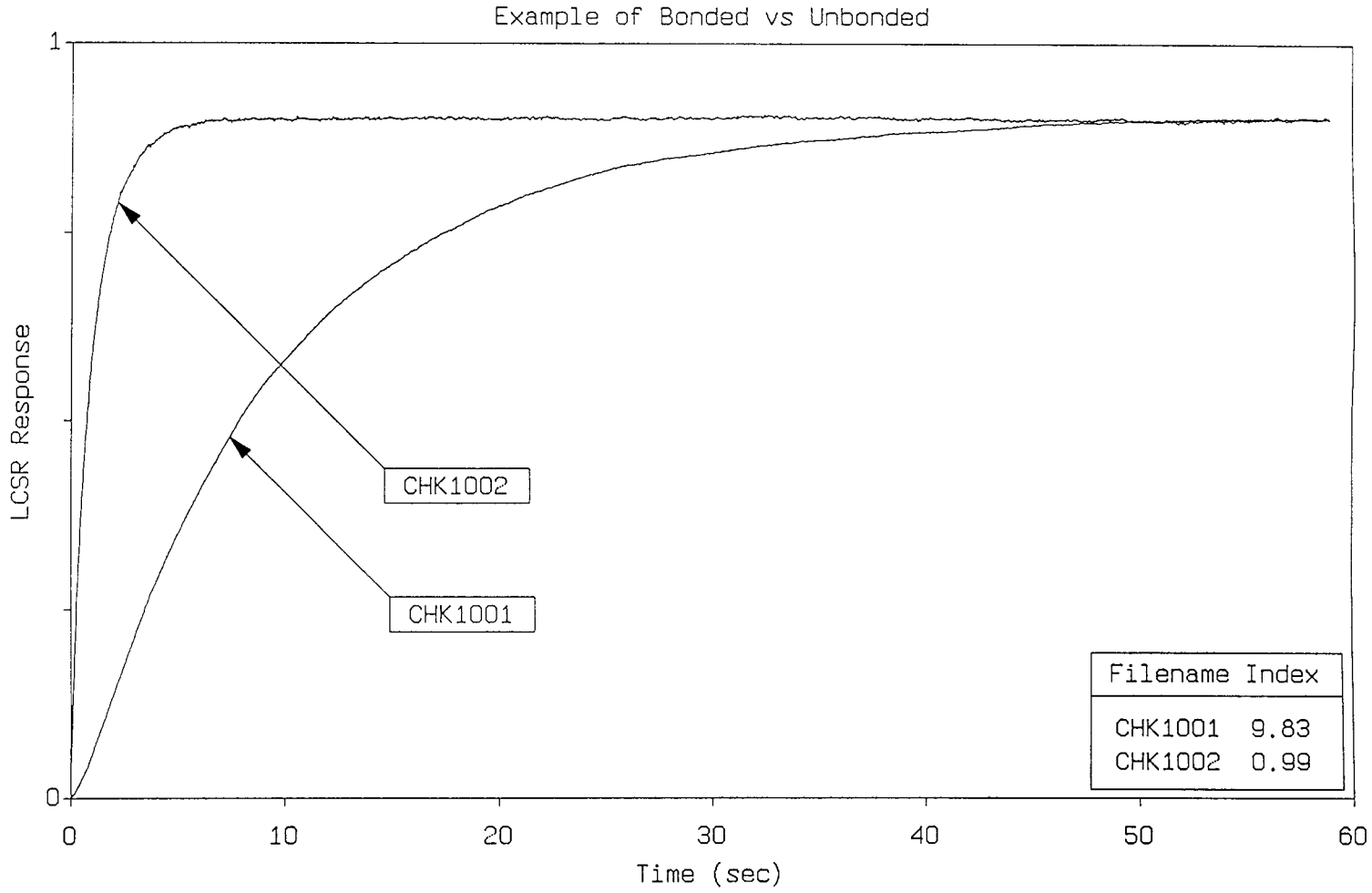

Figure 4.4 Typical LCSR Transients for a Bonded an Unbonded Thermocouple (The Installation Indices of 0.99 and 9.83 Shown in the Box on the Figure Quantify the Bonded and Unbonded Installations, Respectively)

of the project. Figure 4.5 shows a photograph of this equipment. The equipment was shipped to NASA/MSFC at the end of January 1996.

The equipment consists of two units; a LCSR signal generator, and a LCSR signal analyzer. These units are described below.

1. The LCSR signal generator unit contains a variac that can be adjusted to provide the necessary voltages across the thermocouple for the LCSR test. The resulting current that flows through the thermocouple is displayed on an analog ampmeter on the front panel of the LCSR signal generator unit. The unit also contains timing circuitry to adjust the thermocouple heating time, and amplifiers and filters for LCSR signal conditioning. The amplifier gains and the filter settings are accessible on the front panel of the equipment.

2. The LCSR signal analyzer unit consists of a data acquisition computer with a 12-bit analog to digital convertor (A/D) to sample and analyze the LCSR data.

   A user-friendly data acquisition and data analysis software provides a menu with eight options to allow automatic LCSR data sampling and storage, data averaging, data display, etc. The data acquisition software provides the user with a default set of sampling parameters. The user can override the default parameters from the keyboard as necessary to test thermocouples with various dynamic characteristics. For example, for slow thermocouples (e.g., thermocouple with response time greater than 100 seconds), LCSR data is sampled at a low rate (e.g. 0.05 to 0.5 second intervals), and for a long time (e.g., 5 to 10 minutes). Conversely, for fast thermocouples, the LCSR data is sampled at a high frequency (0.01 to 0.03 second intervals) and for a short period of time. Figure 4.6 shows the computer screen with the LCSR menu.

Appendix B contains a copy of the operations manual for the equipment. The manual describes the operation of the equipment including a detailed LCSR test procedure.

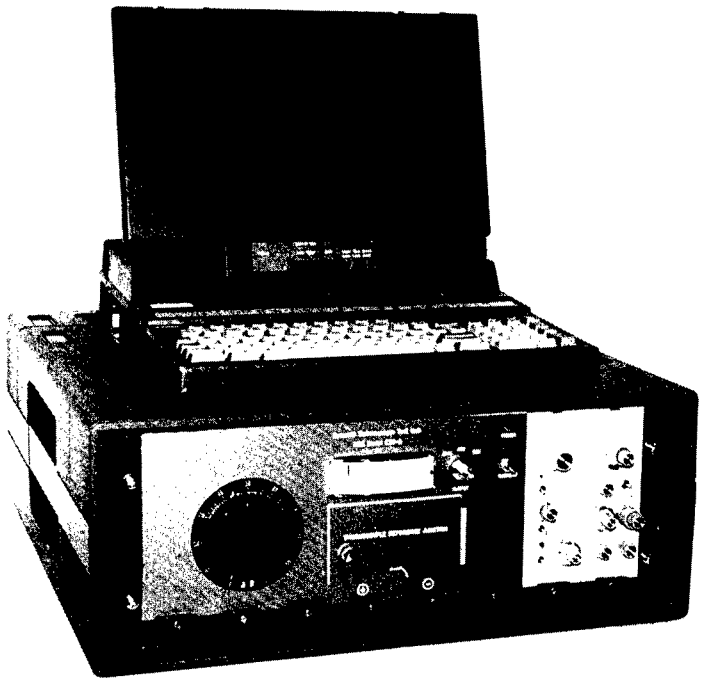

Figure 4.5 Photograph of Thermocouple LCSR Test System Delivered to NASA

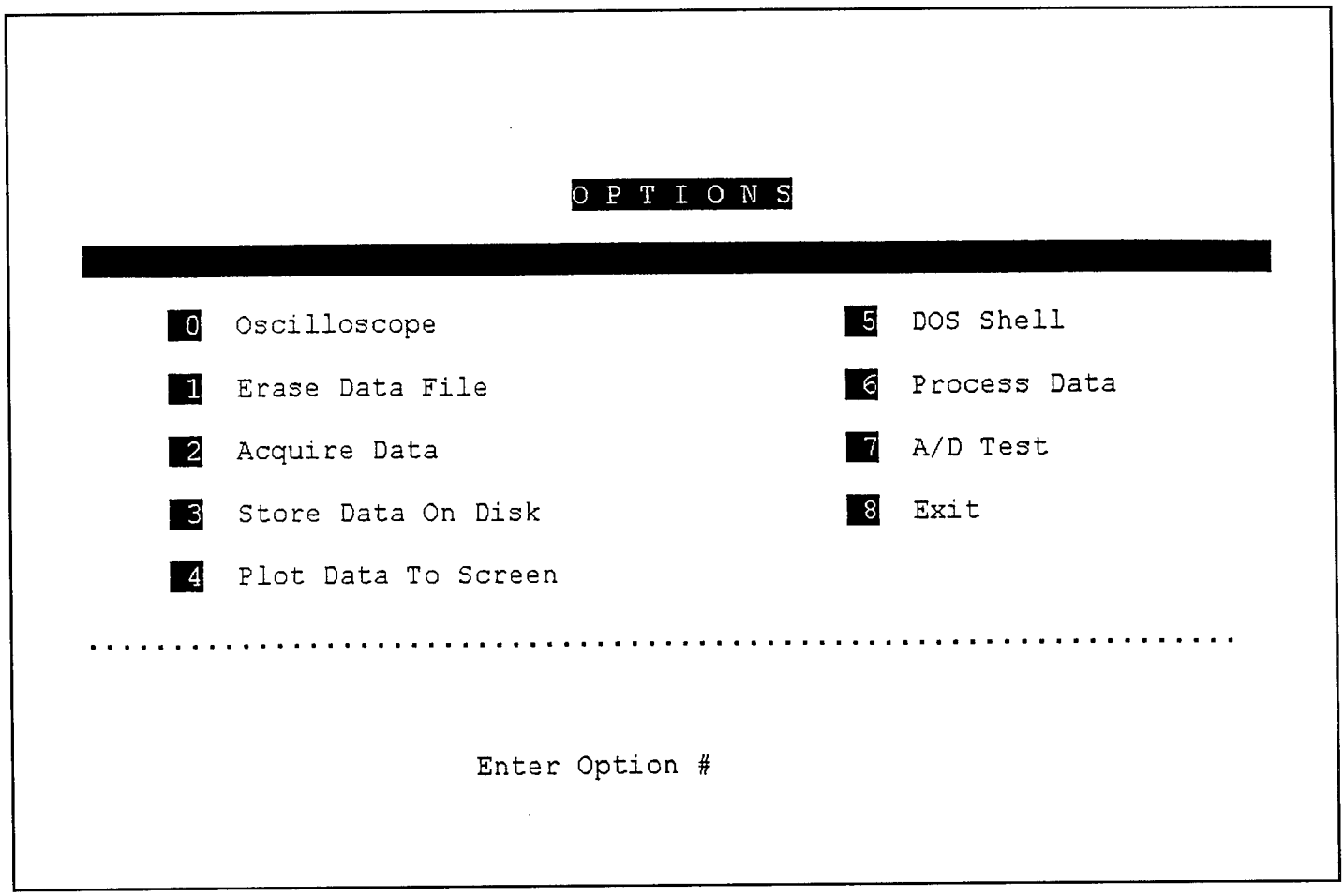

Figure 4.6 Computer Screen Showing the Menu for the User of LCSR Test Equipment

5. DESCRIPTION OF LCSR TEST FOR RTDs AND STRAIN GAGES

The LCSR test of RTDs and strain gages involves a Wheatstone bridge with current switching capability and a variable power supply as shown in Figure 5.1 The sensor is connected to one arm of the bridge and the bridge is balanced using a decade box. As shown in Figure 5.1, when the switch is open, the bridge voltage is dropped across a large resistor (R_s) and a small current (1 to 2 mA) flows through the sensor. When the switch is closed, R_s is bypassed and a larger voltage is then applied to the bridge leading to a high current (40 to 80 mA) through the RTD or strain gage in the bridge. The high current causes internal heating in the sensor and increases its temperature a few degrees (about 5 to 15°C depending on the applied current and the sensor response time) above the ambient temperature. This temperature rise causes the resistance of the sensor to increase with time and results in an exponential transient at the output of the bridge that has a final amplitude of about 0.05 to 0.15 volts. An amplifier is used to increase this voltage to near 10 volts before it is sampled by a computer for analysis. The fixed resistors in the bridge are of the type which do not heat up when the current is increased. As such, the output of the bridge represents predominantly the heating of the sensing element in the RTD or strain gage.

Figure 5.2 illustrates the principle of the LCSR test and Figure 5.3 shows LCSR transients for an RTD and a strain gage that were tested in the laboratory.

The amount of high current that is used for LCSR testing of an RTD or strain gage depends on the response time of the sensor under the conditions that the sensor is tested. If the sensor is slow, then 10 to 20 mA is sufficient. This is because a slow sensor dissipates the heat slowly and leads to a large LCSR signal without a need for a large current or a large

AMS-DWG WBR003X

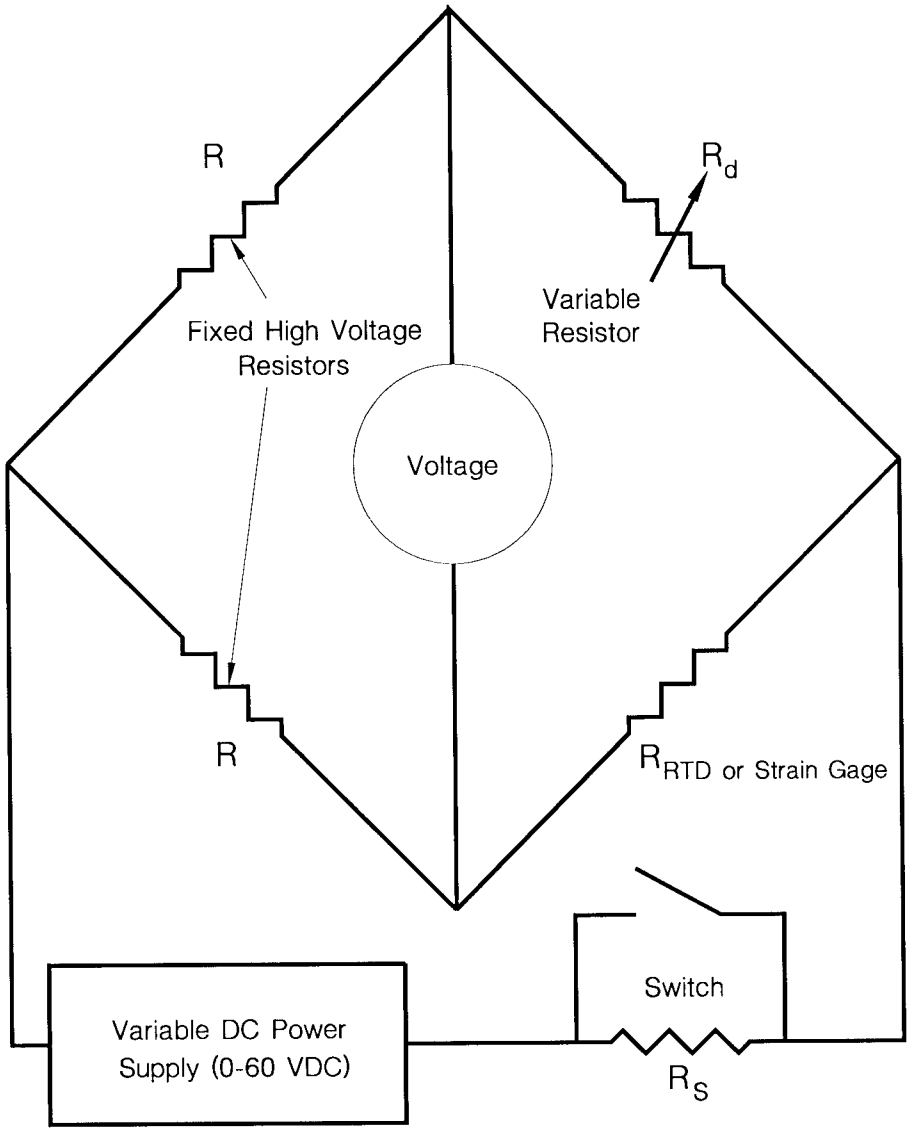

Figure 5.1 Wheatstone Bridge for LCSR Testing of RTDs and Strain Gages

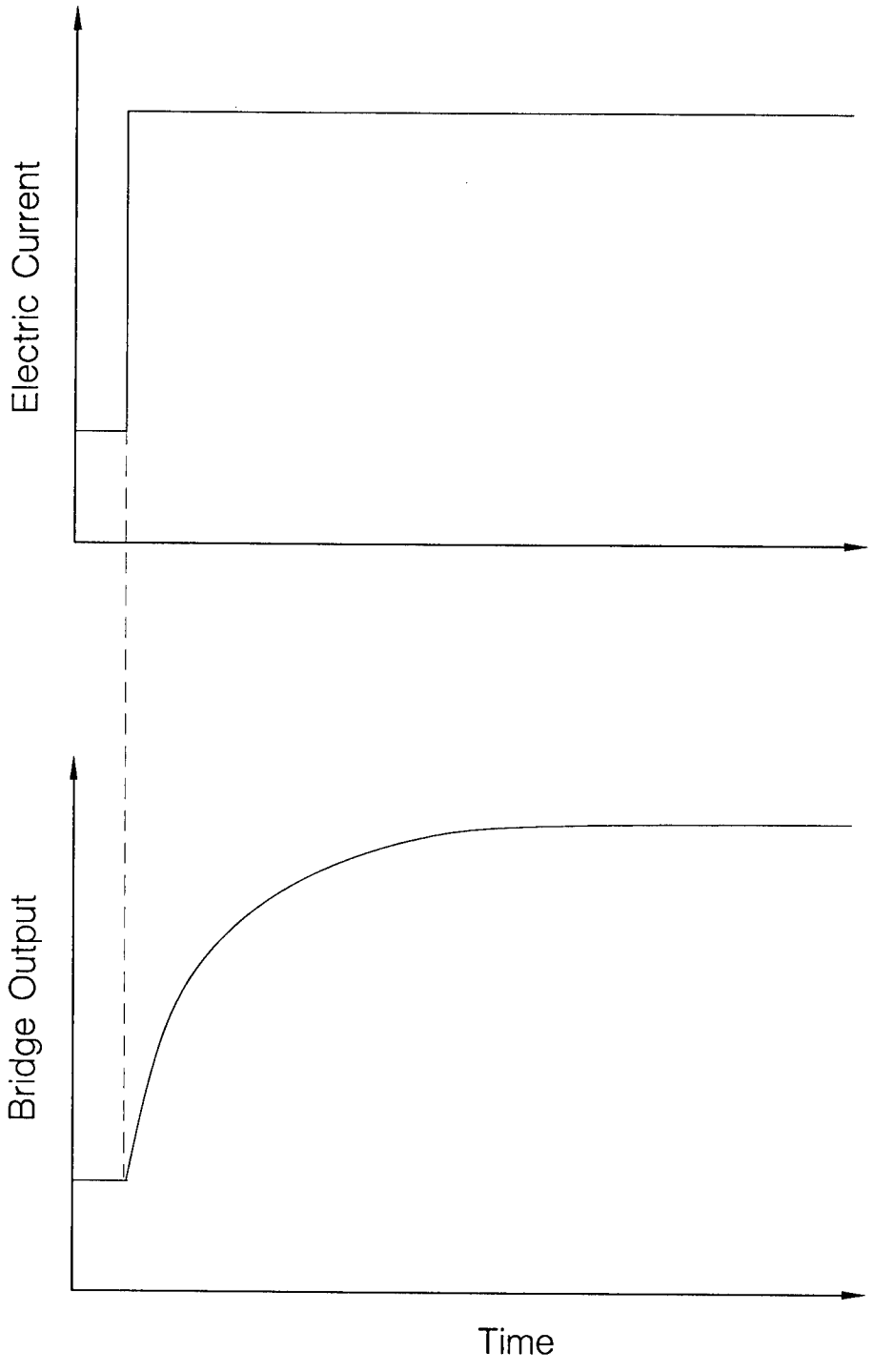

Figure 5.2 Illustration of the Principle of the LCSR Test

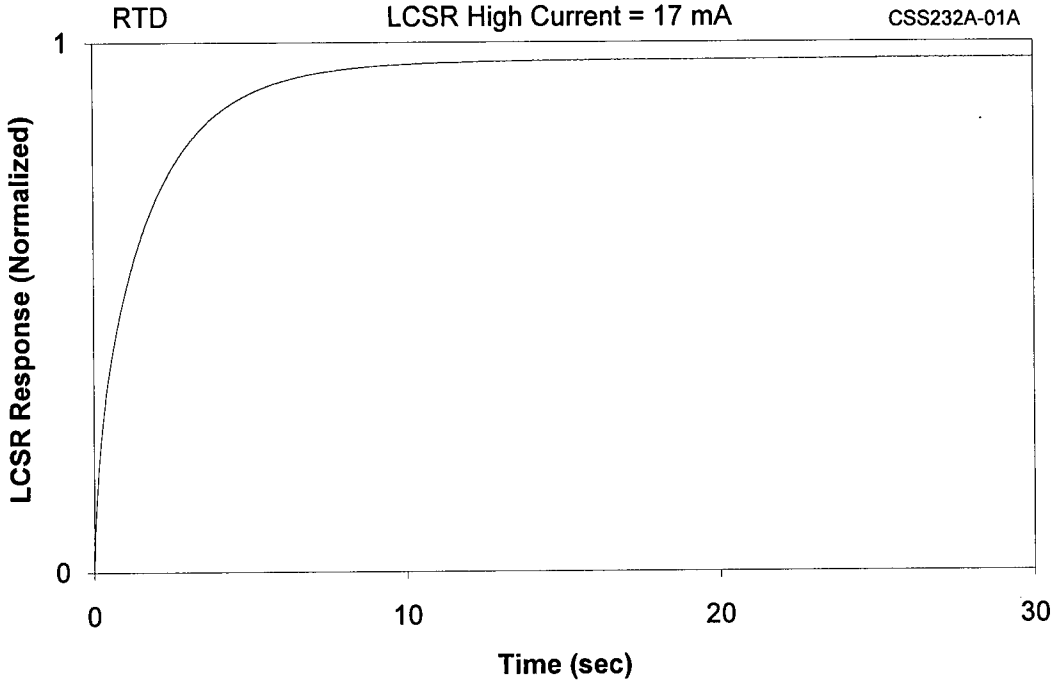

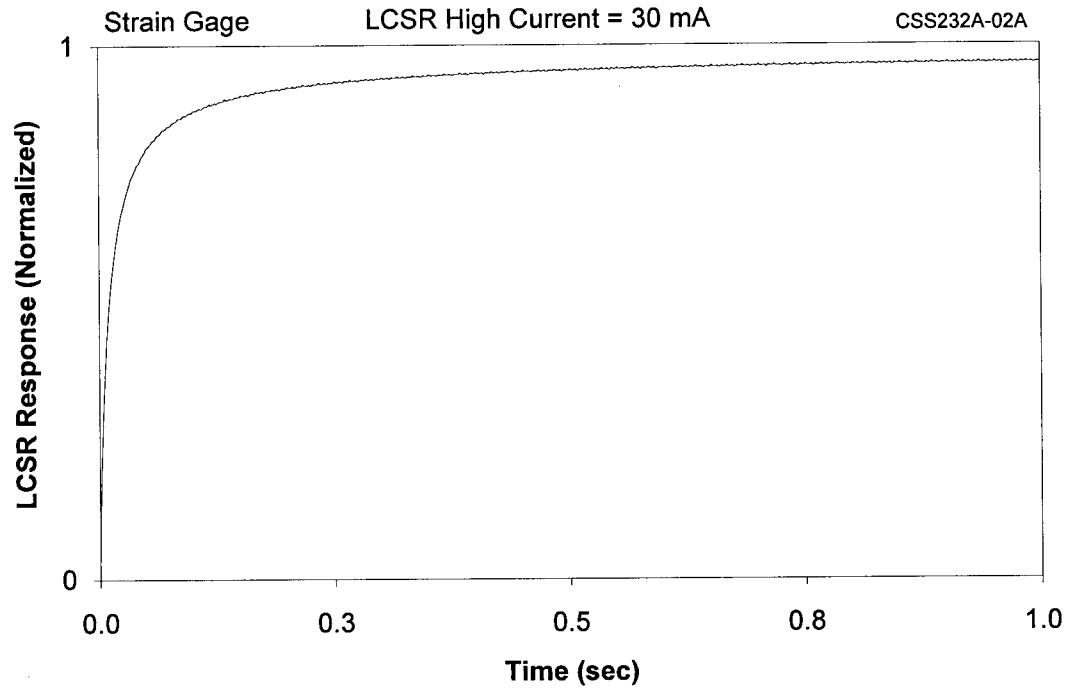

Figure 5.3 LCSR Transients for a RTD and a Strain Gage
Tested in the Laboratory

amplifier gain. On the other hand, if the sensor is fast, such as when the sensor is installed in a flowing fluid, then a larger current (40 to 80 mA) is needed to overcome the ability of the sensor to dissipate the heat. In this case, the larger current helps to provide a useful LCSR signal without having to use a large amplifier gain. It is generally better to use a higher heating current than a larger amplifier gain to obtain a LCSR transient. Large amplifier gains will also amplify any noise on the LCSR signal and must therefore be avoided when there is no restriction on the level of heating current that can be used. Of course, if the heating current must be limited and a high amplifier gain must therefore be used, then a "Low-Pass" filter may be needed to remove any extraneous noise.

Figure 5.4 shows a photograph of the LCSR test equipment that AMS developed years ago and has been using to make response time measurements on RTDs in nuclear power plants and other processes. Referred to as the AMS Model ERT-1, this equipment was used throughout this project to perform LCSR tests on RTDs and strain gages of interest to NASA.

In addition to the ERT-1, AMS has a microprocessor-based data acquisition and data analysis system for LCSR testing of RTDs in nuclear power plants (Figure 5.5). This analyzer is connected to the ERT-1 to perform the LCSR test, analyze the data, calculate the sensor response time, and display the results on a digital indicator on the front panel of the equipment. This analyzer is referred to as the AMS model ELC-1.

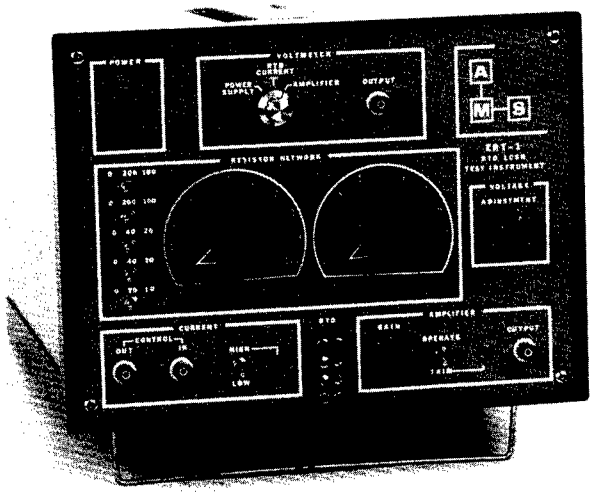

Figure 5.4 Photograph of LCSR Signal Generator, AMS Model ERT-1

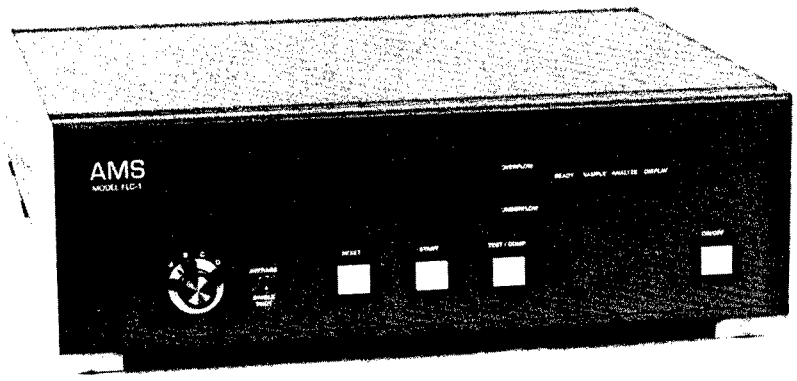

Figure 5.5 Photograph of LCSR Signal Analyzer, AMS Model ELC-1

6. RESULTS OF LABORATORY TESTS OF THERMOCOUPLES

Laboratory tests using the plunge and LCSR methods were performed on representative thermocouples as installed in composite materials to provide baseline data on the dynamic behavior of thermocouples in solids. Furthermore, the laboratory tests were intended to help in interpretating field test results, establishing optimum heating times and heating currents for LCSR testing, quantifying the effect of air gaps on the results of LCSR tests, and examining how thermal compounds used in mounting of thermocouples in solids can help minimize the effect of air gaps on dynamic response of thermocouples. The key results of this work are presented in this chapter.

6.1 Plunge Test Results

A plunge test involves exposing the thermocouple to a sudden change in ambient temperature and recording the thermocouple output to identify its time constant. The time constant is defined as the time that is required for the thermocouple output to reach 63.2 percent of its final steady-state value following a step change in ambient temperature.

Plunge tests were performed in this project to identify the correlation between the results when a thermocouple is plunge tested in air, then installed in a composite block and plunge tested while in the block, and finally, LCSR tested in the block. The results for a sample of five thermocouples are presented here. These thermocouples are identified in Table 6.1 by tag numbers that were assigned to them in this project to track the results. Three of the thermocouples are general-purpose off-the-shelf sensors purchased from OMEGA Engineering, and the other three are small diameter thermocouples made by Delta M Corporation. Delta M

TABLE 6.1

Representative Thermocouples Used for Laboratory Tests

Tag Number	Thermocouple Manufacturer	Sheath Outside Diameter (inches)	Loop Resistance (ohms)	Insulation Resistance (IR) (Mega-ohms)
N28	OMEGA	0.02	49.320	0.10
N29	OMEGA	0.02	47.960	10,000.00
N30	OMEGA	0.02	48.470	10,000.00
N31	DeltaM	0.01	157.043	10,000.00
N32	DeltaM	0.01	156.906	10,000.00
N33	DeltaM	0.01	154.516	10,000.00

has supplied a significant number of specially-made thermocouples to NASA and others for the SPIP program. Appendix C includes a description of the Delta M manufacturing process for thermocouples that are used for special applications.

The plunge tests were performed on thermocouples as installed in a composite material. The composite material, a carbon-phenolic (C-P) sample identified as FM5055, was first machined into a cylindrical sample and thermocouples were fit into holes in the block at two different depths as shown in Figure 6.1. Using a hydraulic plunger, the composite block was suddenly moved into a furnace at 300°F. Figure 6.2 shows a photograph of the furnace and the composite block situated in a position to be moved into the furnace by the hydraulic plunger.

The plunge test results are presented in Table 6.2 in three columns. The first column shows response times of the thermocouples before they were installed inside the composite block. Referred to as the "Bare" time constant, these results were obtained by securing each thermocouple on the hydraulic plunger in air and moving it quickly into the furnace. The second and third columns provide time constant results after the thermocouples were installed in the composite material and plunged into the furnace along with the composite material. The second column gives the time constants of the five thermocouples at a depth of 1/16" from the heated surface, and the other column gives the results for a depth of 1/4" from the heated surface. Note that the time constants increase by an average of less than 10 percent for the five thermocouples when the material thickness is increased from 1/16" to 1/4".

Figure 6.3 shows typical plunge test transients for one of the five thermocouples as installed in the C-P material at two different depths from the heated surface. Two plots are presented in Figure 6.3; one showing an 8000 second trace, and the other showing the first 1000

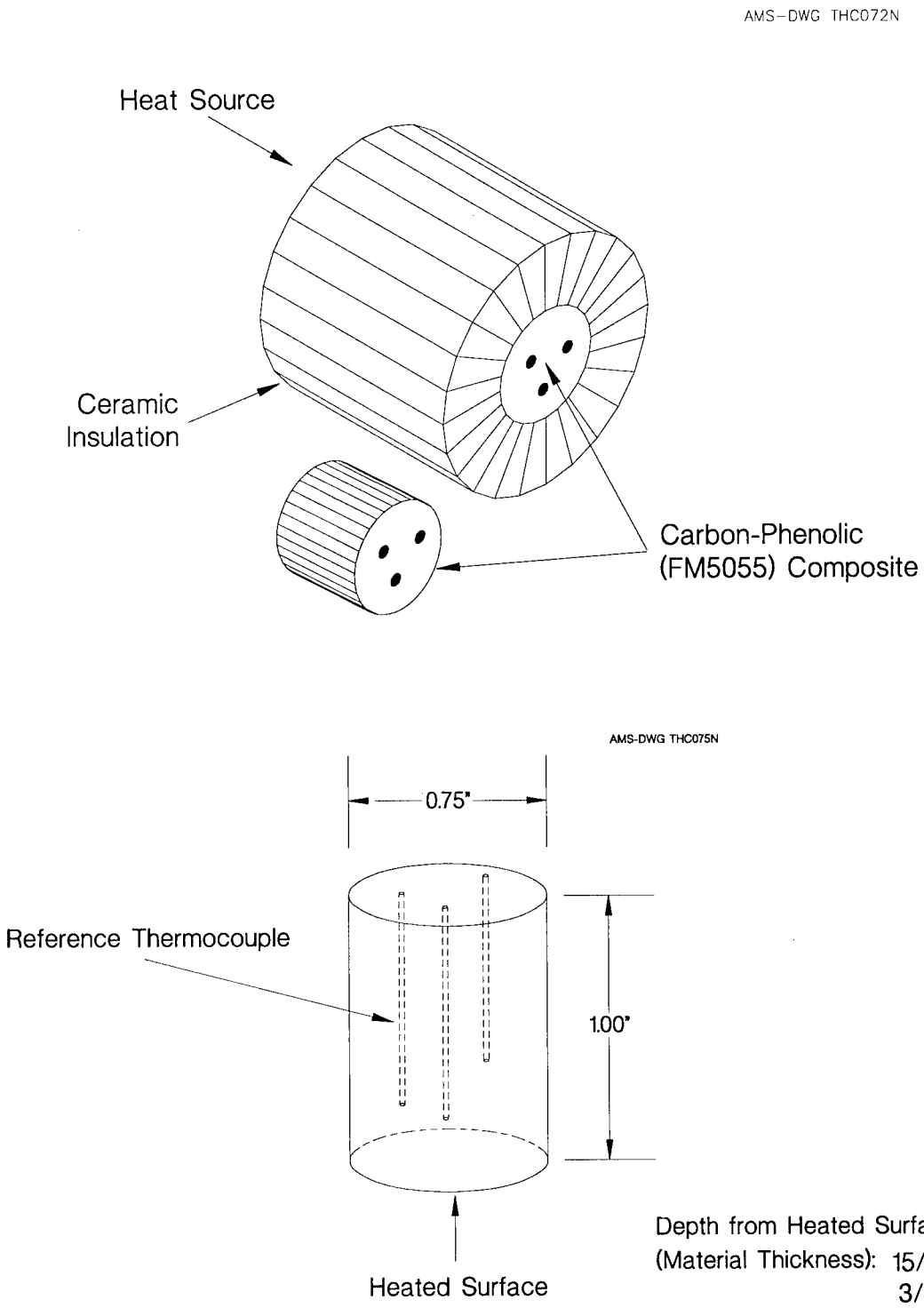

Figure 6.1 Carbon-Phenolic Block with Ceramic Insulation Prepared for Plunge Tests in a Furnace

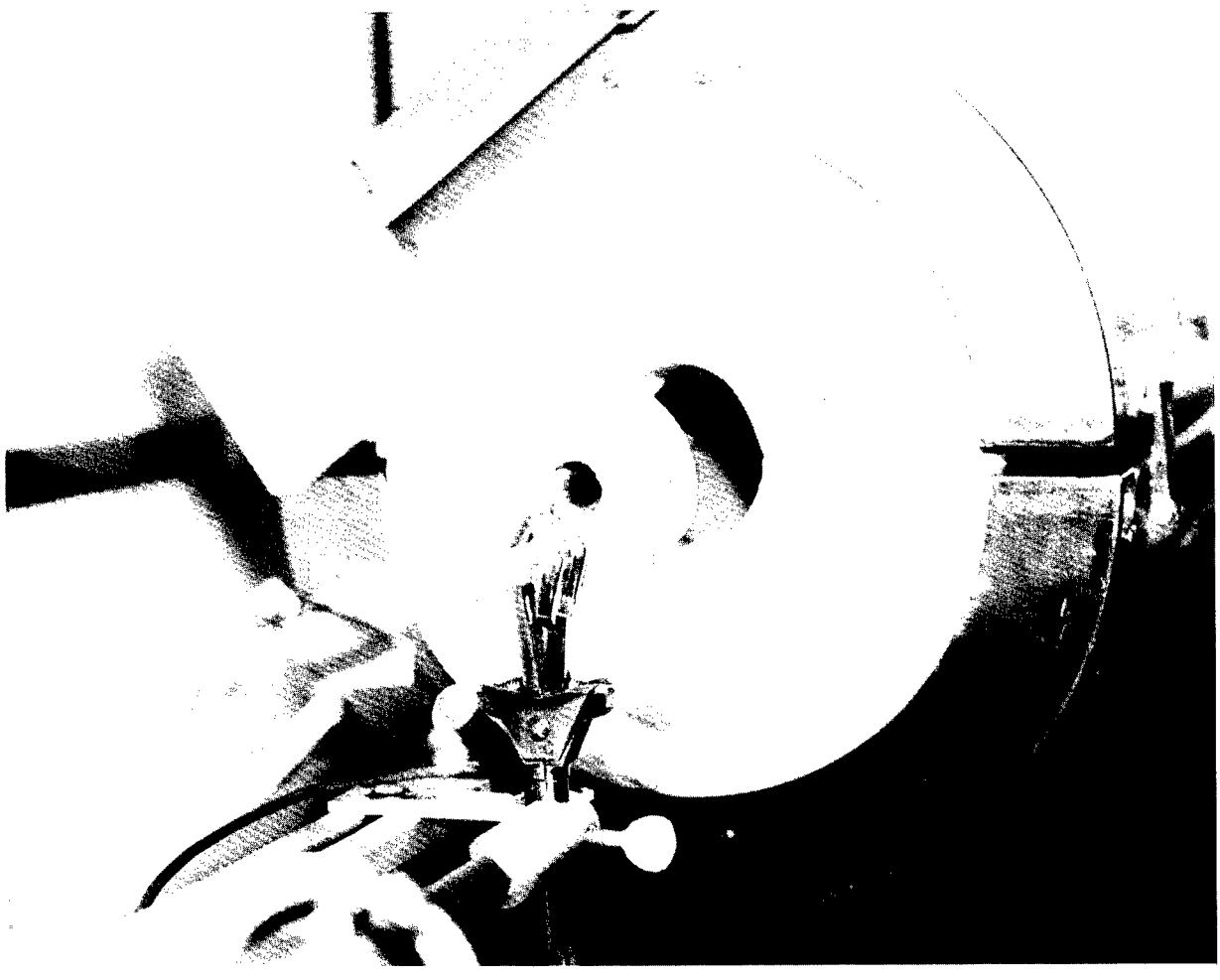

Figure 6.2 Photograph of Furnace and Plunge Test Setup

seconds of the same transient. It is apparent that it takes a little more than one hour for the thermocouple to come to equilibrium with the temperature of the C-P block.

A similar set of plunge tests were performed on a test specimen provided by NASA during the Phase I project. The test specimen was a block of solid material with three embedded thermocouples (Figure 6.4). The three thermocouples were at different distances from the specimen surface that was exposed to the furnace heat during the plunge tests. These distances were identified from the X-ray of the specimen that is shown in Figure 6.4. The plunge test results are given in Table 6.3. Note that the time constant results change by only about 10 percent when material thickness is changed by as much as 0.28".

6.2 LCSR Test Results

The thermocouples that were identified earlier in Table 6.1 were LCSR tested as installed in the composite material while the block was in the furnace at 300°F. The results are listed in Table 6.4 and compared with corresponding results from plunge tests of bare thermocouples and plunge tests of thermocouples as installed in the C-P material.

It is apparent from the results in Table 6.4 that the LCSR test provides results which agree only with the response time of the thermocouples as tested bare rather than the response time of thermocouples in the composite block.

6.3 Effect of Temperature on LCSR Results

The thermocouples identified in Table 6.1 were LCSR tested as installed in a composite material at four different temperatures. The purpose of these tests was to determine if the

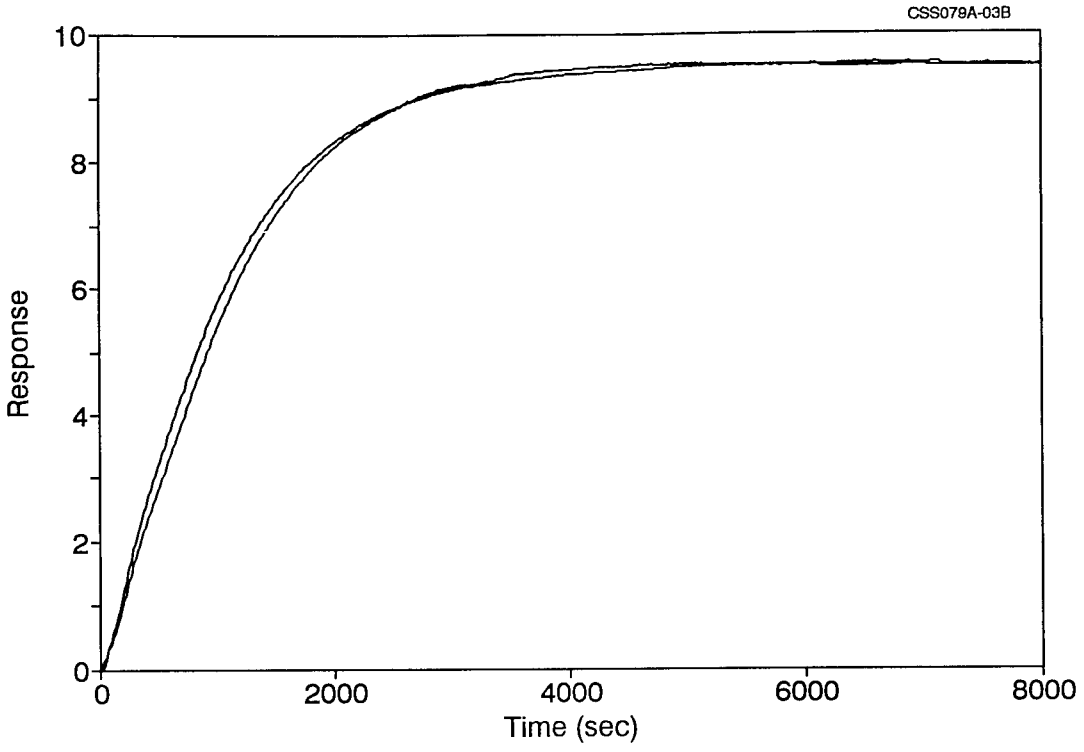

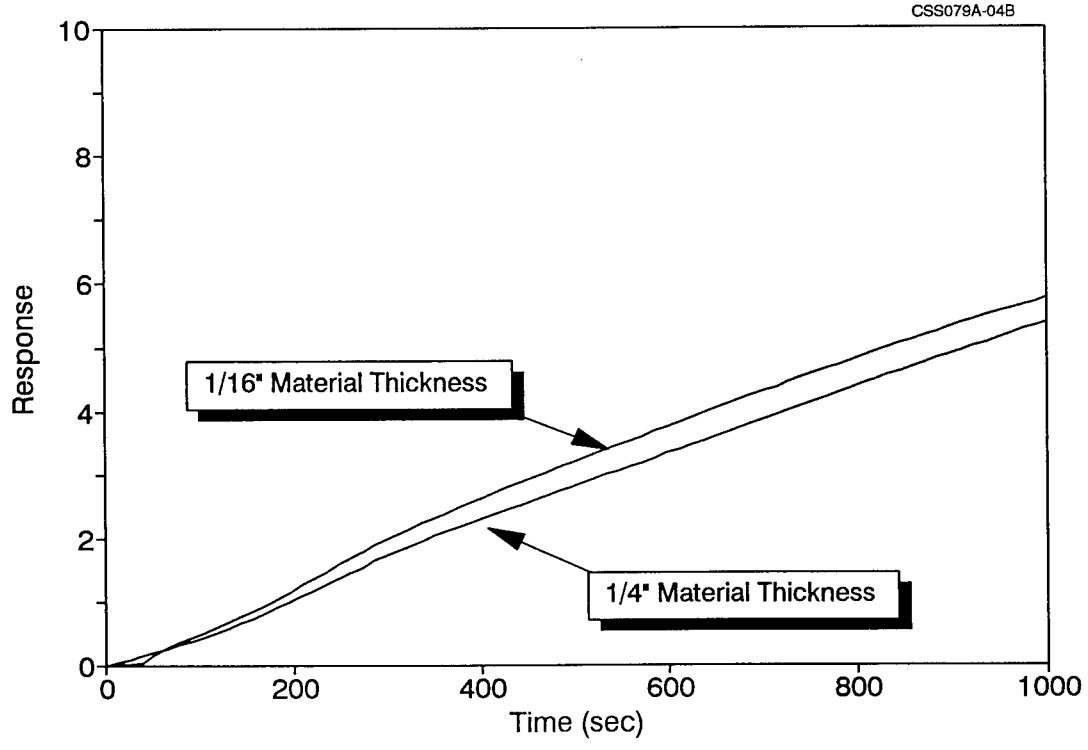

Figure 6.3 Results of Plunge Testing of Thermocouple Number N28

TABLE 6.2

Embedded Thermocouple Response Times Obtained by Plunge Test into a Furnace at 300°F

Tag Number	Time Constant (sec)		
	Bare Thermocouple	1/16" Material Thickness	1/4" Material Thickness
N28	6.0	1026	1176
N29	6.5	1014	1044
N30	5.3	636	756
N31	1.5	846	894
N33	1.6	1080	1140

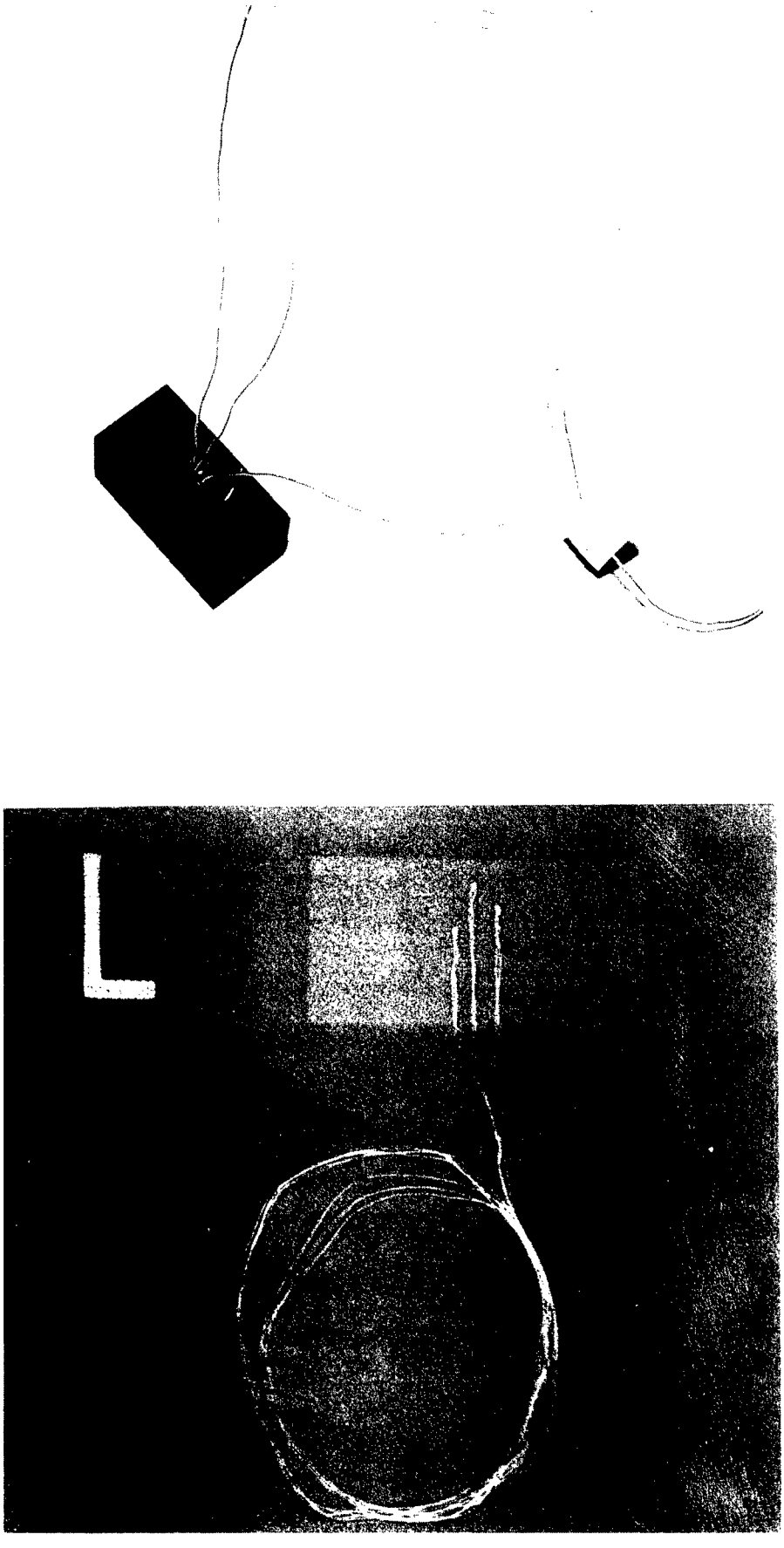

Figure 6.4 NASA Test Block with Three Embedded Thermocouples

TABLE 6.3

Plunge Test Results for Thermocouples in Test Specimen sent to AMS from NASA

Tag Number	Response Time (sec)	Material Thickness (in)
N34	528	0.276
N35	480	0.157
N36	588	0.433

TABLE 6.4

Comparison of LCSR and Plunge Test Results for Representative Thermocouples Tested in a Furnace at 300°F

Tag Number	Plunge Test time Constant (sec)		LCSR Results (sec)
	Bare Thermocouple	Thermocouple Installed in Composite Block	Thermocouple Installed in Composite Block
N28	6.0	1026	3.6
N29	6.5	1014	4.0
N30	5.3	636	4.0
N31	1.5	846	1.4
N33	1.6	1080	1.2

temperature of the composite material has an influence on the dynamic response of the embedded thermocouples. The results are shown in Table 6.5. Each value shown in Table 6.5 is the average of three LCSR results obtained for each thermocouple in three different locations in the block. These results tend to show that the response times of these thermocouples generally increase with temperature.

6.4 Effect of Thermal Compounds on LCSR Results

The five thermocouples identified in Table 6.1 were LCSR tested to illustrate that the use of a thermal compound to install a thermocouple in a composite material can help improve the dynamic response of the thermocouple. Table 6.6 shows the results. These results are from LCSR tests of the thermocouples in holes that were slightly larger in diameter than the thermocouples. The filler material was Boron Nitride which was used in both dry and slurry forms between the outside wall of each thermocouple and the inside wall of the holes in the composite block. The slurry mixture was made by mixing the dry Boron Nitride with a small amount of water. The use of slurry mixture of Boron Nitride has been a common practice in the SPIP program for installing thermocouples inside composites. The mixture has good thermal properties and can help fill any air gap between a thermocouple and the composite block and improve the transient response of the thermocouple.

Figure 6.5 shows LCSR transients for a thermocouple in a C-P composite with and without the use of a thermal compound. It is apparent that the thermal compound can make a significant difference in reducing the sensor-to-solid lag.

6.5 Effect of Air Gap on LCSR Results

In order to quantify the effect of air gaps on response times of thermocouples in solids, LCSR tests were performed on three thermocouples that were installed in a solid material with radial

TABLE 6.5

LCSR Results for Embedded Thermocouples as a Function of Temperature of the Composite Material in Which the Thermocouples were Embedded

Tag Number	LCSR Results (sec)			
	Room Temp.	300°F	600°F	900°F
N28	2.3	3.2	3.0	4.7
N29	2.5	3.9	4.7	6.1
N30	2.7	3.6	4.1	6.3
N31	1.6	1.4	0.9	1.5
N33	1.1	1.1	0.8	1.4

TABLE 6.6

LCSR Results for Thermocouples as Installed in a Composite Block With and Without Filler Material

Tag Number	LCSR Results (sec)		
	No Filler Material	Slurry Filler Material	Dry Filler Material
N28	11.9	7.3	4.1
N29	17.2	4.8	4.2
N30	14.5	9.9	3.3
N31	4.4	0.1	1.4
N33	6.8	0.1	2.2

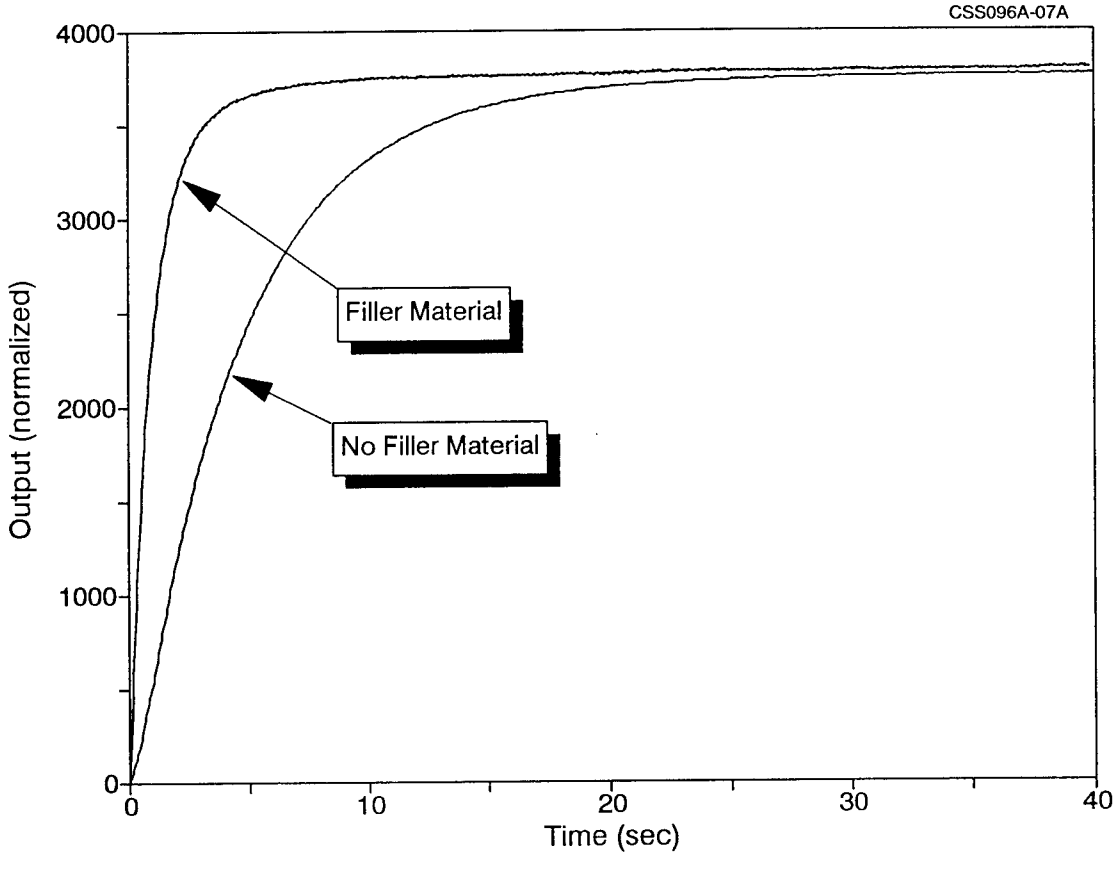

Figure 6.5 LCSR Transients for a Thermocouple Tested With and Without Dry Boron Nitride

gaps of 1/16" and 1/8". The test setup is shown in Figure 6.6 and the results are shown in Figure 6.7 for three types of thermocouples in terms of increases in installation indices due to the air gap. It is apparent that doubling the radial air gap approximately doubles the increase in the installation index. Another way to state this conclusion is to point out that 1/16" of radial air gap increases the LCSR results by 15 to 20 seconds. Figure 6.8 shows representative LCSR transients for one of the air gap experiments.

Laboratory experiments were also performed to determine the effect of air gaps at the tip of a thermocouple that is installed in a solid material. The results are shown in Figure 6.9 in terms of increases in response time due to an air gap (¼") at the tip of the thermocouple. A comparison of results in Figures 6.7 and 6.9 indicates that a radial air gap slows the thermocouple down much more than an air gap at the tip of the thermocouple.

6.6 Effect of Heating Current and Heating Time on LCSR Results

The level of electrical currents that are used to heat a thermocouple for LCSR testing and the heating time are often important in providing reliable LCSR results. Therefore, laboratory experiments were performed on several thermocouples to determine the optimum levels of current and heating times. Representative results are shown in Figure 6.10 in terms of LCSR transients for a 1/16" Type K thermocouple. It is apparent from this figure that 0.5 amps do not provide a very good LCSR transient, while 1.0 amps provide excellent LCSR data. For the same sensor, only two seconds of heating is all that is required to provide a good LCSR transient as shown in Figure 6.11.

Also shown in Figure 6.11 are LCSR transients for another thermocouple (a 1/16" Type J) for which two seconds of heating is insufficient but 5 seconds yields a good LCSR transient. Of course, both the heating currents and heating times that are required for LCSR tests depend very much on thermocouple dimensions, wire resistance, and the heat transfer condition in which the thermocouple is used. The results given in Figures 6.10 and 6.11 were for thermocouples installed

Thermocouple Installed in a Solid with No Air Gap

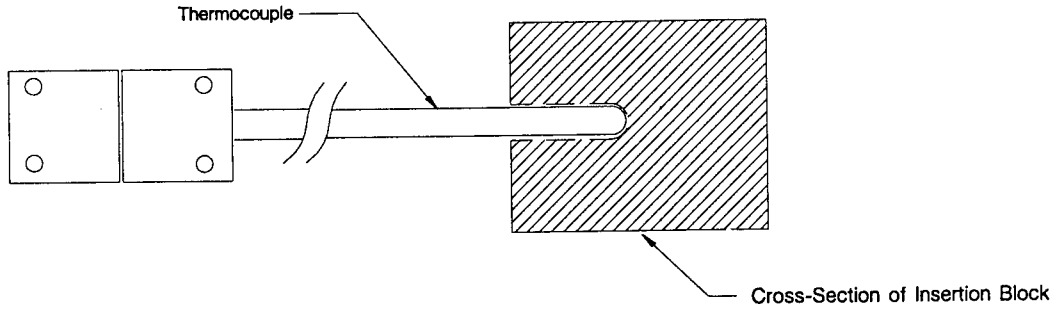

Thermocouple Installed in a Solid with a Radial Air Gap

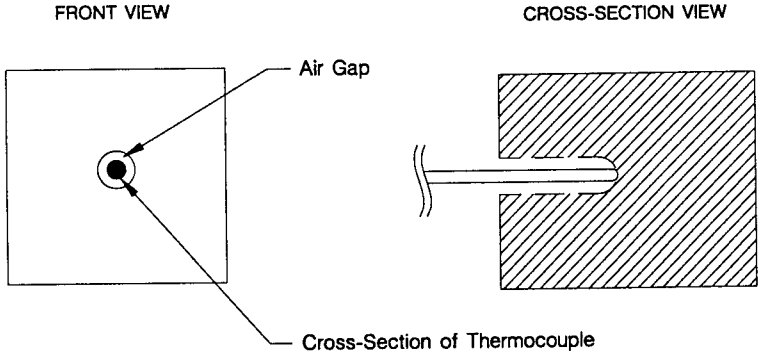

Thermocouple Installed in a Solid with a 1/4" Air Gap at the Tip

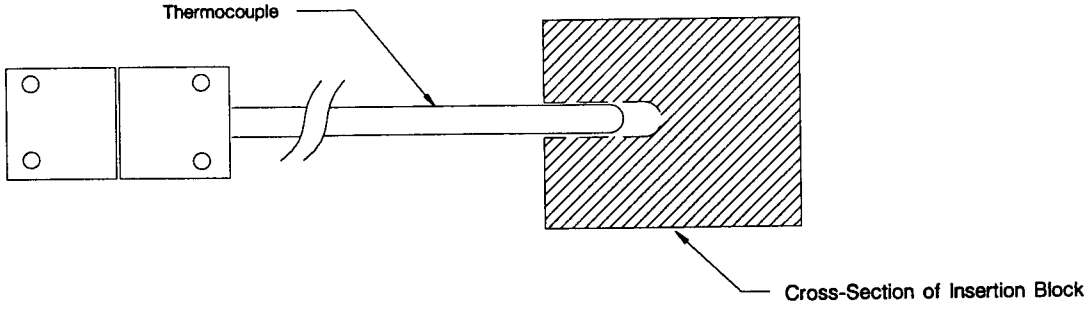

Figure 6.6 Illustration of Thermocouple Installation in Solid Materials for Experiments to Quantify the Effect of Air Gap on Response Time

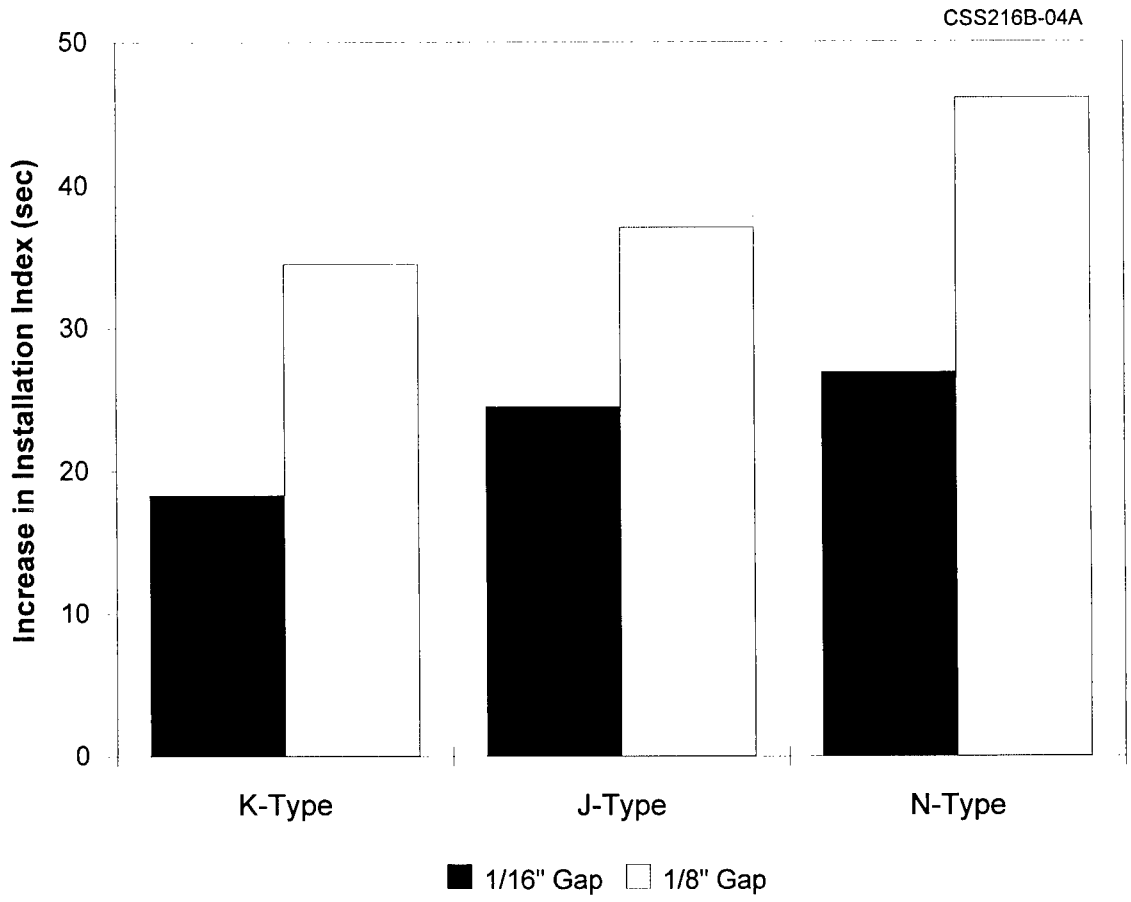

Figure 6.7 Increase in Installation Index Identified by LCSR Testing of Thermocouples in a Solid Block of Copper with 1/16" and 1/8" of Radial Air Gaps

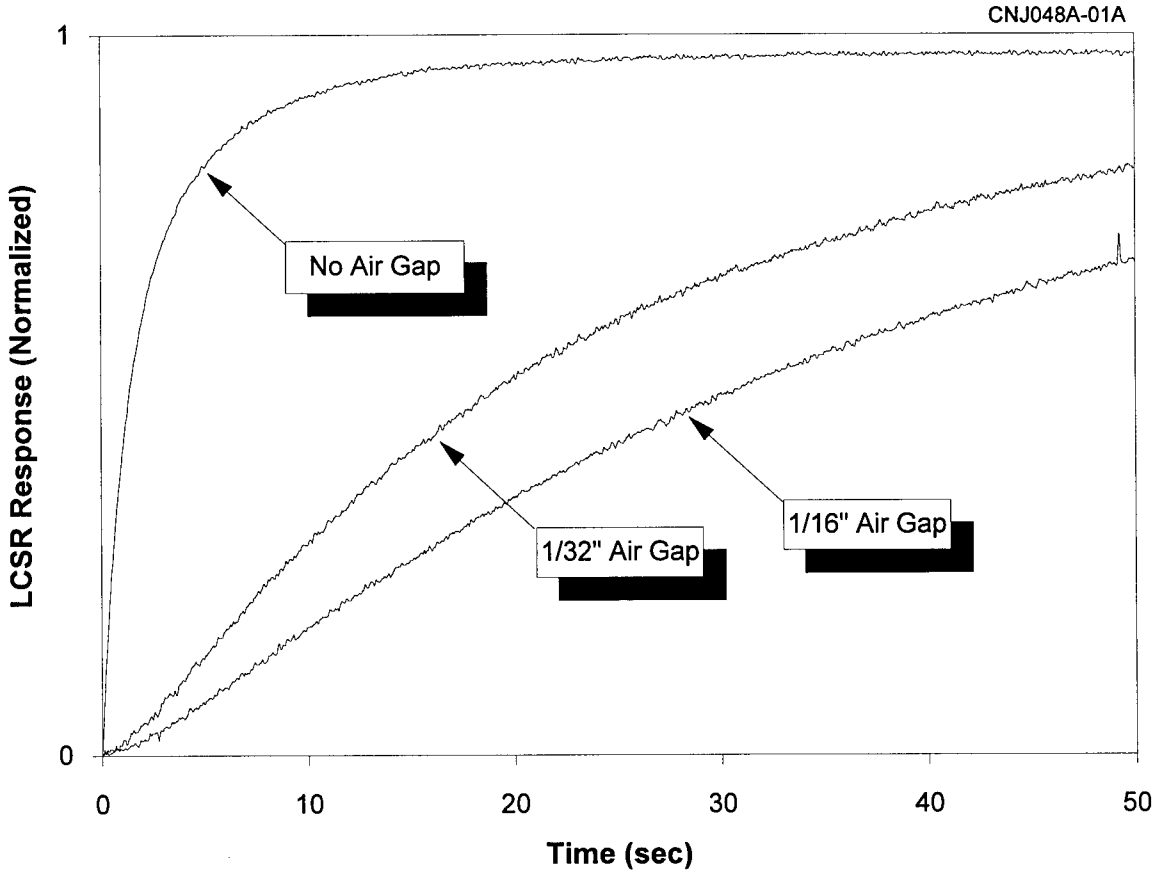

Figure 6.8 Representative LCSR Transients for a Thermocouple Tested in a Solid Material With and Without Radial Air Gaps

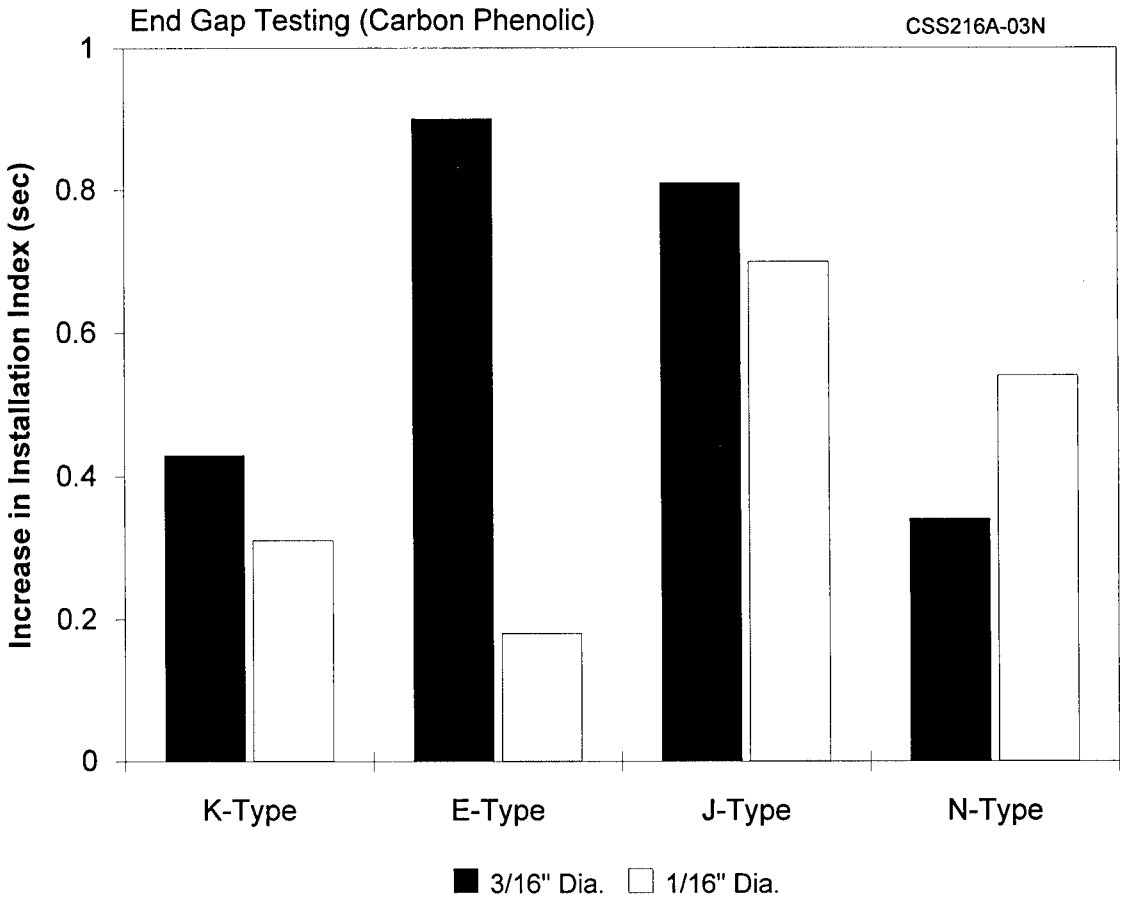

Figure 6.9 Increase in Installation Index for 1/4" Air Gap at the Tip of Thermocouple as Installed in C-P Material. Results are shown for 3/16" O.D. and 1/16" O.D. Thermocouples

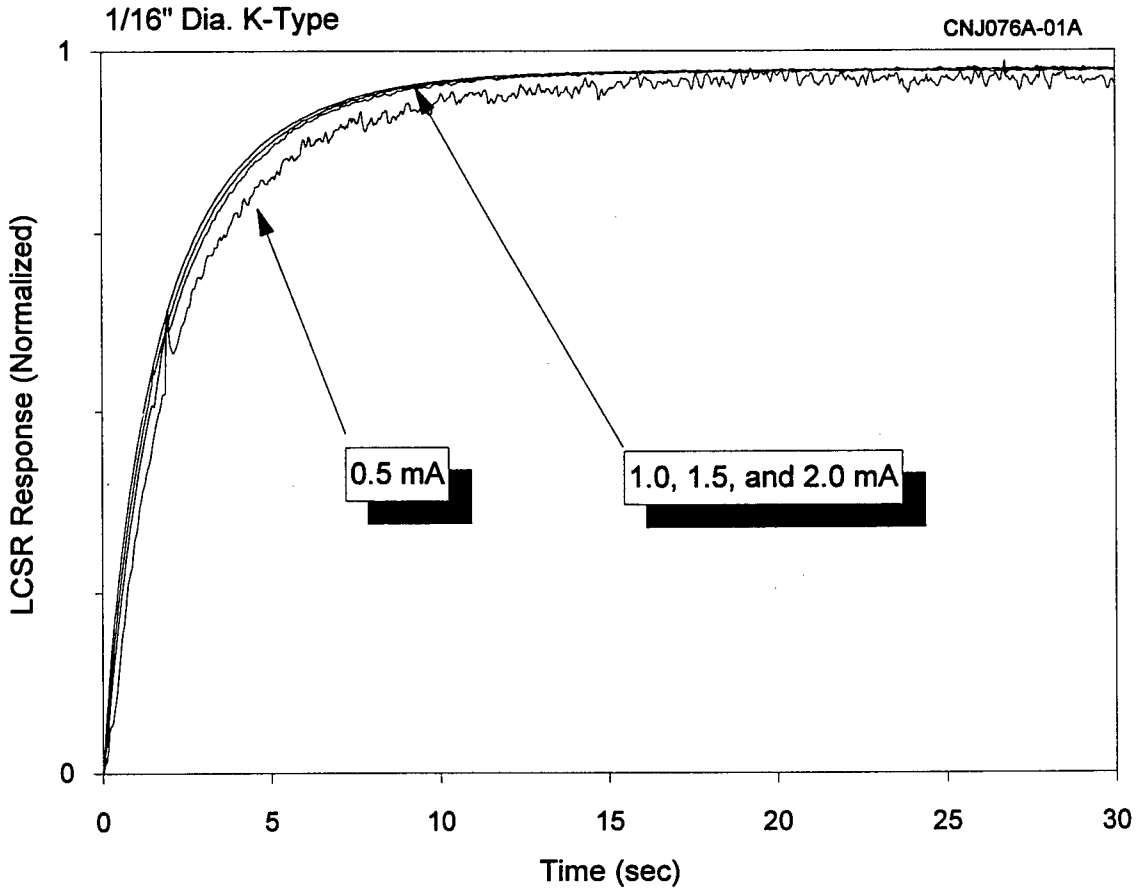

Figure 6.10 Effect of Heating Current on Quality of LCSR data for a Thermocouple

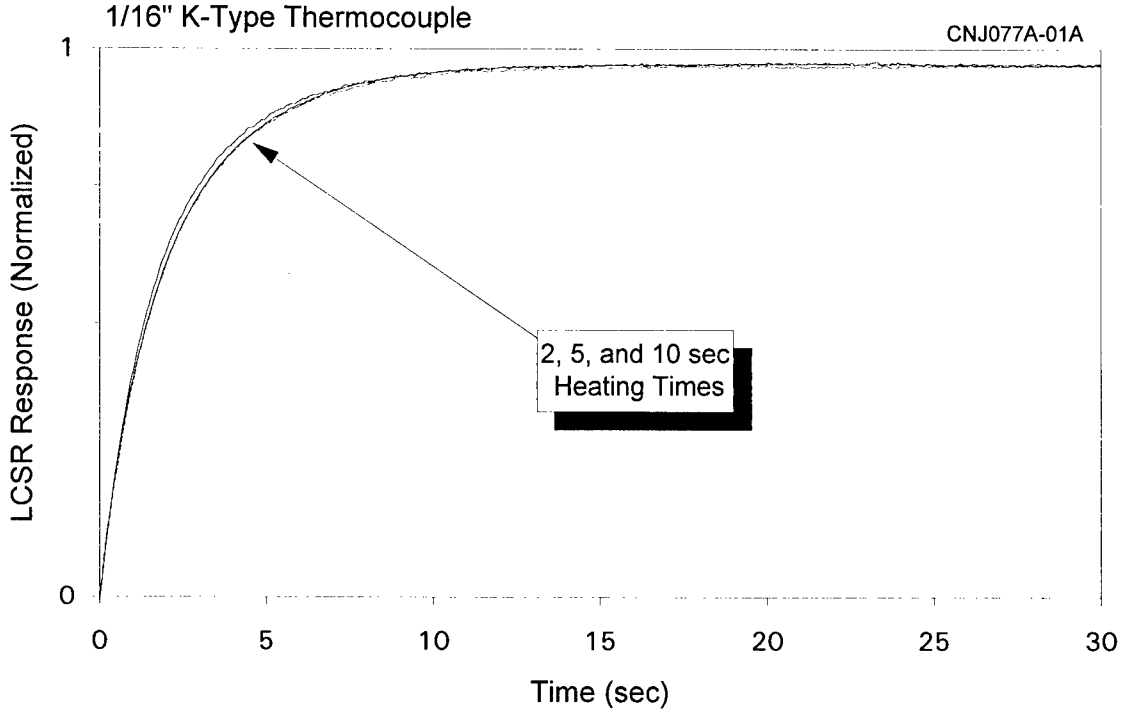

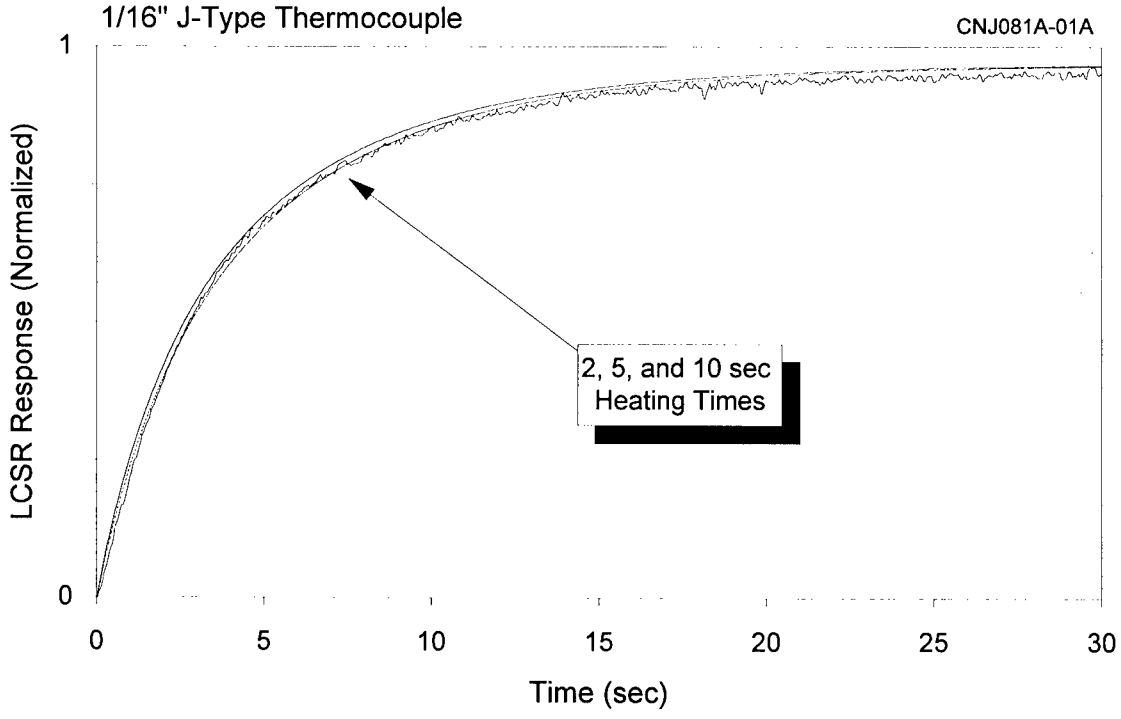

Figure 6.11 Effect of Heating Time on Quality of LCSR Transients

inside a solid block in cylindrical holes that tightly matched the outside diameter of the thermocouple.

A simple procedure can yield the optimum heating time and heating current for LCSR testing of a thermocouple. The thermocouple may be heated with a fixed amount of current (e.g., 0.5 amp) for heating times of as little as 2 seconds to as high as 20 seconds. This experiment will reveal the minimum heating time that is needed to provide a good LCSR transient. The LCSR test unit that was developed in this project for NASA/MSFC is equipped with a timing mechanism which allows the user to adjust the heating time as necessary to conform to this procedure. Alternatively, a default heating time (e.g., 5 seconds) can be used and LCSR tests repeated with various levels of current (from about 0.5 to 3 amps) to identify the optimum current for LCSR testing.

6.7 Repeatability of LCSR Results

LCSR tests were performed on a thermocouple in three different locations in a composite block. The results are shown in terms of LCSR transients in Figure 6.12. The three test transients are superimposed indicating that the response time of the thermocouple is not dependent on its location in the block even though the locations were at different depths in the block. This is consistent with earlier conclusions that the LCSR results for a thermocouple in a solid material is predominantly a function of how well the thermocouple is attached to the solid material. If the thermocouple is tightly installed in the material, then the LCSR result is dominated by the dynamics of the thermocouple itself. On the other hand, if the thermocouple is not in good contact with the solid material, then the LCSR results will depend on the size of any radial air gap between the thermocouple and the material unless the gap is filled with a thermal couplant.

Figure 6.13 shows LCSR transients for the same thermocouples as Figure 6.12, tested in the same three locations in the same block at an elevated temperature (600°F). Again, the LCSR results provide comparable results in the three locations.

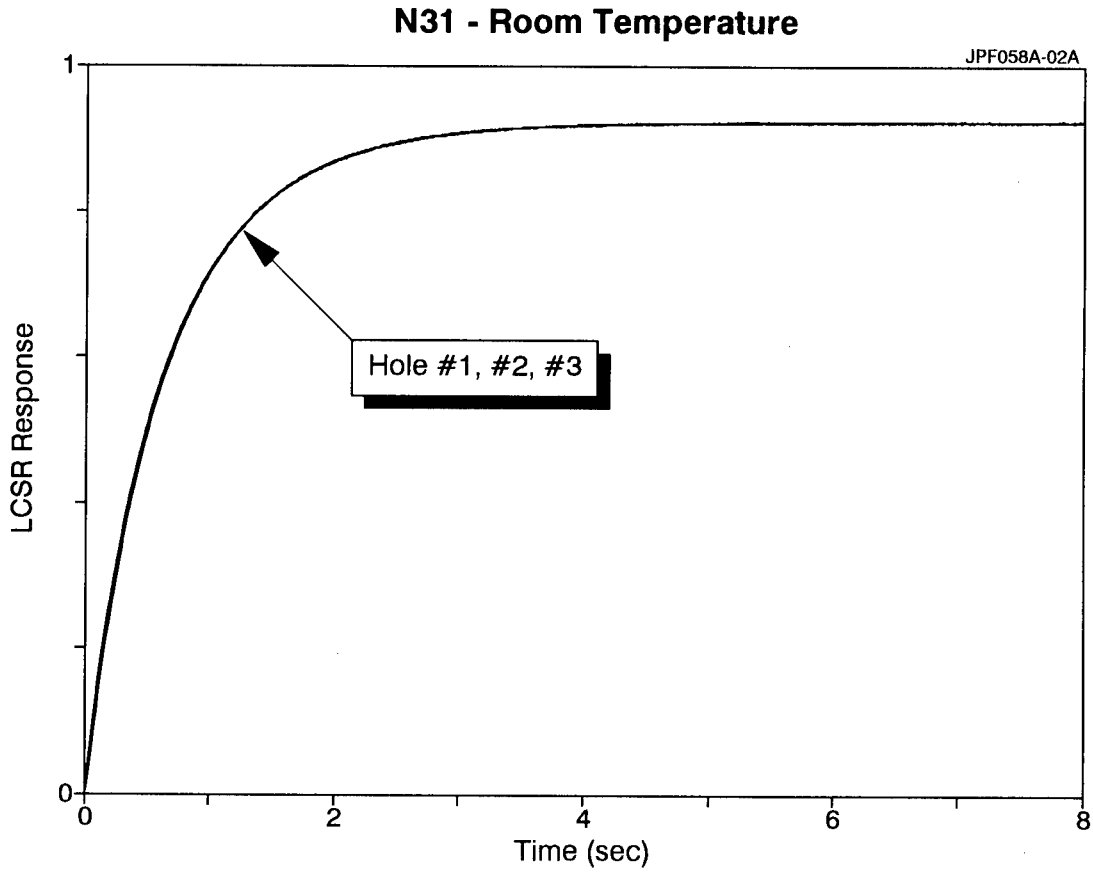

Figure 6.12 LCSR Results for a Thermocouple Tested in Three Different Locations in a Composite Block at Room Temperature

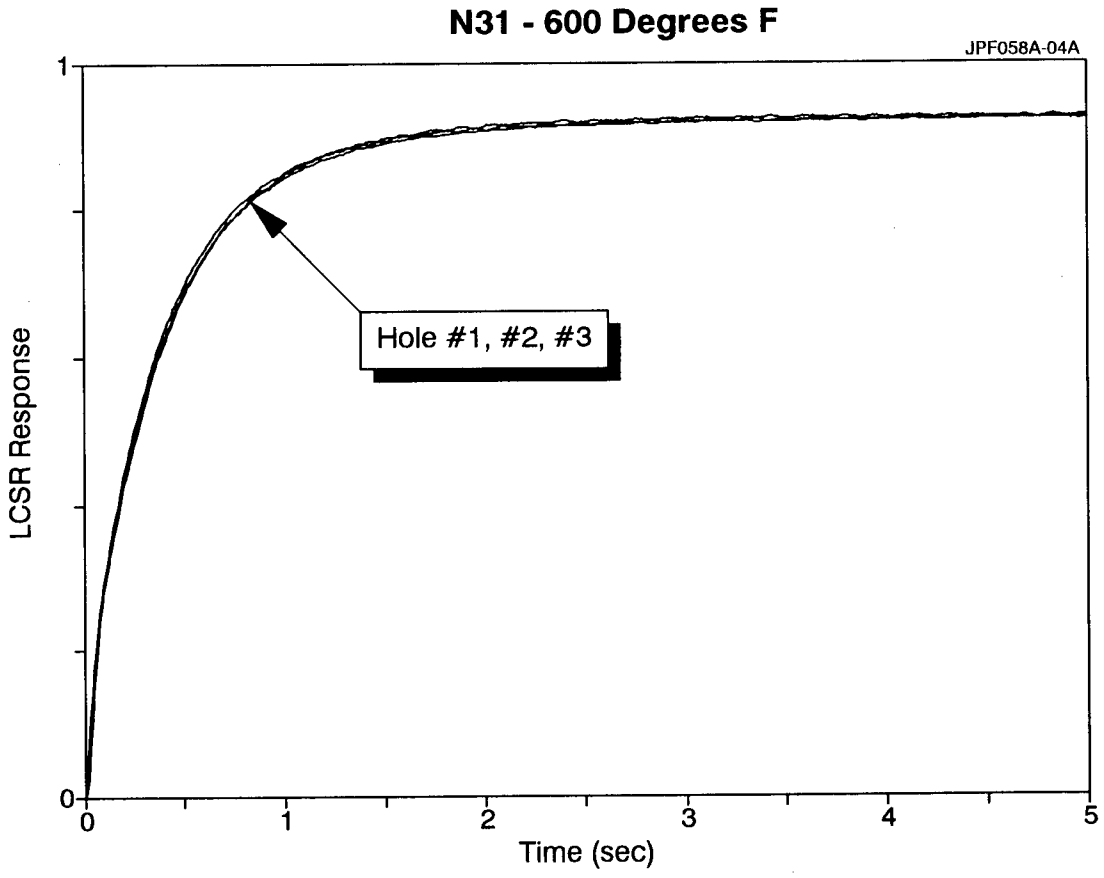

Figure 6.13 LCSR Results for a Thermocouple Tested in Three Different Locations in a Composite Block at 600°F (316°C)

It was stated before that the response time of thermocouples installed in a solid material may increase with temperature. Figure 6.14 shows LCSR results for six thermocouples that were tested in three locations in the same block at three different temperatures. It is apparent that the response times of three of the six thermocouples have increased with temperature. This could be the result of either one or both of the following: 1) the response time of the thermocouple itself increased with temperature, and 2) temperature caused expansion and contraction in the thermocouple and the host material which can change the fit between the thermocouple and the material and affect the response time. It is also important to note that the LCSR results are very repeatable for the three locations in the block. Although the results change with temperature, the LCSR results for each thermocouple are almost the same in the three holes tested.

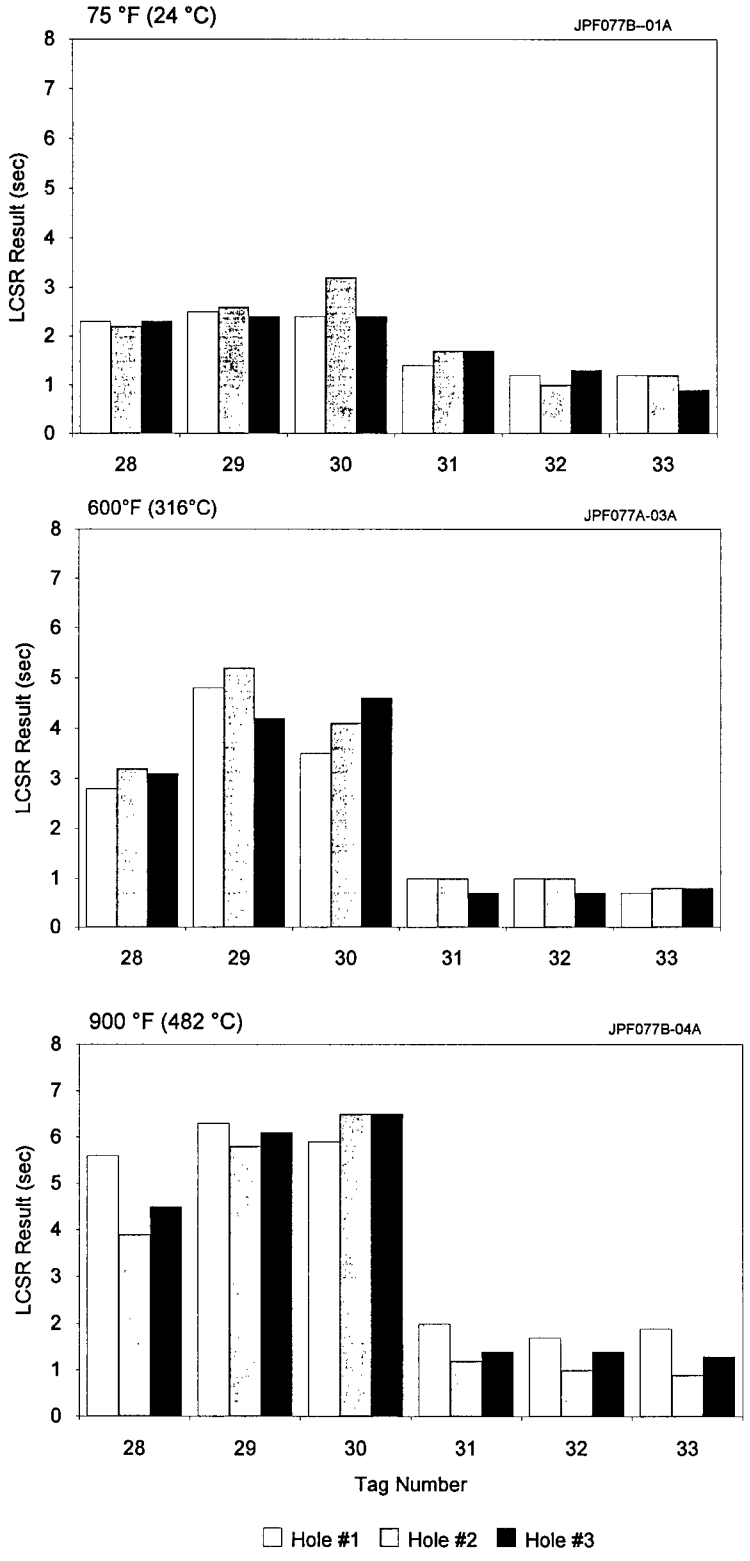

Figure 6.14 LCSR Results Showing the Repeatability of LCSR Results for Each Thermocouple and Indicating the Effect of Temperature on Thermocouple Response

7. RESULTS OF LABORATORY TESTING OF THIOKOL BLOCKS

To increase the value of this Phase II project to NASA, AMS worked with NASA contractors; Thiokol Corporation and Hercules Aerospace Company, who have been involved in development of improved composites under the SPIP/SRM nozzle programs. In particular, AMS performed laboratory testing on thermocouples that were installed in composite materials made by Thiokol. The tests involved forty-two panels known as the "SPIP 94 Analog Test Matrix." Each panel was a composite block of C-P material made by Thiokol under a subcontract with Hercules for NASA. The composite blocks were made using different ply angles and thermocouples were installed in the block using two different mounting procedures. Up to six thermocouples were installed in each block. Some of the thermocouples were installed in a plug inside the block as shown in Figure 7.1, and others were cured into the composite as shown in Figure 7.2. The latter is referred to as cured-in-place or CIP installation meaning that the thermocouple was embedded into the C-P material when the material was manufactured. The test matrix was made for NASA to: 1) determine the difference between the CIP and plug installation techniques, 2) study the effect of ply angle on the performance of composites, 3) identify side gap effects, 4) determine the contributions of Boron Nitride on reducing thermocouple lags, and 5) quantify heat rate effects.

All thermocouples used in the Thiokol blocks were 0.01" O.D., sheathed, Type K thermocouples manufactured by Delta M. The plug installation involved Boron Nitride in the plug to fill any air gap between the thermocouple and the solid material.

The purpose of the AMS tests was to evaluate the CIP and plug installation methods and identify any outlier thermocouples in terms of response time. After AMS testing, the blocks were sent to SRI for firing tests.

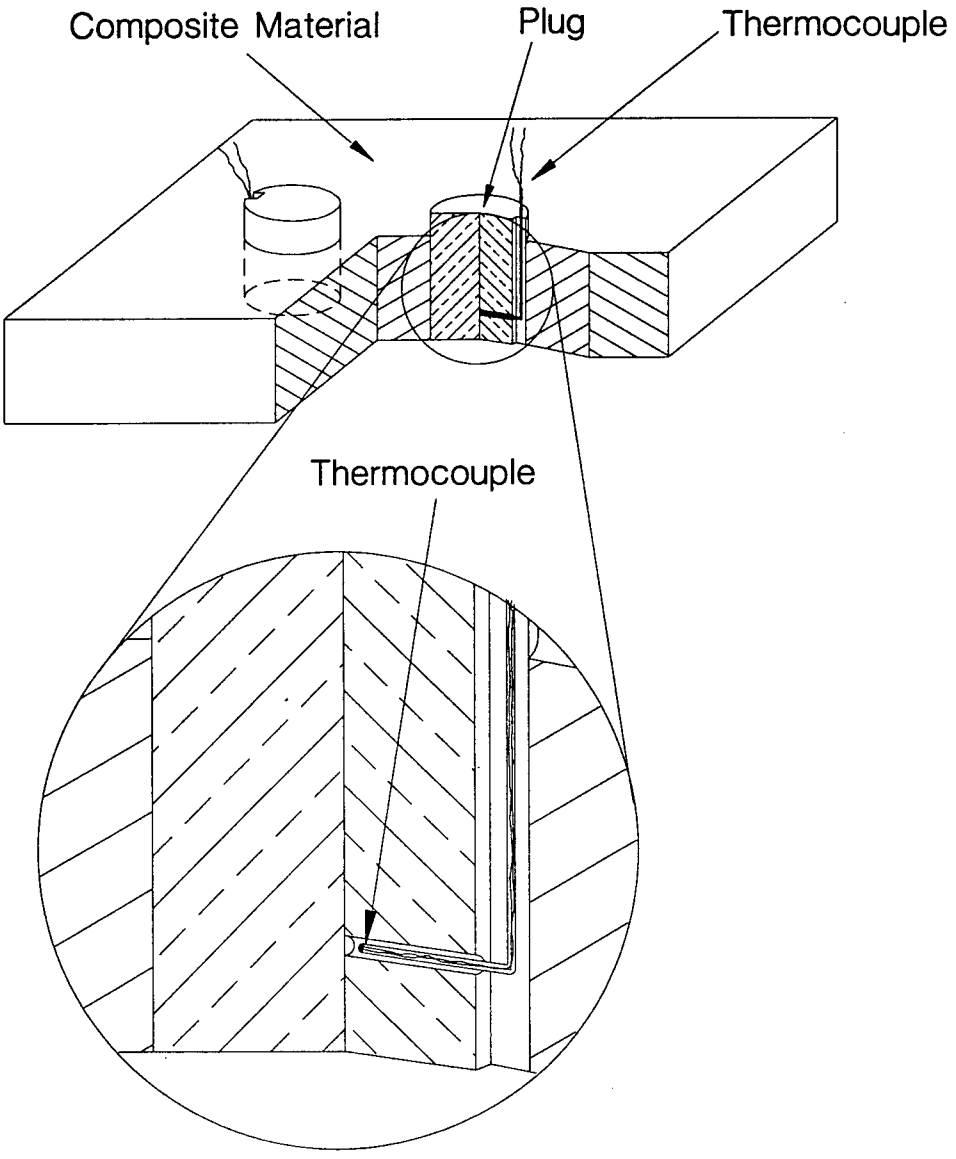

Figure 7.1 Illustration of Plug Installation of a Sheathed Thermocouple in a Composite Block

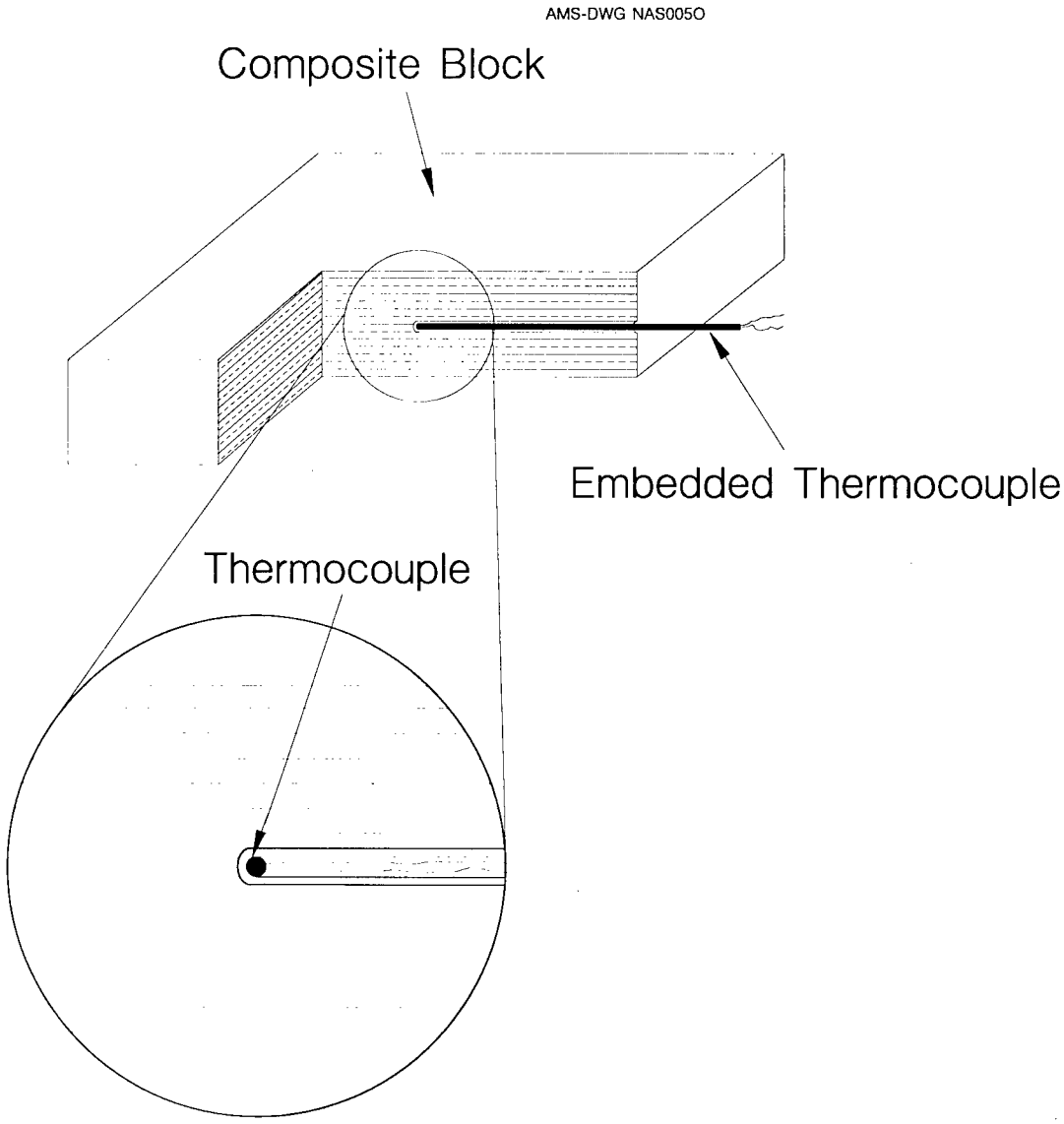

Figure 7.2 Illustration of "Cured In Place" or CIP Installation of a Thermocouple in Composite Material

Figure 7.3 shows LCSR test transients for six thermocouples in one of the Thiokol blocks. The schematic of a typical block is provided in Figure 7.4 showing the three thermocouples that were installed in plugs and the three that were cured into the block. The numbers shown in front of each thermocouple correspond to the distance of thermocouples from the bottom of the block which was fired at SRI.

It is apparent from the LCSR transients in Figure 7.3 that plug installation provides better dynamic response than CIP installation. Intuitively, however, one would think that curing the thermocouple should result in a better contact between the thermocouple and the material than the plug installation. This would have probably been the case if a thermal compound was not used in installing the thermocouples in the plug.

Figure 7.5 shows histograms of LCSR test results for thermocouples that were LCSR tested in the 42 blocks of the SPIP 94 Analog Test Matrix. The details and the individual results are given in Appendix D. The histograms in Figure 7.5 show that the CIP method results in more consistent response times than the plug installation method. More specifically, there is less scatter in the LCSR results for the CIP method than the plug method. Most of the CIP results are in the 0.75 to 1.05 second range which encompasses the mean value of the response time results and constitutes almost a "Normal or Gaussian" distribution. In contrast, the plug installation method has much variation in response time results although it yields faster response times.

Following the laboratory tests at AMS, the Thiokol blocks were sent to SRI where analog temperature data were collected during test firings. Figure 7.6 shows analog test results for six thermocouples in one of the Thiokol blocks (block # SRI-1-21). In all cases, the CIP lags behind

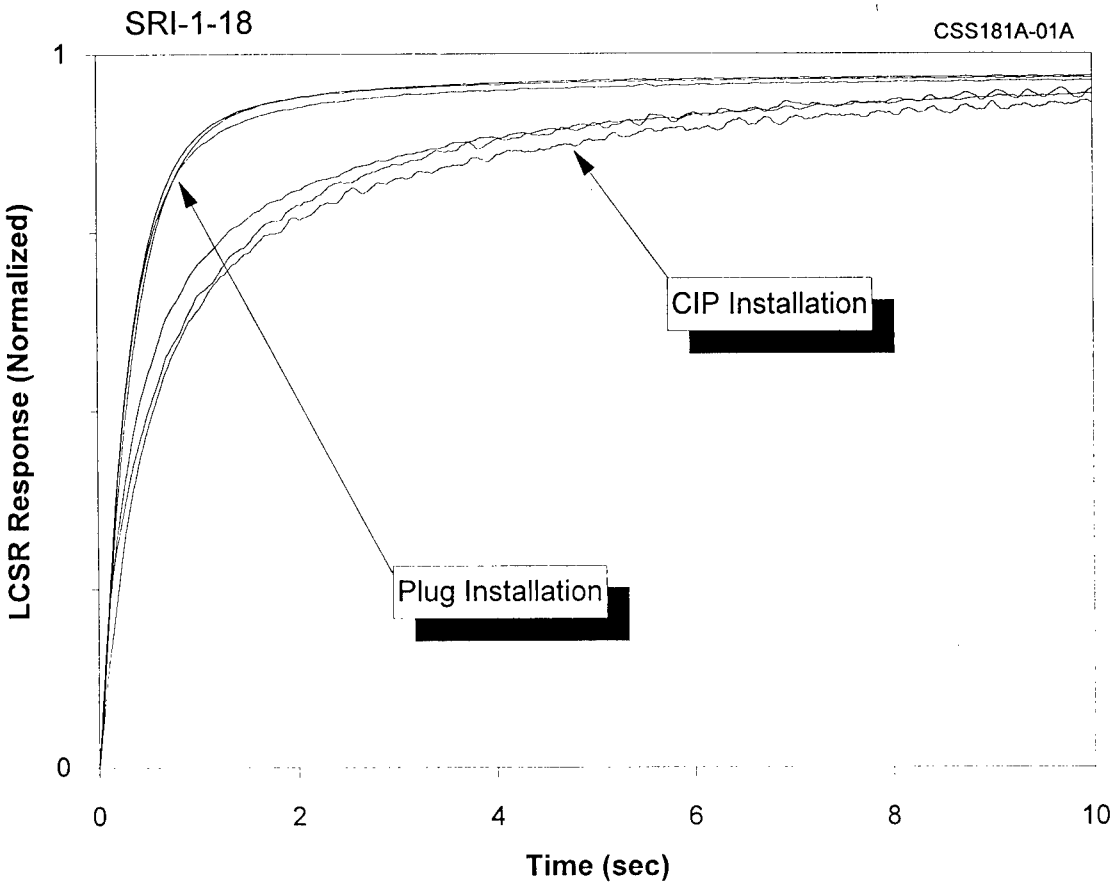

Figure 7.3 LCSR Test Transients for Six Thermocouples Installed in One of Thiokol Test Blocks at AMS at Room Temperature

AMS-DWG NAS020C

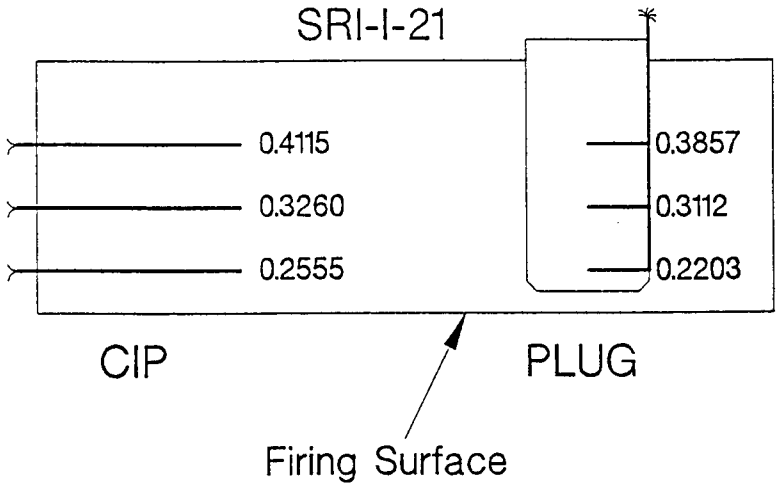

•Note: All dimensions are inches from flame surface.

Figure 7.4 Schematic of a Thiokol Block with Three Thermocouples Installed in a Plug and Three Thermocouples Cured-in-Place. The Numbers Shown are Distances from the Bottom of the Block in Inches

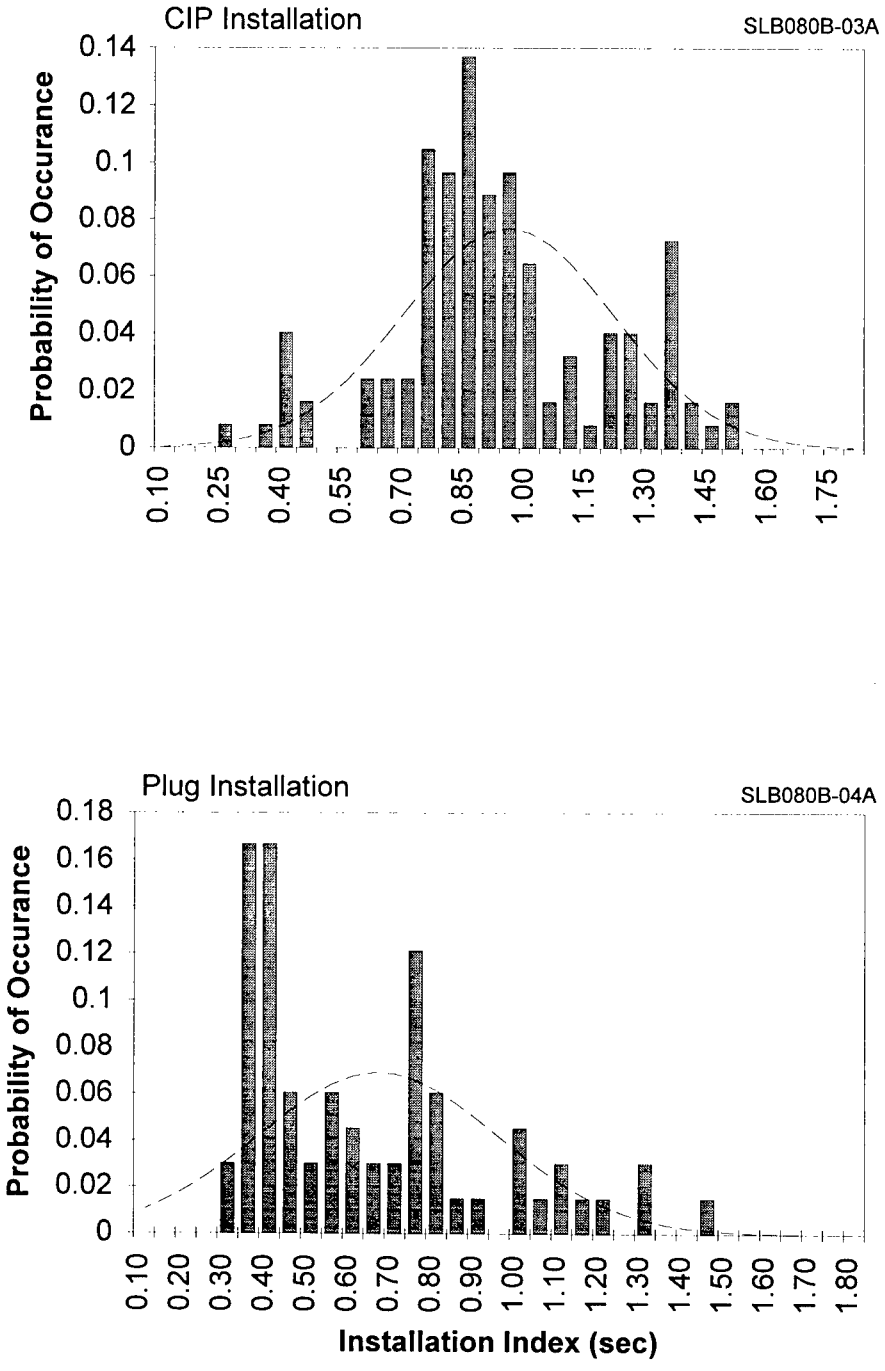

Figure 7.5 Distribution of LCSR Results for CIP and Plug Installation of All Thermocouples in All 42 Blocks of the SPIP 94 Analog Test Matrix

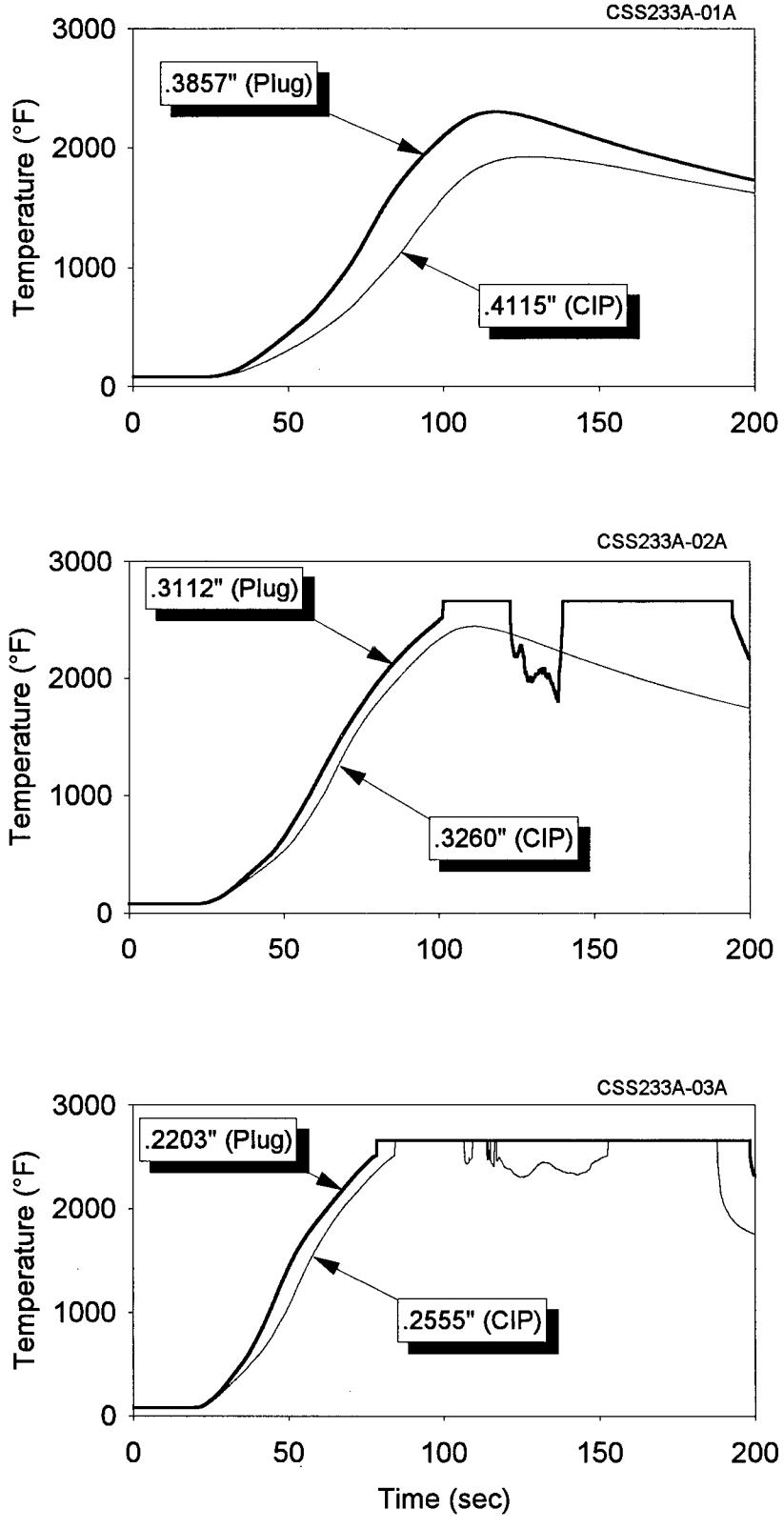

Figure 7.6 Analog Test Results for Six Thermocouples in One of Thiokol Blocks Fired at SRI

the plug. The discontinuities in the LCSR transients in Figure 7.6 are points at which the thermocouples failed due to high temperature.

The analog test at SRI identified fourteen inconsistent thermocouples, twelve of which were identified by LCSR tests at AMS prior to the firing at SRI.

8. TESTING OF BLAST TUBE LINER MATERIAL

The SRM blast tubes are lined with a material to protect the booster against the high temperatures that are involved when the booster is fired. As in the case of composite materials for SRM nozzles, NASA and the aerospace community have been interested in the thermal behavior of the blast tube liner material. As such, thermocouples have been installed in the liner material of test blast tubes (scaled models) to determine the thermal behavior of the material. An array of thermocouples assembled into a unit called an "Erosion Monitoring Thermocouple Array" gage or EMTA gage has been designed to make the temperature measurements in blast tube materials. Figure 8.1 shows the schematic of an EMTA gage.

Thiokol provided AMS with a number of small diameter (0.005"), Type K thermocouples of the types used for temperature measurements in testing blast tube liner material. The bare (not installed in a solid material) thermocouples were LCSR tested in air at the ambient temperature. The purpose of these tests was to show that the LCSR test can be performed on thermocouples successfully, identify optimum LCSR test currents and heating times, and to ensure that the LCSR test cannot harm the thermocouples. Representative results of these tests are shown in Figure 8.2.

Additional testing was then performed on EMTA gage thermocouples while the gage was embedded in a sample of blast tube liner material (Figure 8.3). Figure 8.4 shows how the gage is installed in the material and Figure 8.5 shows LCSR transients for the six thermocouples in the EMTA gage of Figure 8.3.

In addition to the EMTA, a gage manufactured by Medtherm Corporation was sent to AMS for laboratory testing. This gage was of the type that was scheduled to be installed in an scaled

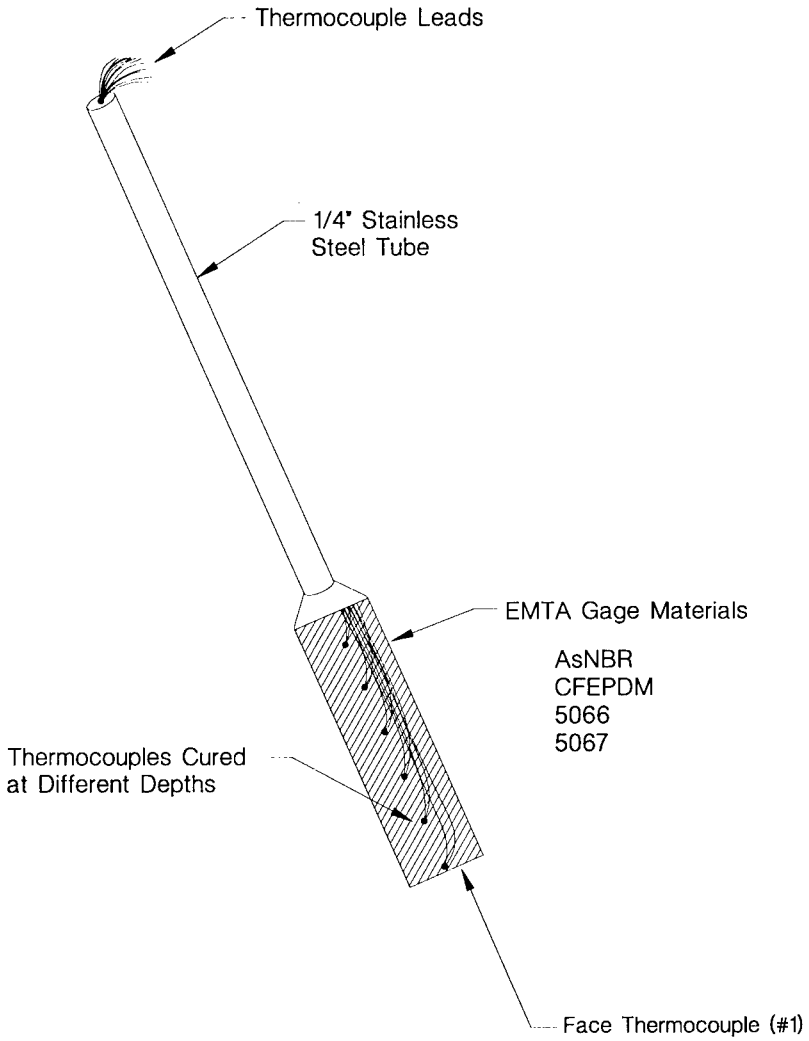

Figure 8.1 Schematic of An Erosion Monitoring Thermocouple Array Gage

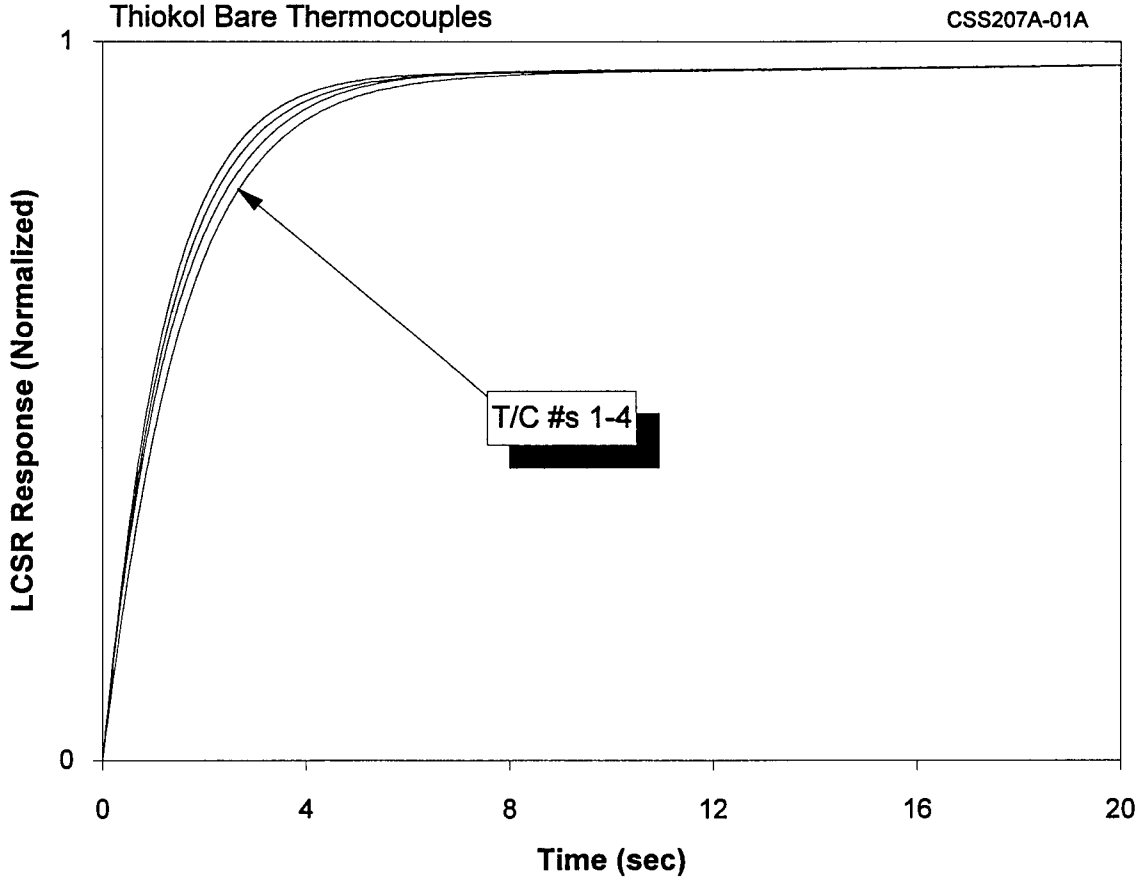

Figure 8.2 LCSR Test Transient for Blast Tube Thermocouples Tested Bare in the Laboratory at Ambient Air

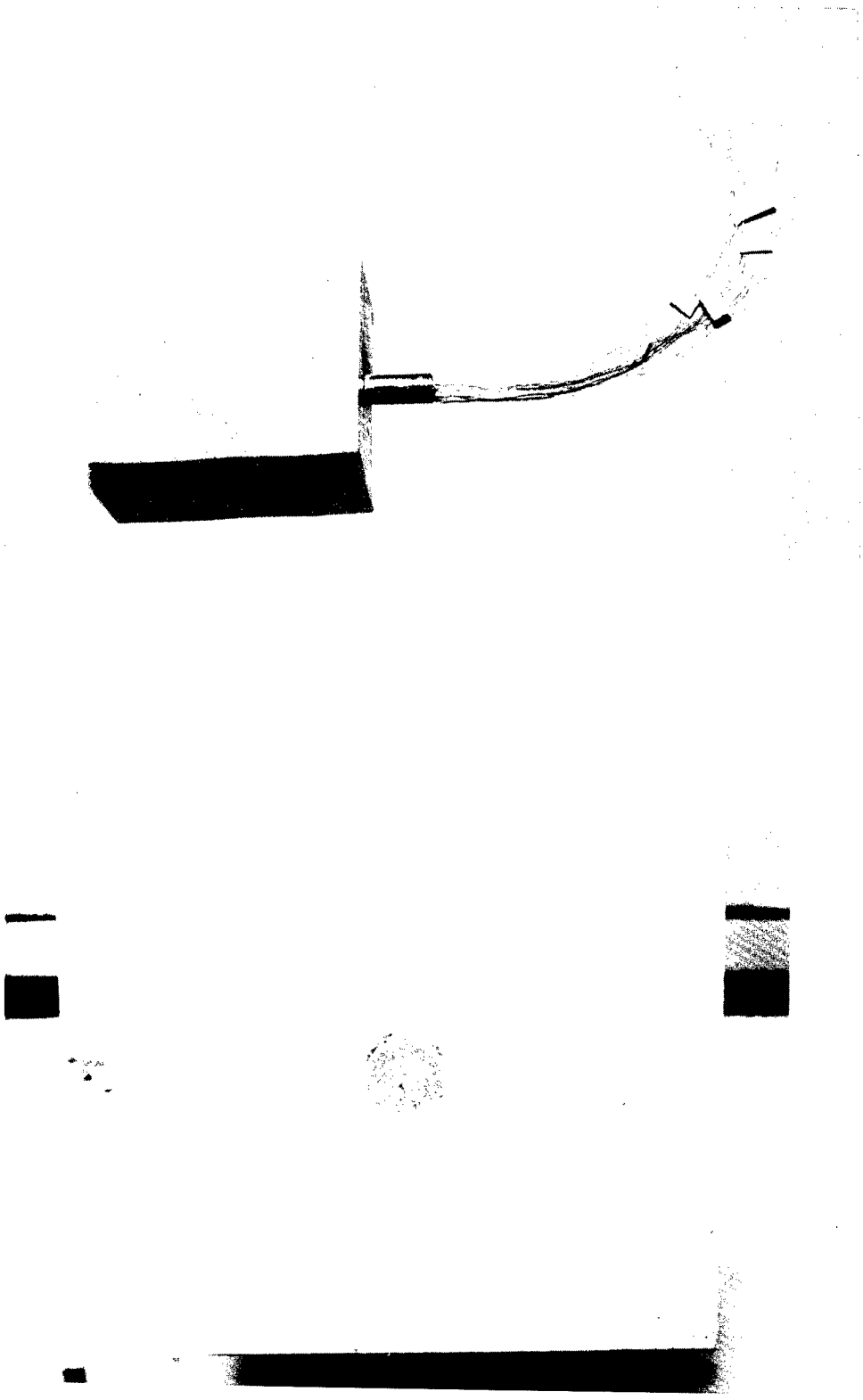

Figure 8.3 Photographs of EMTA Gage as Embedded in a Sample of Blast Tube Liner Material

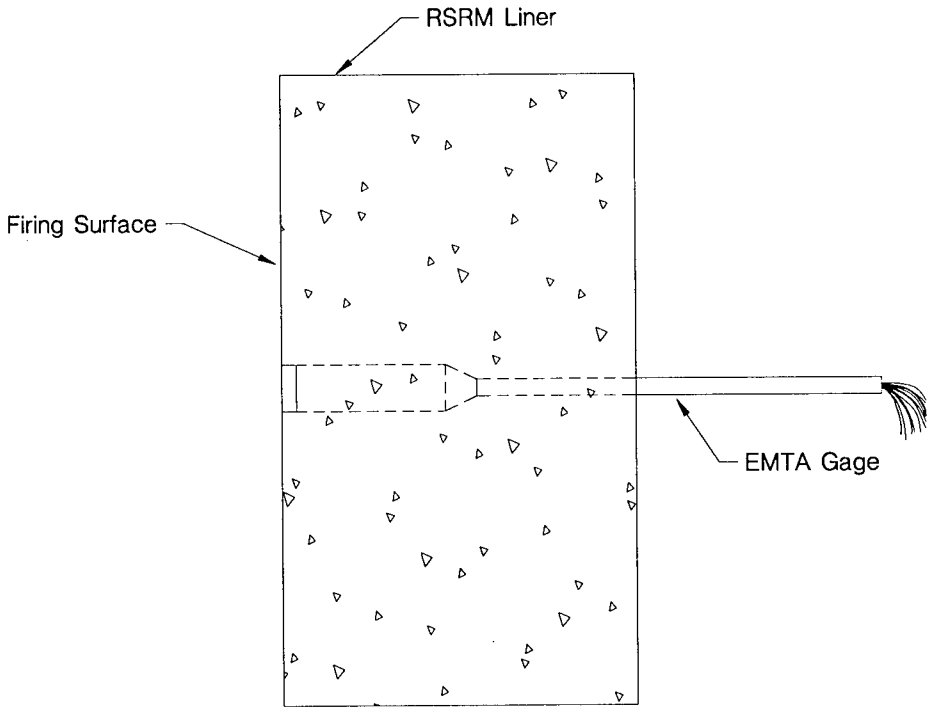

Figure 8.4 EMTA Gage Installed in a Blast Tube Liner Material

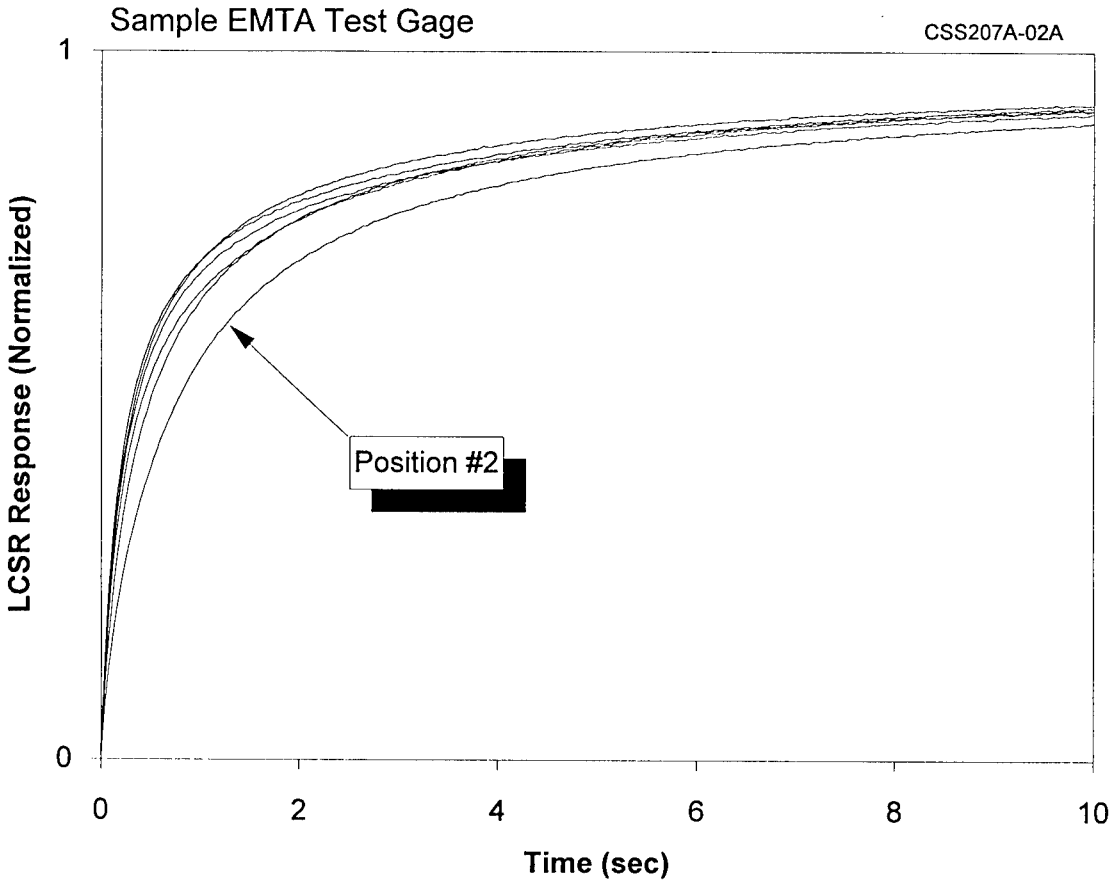

Figure 8.5 LCSR Transients for Thermocouples in EMTA Gage While the Gage was Embedded in a Sample of Liner Material

Redesigned Solid Rocket Motor (RSRM) along with EMTA gages to compare the two gages and determine which type of installation is preferable. Figure 8.6 shows two photographs of a Medtherm gage which consists of six Type K thermocouples installed on a rigid frame which provides support and uniform thermocouple spacing. The Medtherm gages were LCSR tested in stagnant air at AMS. The results are shown in Figure 8.7.

Following the laboratory tests described above, AMS performed field testing on the EMTA and Medtherm gages as installed in RSRMs at MSFC. Both pre-curing and post-curing tests were performed to determine if any changes in thermocouple installation occurred during the curing of the gages within the liner material. The EMTA gages were cured in several different materials; 5055 (carbon-phenolic), 5067 (carbon-phenolic), AsNBR (asbestos filled rubber), and CFEPDM (carbon filler rubber) with each gage containing six 0.005" diameter Type K thermocouples. The pre-curing tests were performed on eleven EMTA gages using the LCSR method. The following observations were made during the pre-curing tests (see Appendix E for identification of gages and a more detailed description of this work).

- Thermocouple #2 in gage #28 and thermocouple #4 in gage #40 had low insulation resistances.
- Thermocouple #1 in seven of the eleven EMTA gages had a slower dynamic response than the other five thermocouples (Figure 8.8).

As a result of AMS tests, EMTA gages #28 and #40 were not cured into the RSRM liner.

After the EMTA gages were cured into the RSRM liner material, a set of post-curing tests were performed. The post-curing tests involved fourteen EMTA gages. Following are the results (see Appendix E for details):

- The following thermocouples were found to be open (not functional):

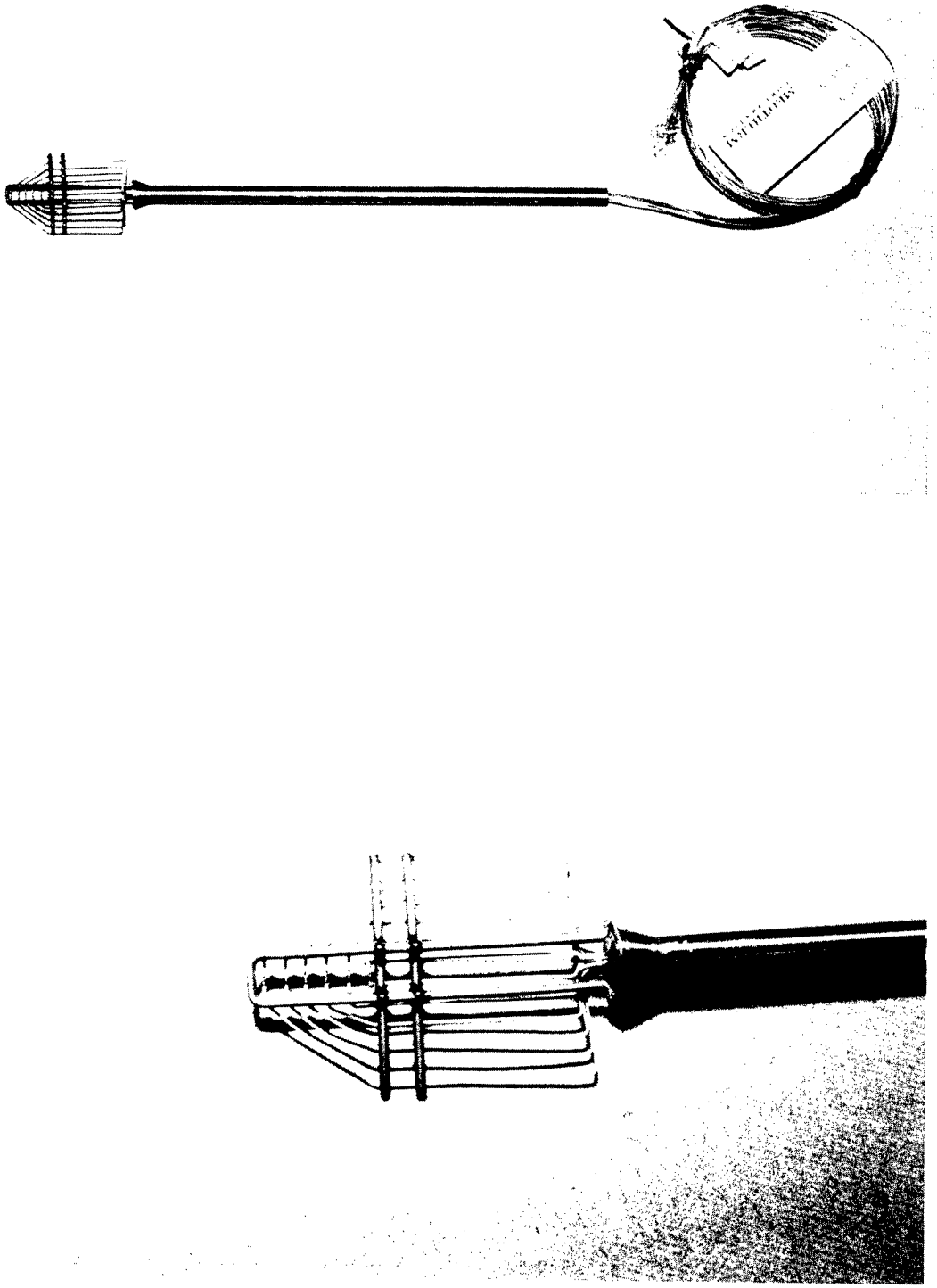

Figure 8.6 Photographs of Medtherm Thermocouples

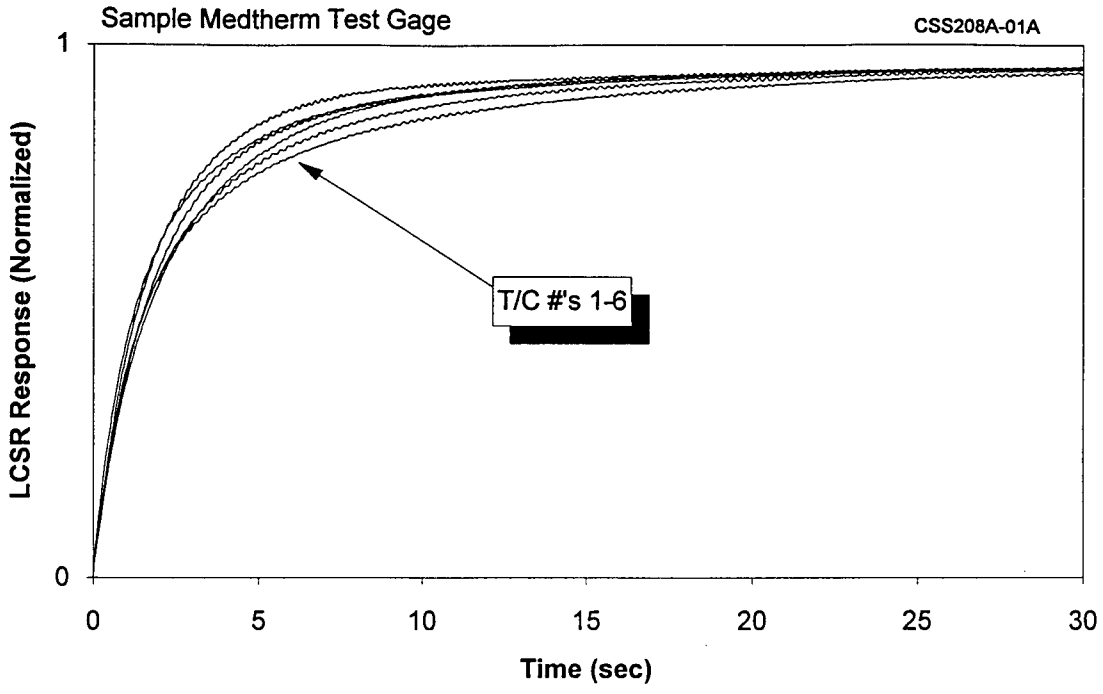

Figure 8.7 LCSR Transients for Medtherm Thermocouples

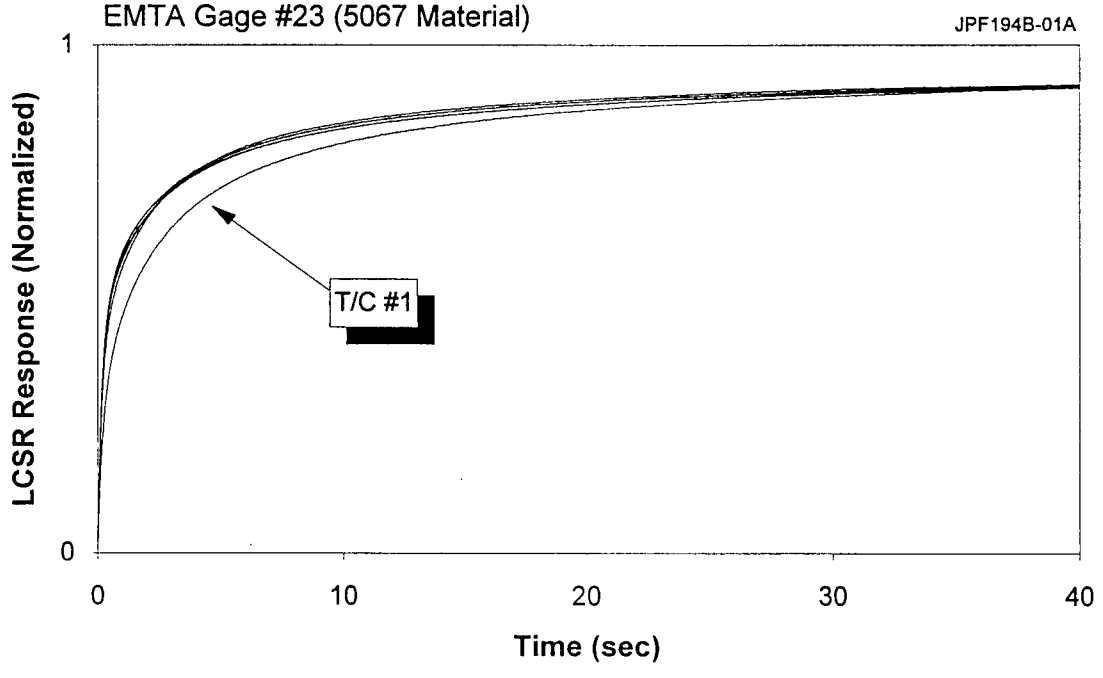

Figure 8.8 LCSR Transients for Thermocouples in an EMTA Gage that was Tested as Installed in RSRM at MSFC

Thermocouple #1 in gage #32
Thermocouple #51 in gage #30
Thermocouple #54 in gage #30

- Thermocouple #4 in gage #34 had a low insulation resistance.
- Thermocouple #1 in gage #'s 20, 25, 29, 30, 31, and 37 had dynamic responses that were different from the other five thermocouples in the corresponding gages.
- The response time of thermocouple #5 in gage #27 was different than the other five thermocouples in the same gage.
- Thermocouple #2 in gage #24 was different in dynamic response than the other five thermocouples in the same gage.

When a comparison was made between the pre-curing and post-curing LCSR transients, it was determined that most of the sensors had a slightly slower response after curing. Figure 8.9 shows a pre-curing and post-curing comparison for one of the gages in the RSRM liner.

Only two Medtherm gages were available for the field tests. All six thermocouples in the Medtherm assembly at the AFT Center 45 degree location were LCSR tested. The results are shown in Figure 8.10. The second Medtherm gage located at the AFT Center 315 degree had only one thermocouple that was tested due to time and schedule constraints. The LCSR transient for this one thermocouple was comparable to that of the corresponding thermocouple in the first Medtherm gage.

Figure 8.11 compares typical LCSR transients for the Medtherm and EMTA gages as installed in the 5066 material. In this graph, the Medtherm transient is faster than the EMTA transient. This type of difference was also noted in the AsNBR material as shown in Figure 8.12.

The overall conclusion of the field tests was that there were no significant changes in the installation integrity of either the EMTA or Medtherm gages that could be attributed to the curing process.

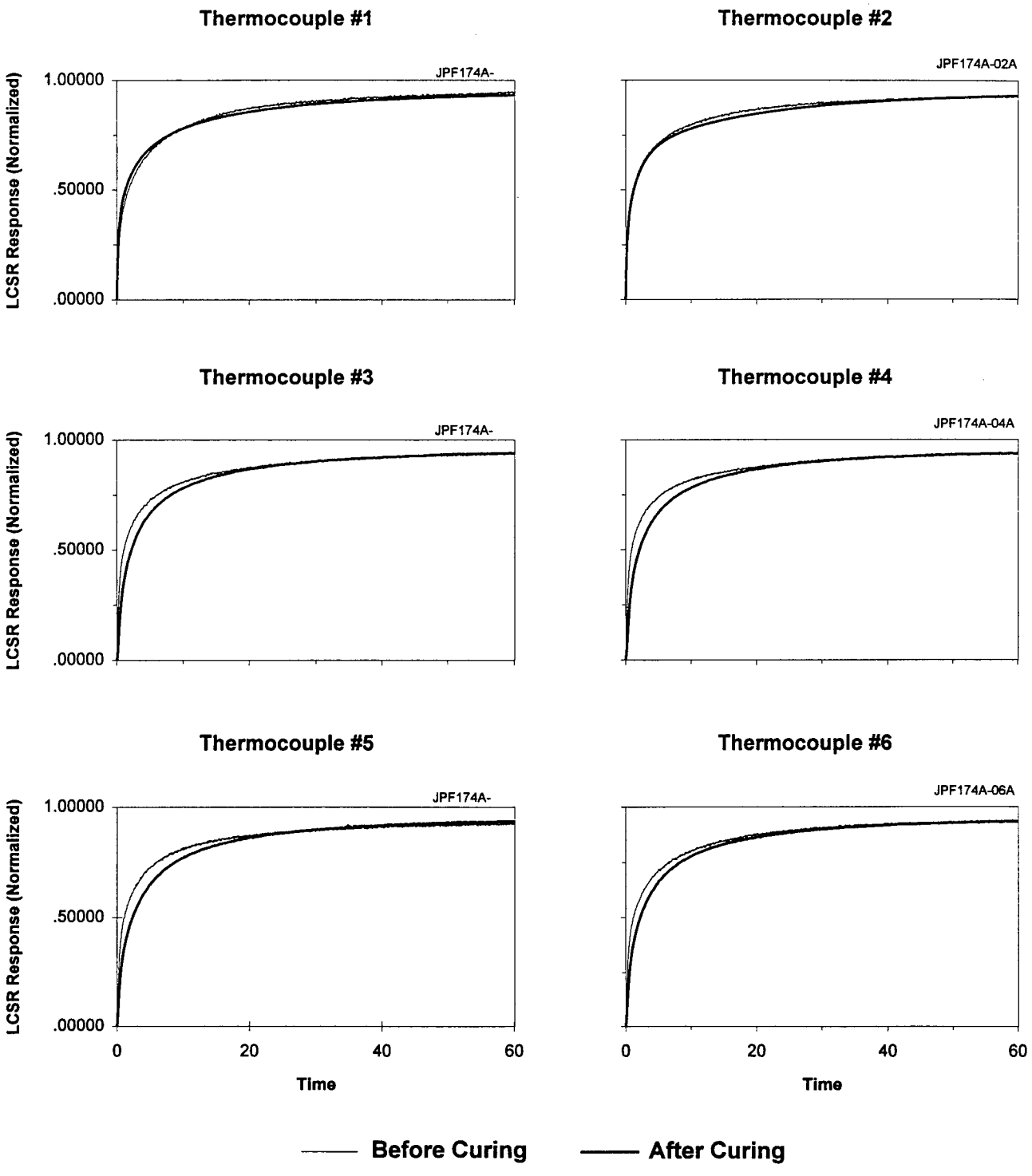

Figure 8.9 Pre and Post Curing LCSR Transients for Six Thermocouples in one of the EMTA Gages

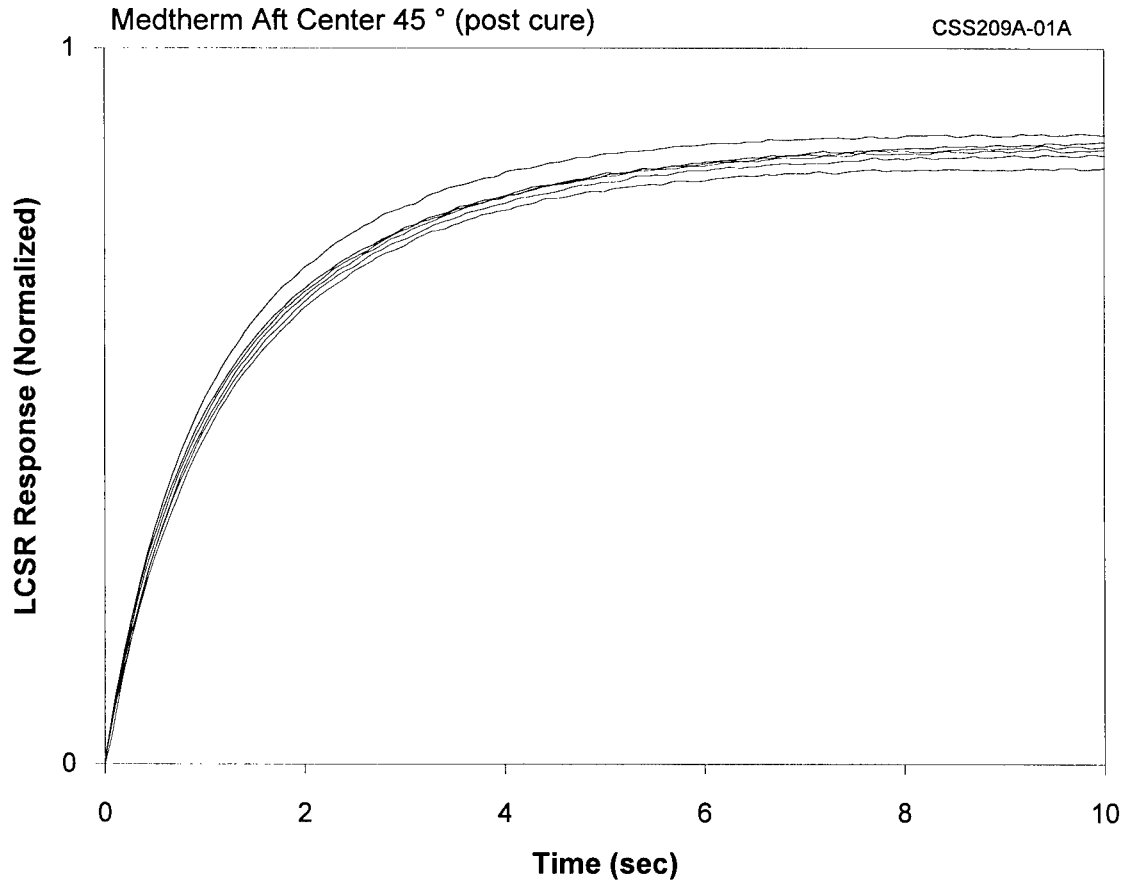

Figure 8.10 LCSR Transients for Six Thermocouples in a Medtherm Gage as Installed in the RSRM Liner

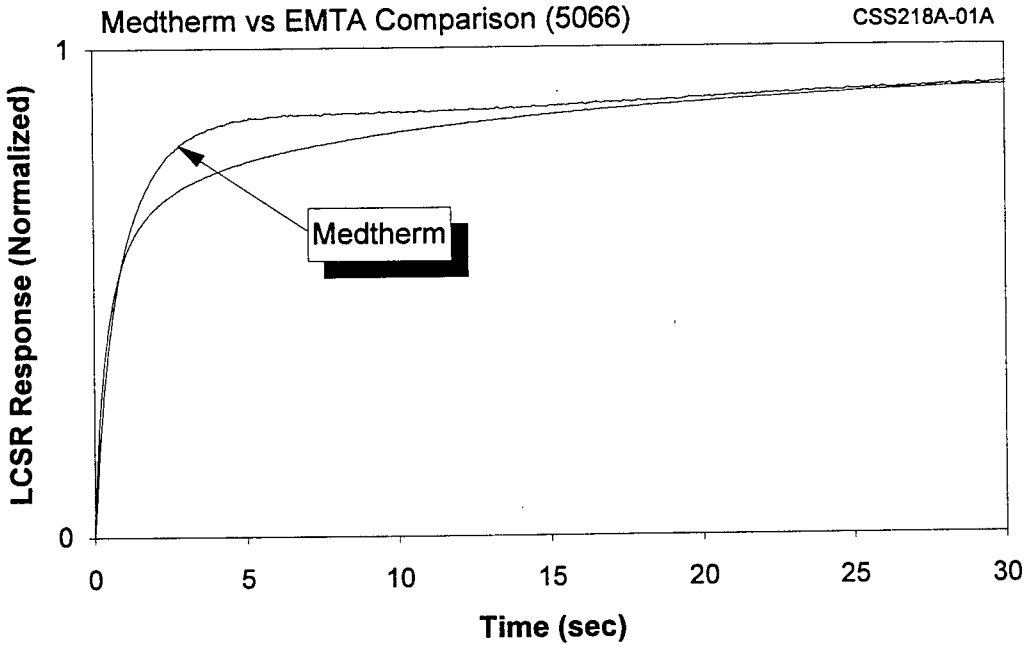

Figure 8.11 Typical LCSR Transients for a Representative Thermocouple in an EMTA Gage and a Medtherm Gage Installed in a 5066 Material

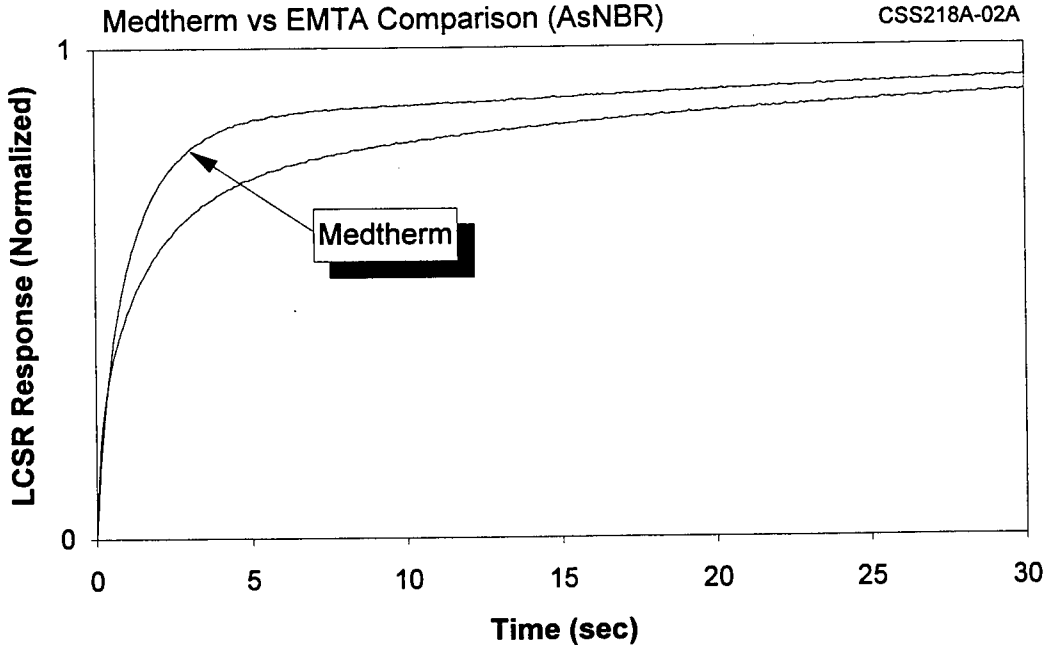

Figure 8.12 Typical LCSR Transients for a Representative Thermocouple in an EMTA Gage and a Medtherm Gage Installed in a AsNBR Material

9. FIELD TESTING OF THERMOCOUPLES AT SRI

9.1 Description of SRI Facilities

On a number of occasions during the Phase I and Phase II projects, AMS provided test equipment, procedures, and personnel on-site at SRI to perform field measurements in conjunction with firing tests of composite samples with embedded thermocouples. The thermocouple tests at SRI were all performed in the Nozzle Ablative Simulation (NAS) apparatus (Figure 9.1). This apparatus contains an electrically heated test-plate for exposing composite specimens to temperatures of up to several thousand degrees.

A schematic diagram of NAS is shown in Figure 9.2. Specimens of composite material are installed in the apparatus between a resistively heated POCO/ATJ graphite element and a load frame. Teflon tape is placed on the bottom of the specimen to decrease the friction between the specimen and plates opposite the specimen. The upper portion of the load assembly is electrically insulated by placing a block of Boron Nitride and pyrolitic graphite against the heater element opposite the specimen. A graphite block is placed above the pyrolitic graphite and a load is then applied to each specimen to restrain the specimen during firing conditions. A photograph of a specimen installed inside the NAS apparatus is shown in Figure 9.3.

Firing of specimens at SRI is performed by applying an electrical current to a graphite heater element in the NAS apparatus via a 44 KVA variable transformer. A line voltage of 240 V is adjusted as necessary using a powerstat. The heater element is connected in series with a transformer and heat fluxes in excess of 800 kW/m^2 can be applied to the specimens. The

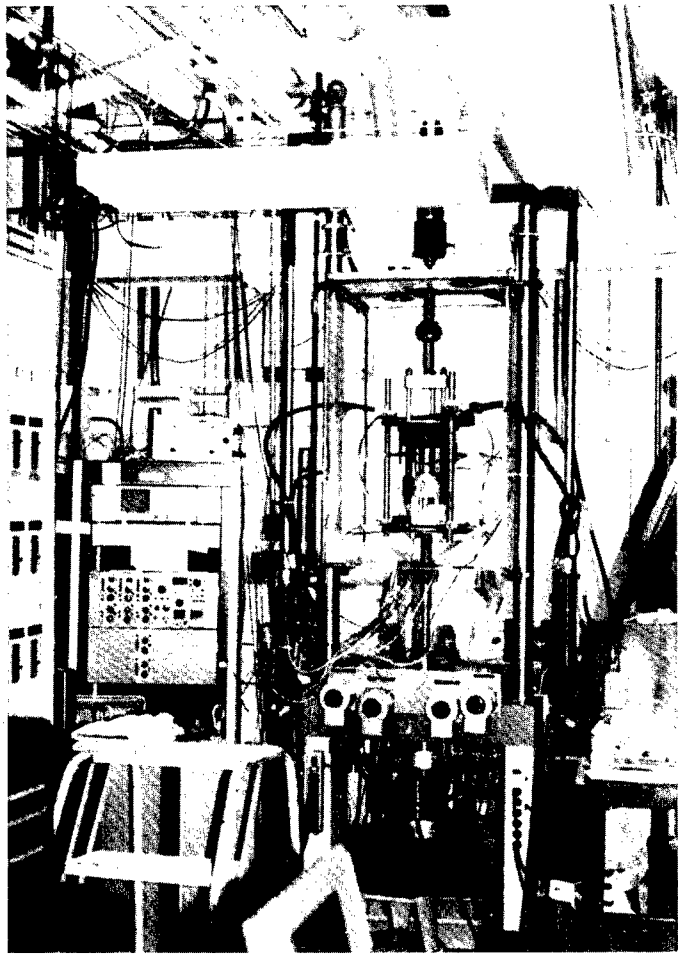

Figure 9.1 Photograph of SRI Nozzle Ablative Simulation Apparatus and Loading Fixture

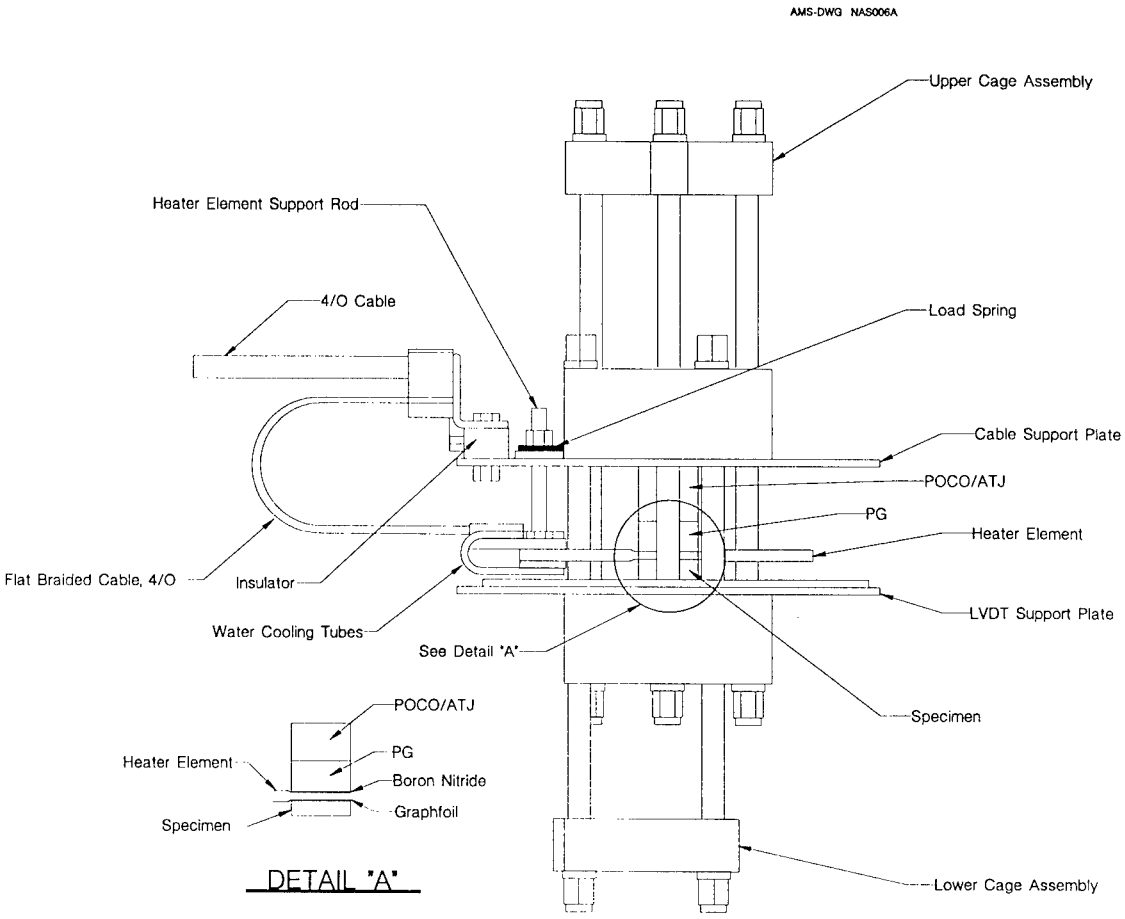

Figure 9.2 Schematic Diagram of NAS Apparatus (Courtesy of SRI)

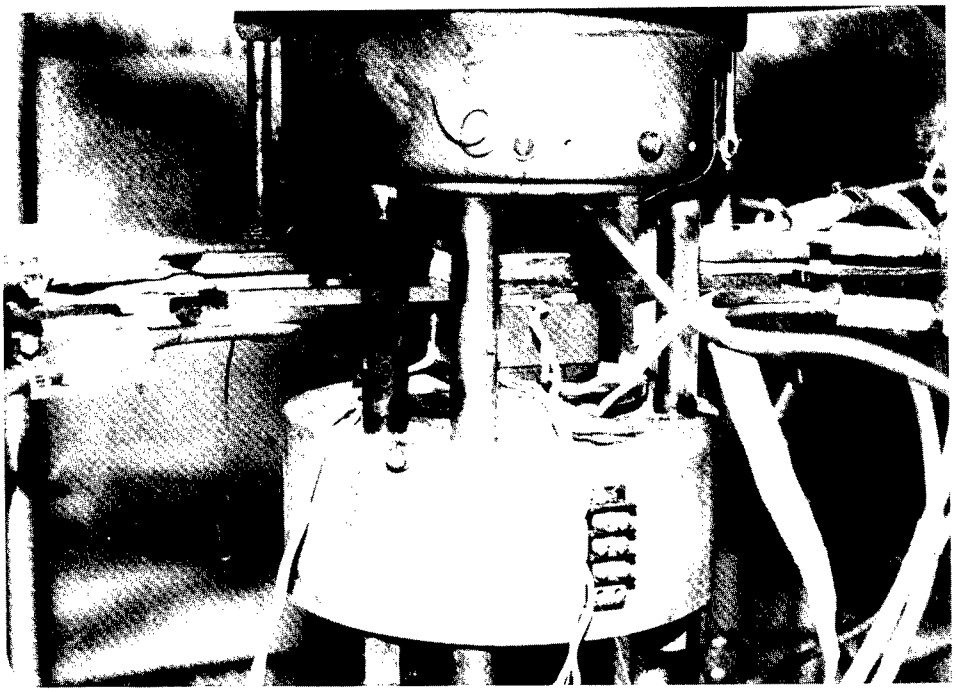

Figure 9.3 Closeup of NAS Apparatus with Specimen Installed in Fixture

specimen's temperatures during the tests are measured using Type K and Type S thermocouples. An optical pyrometer is also used to verify the surface temperature of the composite specimen during the test. The amount of oxidation which occurs during the firing is reduced by injecting a steady flow of nitrogen (moderator) into the test area. In addition, insulation material is placed around the specimen to reduce charring of the specimen and test apparatus.

Figure 9.4 shows temperature data from a NAS firing test at SRI. This type of transient is referred to as analog temperature data. Due to high temperatures involved, some thermocouples, especially those used to record temperatures of the fired surface of specimens, sometimes fail during the tests. Figure 9.5 shows analog temperature data for a case in which the surface thermocouple fails 35 seconds after firing. Figure 9.5 also shows that three of the four embedded thermocouples exhibit erratic behavior as they reach high temperatures within the specimen.

9.2 First Series of AMS Tests at SRI

The first series of tests which AMS performed at SRI involved thirty-nine thermocouples which were used in the "SPIP 48-3 Analog Instrumentation Tests." A listing of these thermocouples is given in Table 9.1. The thermocouples were installed in seven different carbon-phenolic (FM5055) blocks. Each block (or specimen) is identified with an SRI number and a thermocouple number as shown in Table 9.1.

Figure 9.6 shows a photograph of one of the blocks (#28). Both Type K and Type S thermocouples were used in the blocks. Type K thermocouples were first inserted in cylindrical

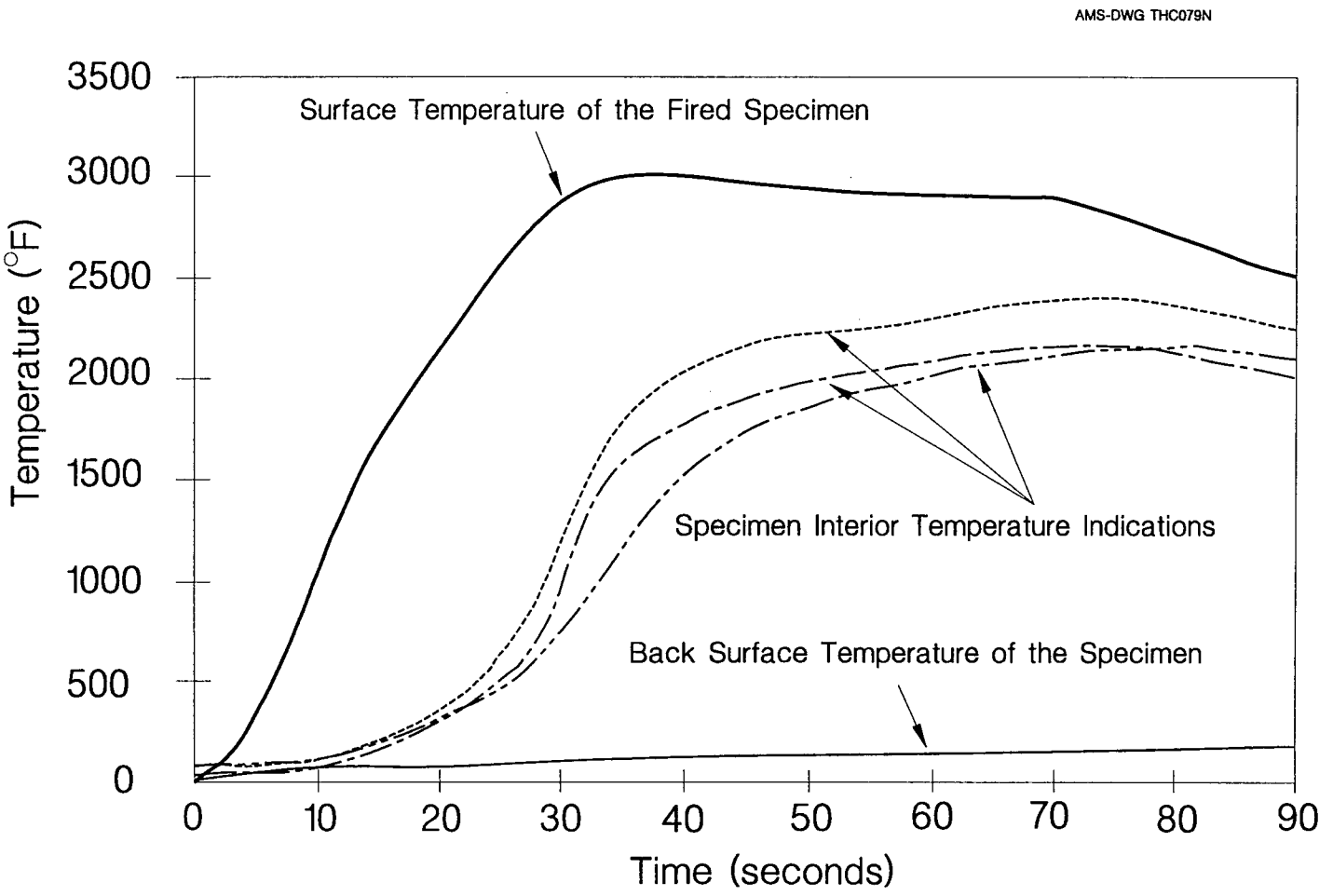

Figure 9.4 Analog Temperature Data Collected at SRI During a Firing Test of a Composite Specimen

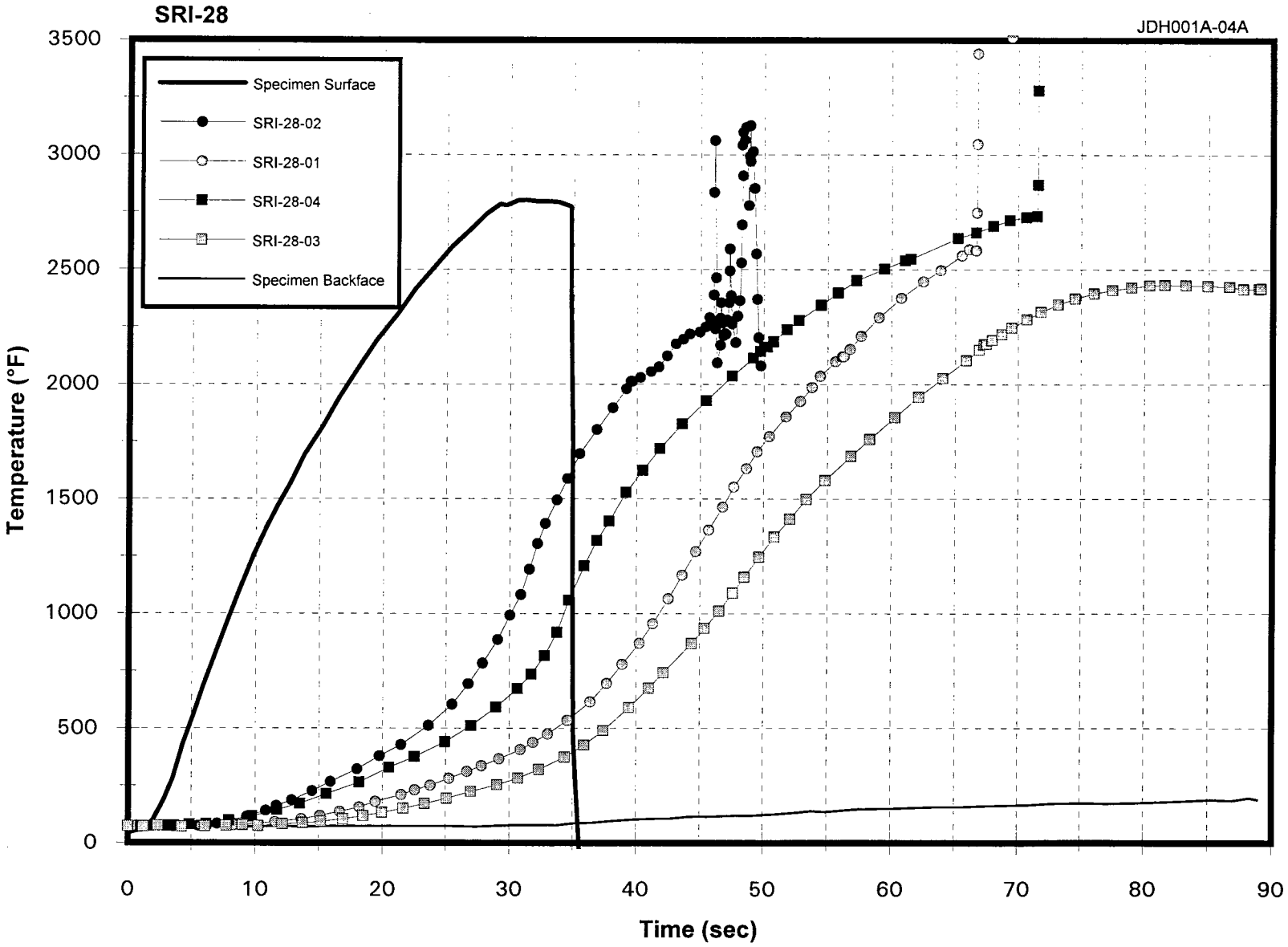

Figure 9.5 Analog Temperature Data Showing a Surface Thermocouple Which Failed and Embedded Thermocouples Which Behaved Erratically During a Firing Test of a Composite Block at SRI

TABLE 9.1

Listing of Thermocouples Involved in the SPIP-48-3 Analog Instrumentation Tests

Item	Thermocouple Tag Number	Thermocouple Type	O.D. (Inches)	Loop Resistance (Ω)	Installation Index Obtained from Pre-Firing LCSR Tests (sec)
1	SRI-29-01	K	0.01	159.68	1.7
2	SRI-29-02	K	0.01	160.03	1.6
3	SRI-29-03	K	0.01	159.85	3.0
4	SRI-29-04	K	0.01	160.42	2.0
5	SRI-29-05	S	0.005	10.7	4.3
6	SRI-30-01	K	0.01	159.75	0.8
7	SRI-30-02	K	0.01	165.02	1.0
8	SRI-30-03	K	0.01	160.26	1.0
9	SRI-30-04	K	0.01	159.58	1.5
10	SRI-30-05	K	0.01	151.17	0.9
11	SRI-30-06	K	0.01	160.31	1.3
12	SRI-30-07	K	0.01	159.23	0.4
13	SRI-30-08	K	0.01	151.88	1.9
14	SRI-30-09	K	0.01	155.98	1.2
15	SRI-20-01	K	0.01	159.36	2.0
16	SRI-20-02	K	0.01	159.08	1.5
17	SRI-20-03	K	0.01	157.64	0.8
18	SRI-20-04	K	0.01	158.3	1.4
19	SRI-20-05	K	0.01	155.86	1.5
20	SRI-20-06	K	0.01	158.86	1.1
21	SRI-20-07	K	0.01	158.1	1.1
22	SRI-20-08	K	0.01	160.41	0.9
23	SRI-20-09	K	0.01	160.33	1.2

TABLE 9.1
(Continued)

Listing of Thermocouples Involved in the SPIP-48-3 Analog Instrumentation Tests

Item	Thermocouple Tag Number	Thermocouple Type	O.D. (Inches)	Loop Resistance (Ω)	Installation Index Obtained from Pre-Firing LCSR Tests (sec)
25	SRI-24-01	K	0.01	158.22	1.0
26	SRI-24-02	K	0.01	152.24	1.5
27	SRI-24-03	S	0.005	10.07	2.5
28	SRI-25-01	K	0.01	164.66	1.6
29	SRI-25-02	K	0.01	160.11	0.7
30	SRI-25-03	K	0.01	153.87	2.5
31	SRI-25-04	K	0.01	159.36	1.7
32	SRI-25-05	S	0.005	10.82	3.3
33	SRI-23-01	K	0.01	154.52	1.7
34	SRI-23-02	K	0.01	142.6	1.7
35	SRI-23-03*	S	0.005	8.33	N/A
36	SRI-28-01	K	0.01	158.43	2.0
37	SRI-28-02	K	0.01	158.67	1.4
38	SRI-28-03	K	0.01	160.1	1.5
39	SRI-28-04	K	0.01	160.77	1.7
40	SRI-28-05	S	0.005	10.88	4.2

* Thermocouple was not testable.

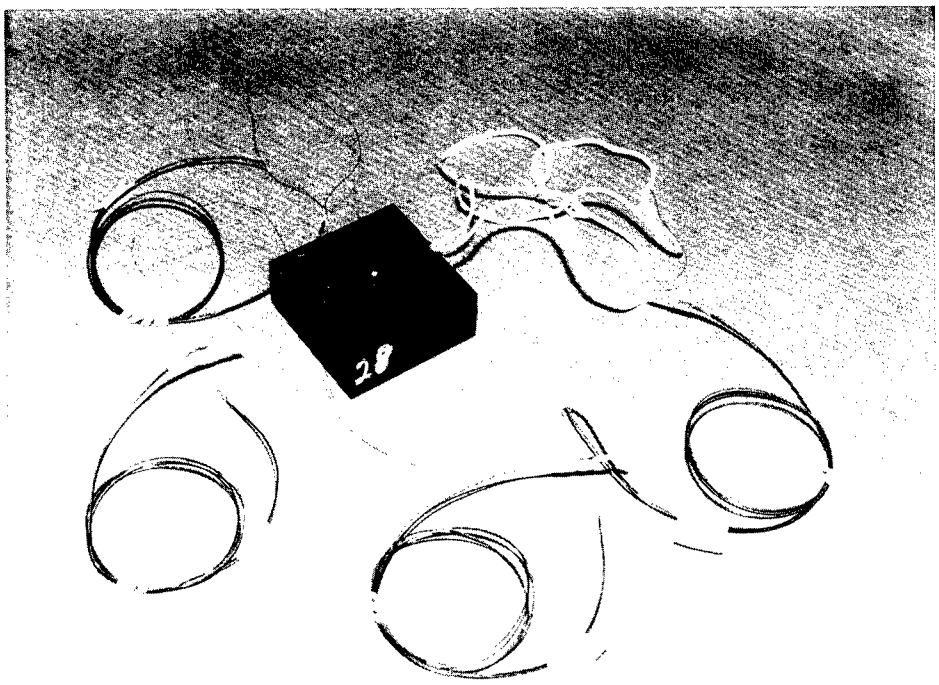

Figure 9.6 Photograph of Specimen #28 Used in the SRI Tests

plugs. Each plug, with up to three embedded thermocouples, was then installed and bonded into a hole machined into the block as shown in Figure 9.7. Each block had up to three plugs.

The thermocouples were embedded in the specimens using different installation techniques. The following is a procedure used by Thiokol for manufacturing of a specimen and the embedding of the thermocouples in the material:

Construction of Plugs

1. Note the ply angle and the orientation for cutting of the plug.
2. Cut the plugs to the appropriate length, be sure to maintain the play angle and the proper orientation.
3. Machine the plugs to 0.375" diameter.
4. Machine a chamfer on the bottom of the plug.
5. Machine a 0.032" slot on the sides and a 0.0064" alignment groove on the top of the plug.
6. Drill 0.020" holes in the plug side for each thermocouple to a depth of 0.25" from the plug O.D.
7. Measure and mark the location of the holes in the sample blocks.

A typical finished plug is shown in Figure 9.8.

Preparation of Specimen Block

8. Using a carbide drill bit, bore a pilot hole to a depth of 0.10" into the specimen block.
9. Using a 3/8" carbide drill bit, bore the hole in the specimen block to a depth of 0.10" short of the final depth.
10. Using a 3/8" carbide end mill, complete the hole depth creating a flat bottom hole.
11. Measure and record the dimensions of the plug and the hole.

AMS-DWG NAS005B

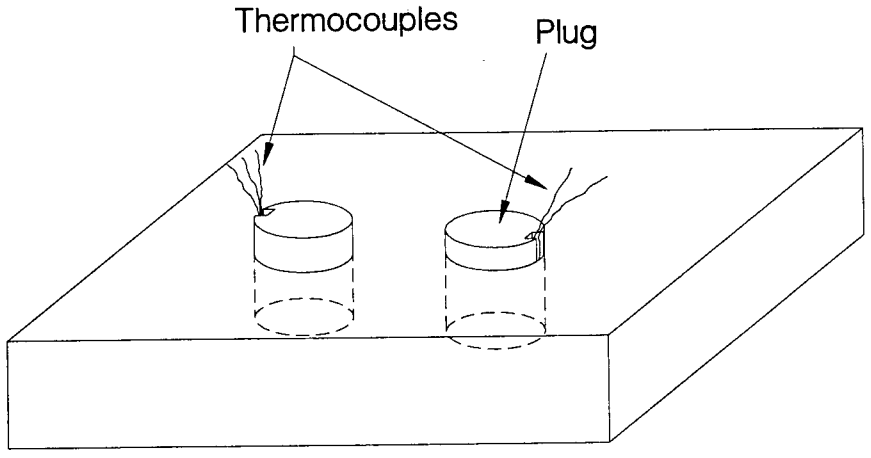

Figure 9.7 Illustration of a Composite Block with Thermocouples Installed in Plugs Embedded in the Block

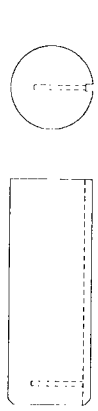

Figure 9.8 Illustration of Finished Plug Used in Carbon-Phenolic Specimens

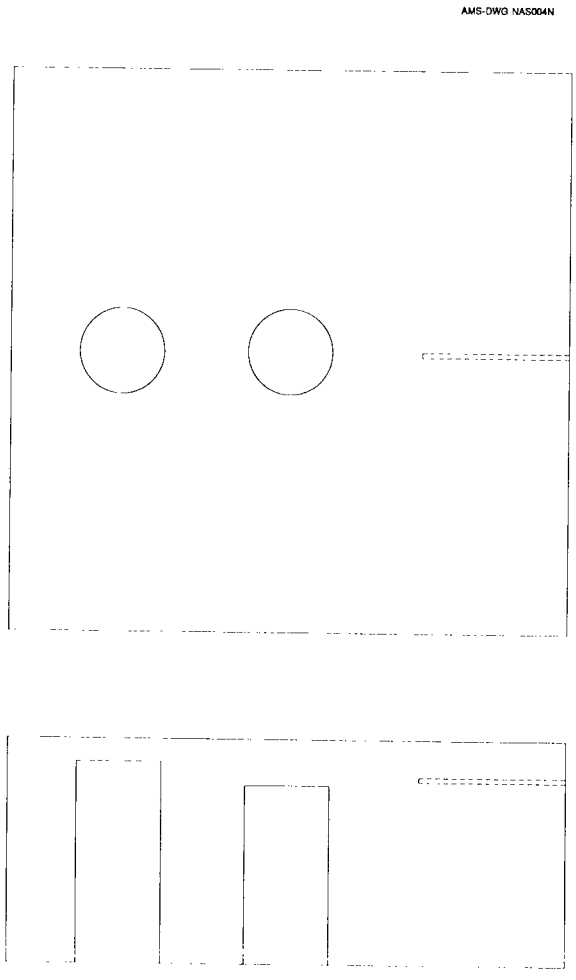

Figure 9.9 Illustration of Finished Specimen Block Used in SRI Tests

12. Measure and record the resistance of each thermocouple.

A typical specimen block is shown in Figure 9.9.

Installation of Plug into Specimen Block

13. Dry fit the plug to the hole in the specimen to assure proper fit.

14. Coat the thermocouples with the proper filler material then bond the thermocouple into the holes in the plug.

15. Clean the instrumented plugs and holes, and allow to air dry.

16. Apply bonding material to the upper two-thirds of each plug.

17. Use a screwdriver in the alignment slot to position plug in the hole in the sample. Tap lightly to ensure seating at the bottom of the hole.

18. Carefully bend the thermocouples over and secure to sample block with tape. Apply a small amount of bonding material over the wire at location of bend.

19. Use tape to apply pressure and maintain proper plug installation until bonding is cured.

20. Bonding should be cured at 70°F or more for 24 hours.

21. After curing, remove restraining devices.

22. Measure and record the resistance of each thermocouple.

Insertion of the SRI Thermocouples

23. Insert the Type S thermoelements through an alumina sleeve and construct the thermocouple.

24. Drill a hole in the specimen block approximately 0.02" diameter along an isotherm.

25. Insert the thermocouple into the dry hole within the block and secure the thermocouple to the outside of the specimen.

Upon completion of the assembly, the specimens are X-rayed to ensure that the thermocouples are accurately installed in the specimen plugs and no inconsistency (such as a

void between the bottom of a plug and the bottom of a specimen hole) is present in any of the specimens.

Figure 9.10 illustrates a composite block and the thermocouples used in the SRI tests. The thermocouples were installed in the specimens in the following five configurations:

1. Sheathed thermocouples installed into a plug with no filler material.
2. Unsheathed thermocouples installed into a plug with no filler material.
3. Sheathed and unsheathed thermocouples installed into a plug with graphite filler material.
4. Sheathed and unsheathed thermocouples installed into a plug with Boron Nitride filler material.
5. Sheathed thermocouples installed on the face of the plug.

9.3 SRI Test Results

Two series of tests were performed at SRI: analog tests conducted by SRI personnel, and LCSR tests performed by AMS.

The analog tests were performed on all thirty-nine thermocouples. The objectives of the analog tests included the following:

- Evaluate the response time of sheathed versus unsheathed thermocouples.
- Verify the manufacturing consistency of plugs installed within the carbon-phenolic specimens.
- Determine/verify the best grounding and shielding configuration for the tests.

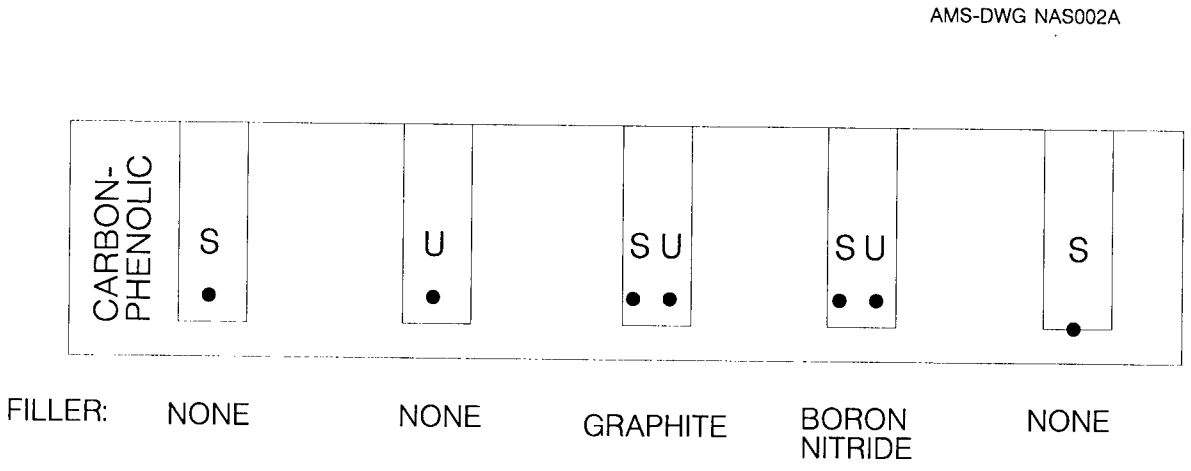

Figure 9.10 Illustration of the Different Specimen/Thermocouple Configurations Used in the SPIP 48-3 Instrumentation Tests

- Evaluate methods of installation and location verification of thermocouples installed within the specimens.
- Evaluate the accuracy and consistency of the plug installation within each specimen.
- Evaluate the response of the thermocouples installed on the face of the plug versus those installed within the plugs.

The overall goal of the analog tests was to determine the best installation configuration and test methods for the thermocouples that were used in a test nozzle which was later fired.

LCSR tests were performed on each thermocouple before and after firing in the NAS apparatus. The purpose of these tests was to provide information about the installation integrity of the thermocouples within the specimens. The post-firing tests were instrumental in determining if any changes in the response characteristics of the thermocouples had occurred during the firing.

The pre-firing LCSR results were given earlier in Table 9.1 and representative analog test data were presented in Figures 9.4 and 9.5. Pre and post-firing results for representative thermocouples tested at SRI are summarized in Figure 9.11 in terms of response times obtained from the analysis of the LCSR data. Of the nine sets of results shown in this figure, three indicate significant increases in response times. Raw LCSR data for two of the nine thermocouples are presented in Figure 9.12. Note in this figure that the post-firing LCSR transient is slower for thermocouple number 24-02 while thermocouple number 24-01 has almost the same post-firing transient as its pre-firing transient. This observation is consistent with the quantitative results presented in Figure 9.11.

Sometimes, the post-firing response times are faster than pre-firing results such as the case presented in Figure 9.13. That is, firing tests can result in any of the following outcomes:

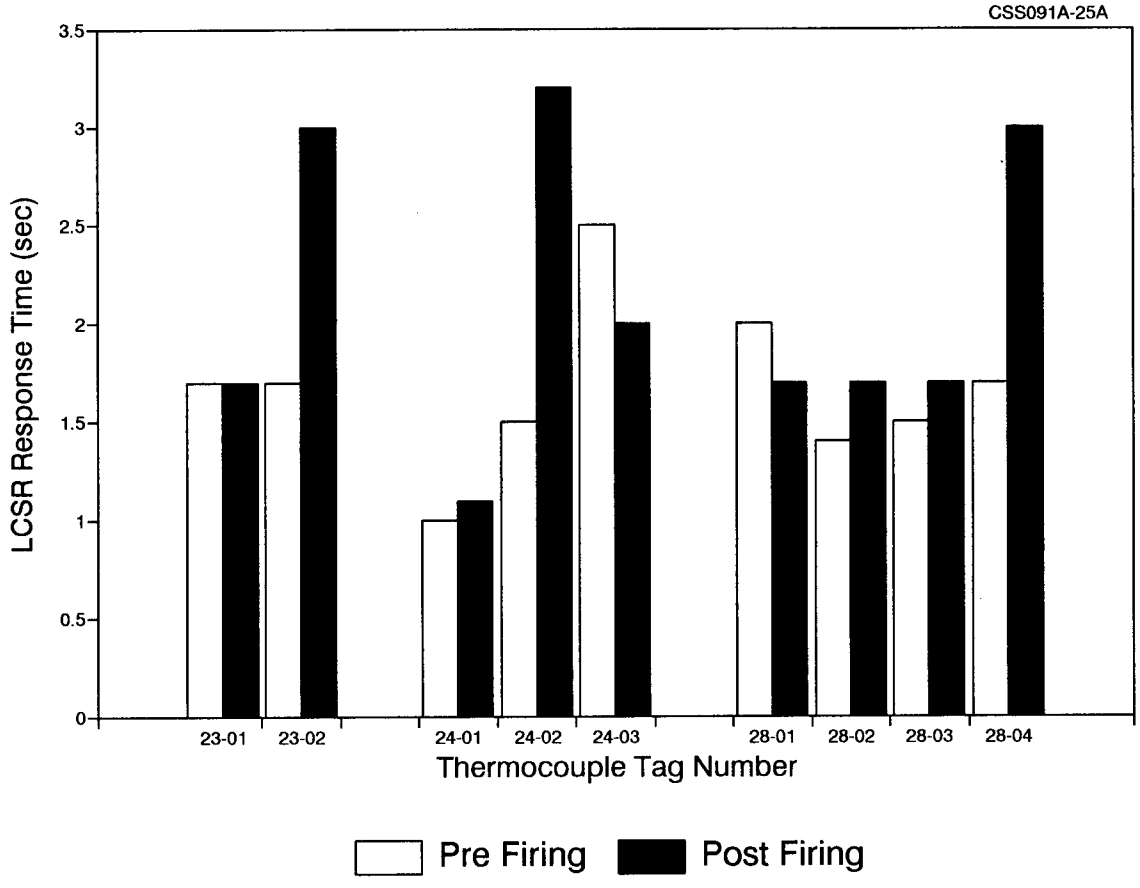

Figure 9.11 Pre and Post-Firing LCSR Results for Representative Thermocouples Tested at SRI

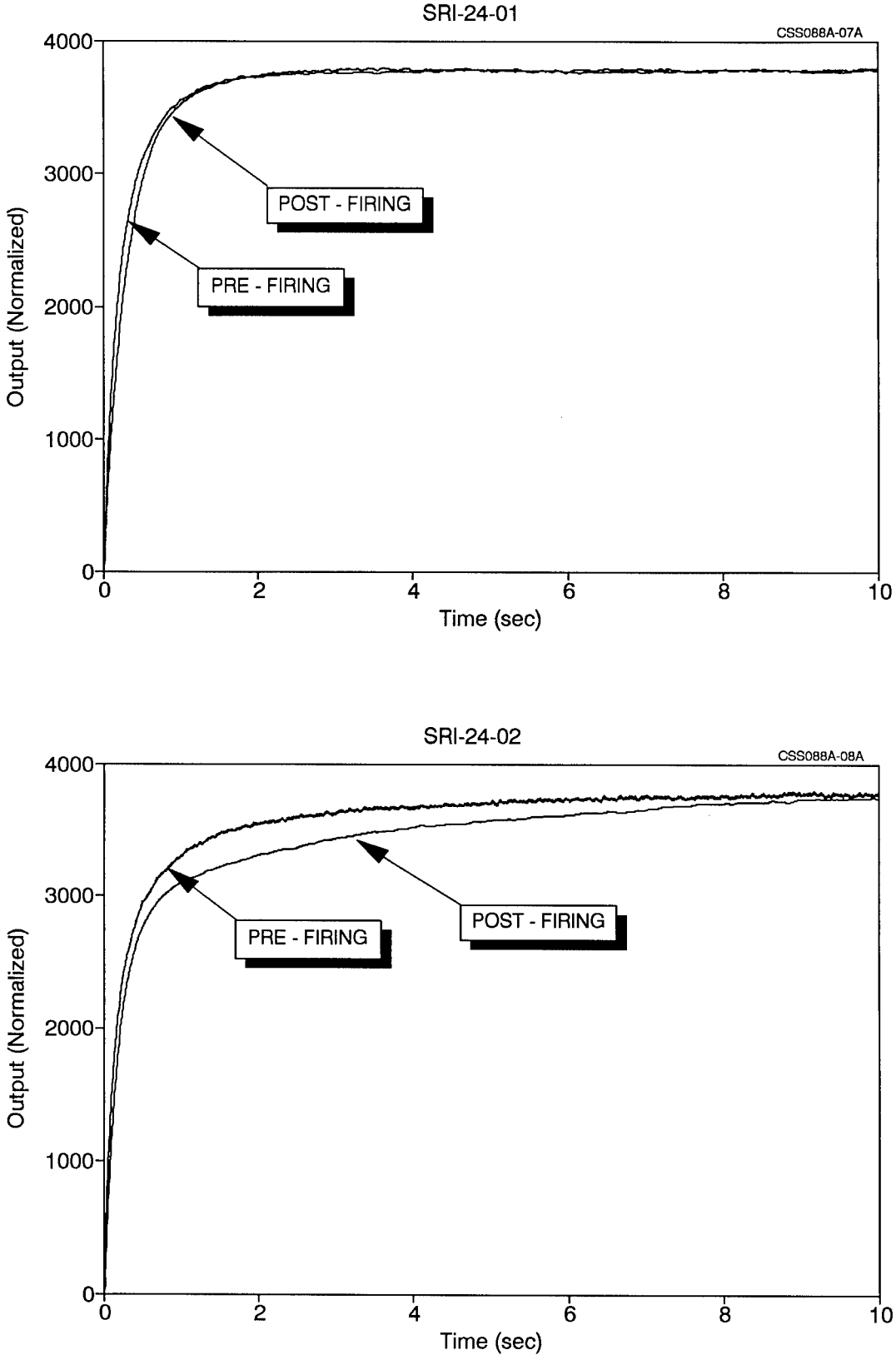

Figure 9.12 Pre and Post-Firing LCSR Transients for Thermocouples in Specimen #24

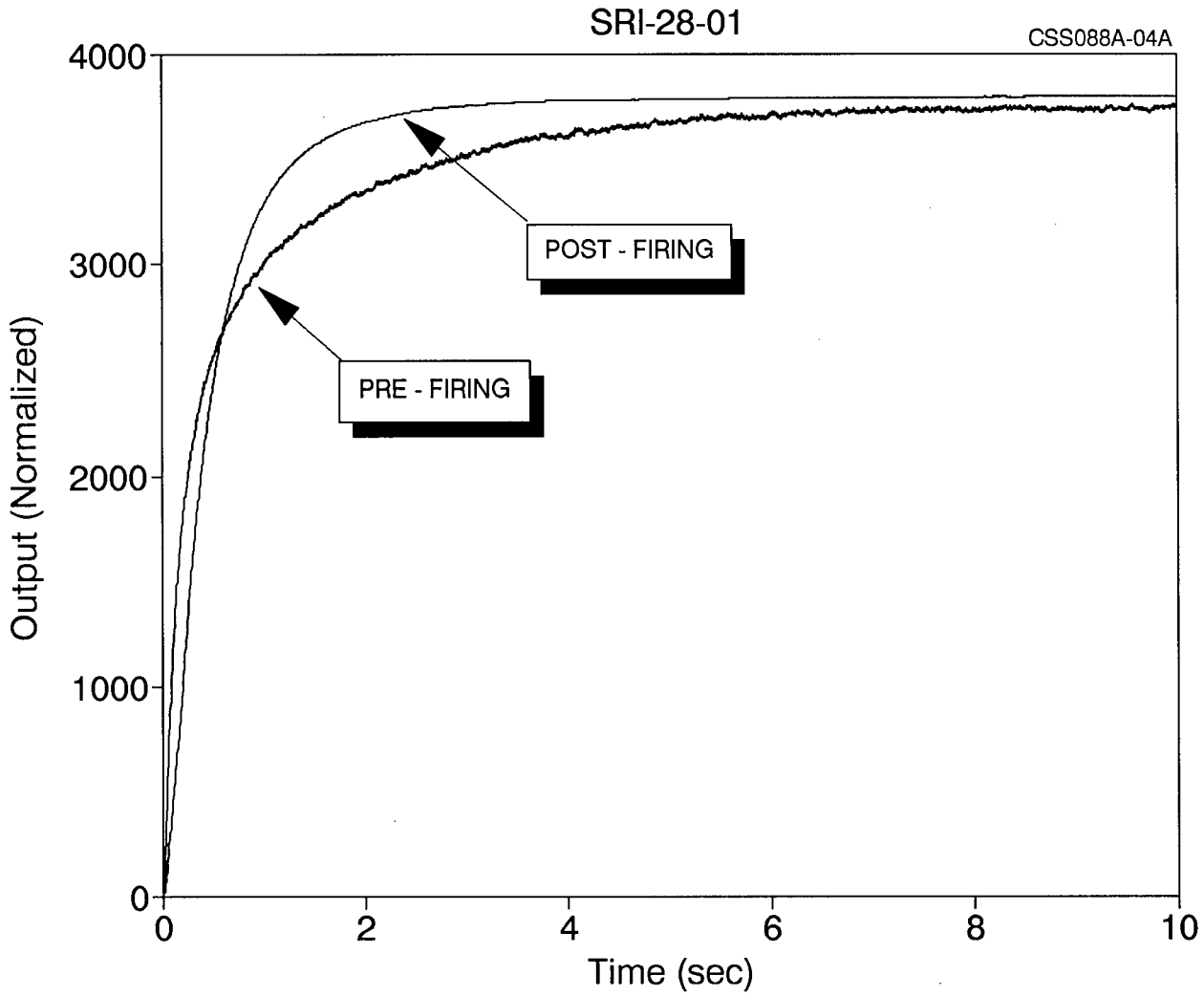

Figure 9.13 Pre and Post-Firing LCSR Transients for Thermocouple #1 in Specimen #28

1) cause no change in thermocouple installation thus leaving the response time unchanged, 2) increase the response time by changing the thermocouple bonding, or 3) decrease the response time by causing the thermocouple to fit better inside the solid material. In any of these cases, it is important for the analyst to know how to account for the thermocouple lag in validating the analytical models of composite materials for SRM nozzles and other applications. The LCSR test provides an excellent tool that can be used to inform the analyst if the thermocouple response time has remained the same, increased, or decreased during the firing tests.

To provide a comparison between results of the analog and the LCSR tests, the amount of time that was required for a thermocouple to reach 1000°F at the SRI tests was calculated for each block. This temperature was selected because all thermocouples in the SRI specimens managed to reach this temperature. The purpose was not to compare LCSR response times with the calculation of response time to reach 1000°F. Rather, the purpose of the comparison was to determine if a thermocouple which indicated a slow response in the analog tests, would also indicate a slow response in the LCSR tests. In most cases, the two results were comparable as shown in Figures 9.14 and 9.15. In each figure, two sets of bar charts are presented. One shows the analog test results and the other shows the LCSR results. As seen in these figures, the analog and LCSR results correlate fairly well. More specifically, when a thermocouple showed up slow in the analog tests, the LCSR test also showed a slower response, and vice versa.

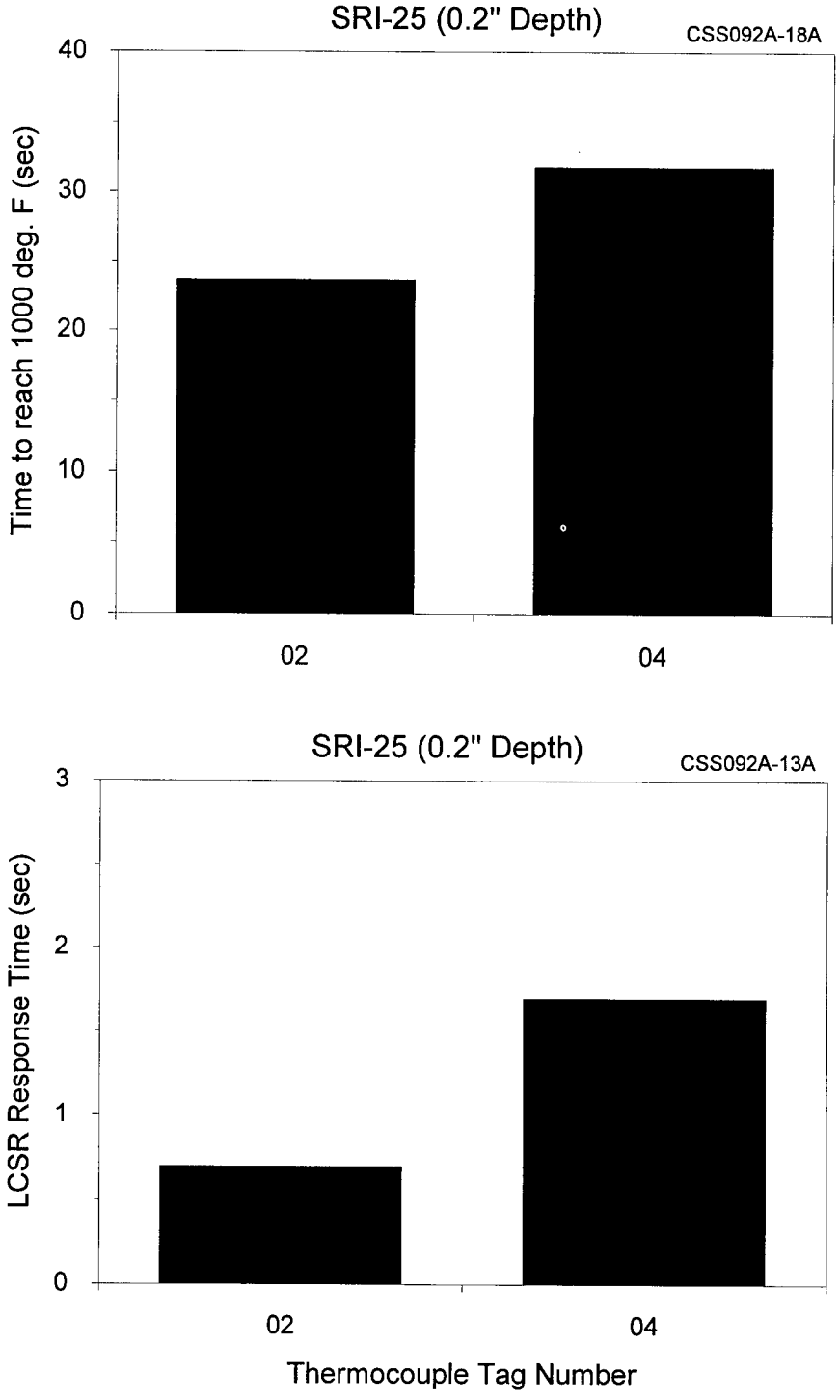

Figure 9.14 Comparison Between Analog Test Results and LCSR Test Results for Delta M Thermocouples in Specimen #25 (0.2" from heated surface)

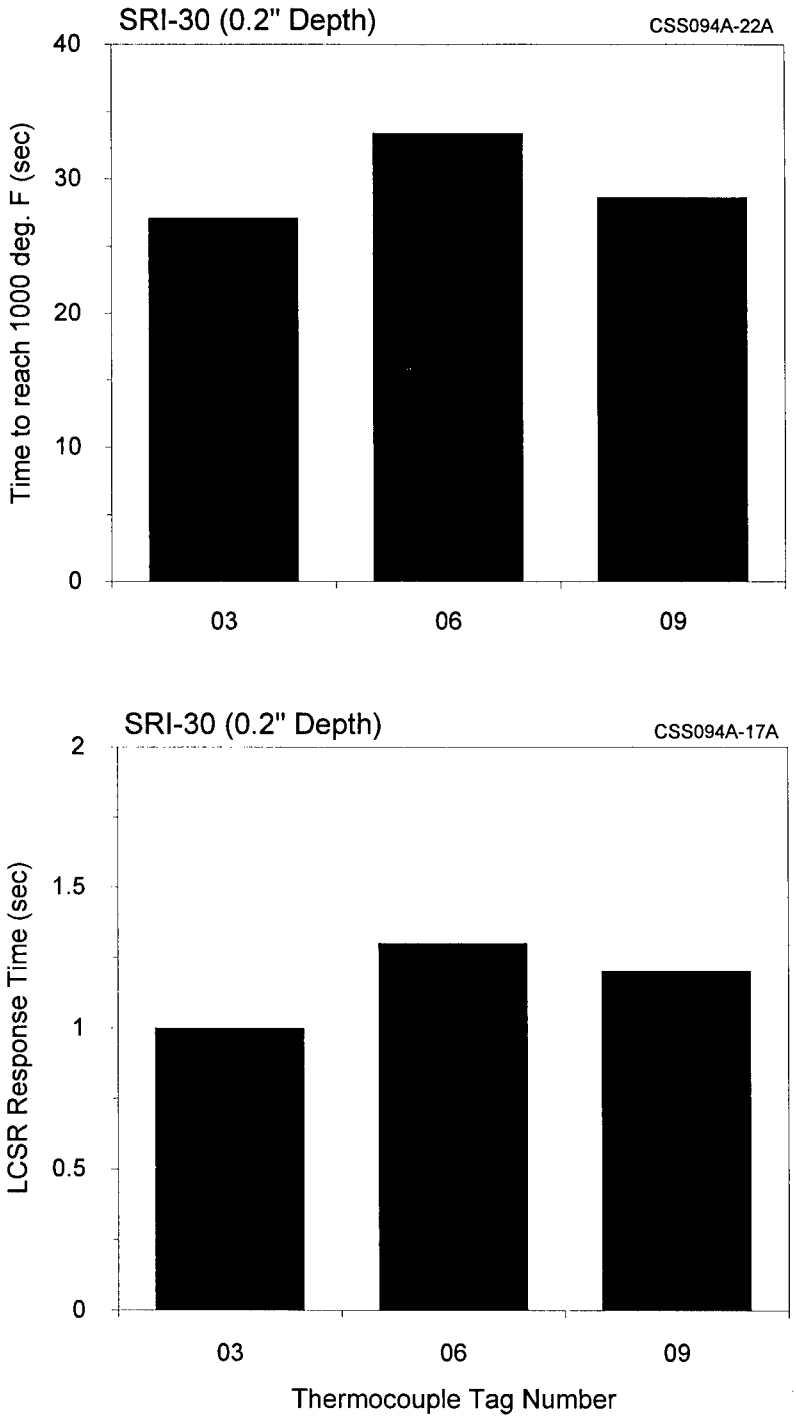

Figure 9.15 Comparison Between Analog Test Results and LCSR Test Results for Delta M Thermocouples in Specimen #30 (0.2" from heated surface)

10. FIELD TESTING OF THERMOCOUPLES AT MSFC

In August 1993, AMS tested forty-four thermocouples embedded in the 48"-3 instrumented scaled nozzle at MSFC. These tests were performed after the completion of the NASA Phase I SBIR project (NAS8-39814) and prior to the NASA Phase II project (NAS8-40165). This testing was performed to assist in the evaluation of the analog temperature data obtained from the nozzle firing tests. The LCSR method was used in these tests for determining the installation integrity of the thermocouples prior to the hot firing of the nozzle.

Figure 10.1 shows a cross sectional view of the scaled nozzle and some of the thermocouples that were installed in the nozzle and were tested in this project. The nozzle is divided into six major areas containing thermocouples. Each area had a group of three thermocouples located radially at different angles around the nozzle with the exception of the 40 and 65 degree throat areas which had only two thermocouples. Four different composite materials (FM5055, FM5952, MX4996 and FM5939) were used at the various thermocouple locations and rotational angles around the nozzle. The temperature sensors embedded in the nozzle were small 0.010" diameter Type K thermocouples manufactured by Delta M. Table 10.1 lists the location of each thermocouple, the material at each location, and the results of thermocouple LCSR testing. These results correlate with the degree of sensor attachment to the host material.

Figures 10.2 and 10.3 show a graphical representation of the response times of each sensor grouped by the type of material in which the thermocouple was installed. As indicated in Table 10.1, four thermocouples were not testable due to open circuits. Also, sensor 85T9116 located at the 270 degree throat location was found to have reversed leads. As illustrated in

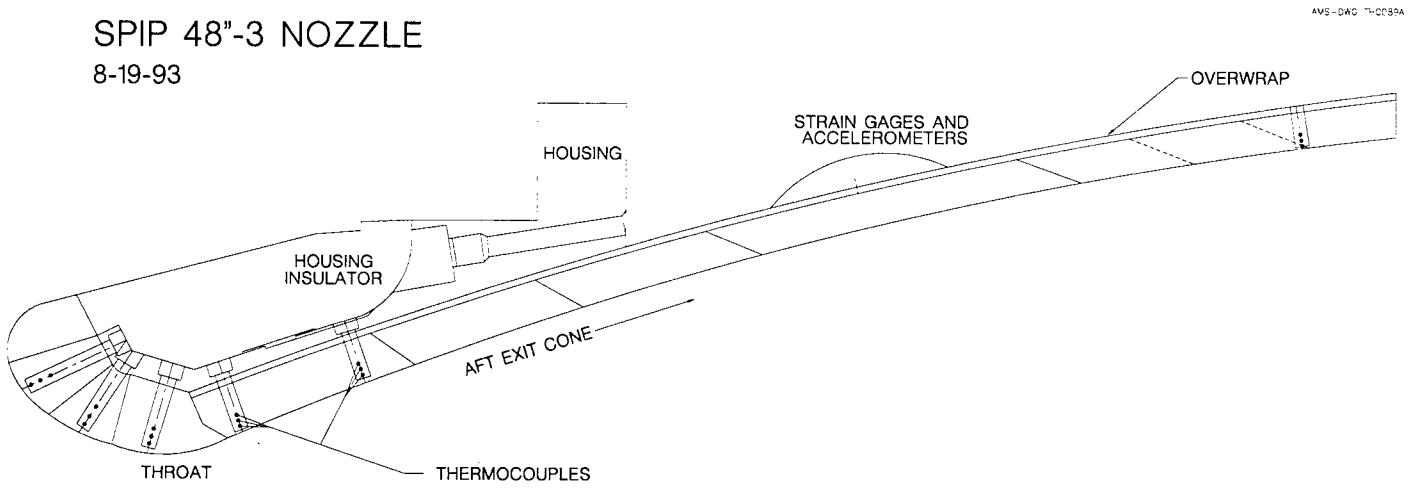

Figure 10.1 Cross Sectional View of Scaled Nozzle

TABLE 10.1

Results of LCSR Testing of Thermocouples in the 48"-3 Instrumented Nozzle at MSFC

Thermocouple Tag Number	Material	Location	LCSR Results (sec)
85T9001	FM5055	85 Degree Fwd Inlet	2.2
85T9002			2.0
85T9003			2.7
85T9004	FM5952	270 Degree Fwd Inlet	1.4
85T9005			1.9
85T9006			2.0
85T9010	MX4996 (2800)	20 Degree Aft Inlet	1.7
85T9011			1.9
85T9012			*
85T9013	MX4996 (2800)	260 Degree Aft Inlet	1.1
85T9014			1.1
85T9015			1.7
85T9119	FM5055	40 Degree Throat	2.2
85T9120			*
85T9121	FM5055	65 Degree Throat	2.8
85T9122			3.5
85T9113	FM5055	85 Degree Throat	*
85T9114			1.4
85T9115			1.6
85T9116	FM5952	270 Degree Throat	**
85T9117			*
85T9118			2.1

* = Not Testable, failed open circuit thermocouple leads
** = Thermocouple leads reversed

TABLE 10.1
(Continued)

Results of LCSR Testing of Thermocouples in the 48"-3 Instrumented Nozzle at MSFC

Thermocouple Tag Number	Material	Location	LCSR Results (sec)
85T9275	FM5055	20 Degree Fwd Exit Cone FWD	1.5
85T9276			2.1
85T9277			1.8
85T9284	FM5055	100 Degree Fwd Exit Cone Aft	1.8
85T9285			1.5
85T9286			1.5
85T9281	FM5952	260 Degree Fwd Exit Cone FWD	1.8
85T9282			1.9
85T9283			1.9
85T9287	FM5952	340 Degree Fwd Exit Cone Aft	2.3
85T9288			2.2
85T9289			1.8
85T9801	FM5939 LDC	100 Degree Aft Exit Cone	2.4
85T9802			1.6
85T9803			1.8
85T9804	FM5939 LDC	340 Degree Aft Exit Cone	3.6
85T9805			4.0
85T9806			3.3

* = Not Testable, failed open circuit thermocouple leads
** = Thermocouple leads reversed

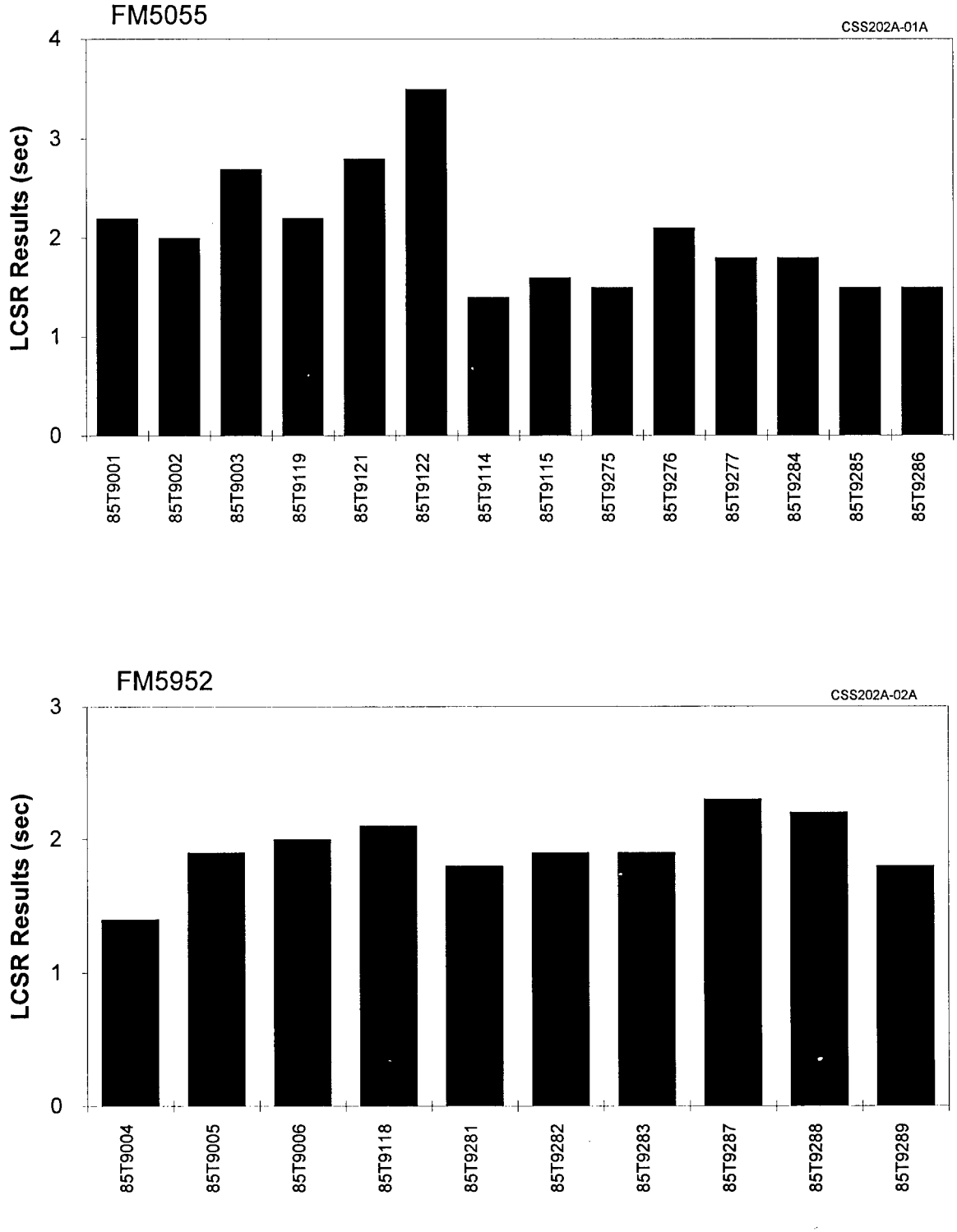

Figure 10.2 LCSR Results for Nozzle Thermocouples in FM5055 and FM5952 Materials

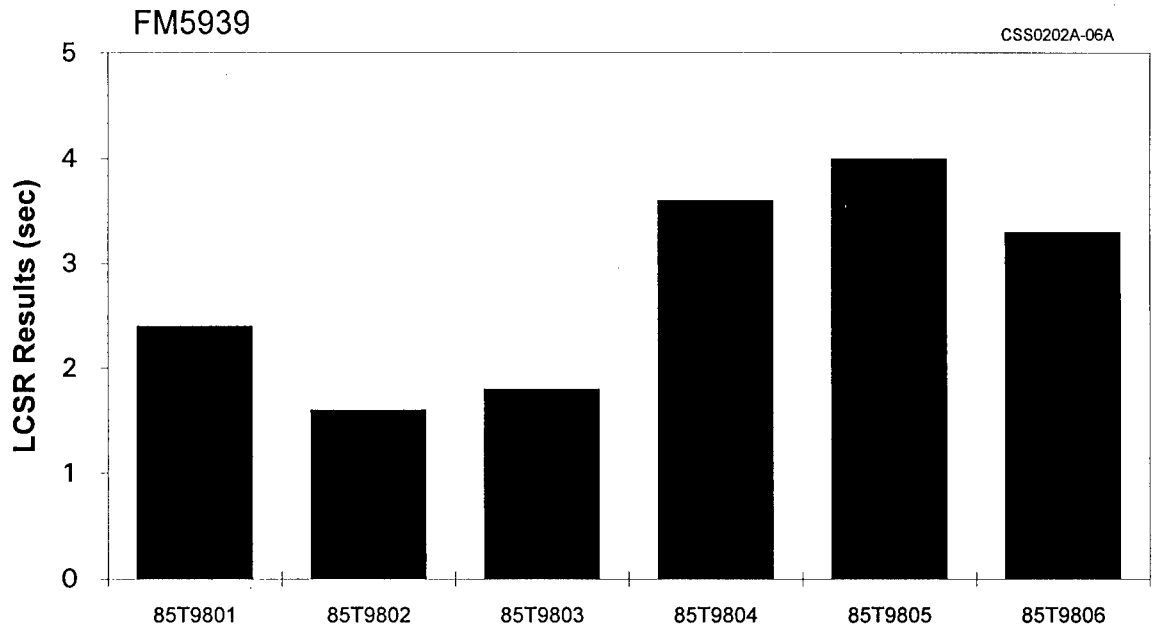

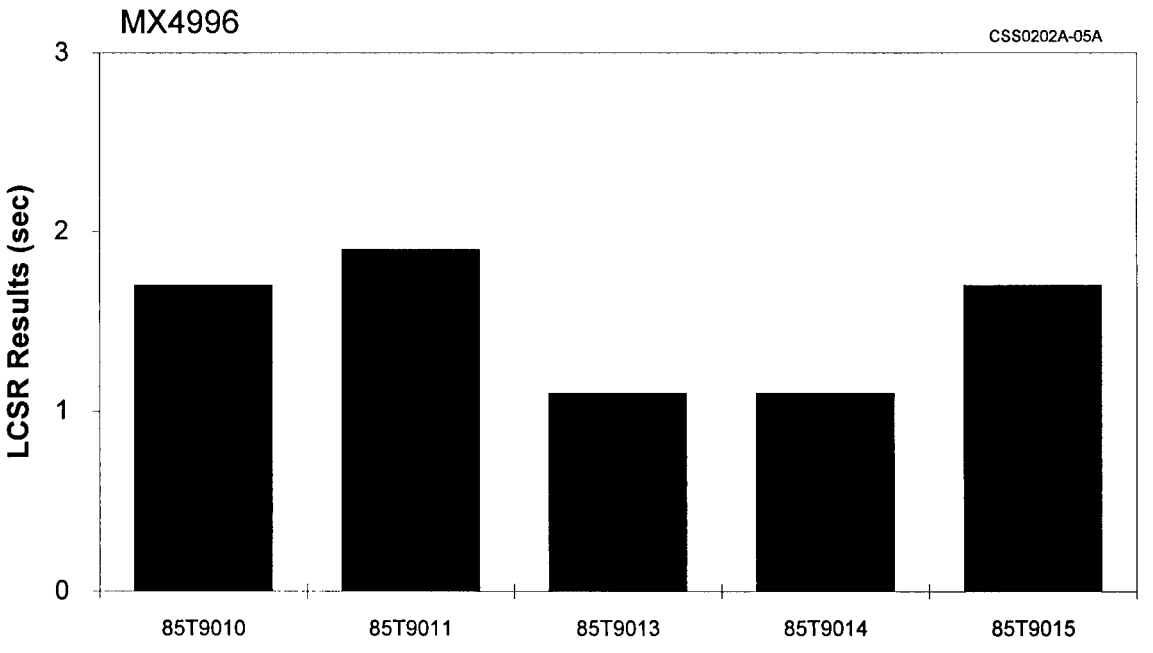

Figure 10.3 LCSR Results for Nozzle Thermocouples in FM5939 and MX4996 Material

Figures 10.2 and 10.3, the average response of the thermocouples is about 2 seconds regardless of the composite material in which the thermocouples are installed except for MX4996 which gave slightly faster responses than the other three materials. In particular, all thermocouples tested in MX4996 had LCSR results of less than two seconds while the response time of some of the thermocouples in other samples exceeded two seconds. The LCSR results for the thermocouples in the four composites ranged from 1 to 4 seconds.

Figure 10.4 shows normalized LCSR transients for the 270 degree throat location thermocouples illustrating the effect of reversed-connected thermocouple on the LCSR transient. This is interesting because it shows that the LCSR method can show not only the relative speed of response of thermocouples, but also provide diagnostic capabilities to identify thermocouple circuit problems. As discussed elsewhere in this report, the LCSR method can reveal secondary junctions and in some cases gross inhomogeneities in thermocouple assemblies or extension wires. The method also has the potential to detect moisture in RTDs and thermocouples.

Additional LCSR transients for some of the thermocouples tested at MSFC are presented in Figures 10.5 through 10.7. Of the thirty-five nozzle thermocouples that were testable at MSFC, most showed results indicative of proper and consistent installation.

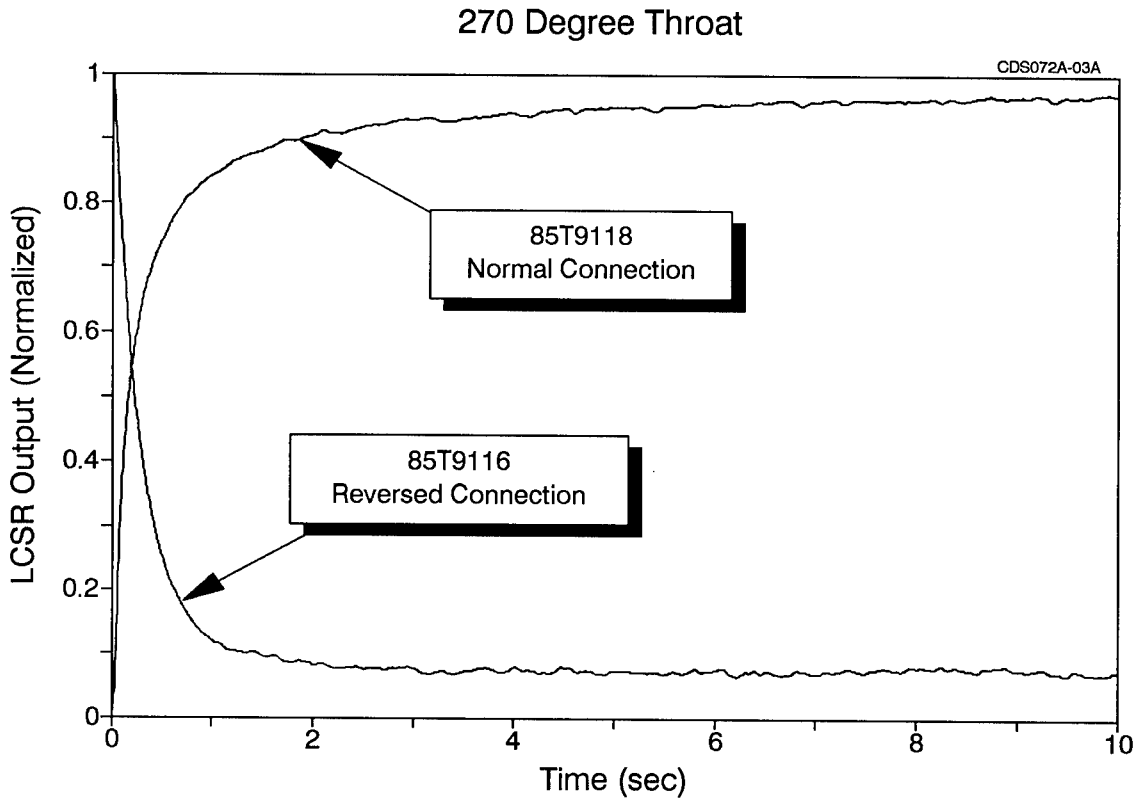

Figure 10.4 LCSR Transient for Nozzle Thermocouples with One Showing a Reversed-Connected Thermocouple

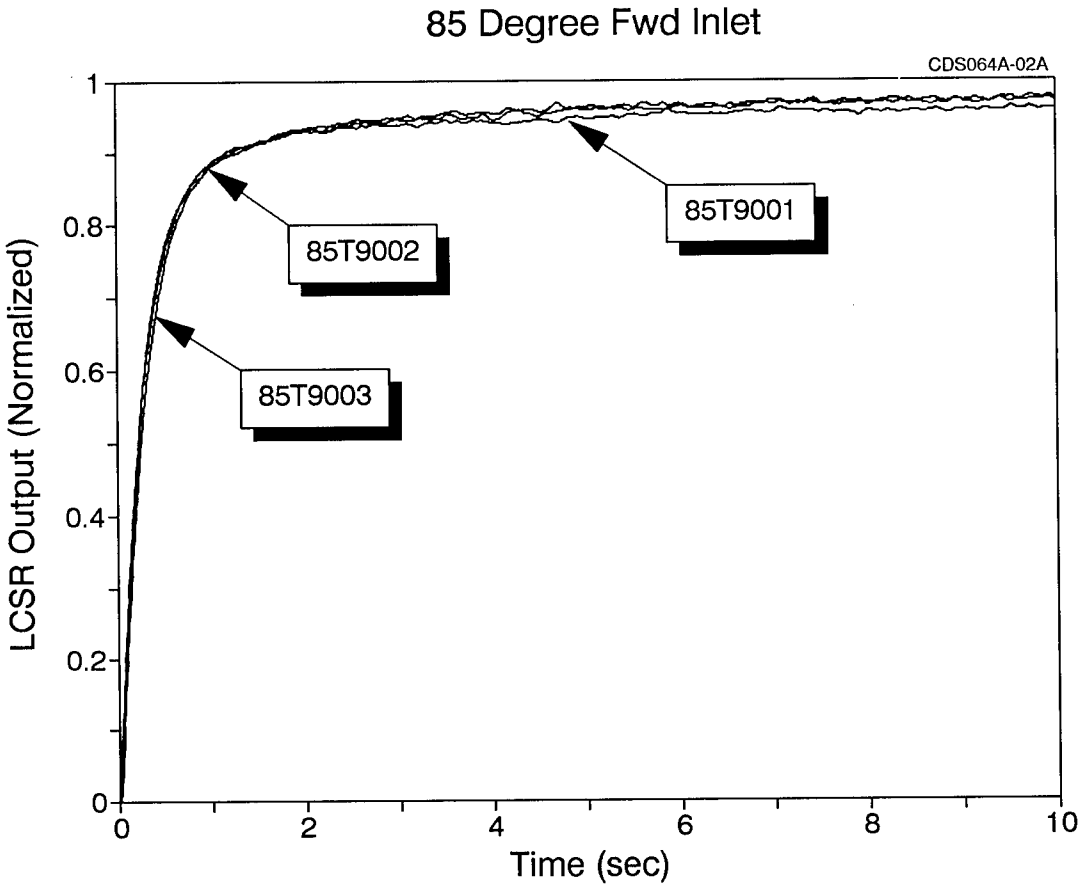

Figure 10.5 LCSR Transients for Nozzle Thermocouples Located at 85 Degree Fwd Inlet

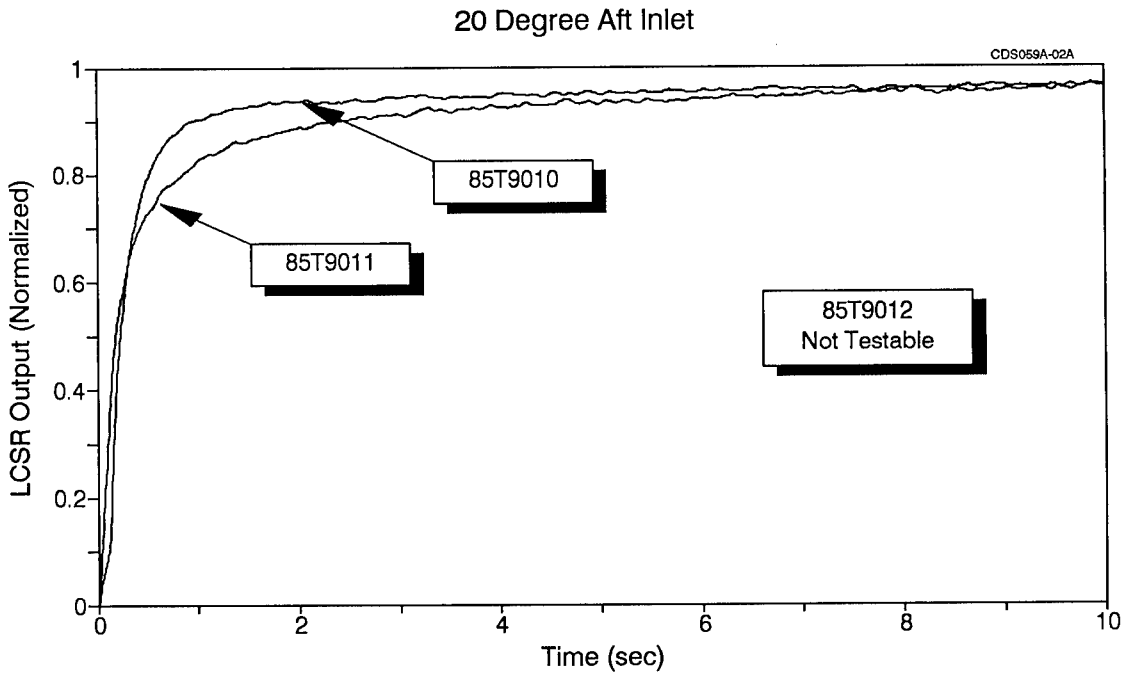

Figure 10.6 LCSR Transients for Nozzle Thermocouples Located at 20 Degree Aft Inlet

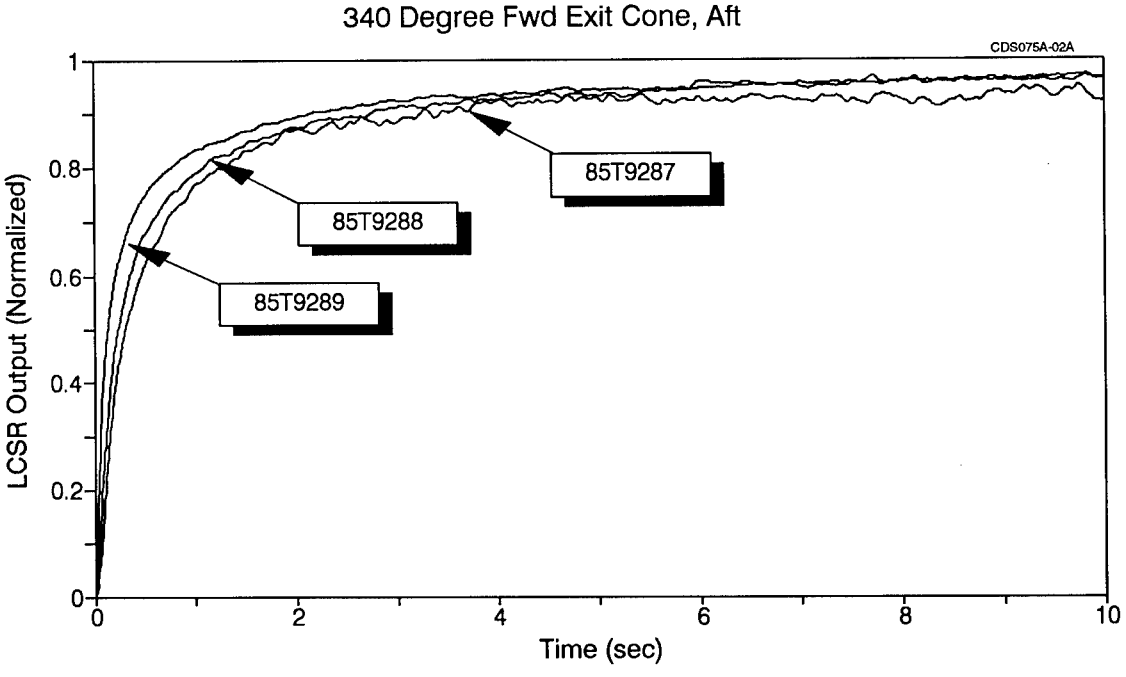

Figure 10.7 LCSR Transients for Nozzle Thermocouples Located at 340 Degree Fwd Exit Cone, Aft

11. TESTING THE ATTACHMENT OF RTDs IN SSMEs

Thin-film, 100 ohm Platinum Resistance Thermometers (PRTs) are bonded to the surface of fuel and oxidizer lines in SSMEs to measure temperature as a means of determining if the line isolation valves are leaking. Referred to as surface-mount or skin-mount RTDs, these sensors should register the ambient temperature unless there is a leaking valve in the line. In this case, the RTDs will show a lower temperature than the ambient temperature. This is because a leaking valve will allow fuel through the line which will lower the temperature of the line.

Since surface-mount RTDs are permanently installed on SSMEs, they are subject to harsh environments during the firing and flight of the space shuttle. As such, the RTDs may become loose or detached from the piping and prevent leak detection. Furthermore, if the bonding between the RTD and the fuel line is poor, the RTD could respond too slowly and prevent timely leak detection.

Each SSME has three locations where surface-mounted RTDs are installed. These locations are:

- Main Fuel Valve discharge (MFV)
- Anti-Flood Valve discharge (AFV)
- Oxidizer Preburner Oxidizer Valve (OPOV)

The piping material to which the RTDs are attached are as follows:

- AFV Material - Inconel 625
- MFV Material - Inconel 718
- OPOV Material - Inconel 625

Figure 11.1 shows the three locations in a SSME where each pair of RTDs is attached to the metallic piping. This is followed by Figure 11.2 with a photograph of an AFV.

Prompt and accurate temperature indications from the RTDs are important in evaluating engine performance during SSME firings. The indications from these sensors are used to determine if engine conditions are appropriate for successful engine operation. An operating SSME can produce severe vibrational environments causing even the finest adhesives to break down and allow sensor debonding to occur. A sensor that is poorly bonded or totally detached from the fuel or oxidizer lines could cause a delay in sensor response and/or produce an erroneous temperature indication. Thus, a method is required to verify that the RTDs are properly bonded.

11.1 Testing of Laboratory-Grade Surface-Mount RTDs

In response to NASA's concerns about the bonding of surface-mount RTDs in SSMEs, a series of laboratory and field tests involving the LCSR method was performed to determine if this method can be used to verify the attachment of RTDs to SSME fuel lines.

These tests involved several commercially-available, thin-film RTDs, purchased from OMEGA. Figure 11.3 shows a photograph of the RTDs. These sensors are not of the type used in SSMEs. Nevertheless, they were obtained for the initial LCSR demonstration tests because they were readily available and inexpensive. The purpose was to demonstrate the feasibility of the LCSR method on these sensors, and then move on to testing higher grade RTDs similar to those used in SSMEs.

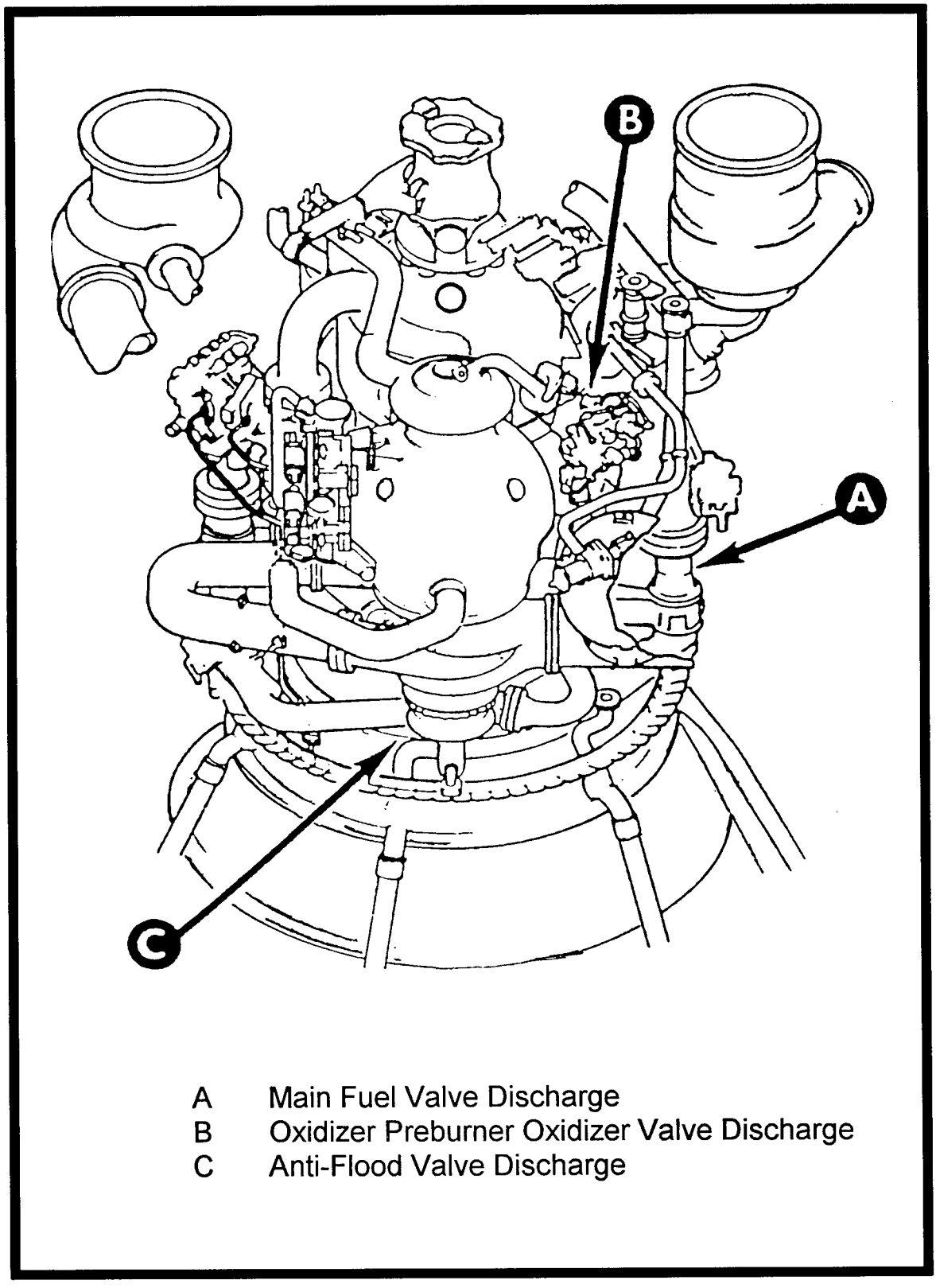

Figure 11.1 Location of Surface-Mount RTDs in Each SSME

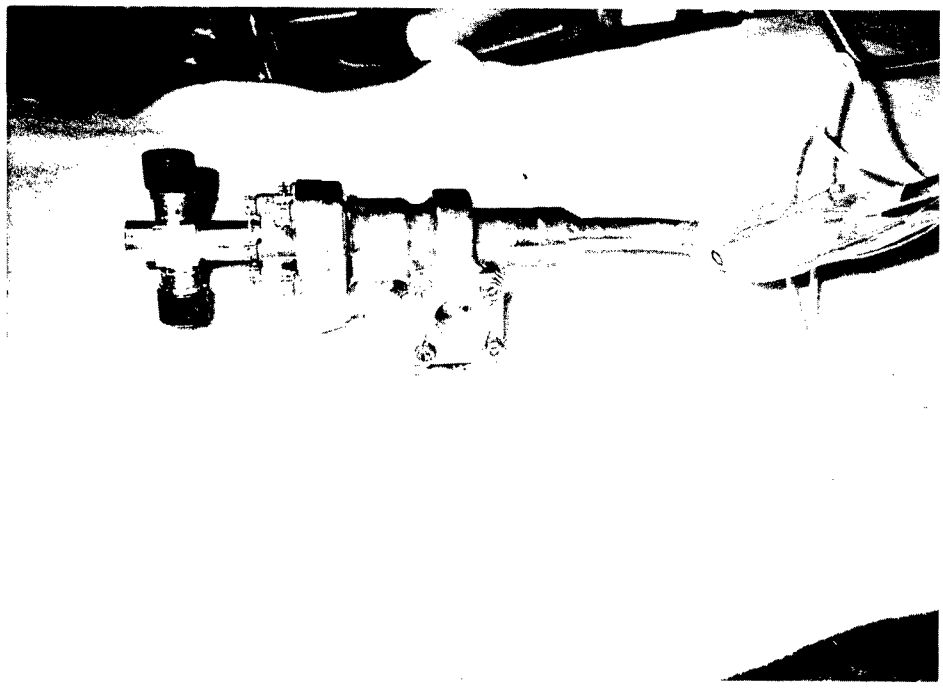

Figure 11.2 Photograph of Anti-Flood Line from the Test Bed SSME

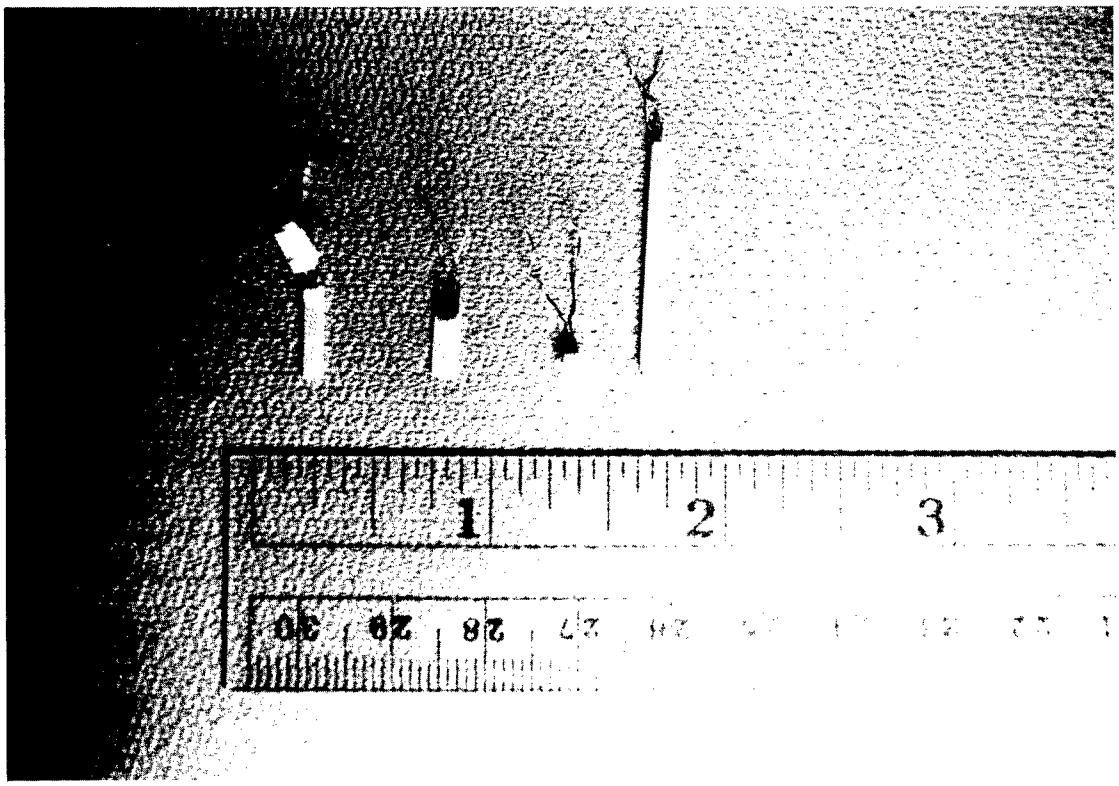

Figure 11.3 Photograph of Surface-Mount RTDs Purchased from OMEGA for the Laboratory Tests

The results of LCSR testing of the thin-film RTDs from OMEGA are shown in Figure 11.4 in terms of laboratory response times measured using the LCSR tests. The results are given in terms of installation indices for the RTDs in both bonded and unbonded conditions. In the bonded case, the sensors were installed on a metallic surface, and in the unbonded case, the sensors were in the ambient air detached from the metallic surface. Note in Figure 11.4 that the installation indices for the unbonded RTDs are from 2 to 20 times larger than the bonded RTDs. This indicates that the LCSR test can readily distinguish a bonded RTD from an unbonded RTD.

Tests were also performed on one of the RTDs when it was first fully bonded to a metallic surface, then partially bonded, and finally unbonded. The results are shown in Figure 11.5 in terms of installation indices obtained from analysis of the LCSR data for the three bonding conditions mentioned.

11.2 Testing of High-Grade Surface-Mount RTDs

Upon successful demonstration of LCSR method for testing the attachment of thin-film RTDs purchased from OMEGA, MSFC provided AMS with two RTDs similar (although not flight qualified) to those installed on fuel and oxidizer lines of SSMEs. In addition, AMS purchased six commercially available high-grade skin-mount RTDs from Rosemount. Figure 11.6 shows a photograph of one of the RTDs purchased from Rosemount (Model 118MGB - top) as well as one of the RTDs obtained from MSFC (Rosemount Model 118BJJ - bottom).

In order to simulate an actual SSME installation, the RTDs mentioned above were mounted on metallic surfaces in the laboratory using the NASA/RocketDyne bonding procedures and were then tested to demonstrate that their attachment quality can be determined using the

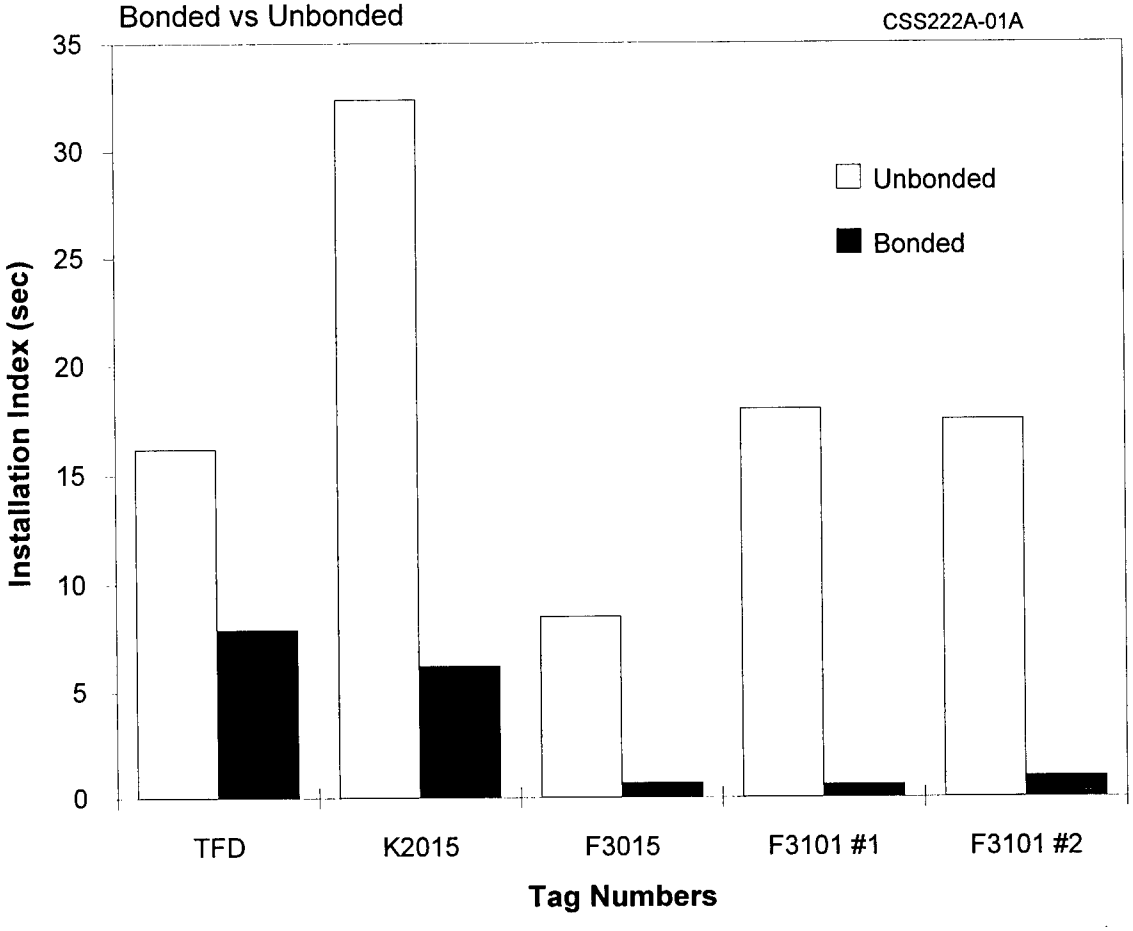

Figure 11.4 Results of LCSR Testing of Thin-Film RTDs

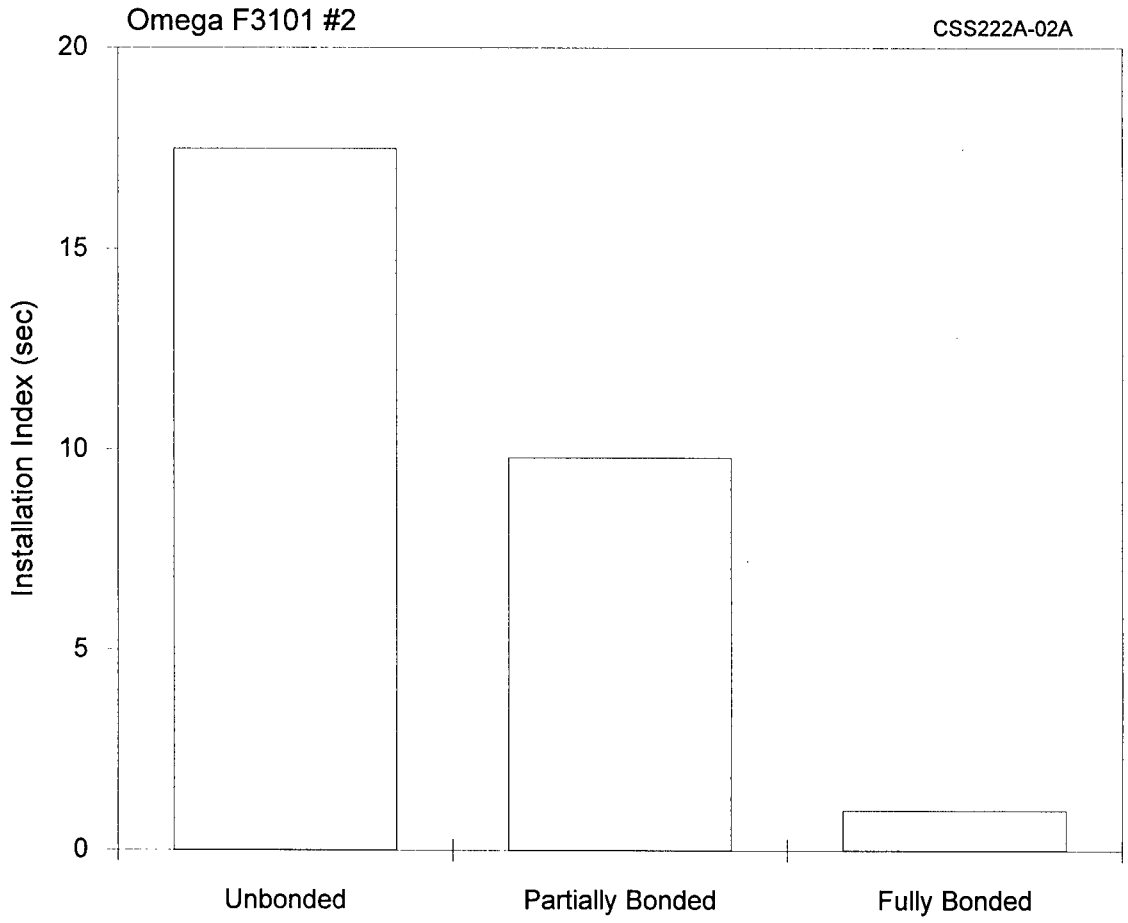

Figure 11.5 LCSR Results for a Thin-Film RTD Tested in the Laboratory

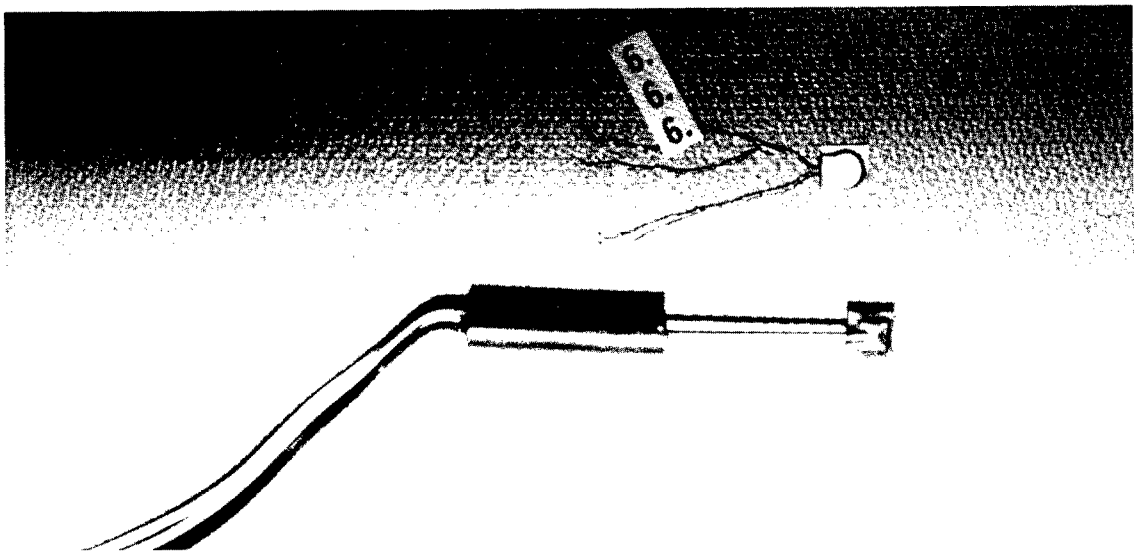

Figure 11.6 Photograph of RTDs of the Type Used on SSMEs for Temperature Measurements on Fuel Lines to Detect Fuel Leak

LCSR method. Thin slices of teflon were used to induce various degrees of RTD installation quality. Figure 11.7 shows LCSR transients for one of the RTDs with varying degrees of bonding. It is apparent that the LCSR test can readily distinguish between a good bond and a bad bond.

In addition to the LCSR method, the self heating test was employed in the laboratory tests to verify that, like the LCSR test, self heating index measurements can help characterize the bonding of an RTD to a solid material. The results are shown in Figure 11.8. The self heating test is based on heating the RTD with an electric current and measuring the steady state increase in RTD resistance per unit of input electric power. The results are expressed in terms of ohms per watt (Ω/w). The self heating test procedure calls for applying various levels of current (I) to the RTD, waiting for the RTD to settle after each current level is applied, and measuring the RTD resistance (R) after it has increased with the application of the current. The results of these measurements are then plotted in terms of RTD resistance as a function of the applied power ($P=I^2R$). The plot for platinum RTDs is usually a straight line. The straight line is referred to as the self heating curve of the RTD, and the slope of the line is called the self heating index (SHI). This index is proportional to the response time of the RTD. Figure 11.9 shows self heating curves for a surface-mount RTD in partially and fully bonded conditions. The corresponding LCSR transients are also shown in Figure 11.9.

11.3 Effect of LCSR Test on RTD Calibration

During the Phase II project, laboratory calibration tests were performed to verify that the LCSR method would not affect the calibration of surface-mount RTDs. In response, a number of surface-mount RTDs were given repeated step changes in current (current cycling) and calibrations were performed before and after the current cycling to determine the effect on RTD calibrations.

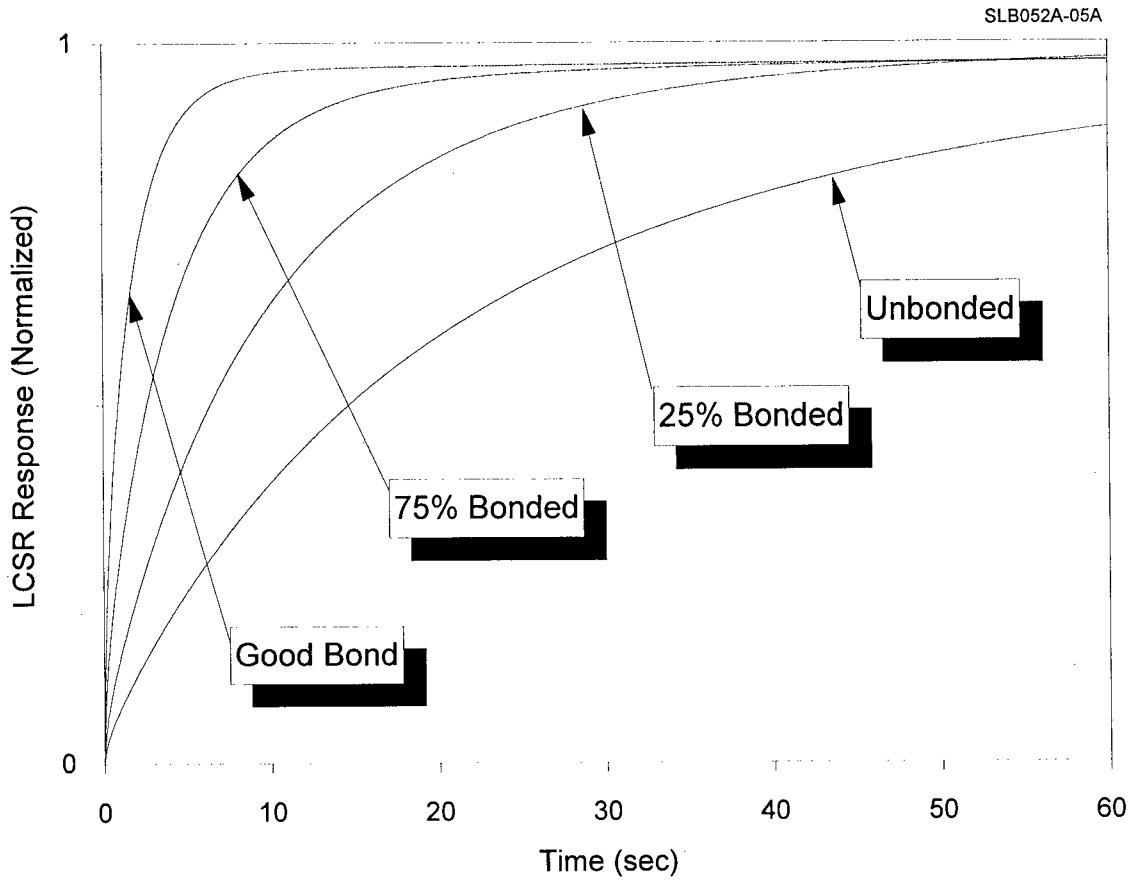

Figure 11.7 LCSR Results for a Thin-Film RTD Tested in the Laboratory

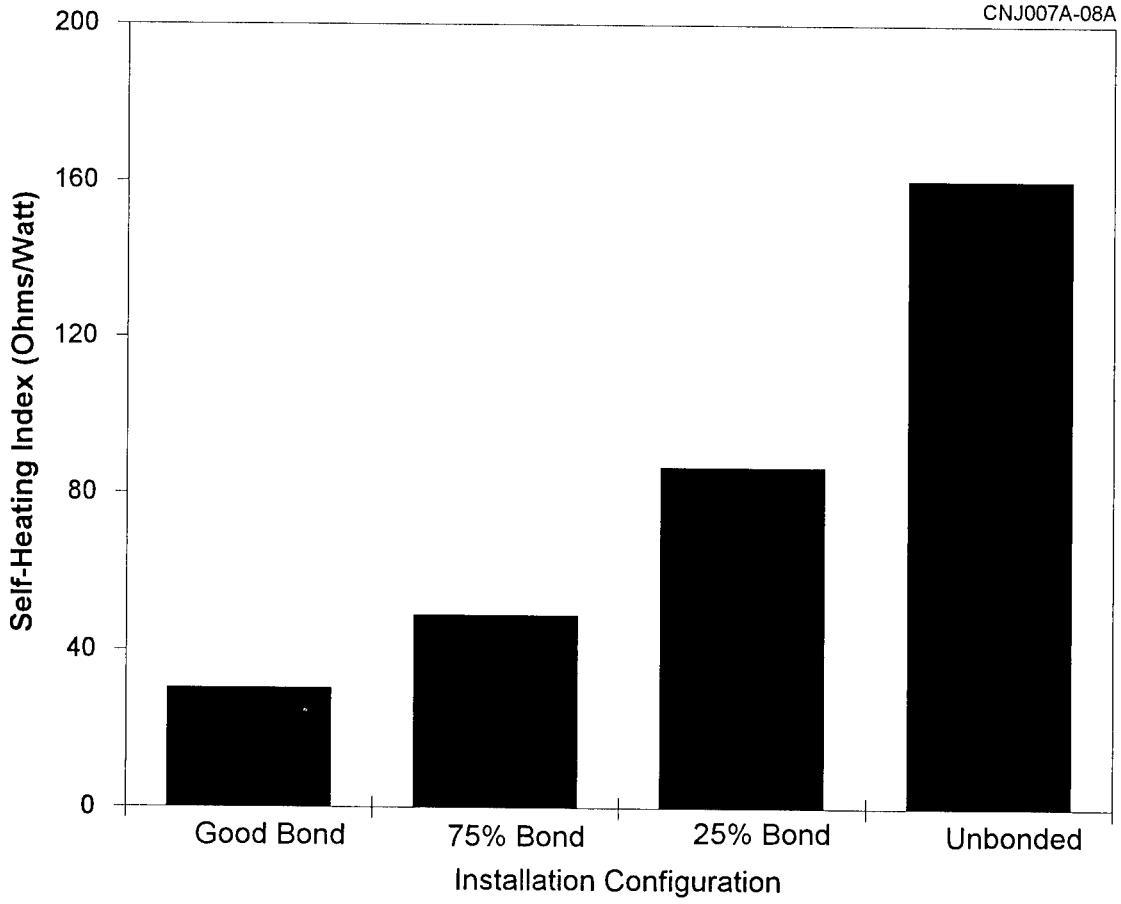

Figure 11.8 Average Self Heating Test Results for Thin-Film RTDs Tested in the Laboratory

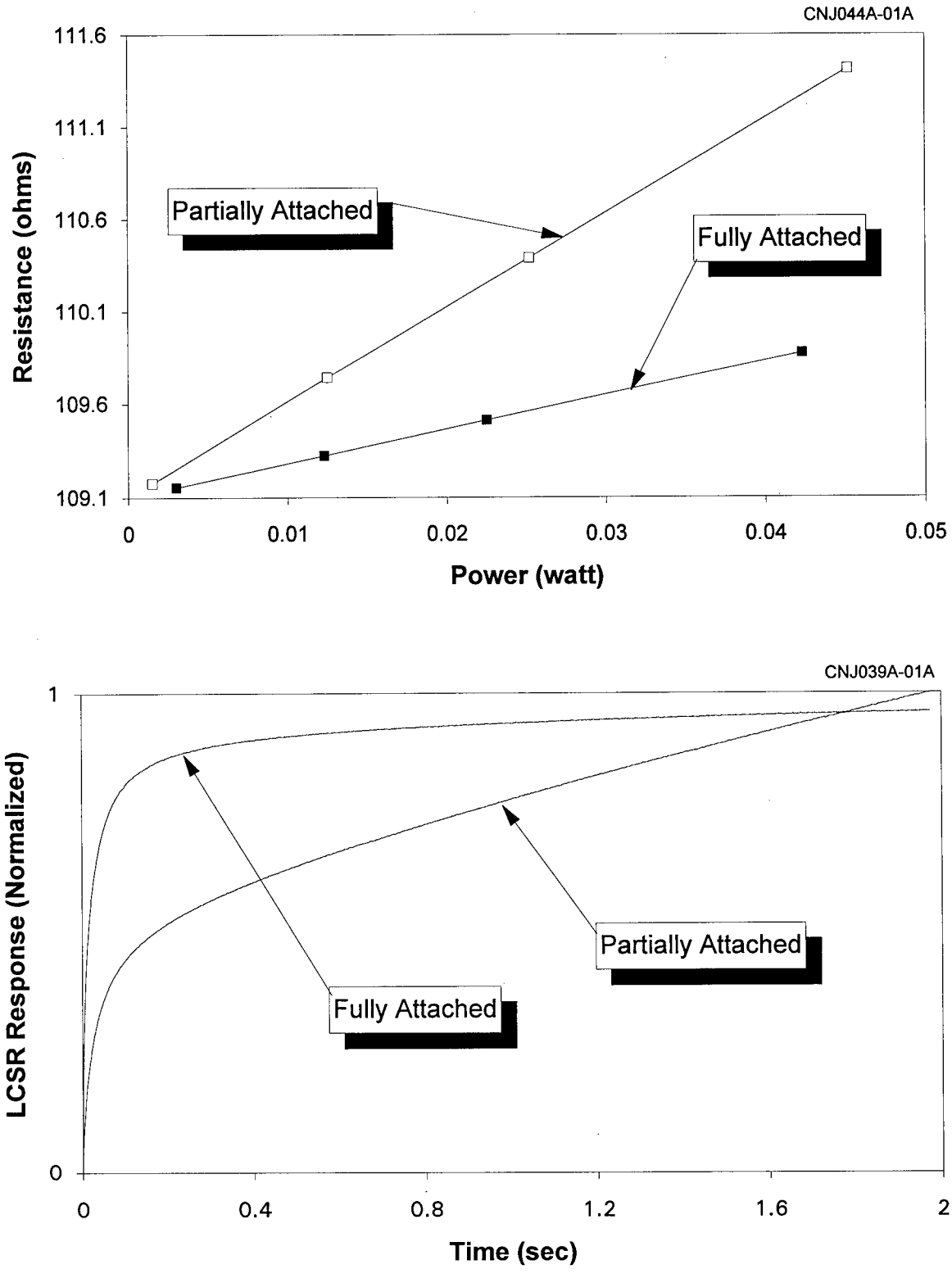

Figure 11.9 Self Heating Curves and Corresponding LCSR Transients for a Skin-Mount RTD Tested in Both Fully and Partially Bonded Configurations

Figure 11.10 shows the results of the calibration tests in terms of the difference in the calibration of RTDs over the range of 0 to 800°F before and after LCSR testing. Results are shown in Figure 11.10 for LCSR cycling using both 60 mA and 30 mA of DC current. At each current level, the RTDs were cycled 720 times and the duration of high current exposure was 60 seconds per each cycle. The differences were almost negligible (less than 0.2°F over the range of 0 to 800°F) indicating that the LCSR tests do not alter the calibration of the RTDs. The calibration differences displayed in Figure 11.10 are said to be negligible because they are comparable to the calibration repeatability of the RTDs. Figure 11.11 shows typical differences between two consecutive calibrations of a surface-mount RTD. This is provided to show the inherent repeatability of the RTD calibrations.

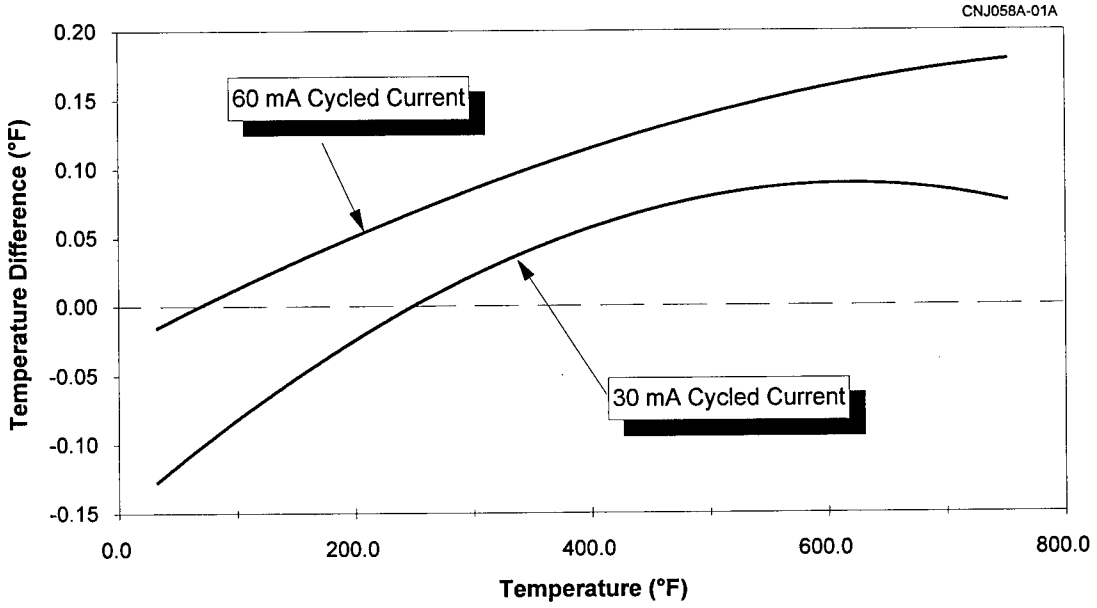

Figure 11.10 Differences in Calibration of a Thin-Film RTD Before and After LCSR Testing

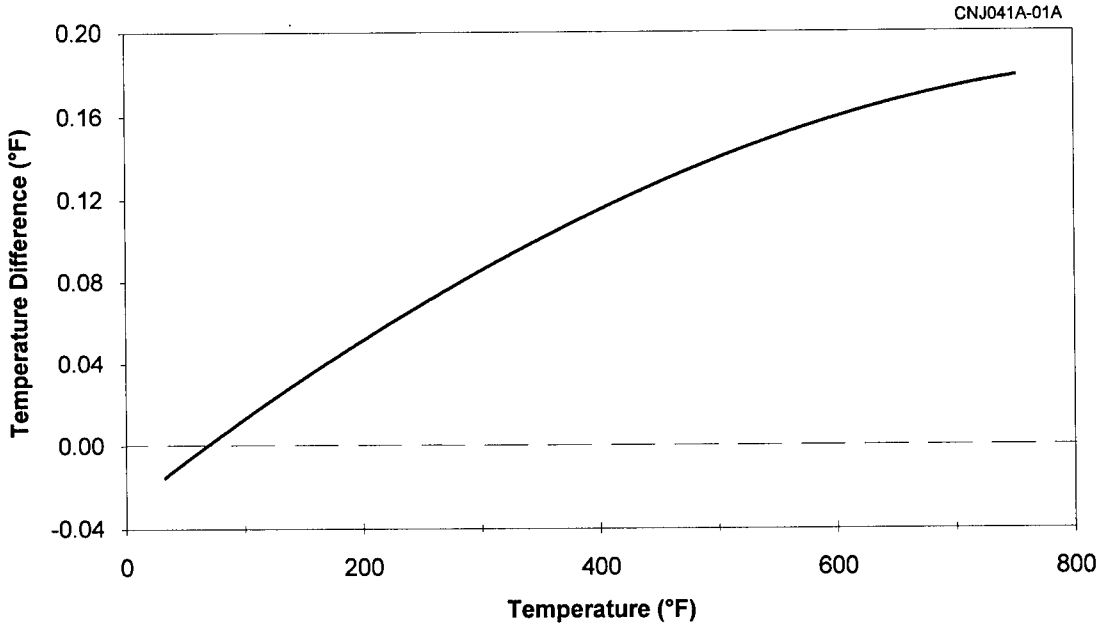

Figure 11.11 Difference Between Two Consecutive Calibrations of a Thin-Film RTD Demonstrating the Repeatability of the RTD Calibration

12. TEST OF BONDING OF STRAIN GAGES IN SSMEs

12.1 Description of SSME Strain Gages

Most strain gages used in SSMEs are either bonded resistance-type strain gages manufactured by Micro-Measurements (Figure 12.1) or weldable strain gages manufactured by HITEC Corporation (Figure 12.2). The bonded resistance type gages are used in moderate temperatures such as the engine support arms, pump & turbine housings, spring-loaded pump end ball bearing cells, and the main injection valve. Figure 12.3 shows a photograph of strain gages installed on a stiff arm in a SSME test bed. Weldable strain gages are used in high temperature applications in locations such as the turning vanes of the SSME turbo pump (Figure 12.4) where the primary focus is on dynamic strains.

The bonding of strain gages not only affects the dynamic response of the gage but also affects the steady-state performance of the gage. Figure 12.5 shows the static response of a strain gage in bonded and unbonded situations.

12.2 Strain Gage Bonding Tests

LCSR and self heating tests were performed on a number of strain gages in the laboratory. The results are shown in Figure 12.6 in terms of LCSR transients and SHIs.

Bonded resistance gages consisting of Constantan foil with a Polyimide carrier matrix were also tested using both the LCSR and SHI techniques. The results showed a strong correlation between dynamic response and bond quality. This led to testing of higher quality and

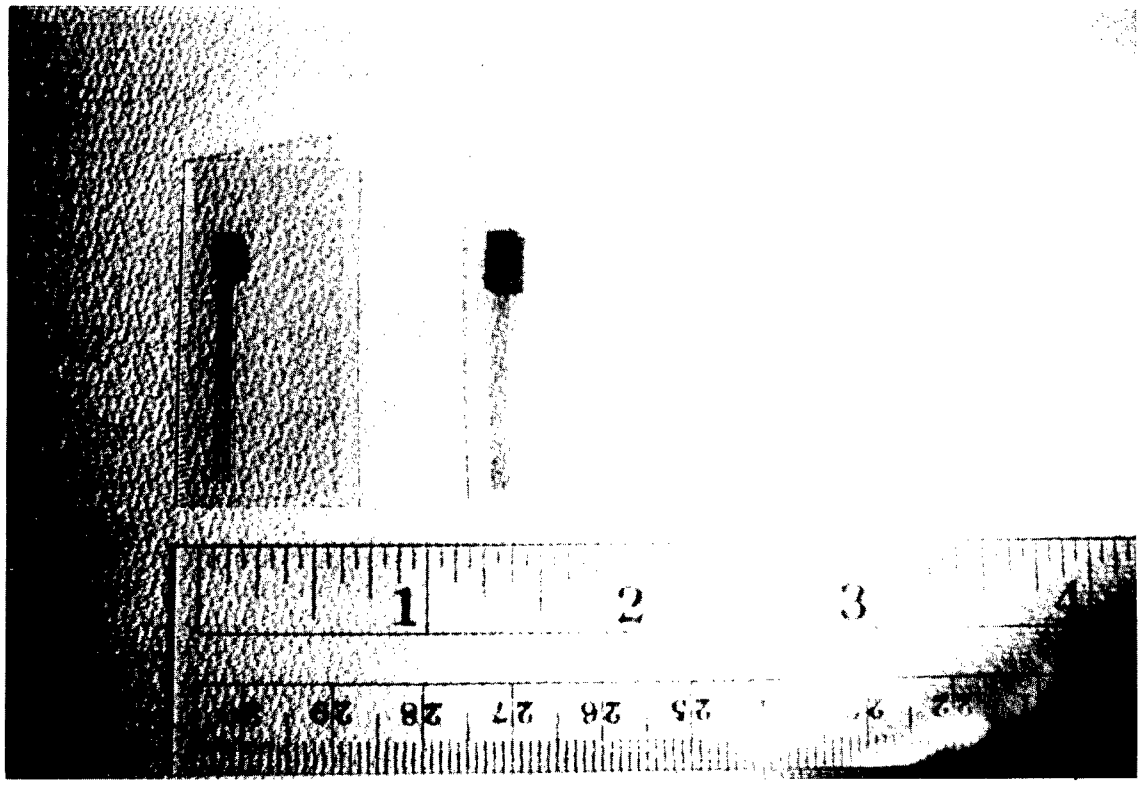

Figure 12.1 Photograph of Strain Gages Manufactured by Micro-Measurements

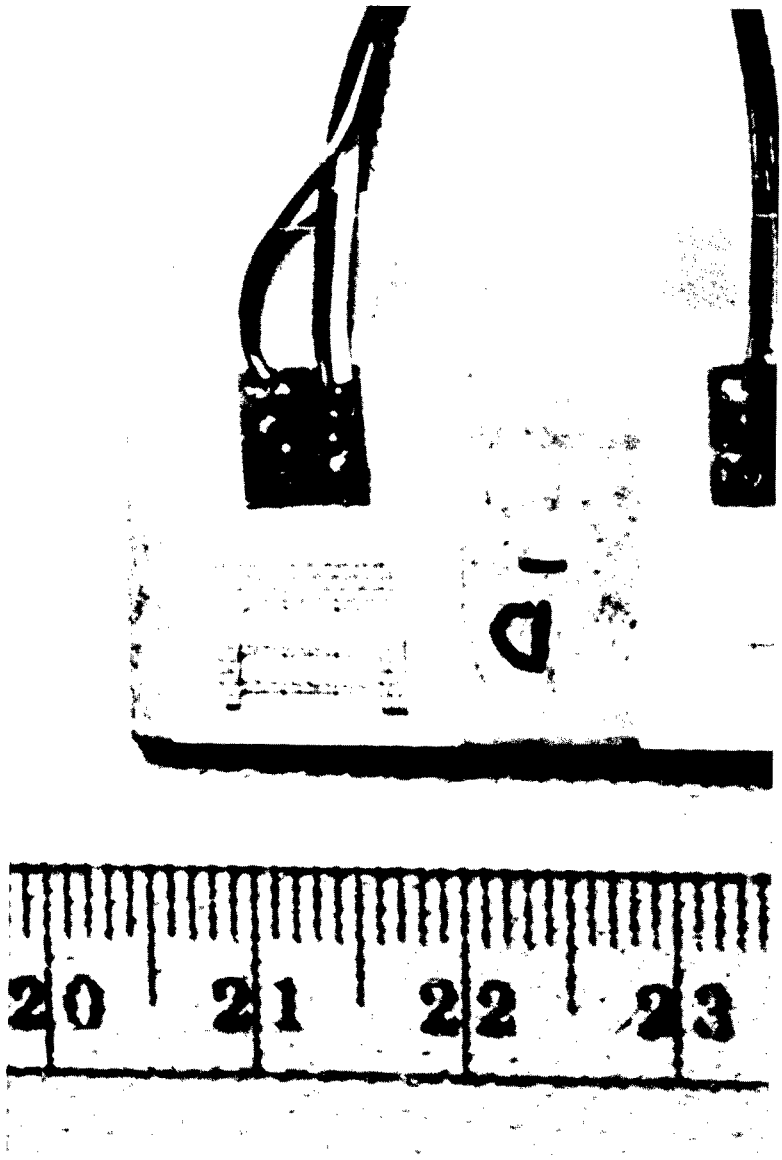

Figure 12.2 Photograph of a Strain Gage Manufactured by HITEC

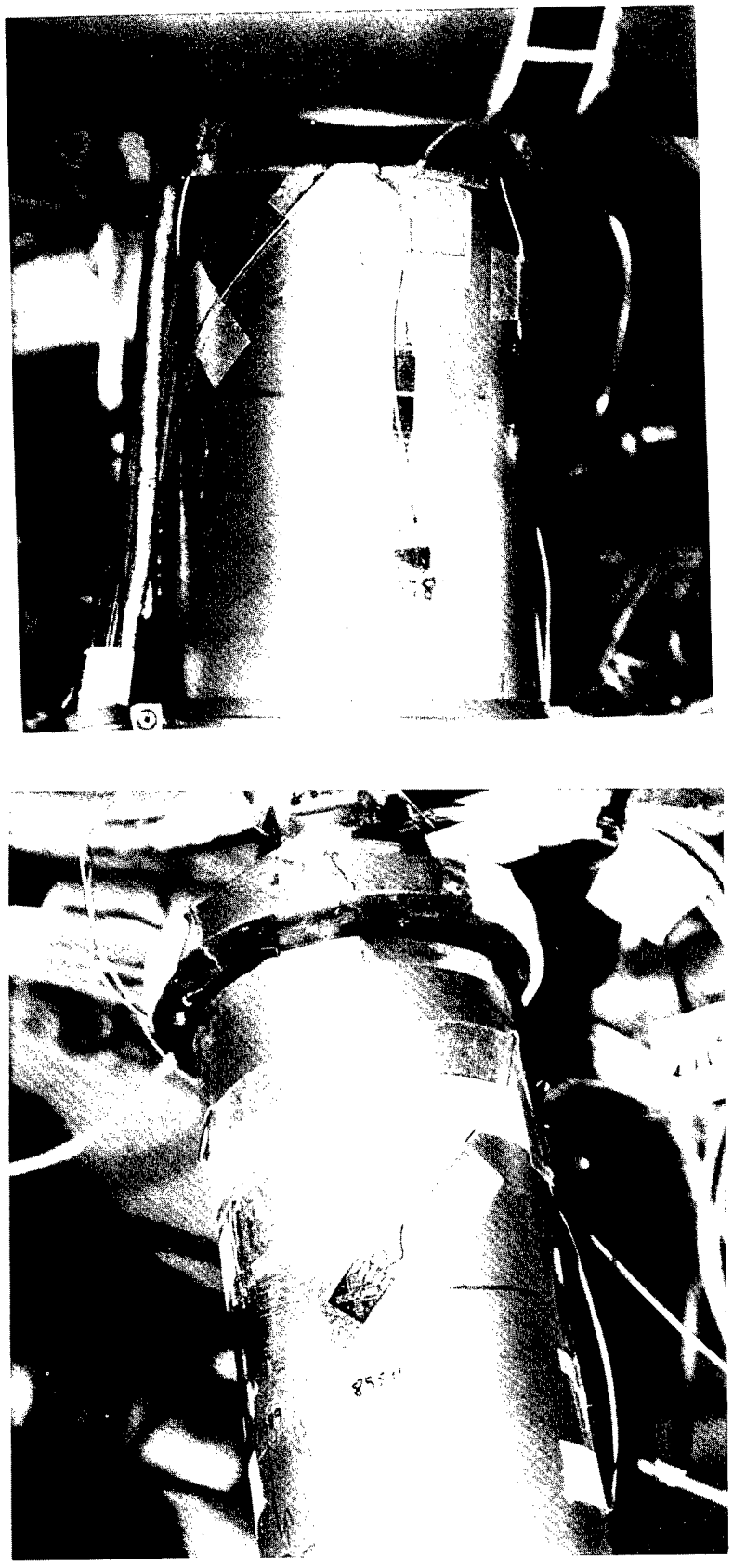

Figure 12.3 Location of Bonded Strain Gages on SSME

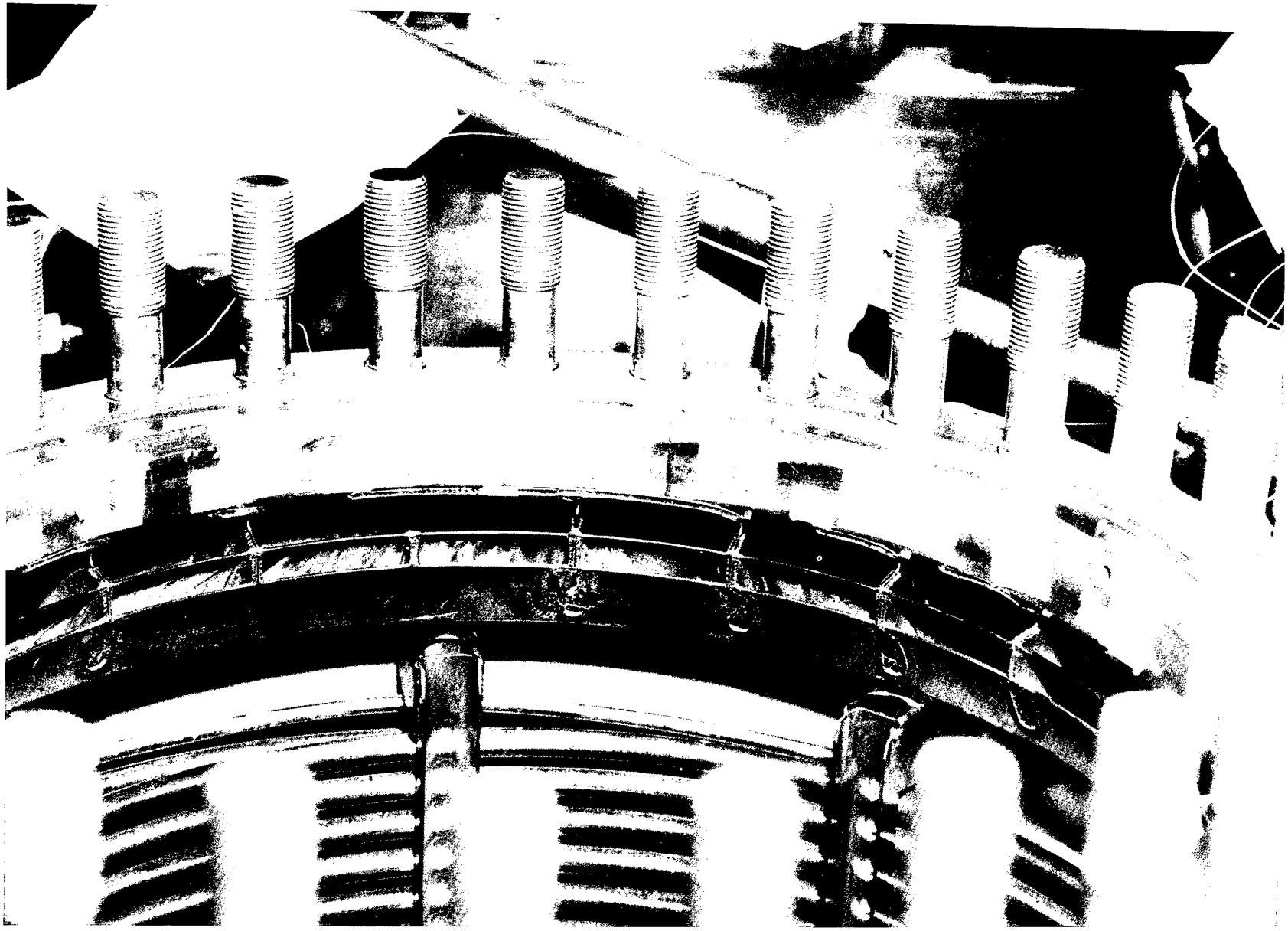

Figure 12.4 Location of Weldable Strain Gages in SSME Turbo Pump

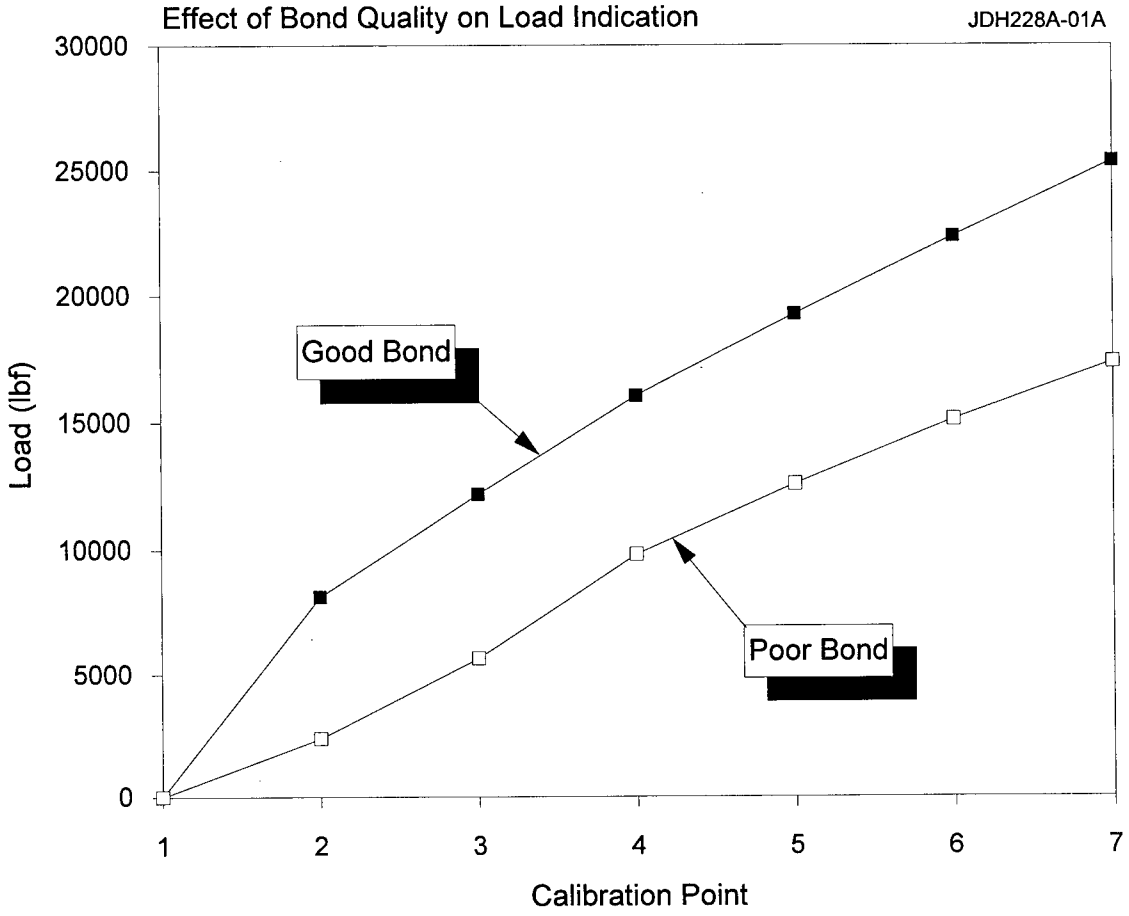

Figure 12.5 Static Response of a Strain Gage for Bonded and Unbonded Situations

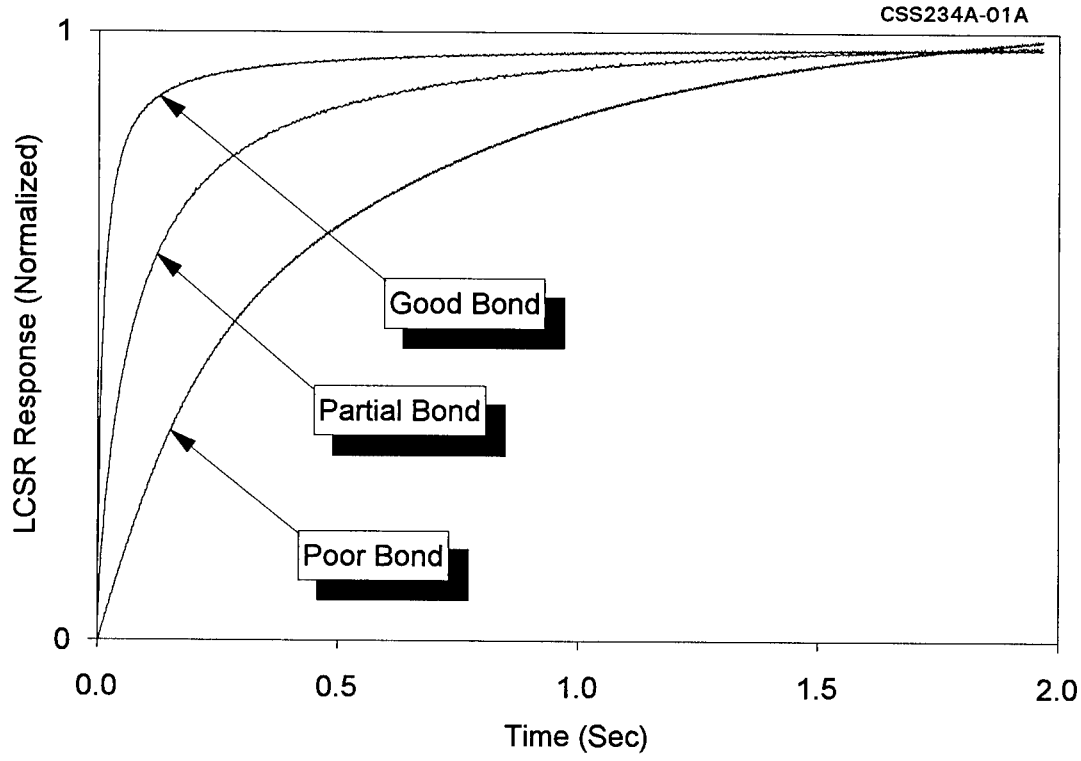

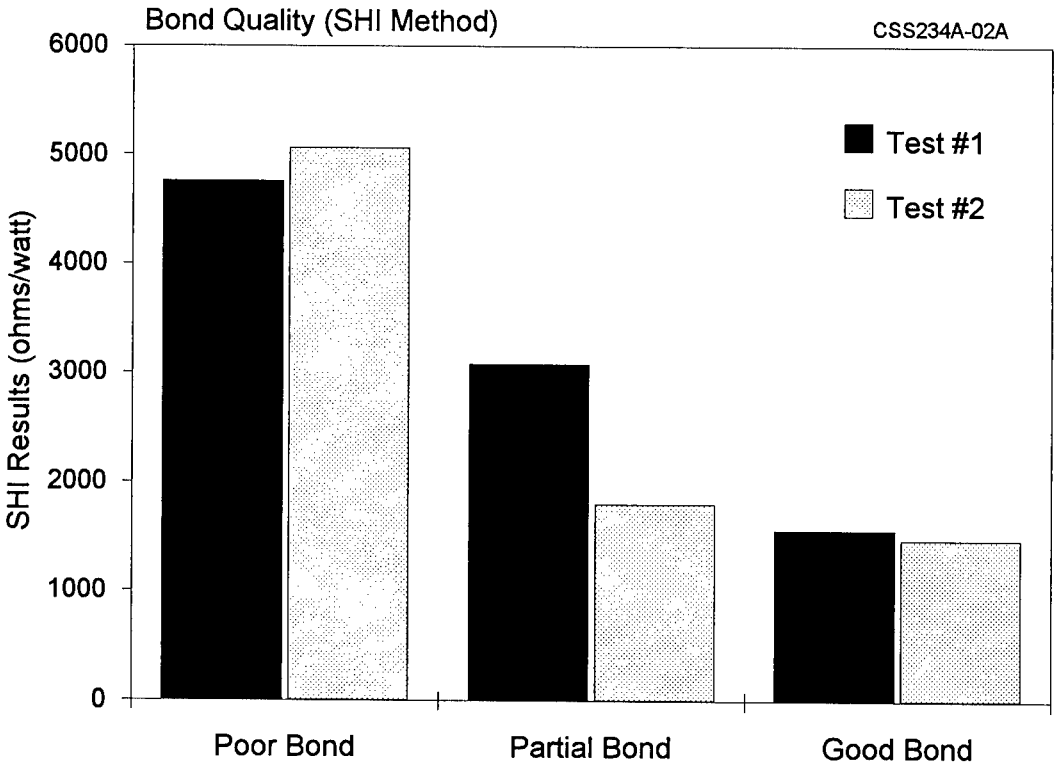

Figure 12.6 Results of Typical Laboratory Tests to Quantify Strain Gage Bonding

more expensive strain gages which were composed of a nickel-chromium alloy fully encapsulated in a glass-fiber-reinforced epoxy phenolic resin. These gages were tested on various materials in both good and bad bond configurations with results showing that the dependance of dynamic response on bond quality is excellent. Figure 12.7 shows typical test results for a number of strain gages that were tested in both fully-bonded and poorly-bonded conditions. The poor bonds were created by intentionally introducing errors into the bonding process. In some cases, the adhesive was not cured at the proper rate or the gage was bonded without using proper surface preparation procedures. In other cases, a small piece of Teflon was placed under the gage during the bonding process and later removed, thus, introducing an air gap between the gage and the host material. The LCSR technique worked well in detecting a poor bond between a strain gage and the host material.

In addition to the bonded resistance type strain gages, high temperature strain gages were tested using the LCSR method. These gages are typically made from platinum or nicrome wire which is directly affixed to the material substrate with a ceramic cement. The bonding process used for high temperature strain gages is much more difficult and not as repeatable as that for bonded resistance type foil gages. After the initial surface preparation, the substrate is coated with 2 to 3 mils of nickel aluminide followed by a 3 to 5 mil Rokide sprayed aluminum oxide coating (precoat). The platinum or nicrome wire is then placed on the aluminum oxide coating and covered with an additional coating of Rokide to hold the sensor in place. This bonding process is shown in Figure 12.8. It has been determined that repeatability problems in bonding of strain gages to solid materials can easily result in 1 - 2 mil of variations in coating thickness (mil is 1/1000"), and make a difference in the strain gage output.

LCSR tests were performed on four high temperature gages with varying precoat

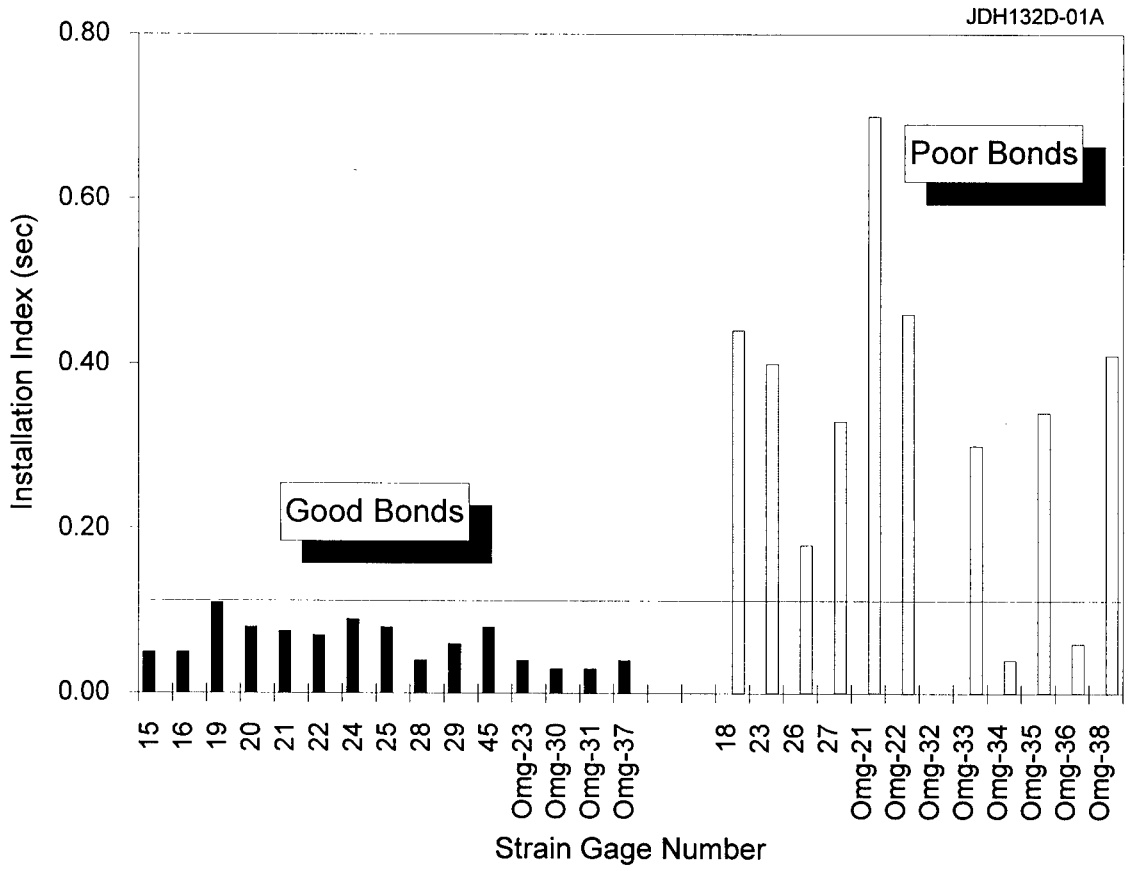

Figure 12.7 LCSR Results for a Number of Gages that were Tested in Fully Bonded and Partially Bonded Configurations

AMS-DWG NAS034A

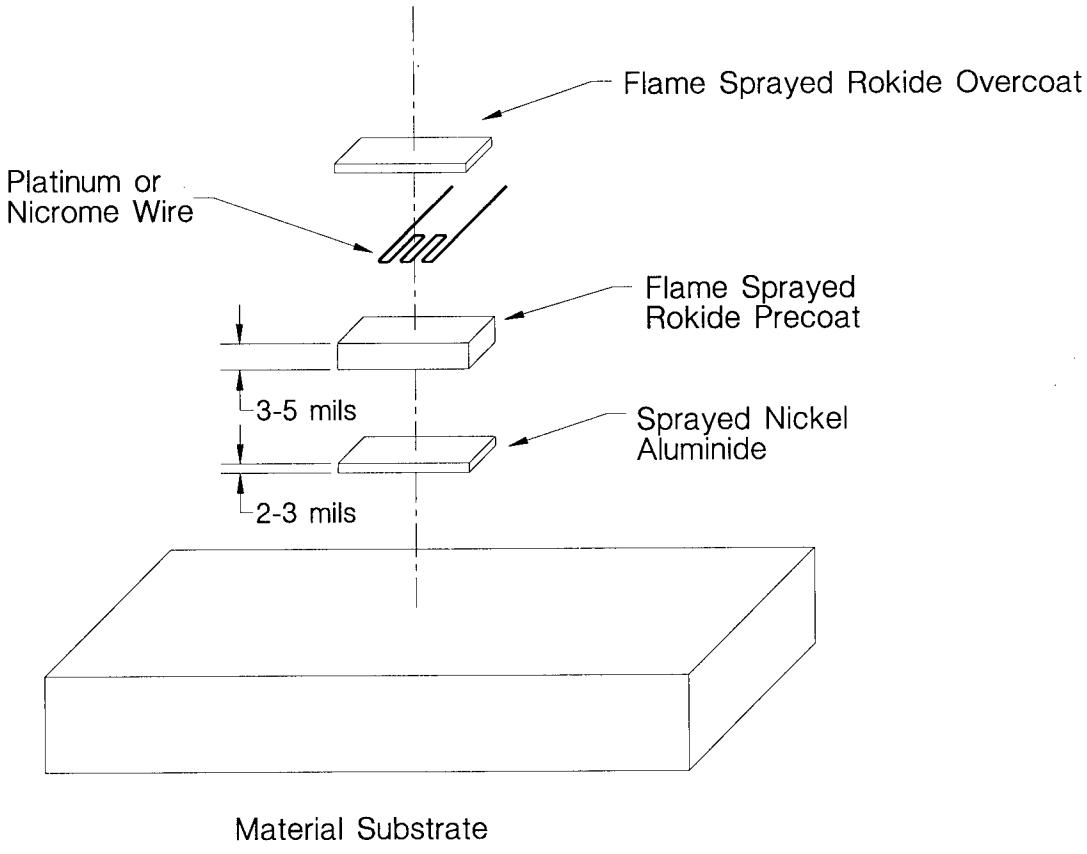

Figure 12.8 Illustration of Bonding Process for High Temperature Strain Gages

thicknesses and overcoating voids (Figure 12.9). The gages were provided by HITEC Corporation along with a description of the bond quality for each gage. Gage A was a good installation with a 5 mil precoat. Gage B was a good bond with a 3 mil precoat. Gage C was installed with encapsulation voids deliberately created around the strain gage filaments, and Gage D was an uninstalled gage taped to the test specimen. The results are summarized in Table 12.1. Gage A, which had a 5 mil precoat, exhibited an installation index of 0.19 seconds. Gage B had a 3 mil precoat and an installation index of 0.06 seconds. Gage C had voids around the strain gage filament which normally would increase the dynamic response but the Rokide precoat was only 2 mils thick resulting in an installation index of 0.10 seconds. The last gage, D, was very different from the other gages. In particular, Gage D had an inverse output (Figure 12.10), and an installation index of 0.66 seconds.

12.3 Effect of LCSR Test on Calibration of Strain Gages

To verify that the LCSR test does not normally alter the calibration of strain gages, two material samples were instrumented with several strain gages and calibrated before and after LCSR testing. Figure 12.11 shows the two instrumented blocks. The samples were loaded using the Instrom tensile testing equipment at the University of Tennessee. The samples were compressively loaded from 0 to 14,000 lbs while data was acquired in 2000 lb intervals. The calibration was performed twice to establish repeatability. After initial calibrations, the blocks were LCSR tested repeatedly using DC currents of up to 90 mA. The samples were then post-calibrated and the results were compared to the initial calibrations. Figure 12.12 shows that the accuracy of the post-calibration is within the repeatability of the calibration. Therefore, it was concluded that the LCSR test does not normally alter the calibration of strain gages. Additional strain gage calibration data before and after LCSR testing is shown in Figure 12.13.

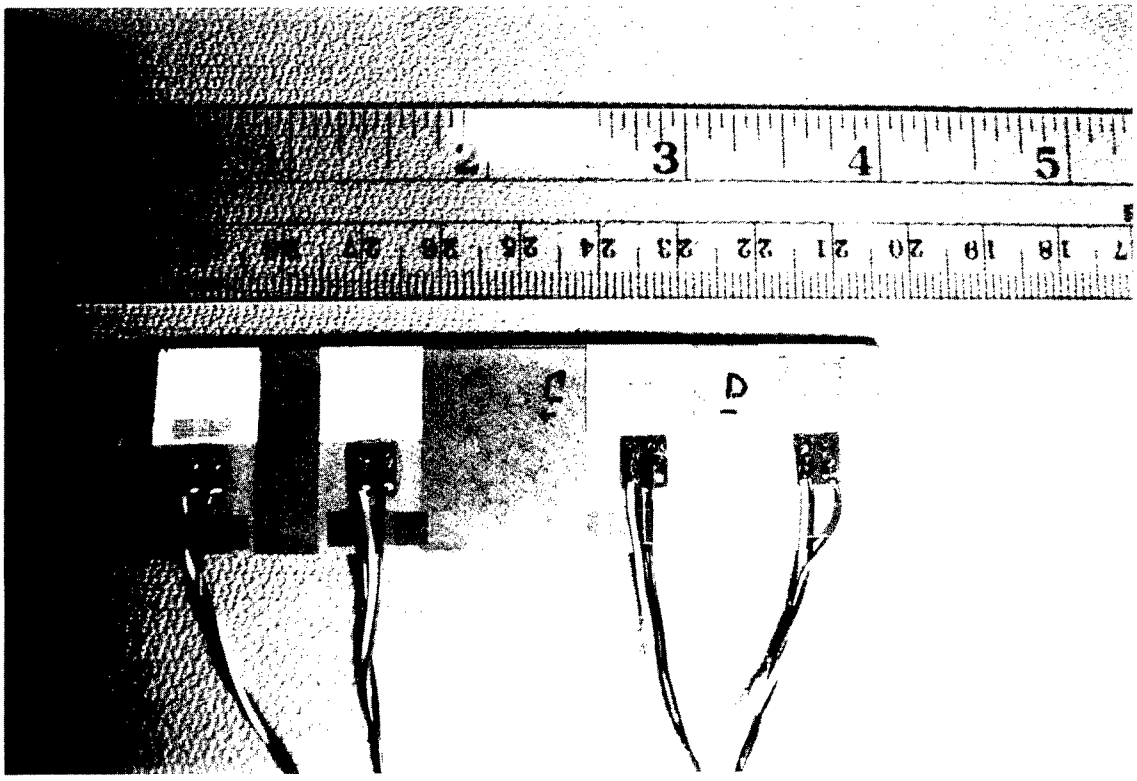

Figure 12.9 Photograph of High Temperature Strain Gages

TABLE 12.1

Results of LCSR Testing of High Temperature Strain Gages

Gage I.D.	Precoat Thickness (mil = 1/1000 inch)	Installation Index (sec)
Gage A	5	0.19
Gage B	3	0.06
Gage C	2	0.10
Gage D	N/A	0.66

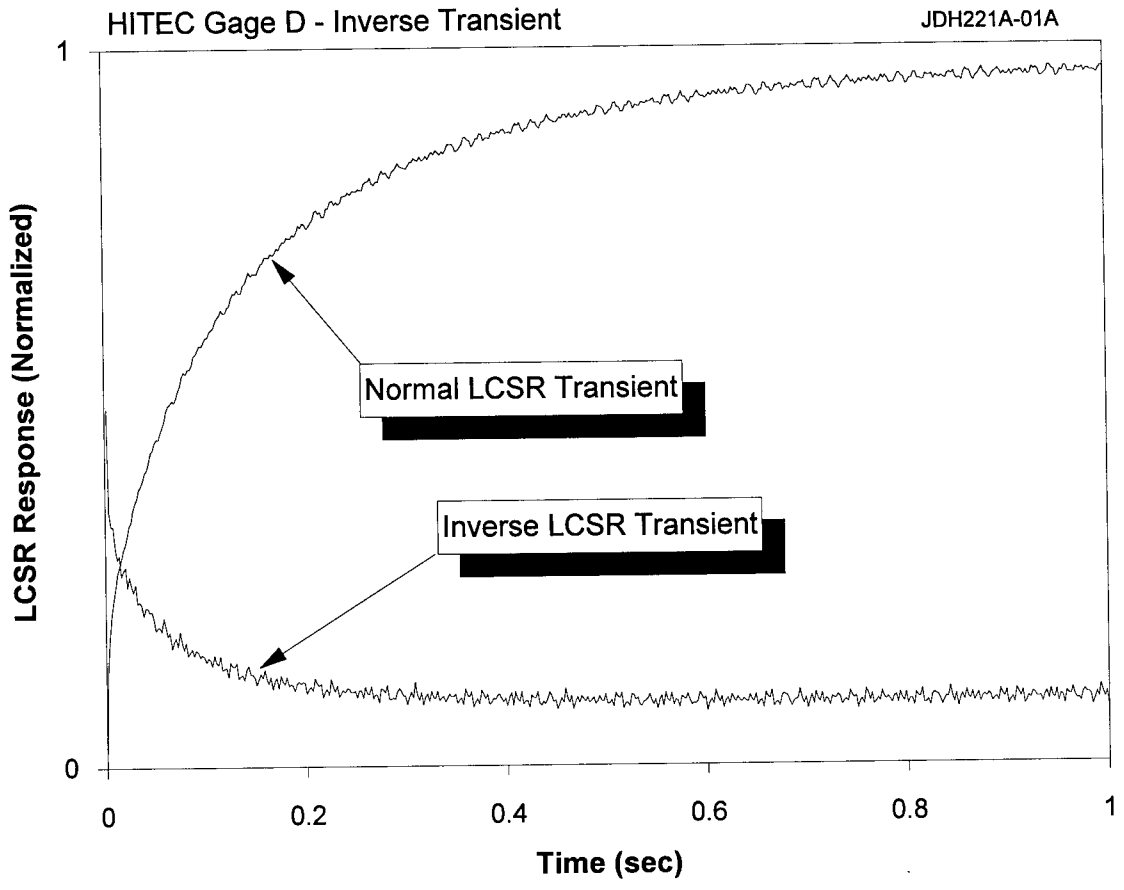

Figure 12.10 Normal and Reversed LCSR Transients for Strain Gages

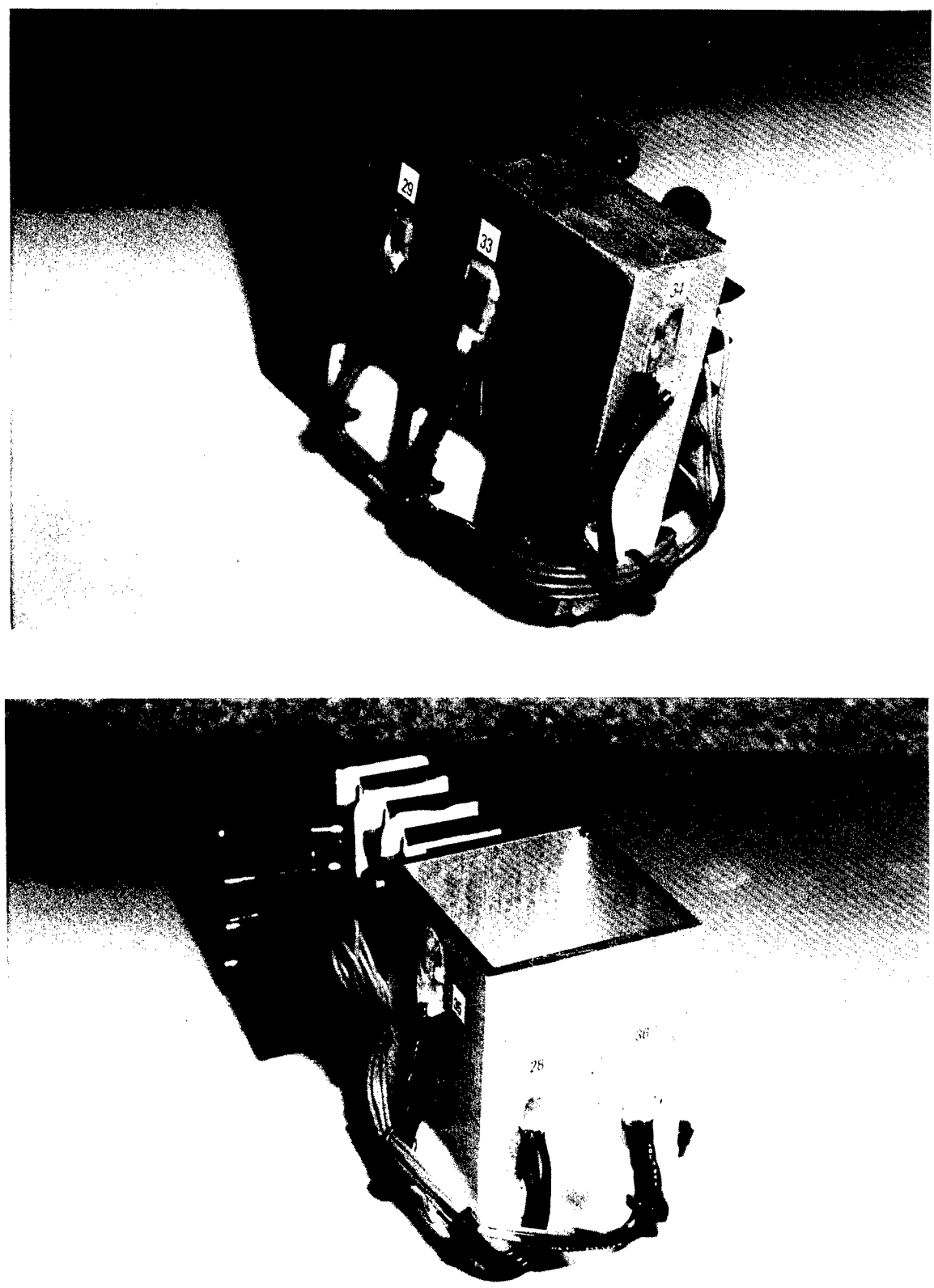

Figure 12.11 Instrument Blocks for Testing the Calibration of Strain Gages Before and After LCSR Tests

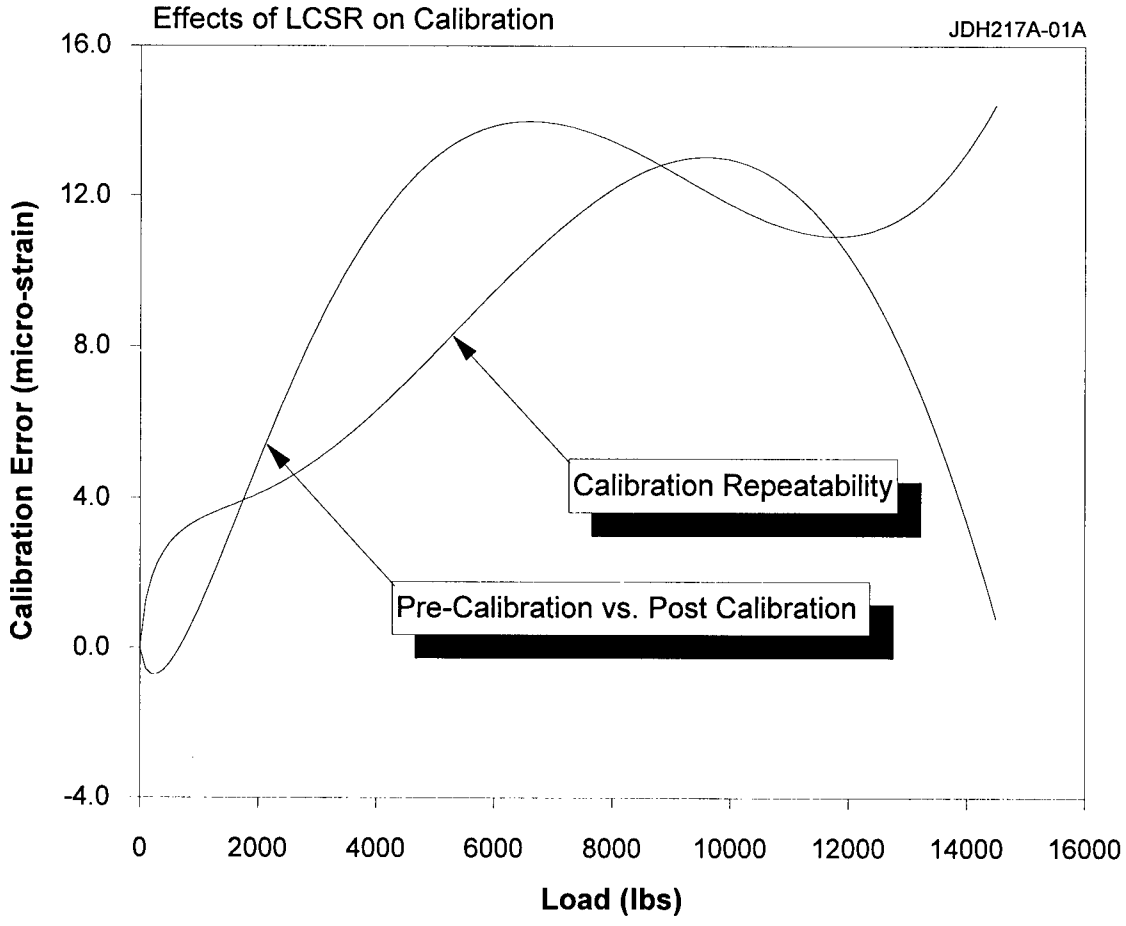

Figure 12.12 Difference Between Calibration of Strain Gages Before and After LCSR Tests. The Strain Gage Calibration Repeatability is Also Shown for Comparison.

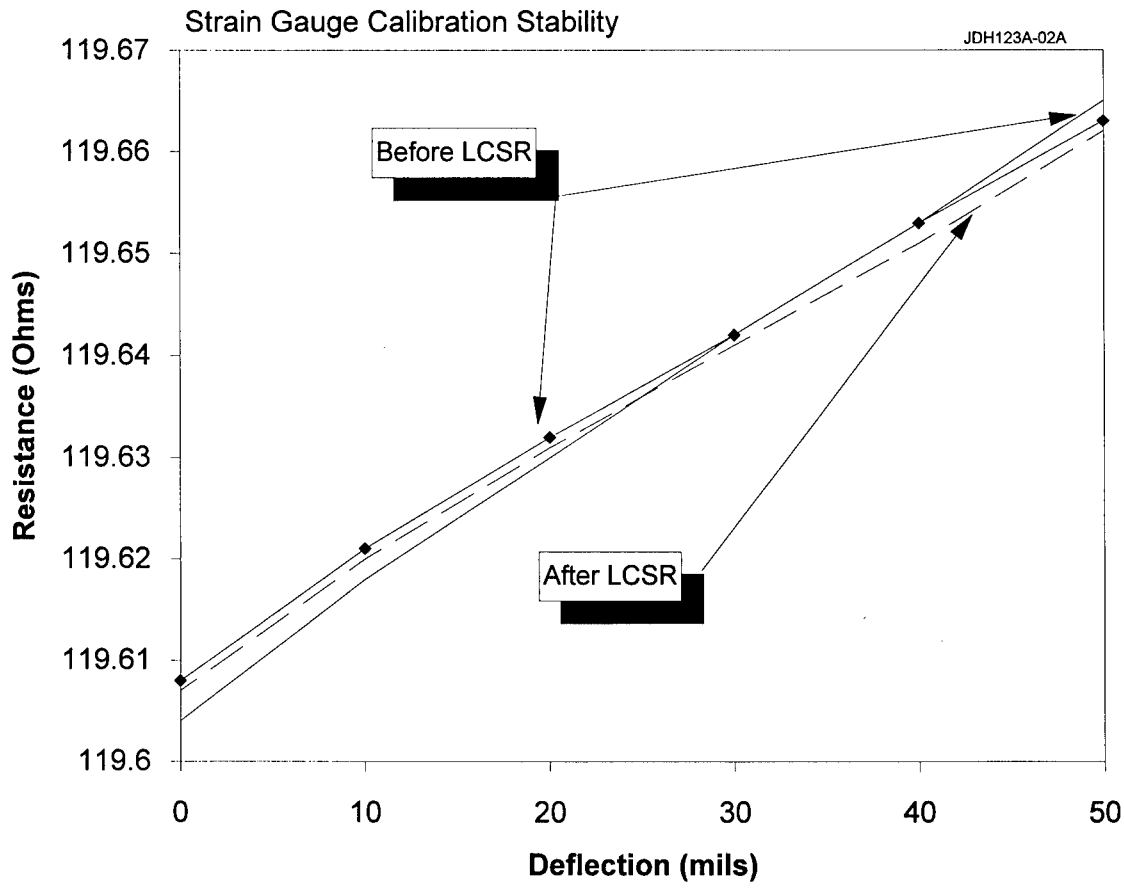

Figure 12.13 Strain Gage Calibration Curves Before and After LCSR Testing

13. TESTING RTDs AND STRAIN GAGES AT MSFC

Field trips were made to MSFC to test RTDs and strain gages to determine bonding quality. More specifically, the following laboratory and field tests were performed in cooperation with MSFC: 1) testing of RTDs as mounted on SSME anti-flood lines, 2) laboratory testing of RTDs and strain gages that were attached to a specially prepared anti-flood line, and 3) examination of Cryogenic Linear Temperature Sensors (CLTS). A major facility at MSFC that was used in this project was the Technology Test Bed (TTB). This is a rocket test-stand facility used for testing various components of SSMEs. Figure 13.1 is a photograph of TTB. AMS tested RTDs and strain gages as installed on a test SSME mounted on the TTB (Figure 13.2).

13.1 RTD Testing

Three Rosemount/RocketDyne model 118AUL-1 110Ω, flight-qualified, thin-film RTDs were tested including two (PID-1420A, PID-1421A) that were attached to an AFL recently removed from an SSME, and an unattached sensor (HJ80) that was still in its Rosemount shipping package. Figure 13.3 shows the removed AFL.

Insulation Resistance (IR) measurements were first made on all three sensors. The results for sensors PID-1420A, PID-1421A, and HJ80 were 2.0 GΩ, 100.0 MΩ, and 90.0 GΩ, respectively. These results are well above the Rosemount IR specification of 10.0 MΩ. Resistance measurements on PID-1421A showed an open circuit.

Following the IR and resistance measurements, LCSR and SHI tests were conducted on PID-1420A and HJ80. The results are shown in Figure 13.4 in terms of LCSR transients and self

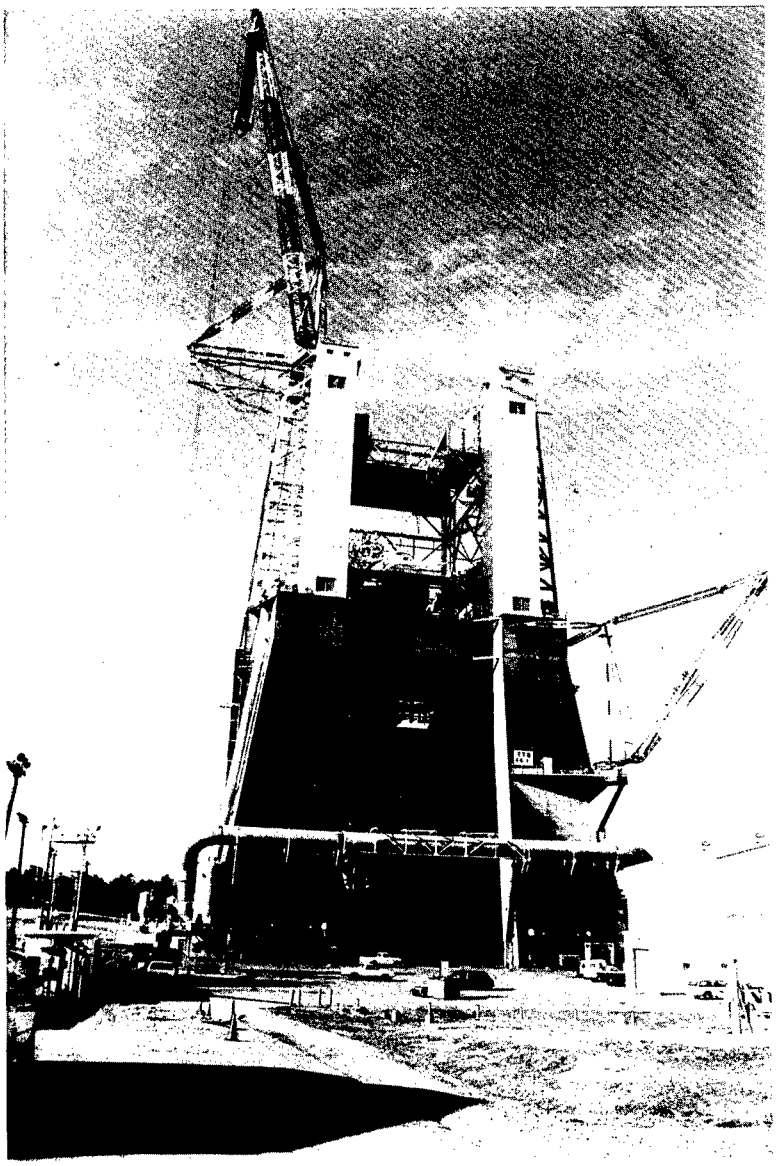

Figure 13.1 Photograph of TTB at MSFC

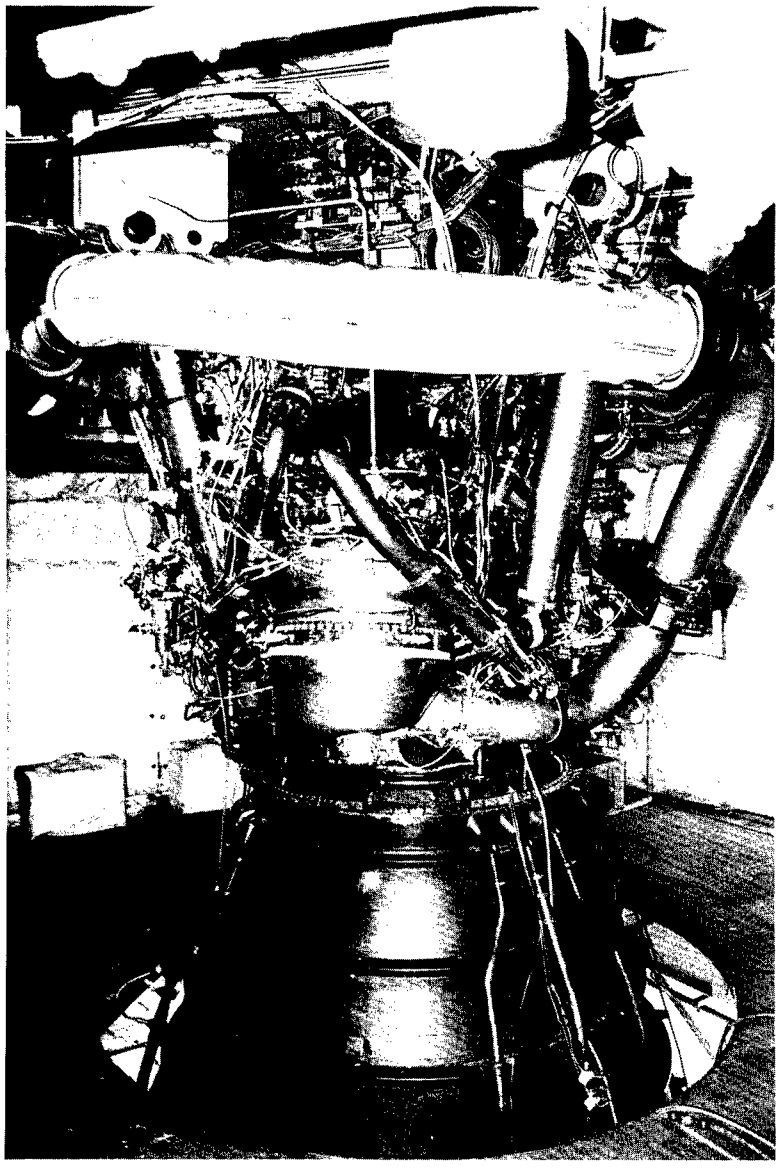

Figure 13.2 Photograph of an SSME That Was Installed in TTB

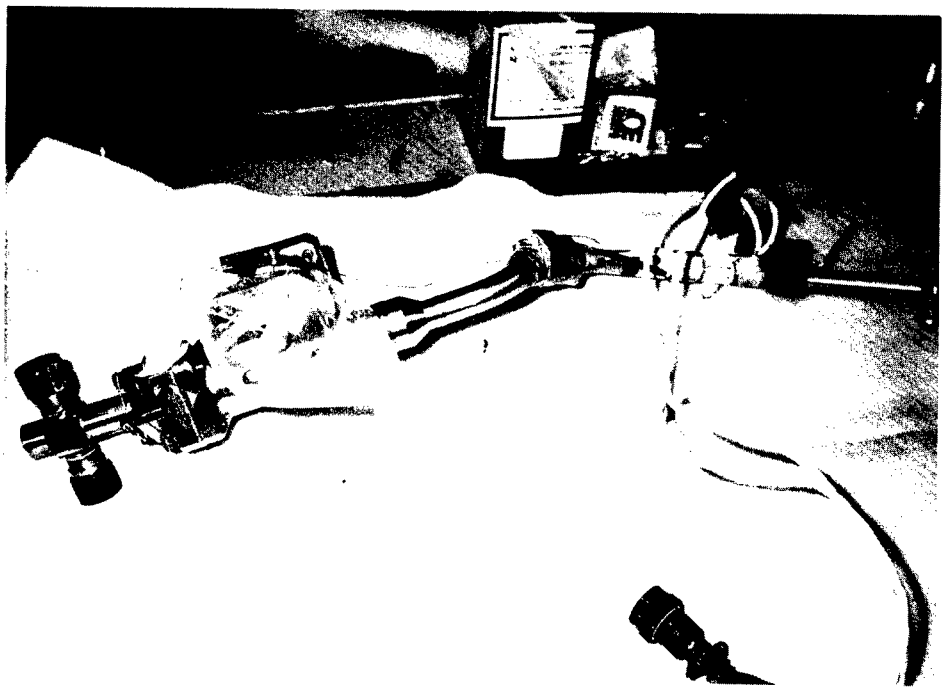

Figure 13.3 Photograph of an Antiflood Line Used in SSMEs

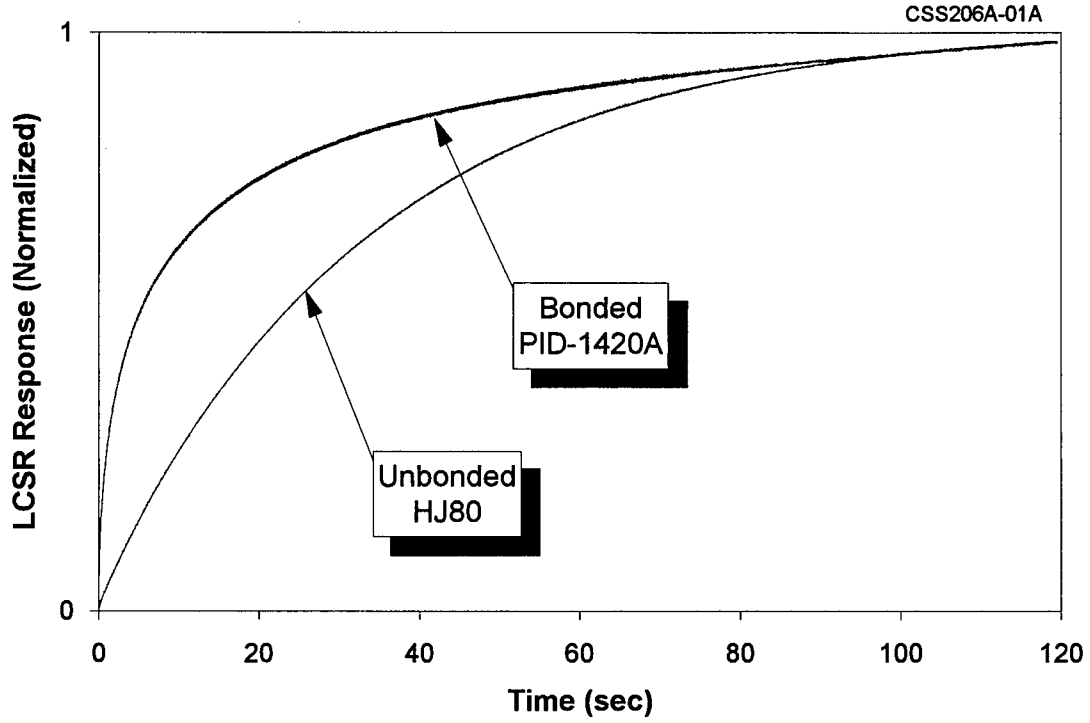

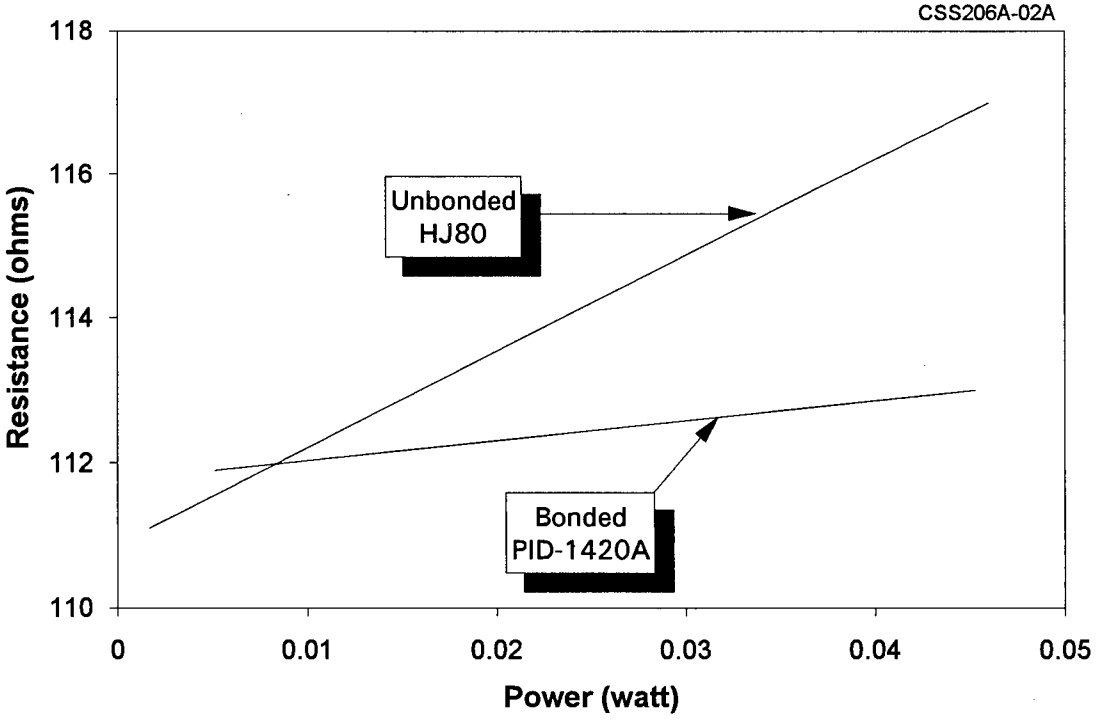

Figure 13.4 LCSR and Self Heating Test Results of SSME RTDs

heating curves. In a more recent field test, several surface-mounted RTDs were tested at MSFC as they were attached to two AFLs. One of the AFLs, #2, was installed on the SSME in preparation for a firing test, while the other AFL, #1, had been removed from the SSME. A pair of surface-mounted Rosemount/RocketDyne model 118AUL-1 RTDs were attached to the AFL #2. Figure 13.5 shows LCSR transients for the two RTDs. The high frequency noise on the LCSR signals is attributed to SSME test electronics. The difference in the two LCSR transients is small indicating that the two surface-mount RTDs had comparable installations.

In addition to the two RTDs on AFL #2, sensor 1420A was tested as it was attached to AFL #1. In an earlier AMS field trip to MSFC, this RTD was LCSR tested before an engine firing test. The retest of this RTD enabled AMS to analyze the bonding ramifications of a firing test. Figure 13.6 shows the pre-firing and post-firing results. A small change in the degree of bonding is evident in the results. The change could have occurred when the sensor was exposed to the harsh environment of an engine test, or in handling of the RTD during the installation or removal of AFL #1. Without the reinforcement of the SHI results, the small difference in the LCSR transients of sensor 1420A would have probably been attributed to repeatability. Therefore, the self heating test should be used in conjunction with the LCSR test when it is necessary to resolve small changes in bonding of RTDs to solid materials.

13.2 Strain Gage Testing

Two Micro-Measurements type WK-13-062AP-350 (Tag #8886 and Tag #8887) gages located on the main injector, and two M-M type WK-13-500AF-350 (Tag #8582 and Tag #8589) gages located on the support arm of the SSME were LCSR tested at MSFC. Figure 13.7 shows typical results. The support arm gages were tested using LCSR parameters similar to those used

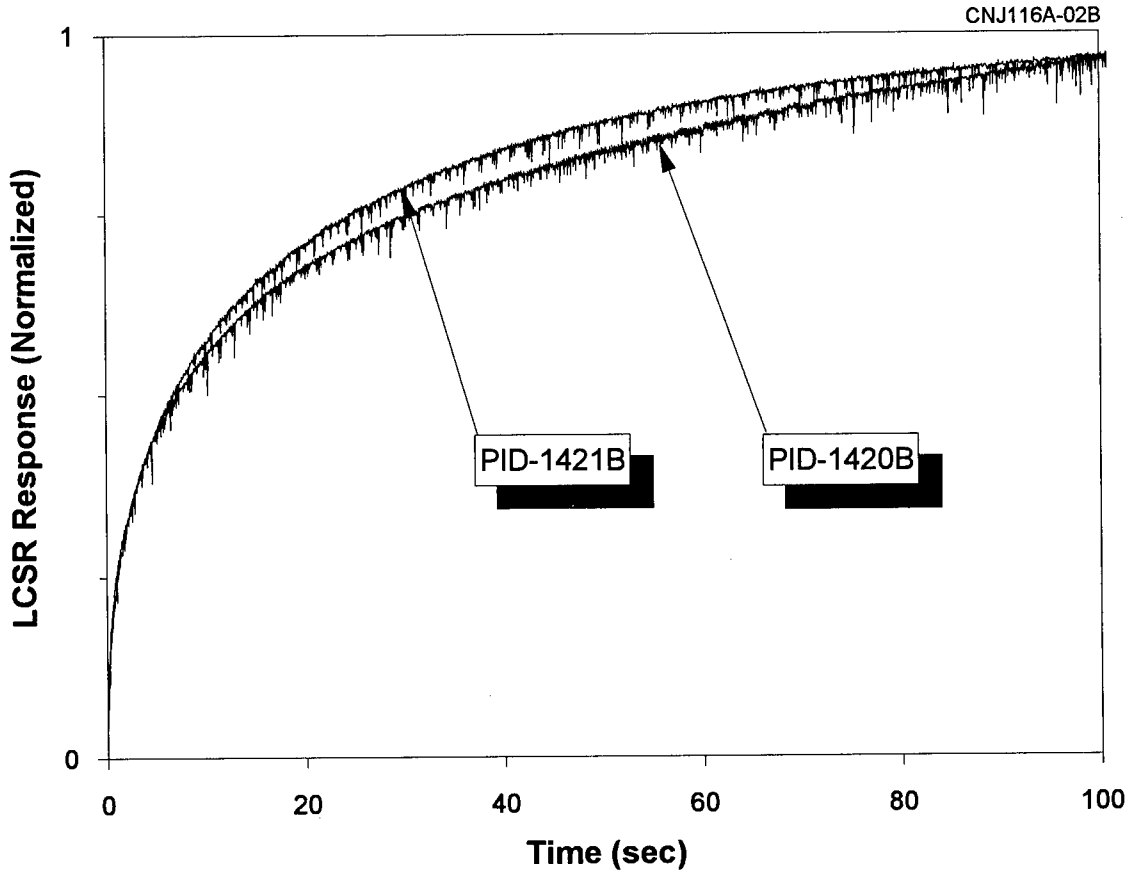

Figure 13.5 Results of LCSR Testing of RTDs on SSME

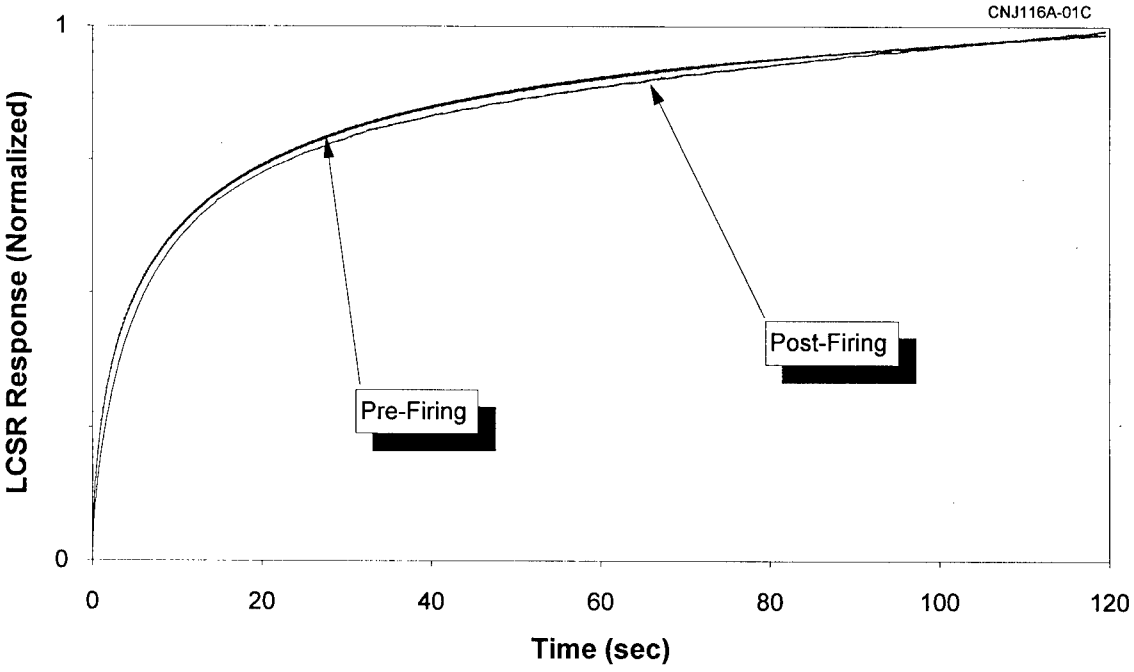

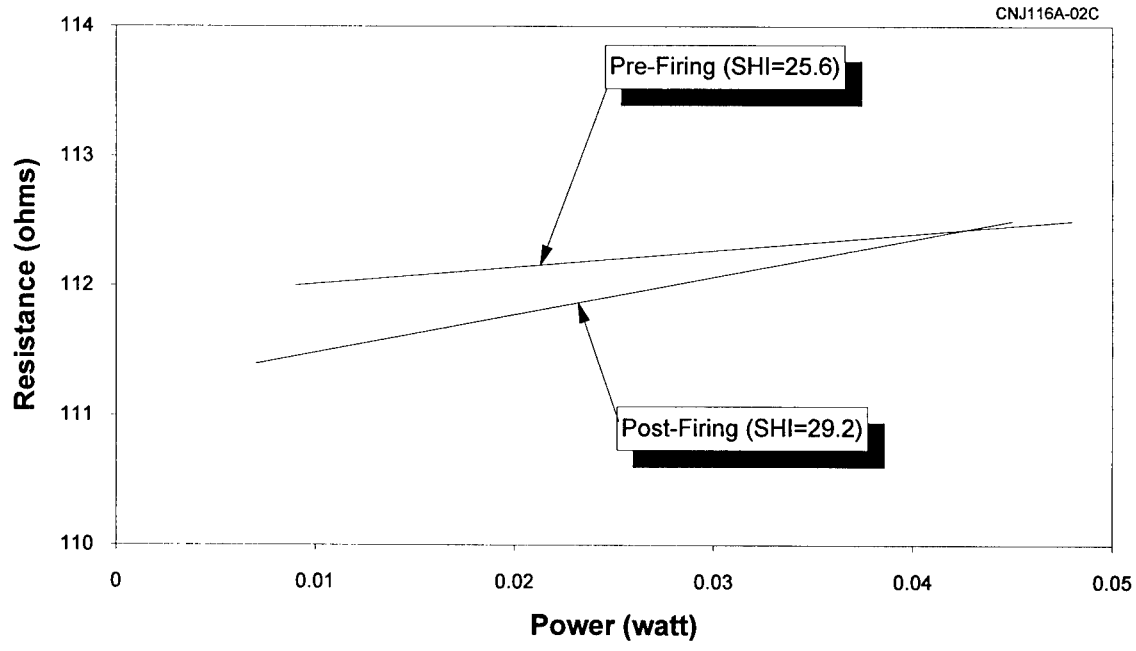

Figure 13.6 LCSR and Self Heating Curves of RTD PID-1420A in AFL #1 Before and After Engine Firing Tests

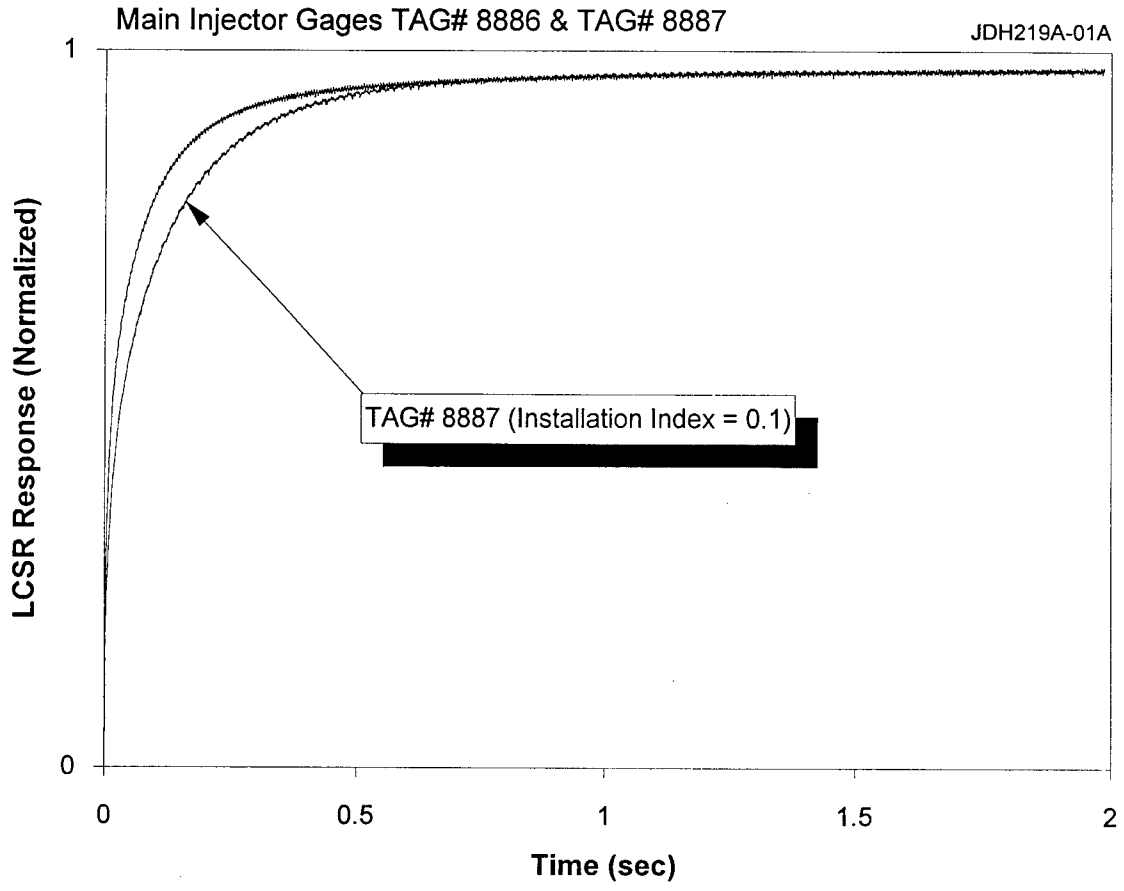

Figure 13.7 Results of LCSR Testing of Strain Gages on a Test Bed SSME

for the main injector gage tests. Strain gage #8582 had an installation index of 0.07 seconds indicative of a good bond, while sensor Tag #8589 had an index of 0.16 seconds indicative of a poor bond.

13.3 Testing of RTDs and Strain Gages on a Spare AFL

A specially prepared AFL (#3) was provided to AMS by NASA/MSFC for laboratory tests. The AFL was instrumented with a pair of Rosemount/RocketDyne 118AUL-1 RTDs (designated as A and C) mounted radially at one location and four Micro-Measurements strain gages (designed as 1 through 4) mounted radially in a separate location on the AFL. LCSR and self heating tests were performed on these RTDs with typical results shown in Figure 13.8 for the RTDs and Figure 13.9 for the strain gages. Two of the four strain gages (#1 and #2) had open circuits and were thus not testable. RTDs A and C exhibited very similar dynamic response indicating similar installation qualities. SHI values were also indicative of very similar installation qualities for sensors A and C.

13.4 Testing of CLTS

NASA provided AMS with two CLTSs for laboratory testing. The CLTSs are small, surface-thermometer gages consisting of a thin foil sensing grid laminated into a glass-fiber reinforced epoxy-resin matrix, and electrically connected in series. These sensors are very desirable because of their low thermal mass, thin construction (0.10 mm), and good linearity at low temperatures (-452°F to 150°F). CLTSs are also very stable.

The CLTS sensors provided to AMS for the laboratory tests had been attached by NASA to a small cylindrical sample of graphite composite. Figure 13.10 shows LCSR transients for the

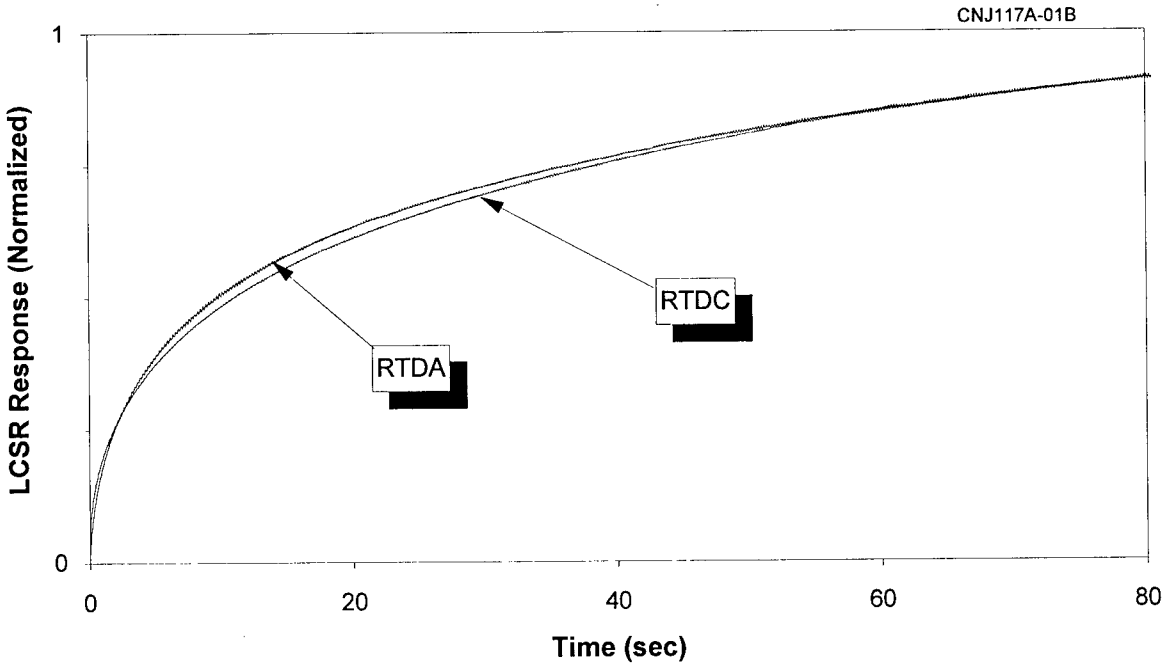

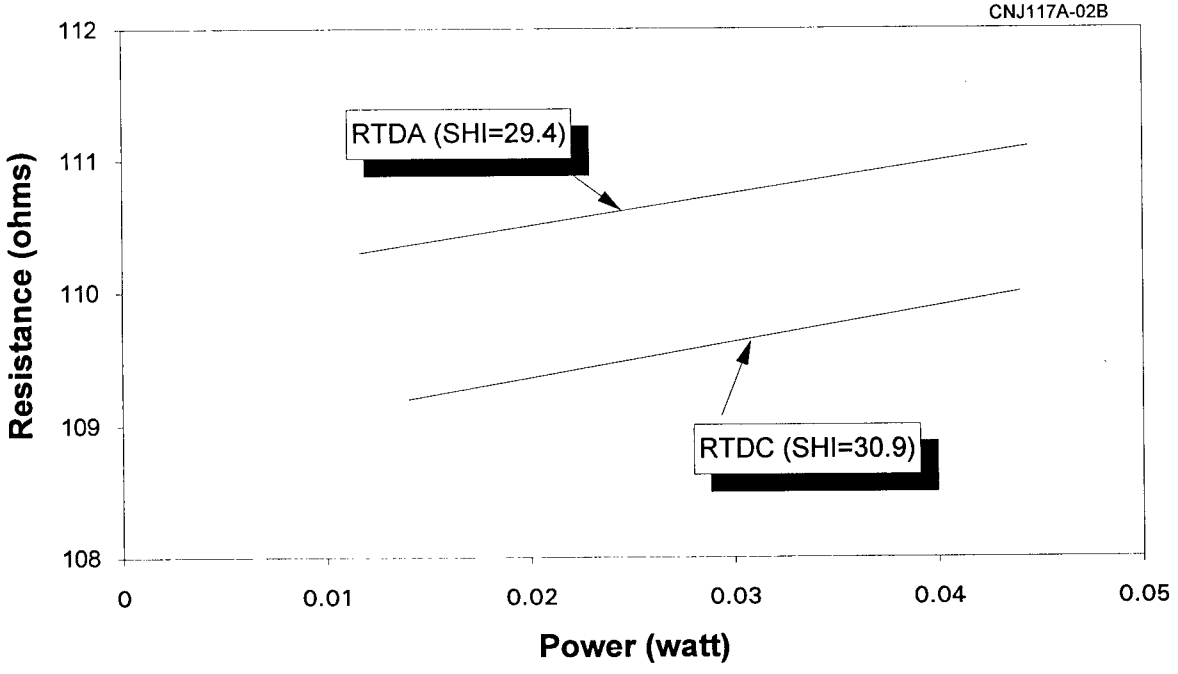

Figure 13.8 LCSR Transients for Radially Mounted RTDs on AFL #3

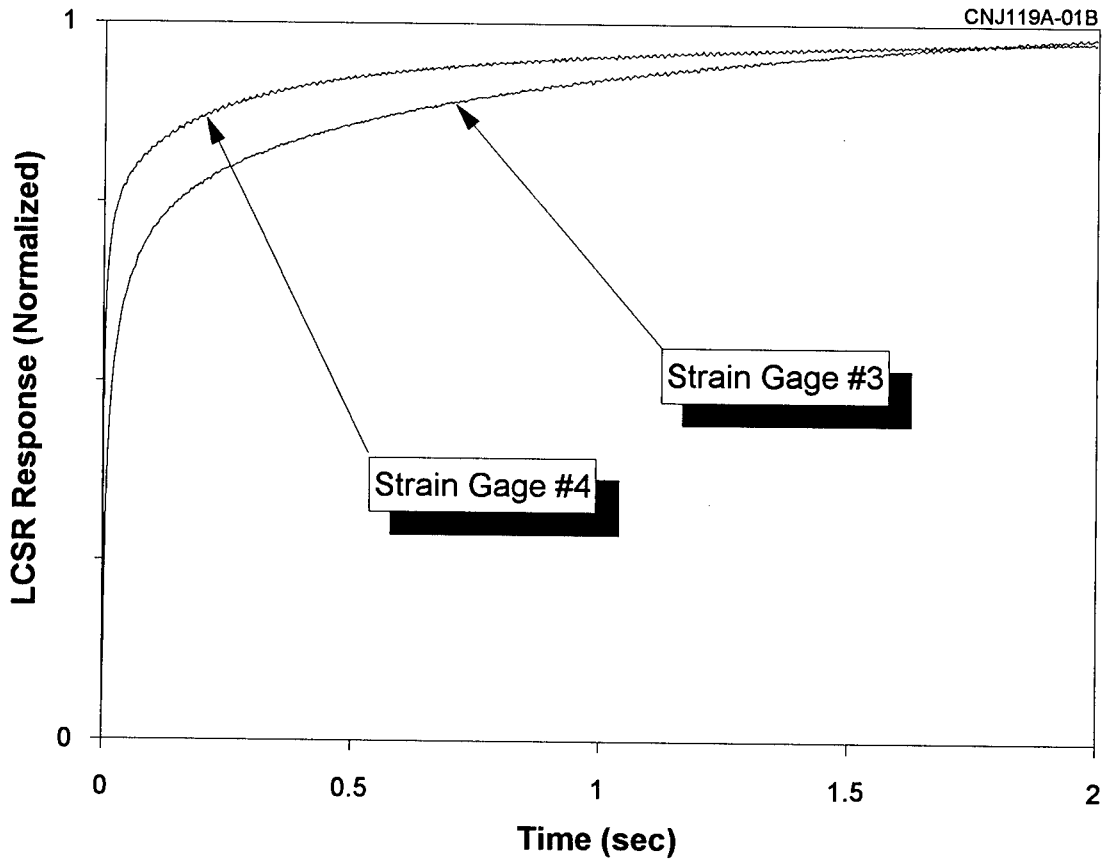

Figure 13.9 Dynamic Response of Radially Mounted Strain Gages on AFL #3

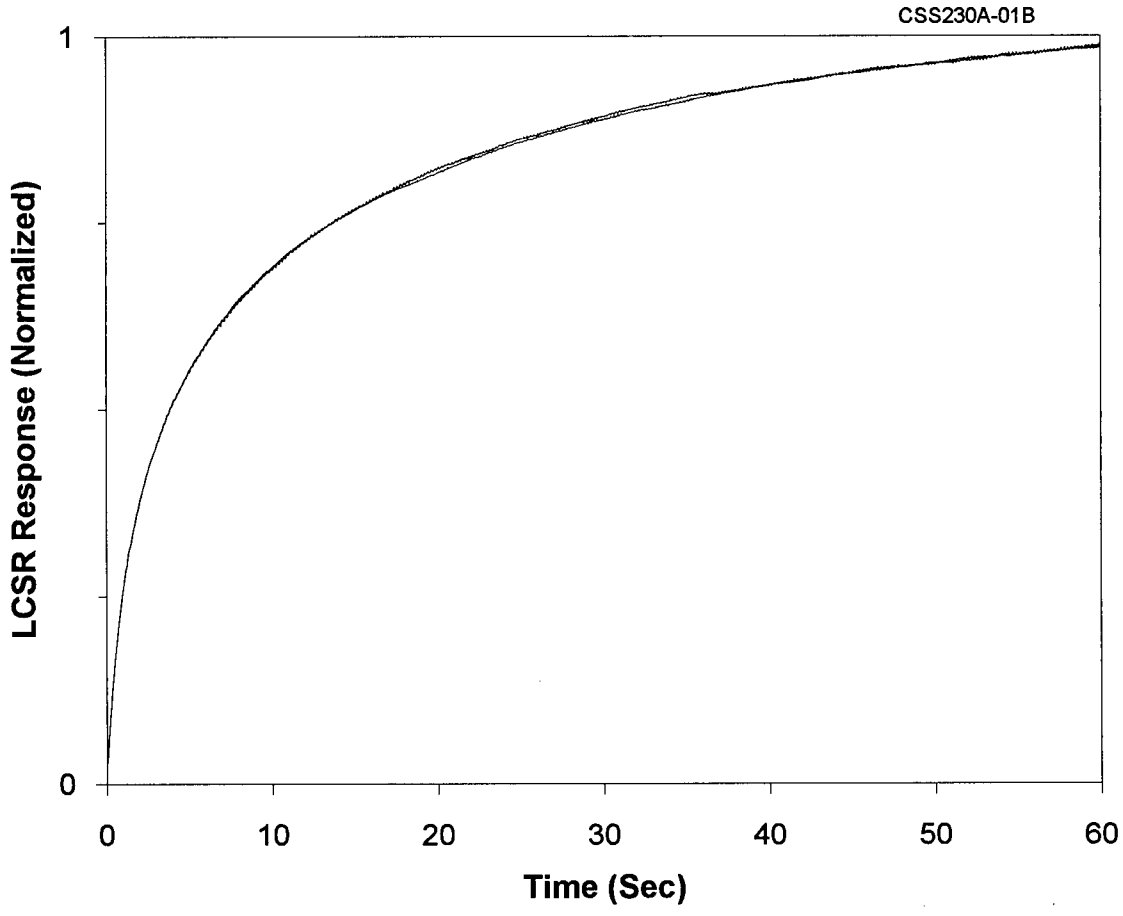

Figure 13.10 LCSR Response of Cryogenic Linear Temperature Sensors

two CLTS sensors as tested in the AMS laboratory. The two LCSR signals, which are superimposed in Figure 13.10, were obtained using 16.5 mA of DC current. The two sensors exhibited almost identical dynamic characteristics. From the limited laboratory tests performed here, it appears that the CLTS sensors are LCSR testable.

14. EVALUATION OF THERMAL COMPOUNDS

Thermal compounds such as Boron Nitride are used in installation of thermocouples in solid materials. The purpose of the compound is to fill up any air gap between the thermocouple and the solid material and minimize the lag in transient temperature measurements.

In some nuclear power plants, a thermal compound called Never-Seez was once used in the thermowells of the reactor coolant RTDs to improve the response time. It was later discovered that Never-Seez could loose its excellent thermal properties at high temperatures (greater than 500°F) and cause the RTD response time to increase. As such, the use of Never-Seez for RTD response time enhancement is no longer prevalent in nuclear power plants.

The effect of temperature on thermal properties of eight thermal compounds were investigated in this project. This investigation involved the LCSR method. The method was used to measure the response time of an RTD as installed in each of the eight compounds at temperatures of up to 1000°F. The goal of the laboratory tests was to determine: (1) how the heat transfer characteristics of thermal compounds affect the response time of a temperature sensor, and (2) how thermal compounds react at high temperatures.

Furthermore, a survey of several manufacturers and users of thermal compounds was performed to: (1) identify the current problems and solutions, (2) discuss how thermal compounds are used in various applications, and (3) identify optimum mounting techniques. The results of these efforts are discussed below.

14.1 Laboratory Testing of Thermal Compounds

Eight thermal compounds that may be used in the installation of thermocouples and other sensors in solid materials were tested. Table 14.1 lists the eight compounds and their temperature specifications as provided by the manufacturers. One of the compounds, the GIT (Gallium-Indium-Tin), was obtained from the Oak Ridge National Laboratory (ORNL). This is a patented material that is intended for a number of applications which include using it as a thermal compound to improve the response time of thermowell-mounted RTDs and thermocouples. No temperature data was available for this compound. Figure 14.1 shows a photograph of the eight compounds that were tested in this project.

LCSR tests were performed on an RTD as installed in each compound. The tests were performed with the compound at various temperatures starting with room temperature and extending to 1000°F in 200°F increments. The test results are shown in Figure 14.2. These results indicate that temperature either does not change the thermal characteristics of these compounds or improves them. The reductions in the LCSR results indicates that these compounds become better heat transfer agents at higher temperatures. It should be pointed out, however, that long-term exposure to high temperatures may reverse the heat transfer ability of the compounds and cause the response time to increase.

Further evaluation of test results in Figure 14.2 illustrates the temperature dependency of thermal conductivity of each compound. The 70°F and 200°F bar charts show that the ORPAC yielded the fastest dynamic response and ECHOTEMP produced the slowest response. For 400°F and 800°F data, the GIT produced the fastest response while ECHOTEMP was still the slowest. At 800°F, the fastest response was produced by PYROGEL and the slowest by TJC

TABLE 14.1

Listing of Thermal Compounds Tested in this Project

ITEM	THERMAL COMPOUND	MAXIMUM TEMPERATURE
1	(GIT) Gallium-Indium-Tin	Not Available
2	(TJC) Thermal Joint Compound	100°F
3	Omegatherm	392°F
4	Sonotemp	900°F
5	Never-Seez - Pure Nickel Special	2,600°F
6	Echotemp	1,200°F
7	Pyrogel Grade 100	500°F
8	Alumina Based Paste (ORPAC)	1,600°F

Figure 14.1 Samples of Thermal Compound Tested for Thermal Characteristics and Temperature Tolerance

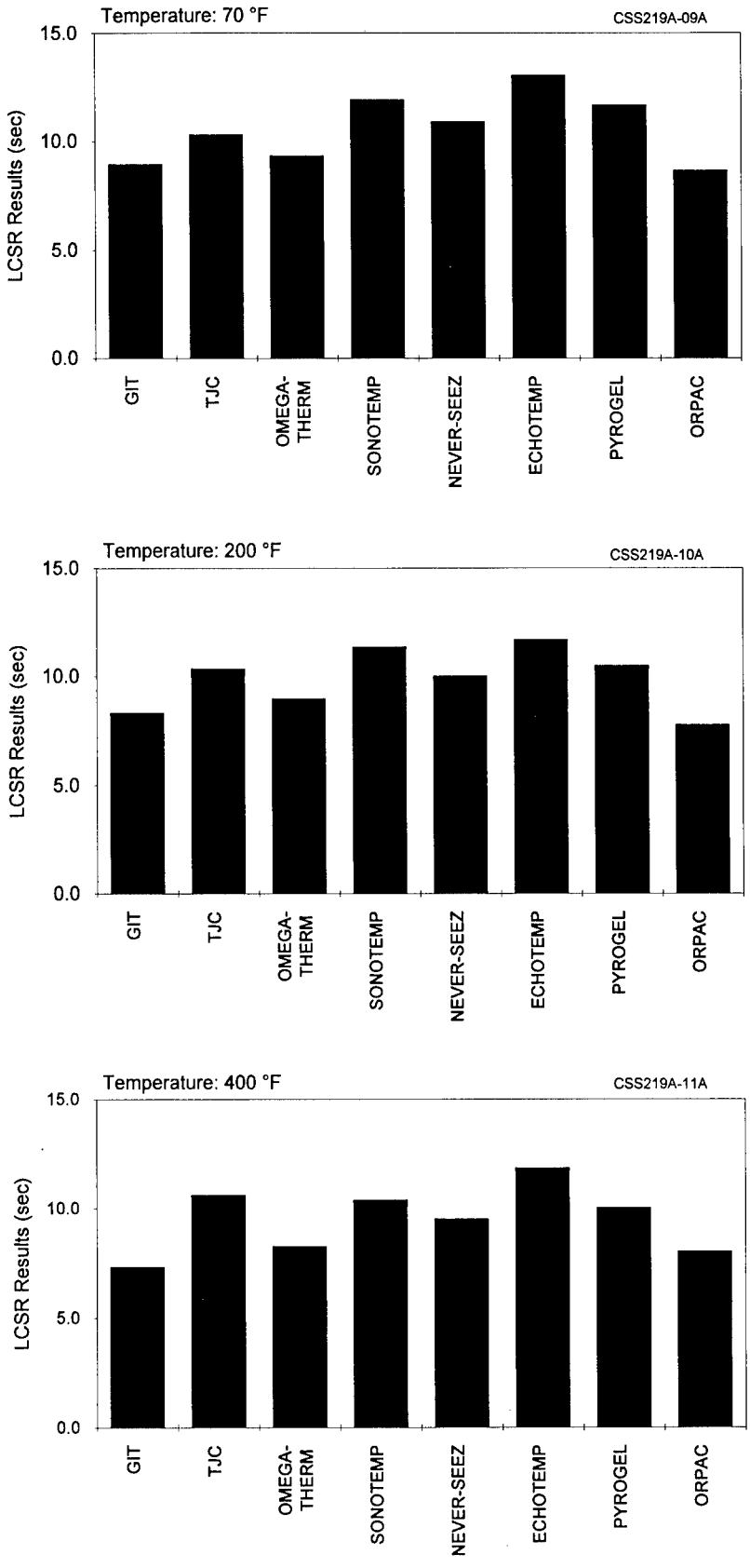

Figure 14.2 Results of LCSR Testing of Thermal Compounds at Different Temperatures

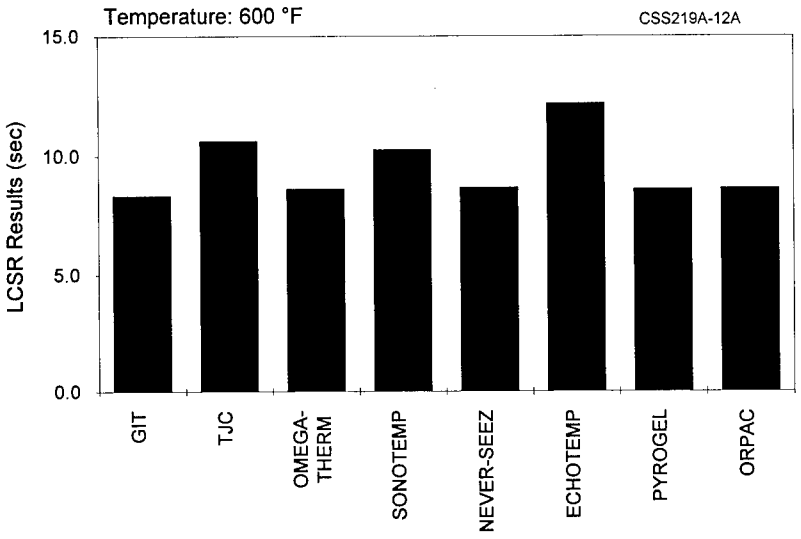

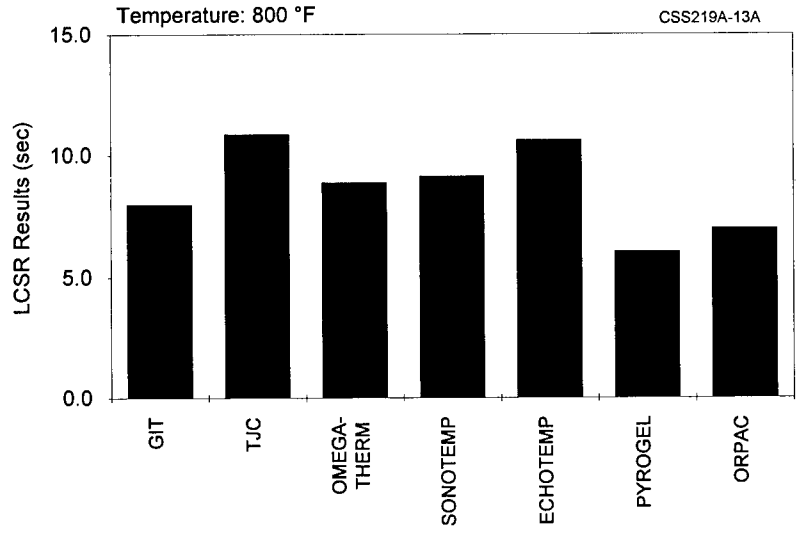

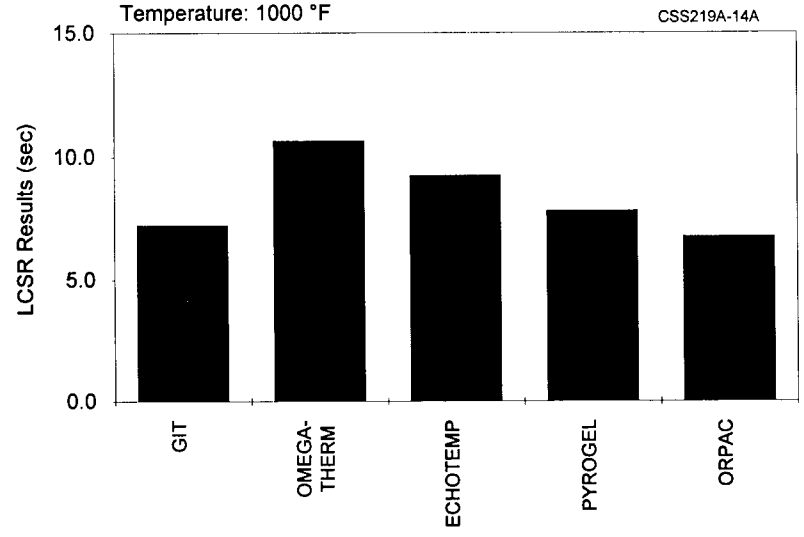

Figure 14.2 (Continued)

(Thermal Joint Compound), while at the 1000°F, the best thermal response was given by ORPAC and the slowest by TJC. In summary, it seems that each thermal compound has a temperature at which its thermal characteristics are optimum.

14.2 Industry Survey

An informal survey of various manufacturing and research facilities was conducted to determine typical sensor bonding problems and solutions and investigate adhesives that are currently used to install temperature sensors in solid materials. Participants in the survey included aerospace companies (Boeing-Seattle, Thiokol-Alabama and Utah), sensor and adhesive manufacturers (HITEC, Entran Devices, Micromeasurment), and research facilities (NASA-Marshall and Lewis, University of Tennessee).

The survey provided: (1) an insight into the type of adhesive bonding performed and adhesives or thermal compounds used at various sites, (2) details on specific bonding procedures and bonding problems encountered, and (3) details on particular thermal compounds, adhesives, and attachment methods that have provided successful sensor attachment results. The results of the survey are attached in Appendix F. These results along with a literature survey were used to prepare bonding techniques for surface-mounted RTDs and strain gages. These techniques are attached in Appendix G including a copy of a NASA procedure for strain gage installation.

15. EFFECT OF HIGH TEMPERATURE ON THERMOCOUPLE RESPONSE TIME

Although properly made thermocouples can normally tolerate temperatures of up to 3000°F, there is always a chance that exposing a thermocouple to temperatures higher than 1000°F may cause measurable calibration or response time changes.

The effect of high temperature on thermocouple response time was investigated in this project in two ways. One way involved measuring the response time of thermocouples before and after they were exposed to high temperatures, and another way involved measuring the response time of thermocouples by plunge testing into a furnace at high temperatures. The results are described below.

15.1 Response Time Before and After Exposure to High Temperatures

This work involved plunge tests in room temperature water flowing at 3 feet per second. A number of thermocouples were plunge tested before and after exposure to high temperatures. The exposure time at the high temperatures was 2 to 3 hours. The thermocouples that were tested included Type T (Copper-Constantan) and Type K (Chromel-Alumel), and Type J (Iron Constantan) sheathed thermocouples with ODs ranging from 1/16" to 3/8." Representative results are provided in Figures 15.1 (Type T) and 15.2 (Type K and J). It is apparent from these results that the response times of these thermocouples remain basically the same even after the thermocouples were exposed to temperatures as high as 1750°F.

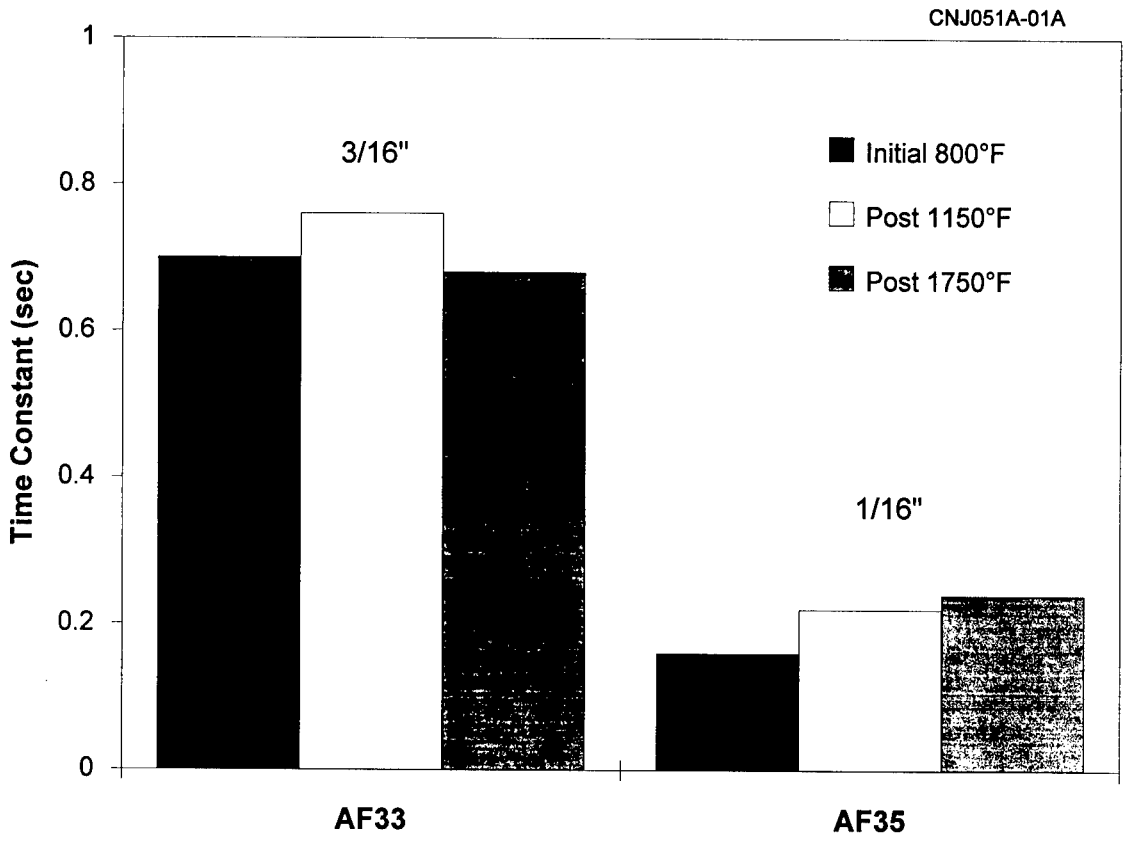

Figure 15.1 Response Time Testing Results for Type K Thermocouples

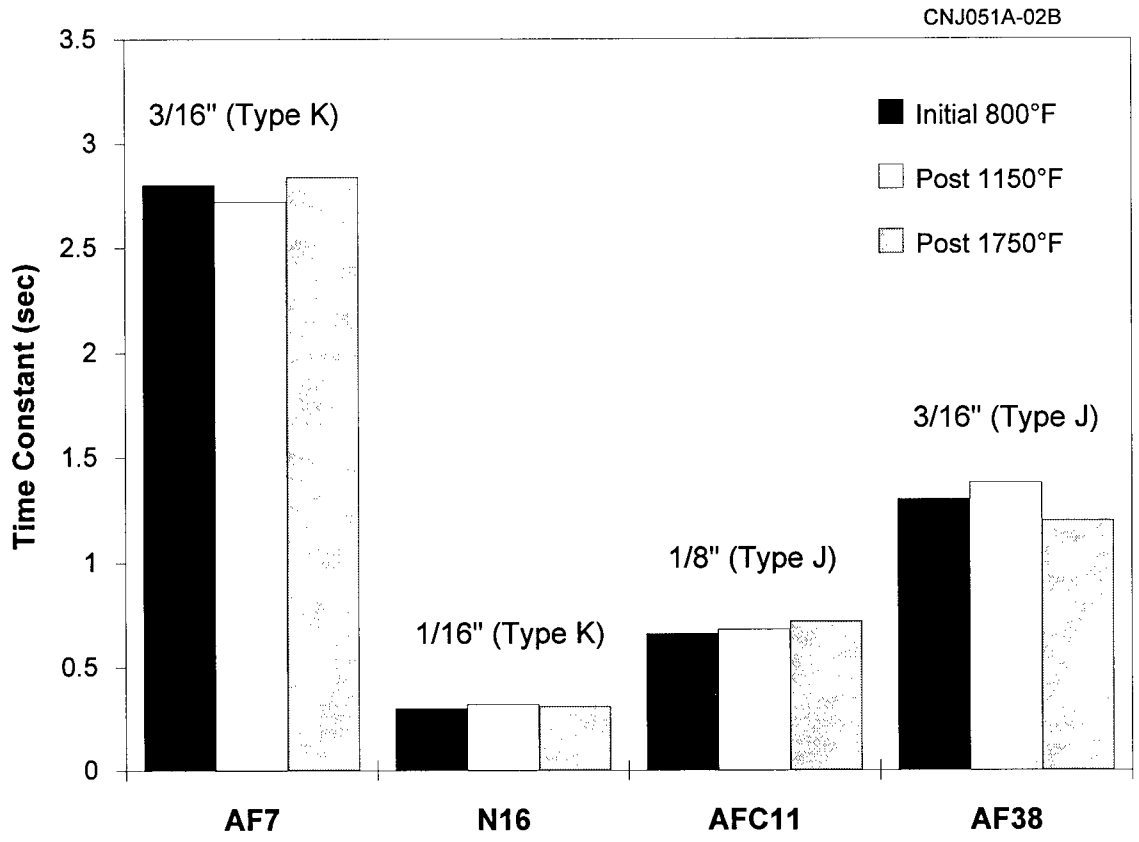

Figure 15.2 Response Time Testing Results for Two Type K and Two Type J Thermocouples After they were Exposed to High Temperatures

15.2 Response Time Measurements By Plunge Testing Into High Temperatures

The response time of eight thermocouples were measured by plunge tests in a furnace in stagnant air at temperatures up to 1200°F. The purpose was to quantify the effect of temperature on response time.

The outcome of the tests are shown in Figure 15.3. It is apparent that as these thermocouples are plunged into high temperatures, their dynamic responses improve. Results shown elsewhere in this report and in other literature, however, indicated an increase in response time with temperature. This type of discrepancy is typical for thermocouples, RTDs, and other temperature sensors. Industrial thermometry literature have shown that the effect of temperature on response time of thermocouples (and RTDs) is unpredictable. That is, for some sensors, the response time decreases at high temperatures, and for others, the response time increases. This is because temperature can cause changes in material properties of sensors and in air gaps that exist in the sensor construction material. The thermal conductivities of sensor material often increase with temperature and should result in improved dynamic responses. However, air gaps in sensor material can experience expansion or contraction, and oppose any improvement in response time due to increased thermal conductivities. In fact, the expansion and contraction of air gaps can not only null any improvement in response time due to increased thermal conductivities, but also proceed so far as to cause the response time of the sensor to increase significantly with temperature.[3]

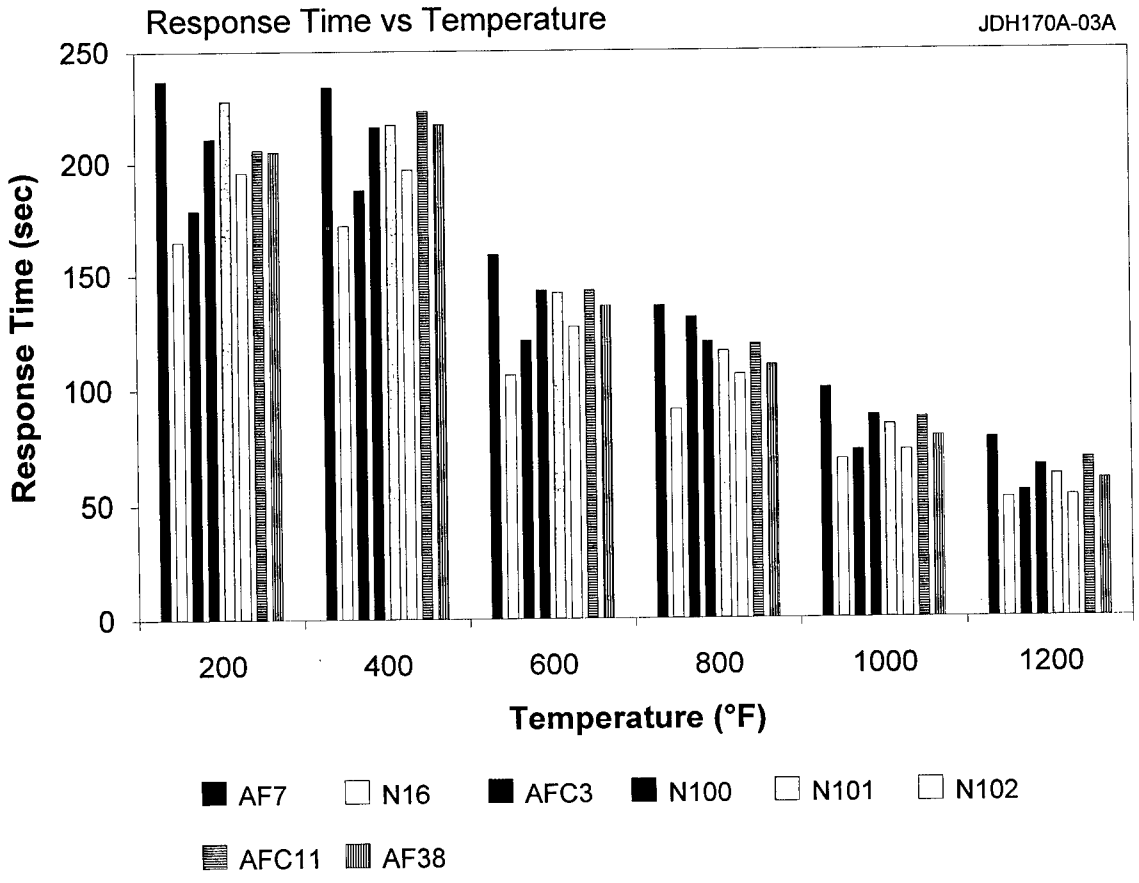

Figure 15.3 Response Time of Eight Different Thermocouples in Stagnant Air as a Function of Temperature in a Furnace

16. HIGH TEMPERATURE MEASUREMENTS WITH THERMOCOUPLES

16.1 Principle of Range Extension Technique

SRM nozzle tests and other aerospace applications may require temperature measurements to nearly 4000°F. Optical pyrometers may be used for these measurements, but high accuracy requirements and practical considerations sometimes preclude the use of pyrometers. Thermocouples can provide better accuracies than pyrometers, in some cases, and are adaptable to a more diverse set of applications. However, thermocouples are usually limited to 2000°F. Thus, a new technique called "thermocouple range extension" was developed and validated in this project for measurement of high temperatures using conventional thermocouples.

The new technique uses a combination of temperature measurements and extrapolation to provide a means to accurately estimate high temperatures in lieu of measurements. The principle of this technique is shown in Figure 16.1. The thermocouple is exposed to the temperature to be measured and its output is recorded as the temperature is increasing until the thermocouple reaches its temperature limit (e.g., 2000°F). At this point, the sensor either fails or is removed from the heat source and the resulting data is extrapolated to estimate the temperature that the thermocouple would have indicated. In essence, the method is like a plunge test. The plunge test is used to measure the response time of a temperature sensor by exposing the sensor to a step change in temperature, recording the transient output of the sensor, identifying the final value of the transient response, and measuring the time which corresponds to where the transient output of the sensor attains 63.2 percent of the final value. In the case of a plunge test, the problem is one of measuring the final value to identify the sensor response time, while in thermocouple range extension, the problem is one of identifying the final value using a known value of response time.

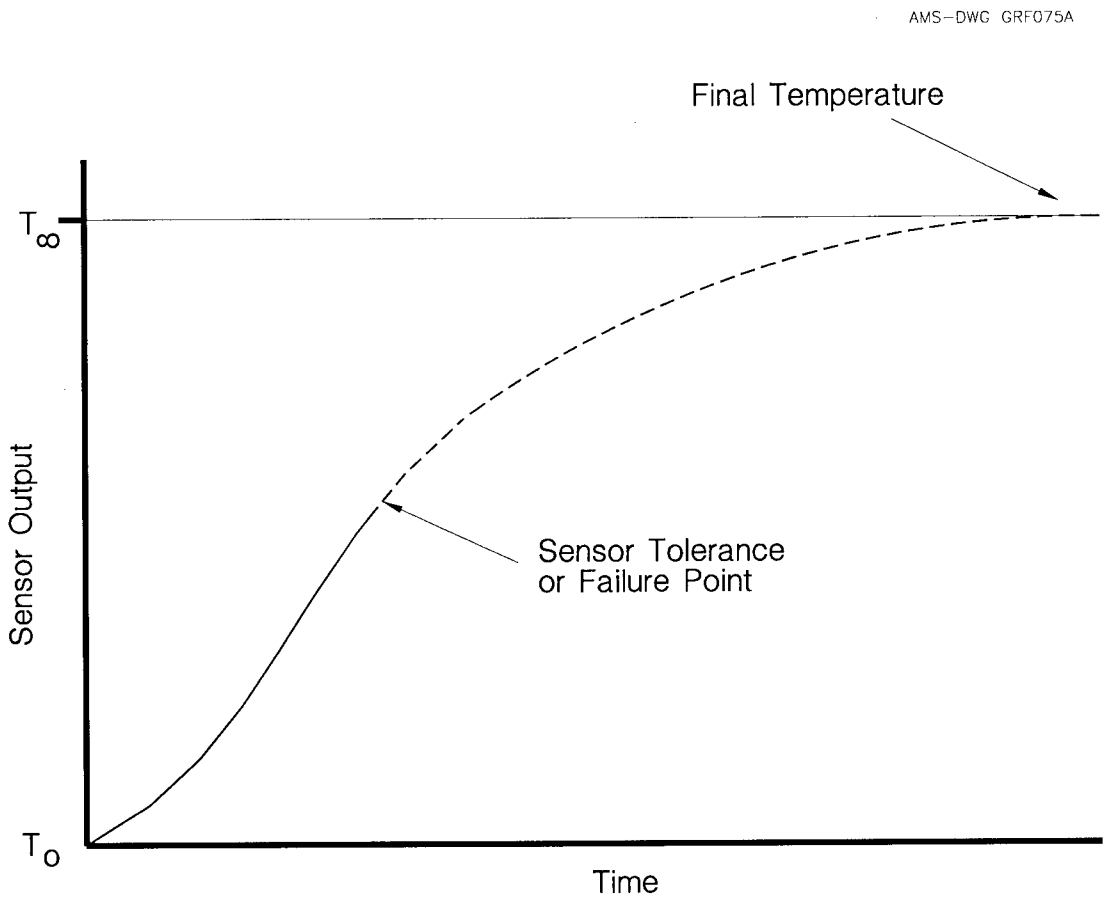

Figure 16.1 Extending the Temperature Range of Thermocouples By Extrapolation

The range extension technique requires a knowledge of the thermocouple response time which can be measured with the LCSR method in a baseline test. Once the response time is known, the final temperature (T_∞) can be calculated by a least square fitting of the transient temperature data to the following equation assuming, for the sake of simplicity, that the thermocouple is a first order system.

$$T(t) = T_\infty(1-e^{-t/\tau}) \qquad (16.1)$$

In this equation, τ is the time constant in seconds, t is time, and T(t) is the transient response of the thermocouple.

16.2 Validation of Range Extension Technique

To determine the validity and establish the accuracy of the range extension technique, laboratory plunge tests were performed on nine thermocouples to determine their response time as follows. The plunge tests were performed in a high temperature furnace at approximately 200°F and response times of thermocouples were identified. The thermocouples were then exposed suddenly to 800°F. Using Equation 16.1 and the response time measured at 200°F, the thermocouple output was extrapolated to 800°F. The extrapolated data were then compared with the measured data, and the difference between the measured and calculated values of the final temperature was identified.

Figure 16.2 shows the transient response of one of the thermocouples to step changes of 200°F and 800°F. To identify T_∞, the first few seconds of the 800°F plunge transient was fit to Equation 16.1 and the response time of the 200°F plunge test was substituted for τ. The resulting T_∞ was compared with the measured final temperature and the difference was calculated in terms of a percent error. The percent error as a function of time is shown in Figure 16.3.

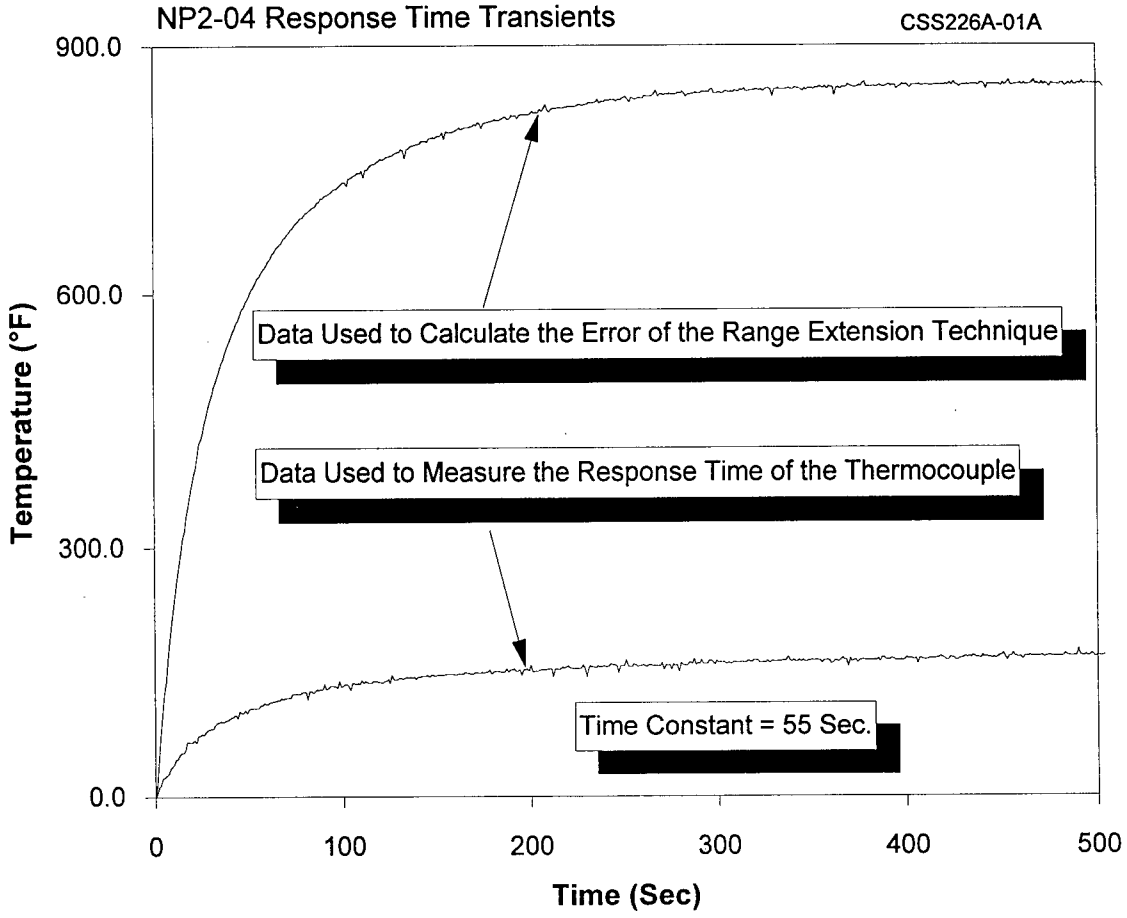

Figure 16.2 Typical Plunge Test Transient from Measuring the Response Time of Thermocouples in a Furnace

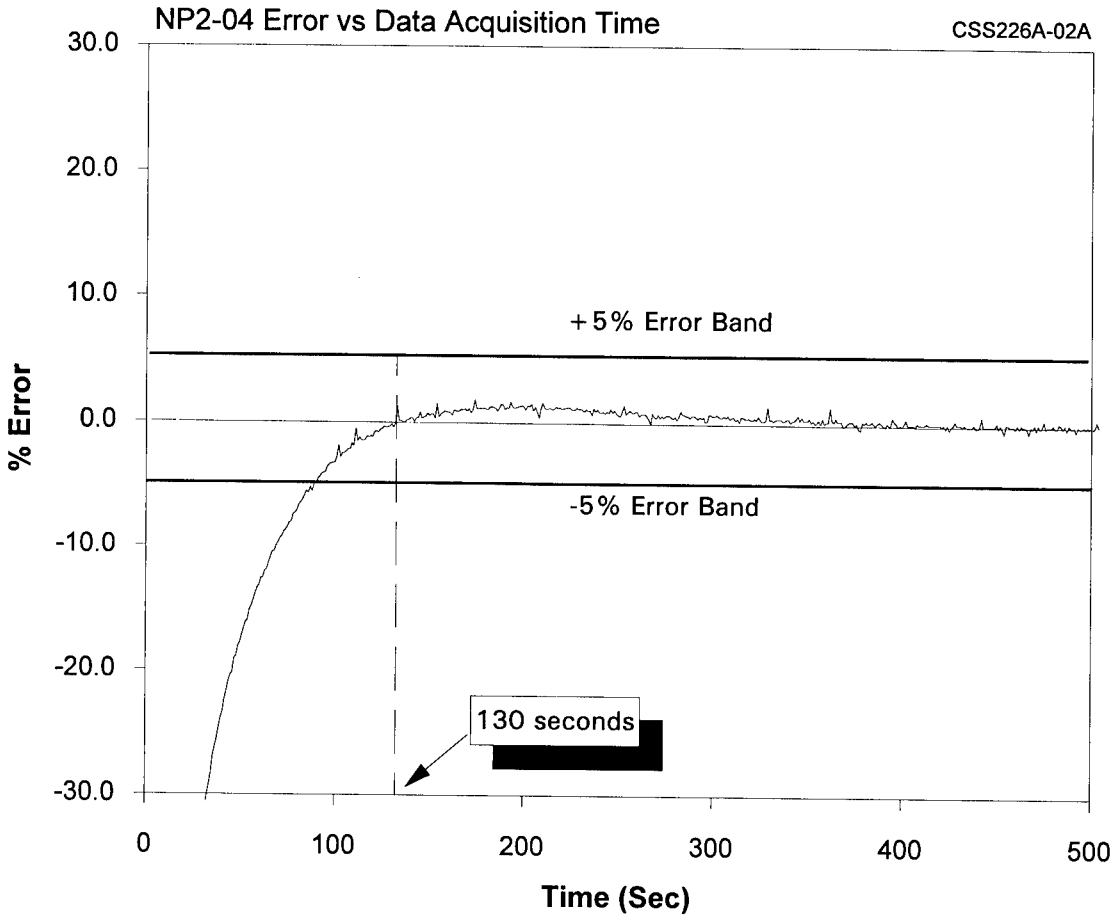

Figure 16.3 Error in Measurement of 800°F by the Range Extension Technique

Figure 16.3 indicates that the temperature of the thermocouple can be estimated with less than 5 percent error if 90 seconds or more data is collected before the thermocouple is removed, melted, or destroyed by high temperature. At about 130 seconds, the error is virtually negligible as shown in Figure 16.3. That is, if the thermocouple is exposed to the high temperature and data is recorded for 130 seconds before the thermocouple is removed, then the calculated temperature using the range extension technique will be very accurate.

The accuracy of the range extension technique depends on the response time of the sensor, and the sensor response is a function of temperature. Figure 16.4 presents laboratory test results conducted in this project to determine the temperature dependance of thermocouple time constant. Although the data in Figure 16.4 indicates a decrease in response time with temperature, as indicated before, thermocouple response time as a function of temperature is often unpredictable. Thus, it should be pointed out once again that although most results in this report have shown that thermocouple response time improves with temperature, there is literature that shows the opposite to be the case.

One method that can be used to estimate the response time of a thermocouple at the temperature to be measured involves developing a response time versus temperature curve for the thermocouple and extrapolating the results to high temperatures as shown in the two sets of data presented in Figure 16.5.

Figure 16.6 shows the amount of data that is needed to accurately predict the final temperature of a thermocouple (i.e., T_∞). These results show that the range extension method, when used in conjunction with the sensor response time-versus-temperature curve, can provide a useful tool for accurate estimation of high temperatures.

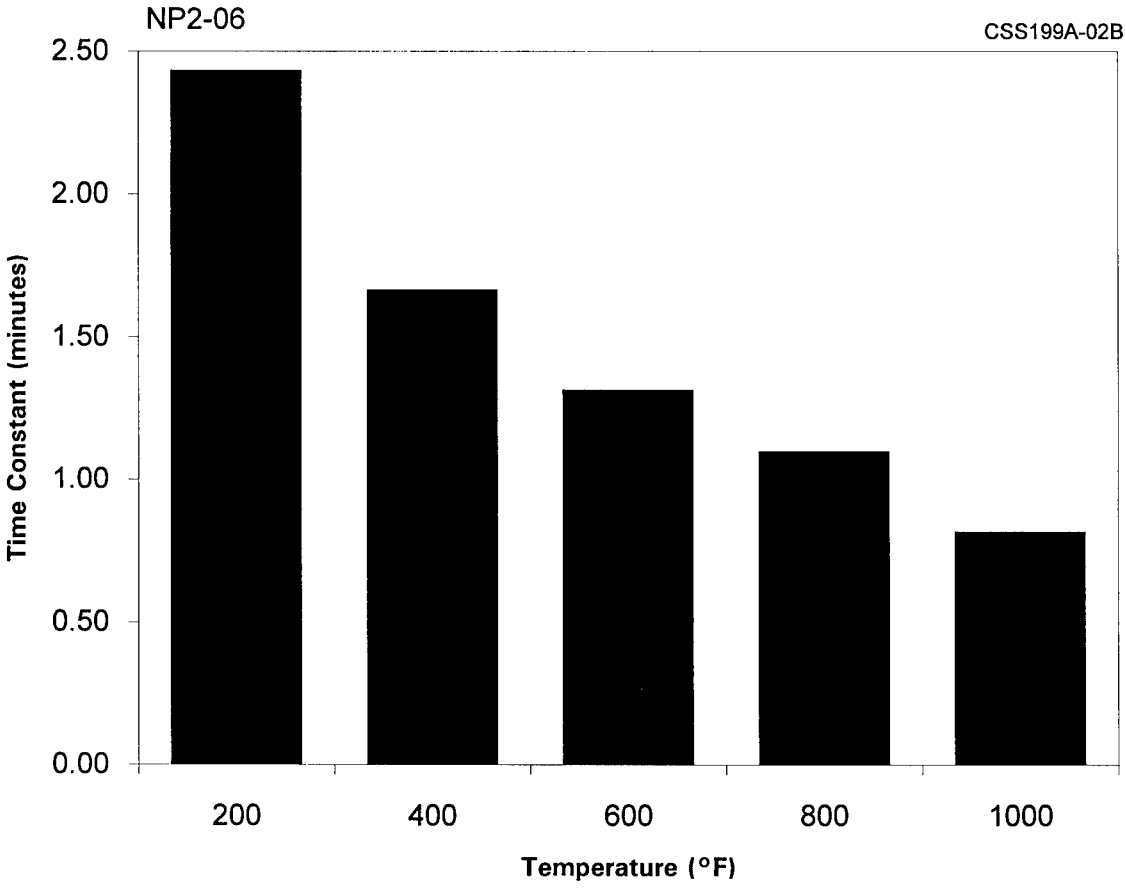

Figure 16.4 Response Time of a Thermocouple Sensor as a Function of Temperature in a Furnace in Stagnant Air

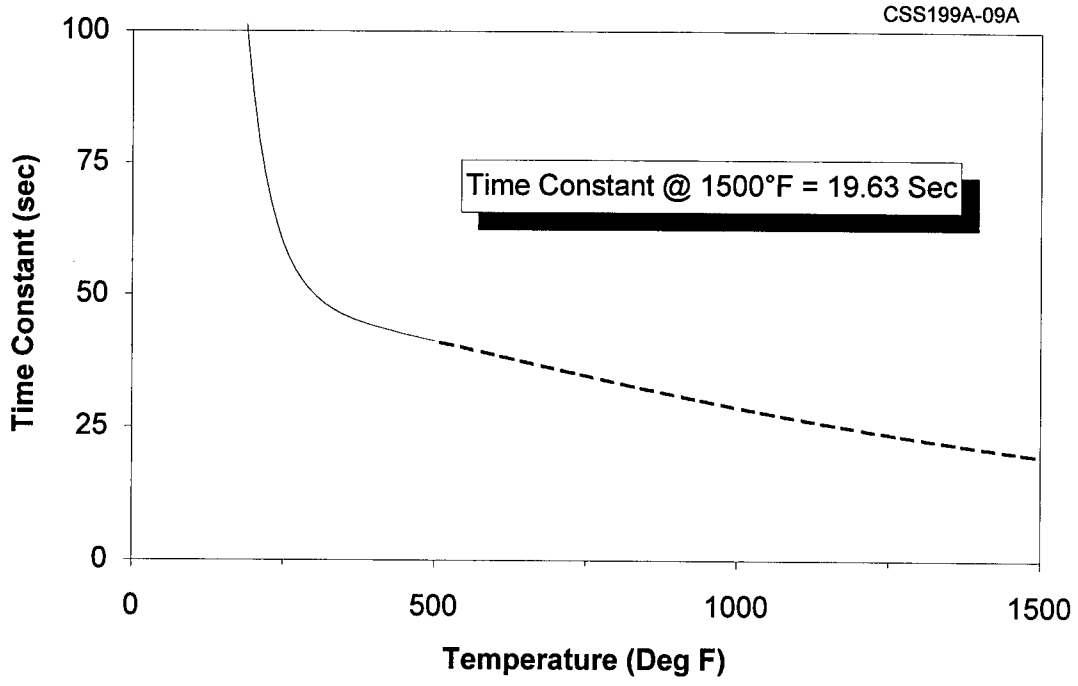

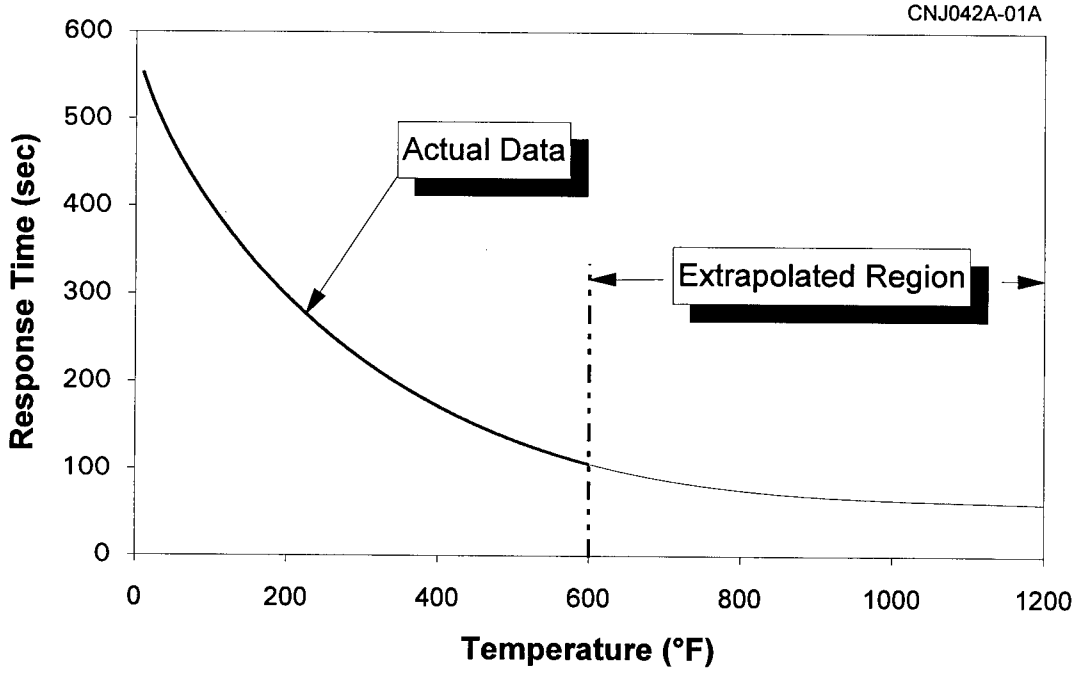

Figure 16.5 Typical Results of Extrapolation of Response Time Measurements to High Temperatures

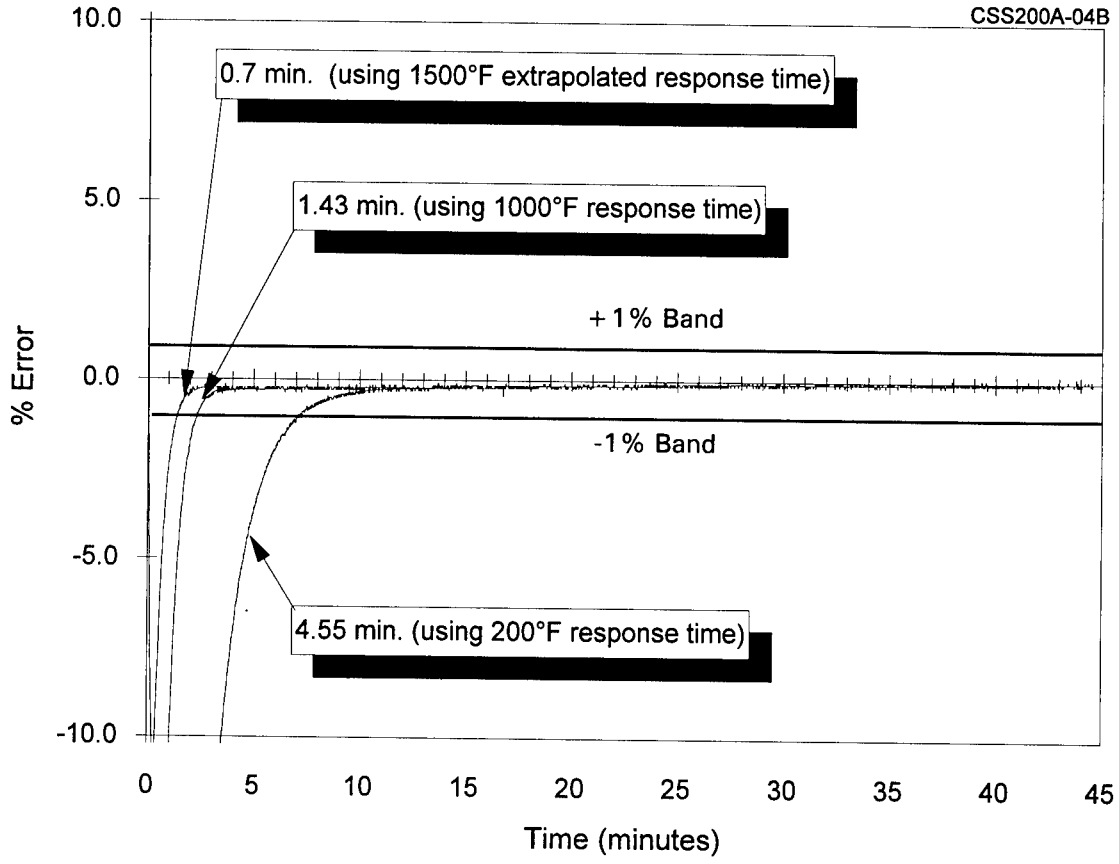

Figure 16.6 Illustration of the Amount of Data that is Required to Measure 800°F with Less than 1 Percent Error Using the Range Extension Technique

17. IN-SITU RESPONSE TIME TESTING OF THERMISTORS

Although thermistors were not found to have been of much use at the SPIP or SRM nozzle improvement/development programs sponsored by NASA, they were nevertheless included in the project to provide a complete picture of LCSR applicability to industrial temperature sensors. In particular, the LCSR method was used to measure the response time of the thermistors in air and compare the results with corresponding plunge test time constants to establish the validity and accuracy of the LCSR test. The results are presented in this chapter.

17.1 Principle of Operation of Thermistors

Thermistors are thermally sensitive resistive elements made of semiconductive ceramic materials. They are typically constructed from a combination of manganese, nickel, and cobalt oxides. These elements have resistivities ranging from 100 to 450,000 Ohms-Cm.

Thermistors are manufactured with either a positive temperature coefficient of resistance (PTC), or a negative temperature coefficient of resistance (NTC), with the NTC being the most commonly used. Figure 17.1 shows a temperature versus resistance curve for a typical NTC thermistor. This temperature versus resistance relationship is characterized by the following equation:

$$R(T) = R_0 \exp\left[\beta\left(\frac{1}{T} - \frac{1}{T_0}\right)\right] \qquad (17.1)$$

where R(T) = resistance at temperature T (in Kelvin)

R_0 = resistance at temperature T_0 (in Kelvin)

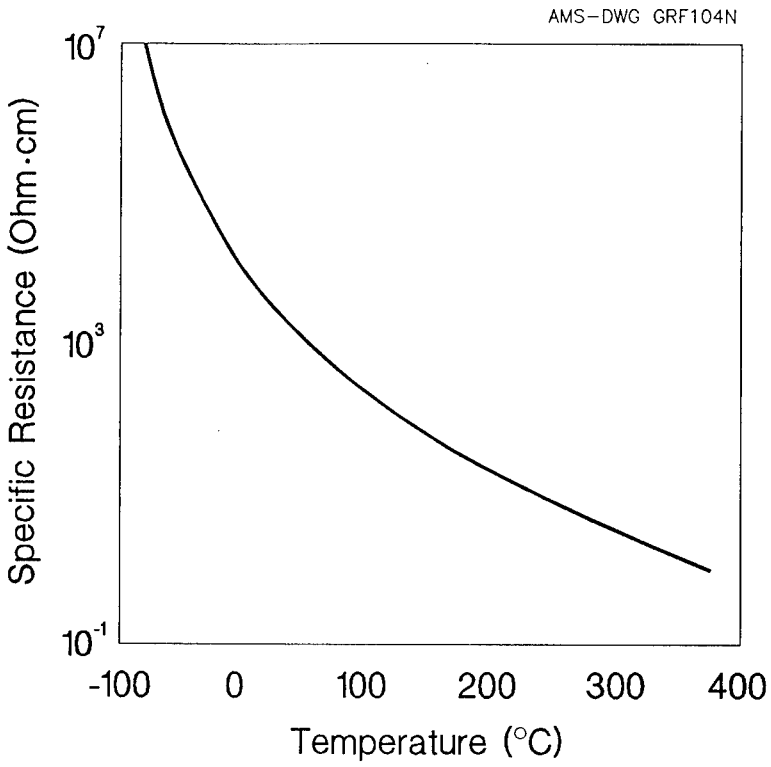

Figure 17.1 A Typical Resistance Versus Temperature Curve for a Thermistor with a Negative Temperature Coefficient of Resistance (NTC)

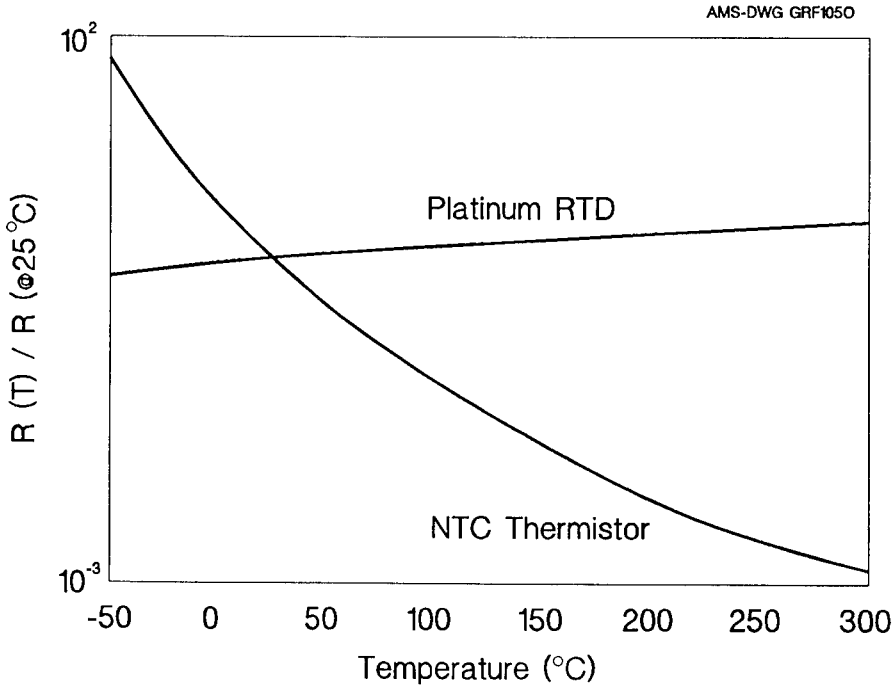

Figure 17.2 Temperature Coefficient of Resistance for a Platinum RTD and a Thermistor

β = constant, determined by thermistor type

The change in resistance as a function of temperature of a platinum RTD is small (about 0.4 percent per °C) compared with that of a typical thermistor (as much as 4 percent per °C). This means that thermistors are much more sensitive than RTDs at low temperatures (-50 to 300 °C). Figure 17.2 is a graphical representation of temperature coefficient of resistivity for both a platinum RTD and a thermistor over the range of -50 to 300°C.

17.2 Validation of LCSR Method for Thermistors

Laboratory tests were performed to determine if the LCSR method can be used to identify the response time of thermistors. The thermistors that were tested included both sheathed and bead-type sensors with various nominal resistances. Figure 17.3 is a photograph of thermistors that were tested in this project.

Thermistors are LCSR tested in the same manner as RTDs and strain gages. The sensor is connected to one arm of a Wheatstone bridge and a current of about 5 mA is used to induce Joule heating (V^2/R), which causes the sensor resistance to decrease for NTC thermistor. The decrease in resistance causes the bridge current to increase gradually and cause further Joule heating. This effect, called an "auto-catalytic" response, increases until the heat transfer to the surroundings is equal to that of the Joule heating.

To determine the baseline response time of thermistors, plunge tests were performed in an air flow loop (Figure 17.4) at various flow rates. The thermistors were also LCSR tested at the same flow rates. The LCSR data were then analyzed using the same analysis procedure and

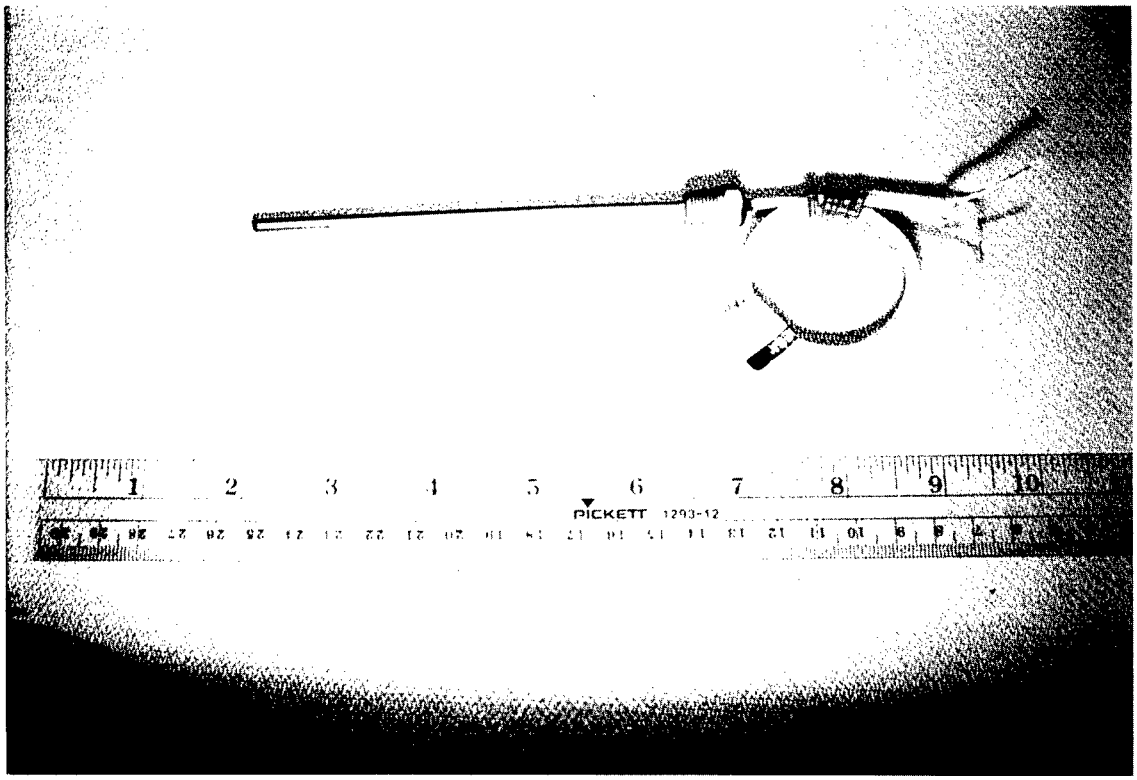

Sheathed Thermistor Probe

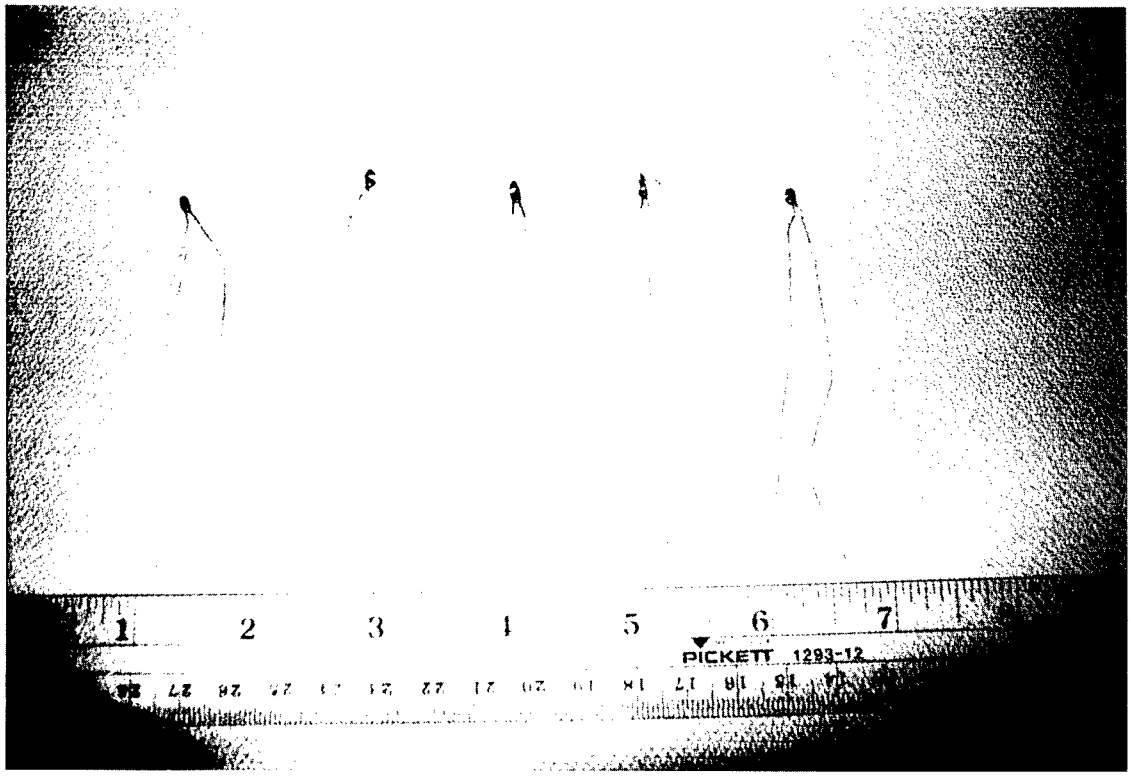

Bead-Type Thermistors

Figure 17.3 Photograph of Thermistors Tested

AMS-DWG THC020J

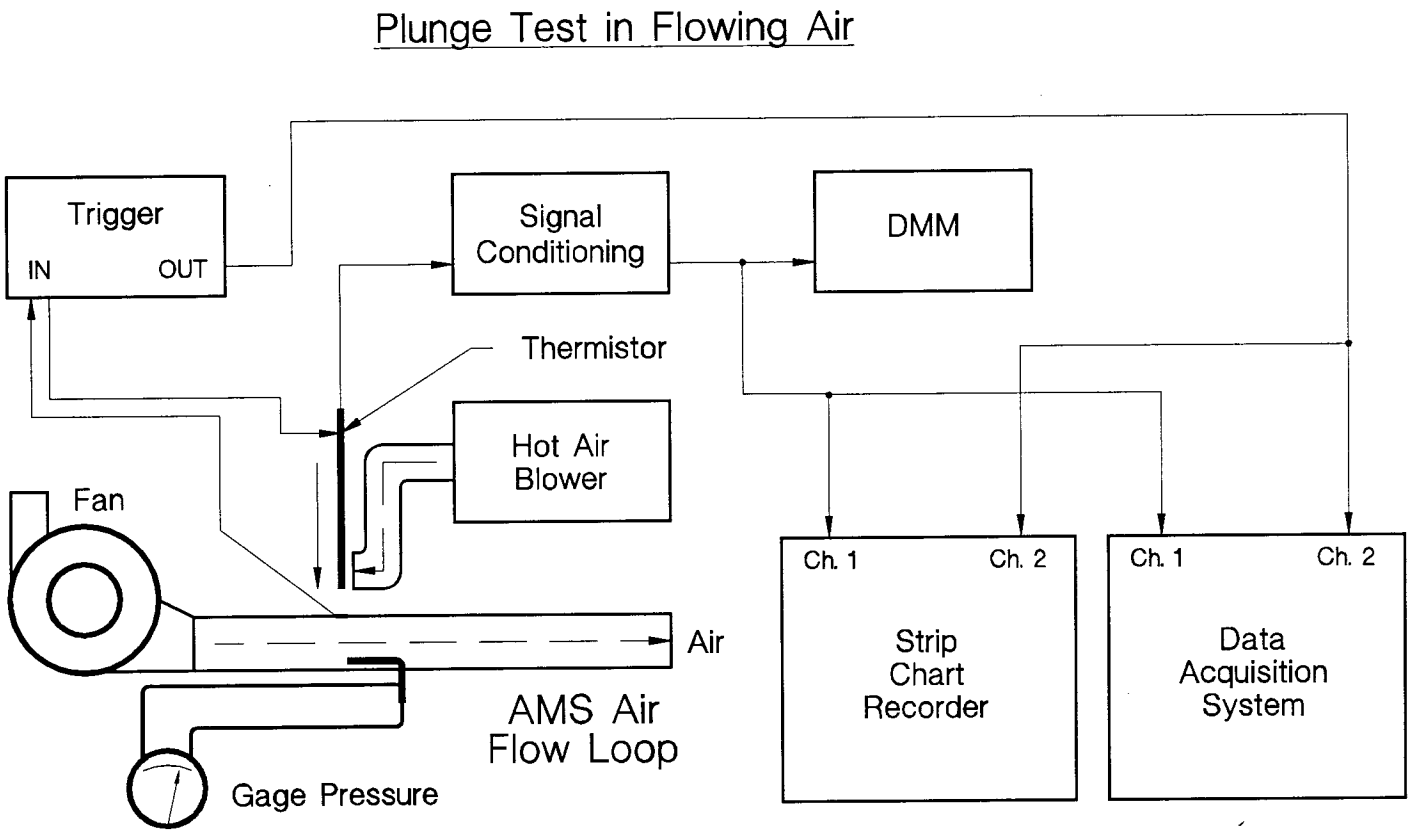

Figure 17.4 Schematic of Air Flow Loop for Measurement of Response Time of Temperature Sensors in Flowing Air

software that have been used for RTDs and strain gages. Figure 17.5 shows typical LCSR transients for two thermistors tested at different flow rates. It is evident that as the flow rate increases, the response time of the sensors decreases. Table 17.1 shows a comparison between representative response time results from plunge and LCSR tests. These results show that the LCSR method can identify the response time of thermistors with an average accuracy of about 5 percent. Figure 17.6 shows additional validation results in terms of bar charts comparing time constants from plunge and LCSR tests.

17.3 LCSR Test to Verify the Installation of Thermistors

The installation quality of thermistors was also evaluated using the LCSR technique. Several thermistors were attached to a solid copper block and tested using the LCSR method. The results were then compared to the LCSR results for the unattached thermistor. Figures 17.7 presents the outcome in terms of LCSR transients for three different thermistors. This indicates that the LCSR technique is successful in detecting a degraded bond in a thermistor.

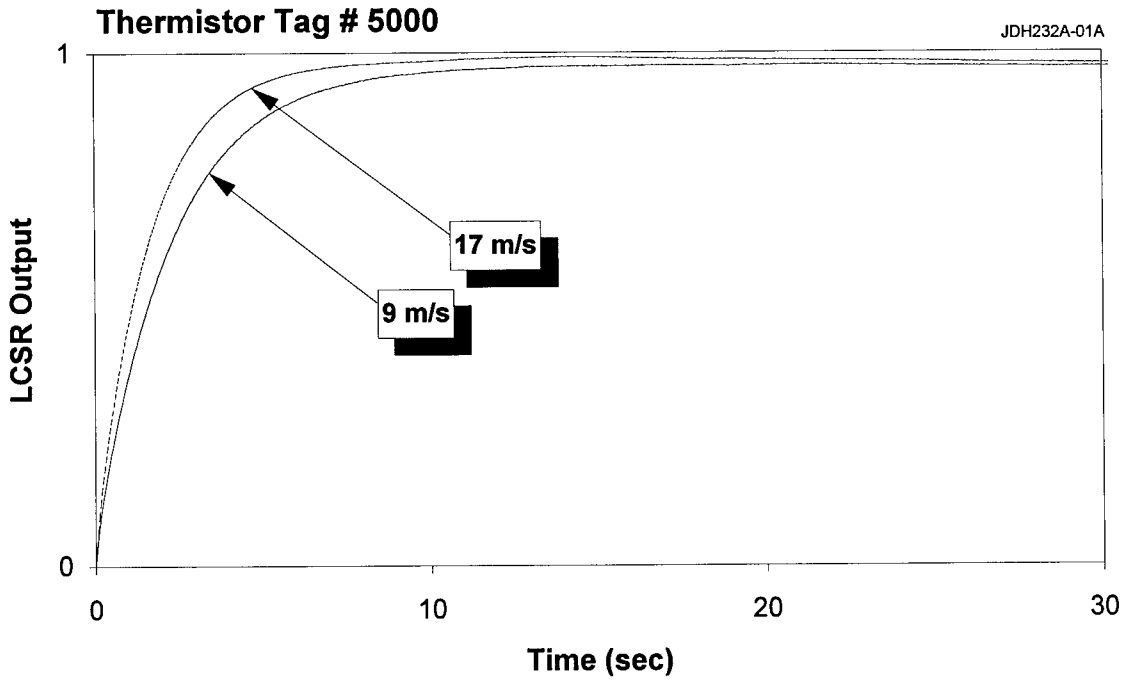

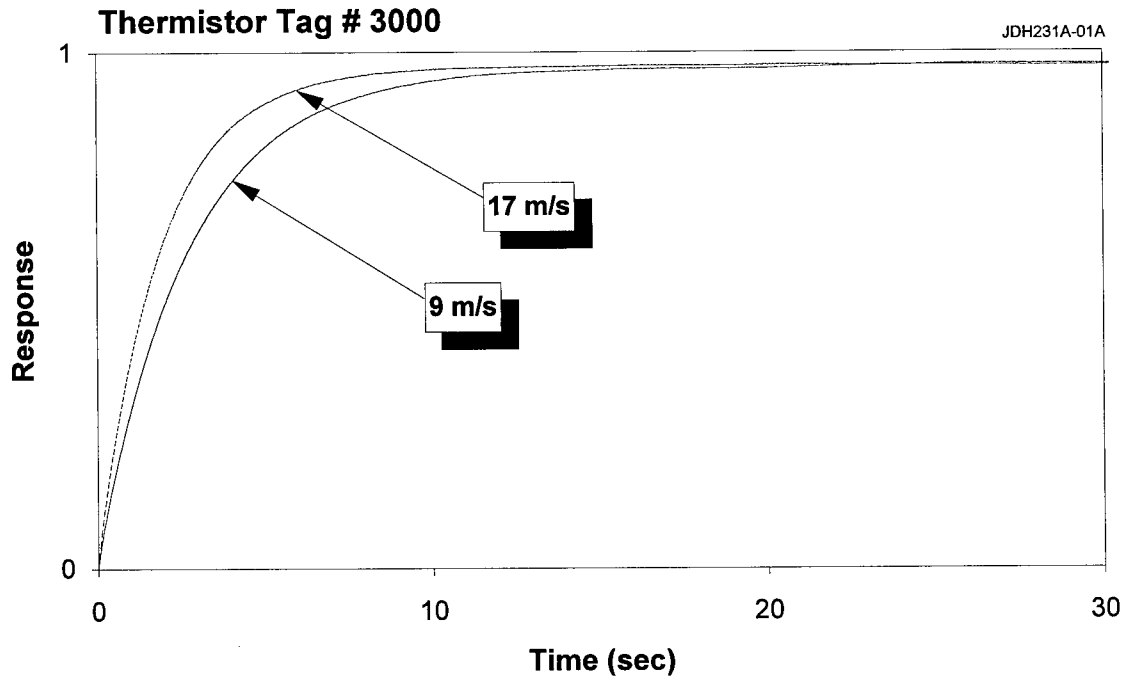

Figure 17.5 Typical LCSR Transients for Two of the Thermistors Used in this Project

TABLE 17.1

Representative Results of LCSR Validation for Response Time Testing of Thermistors

Tag Number	Response Time (sec)		Percent Difference
	Plunge Test	LCSR Test	
50 Ft/Sec			
10000	2.7	2.5	-7.4
2252	2.1	2.2	+4.8
3000	1.9	1.9	0
25 Ft/Sec			
10000	3.4	3.8	+11.8
2252	2.9	3.0	+3.5
3000	2.9	2.9	0
Average Difference (Percent)			4.6

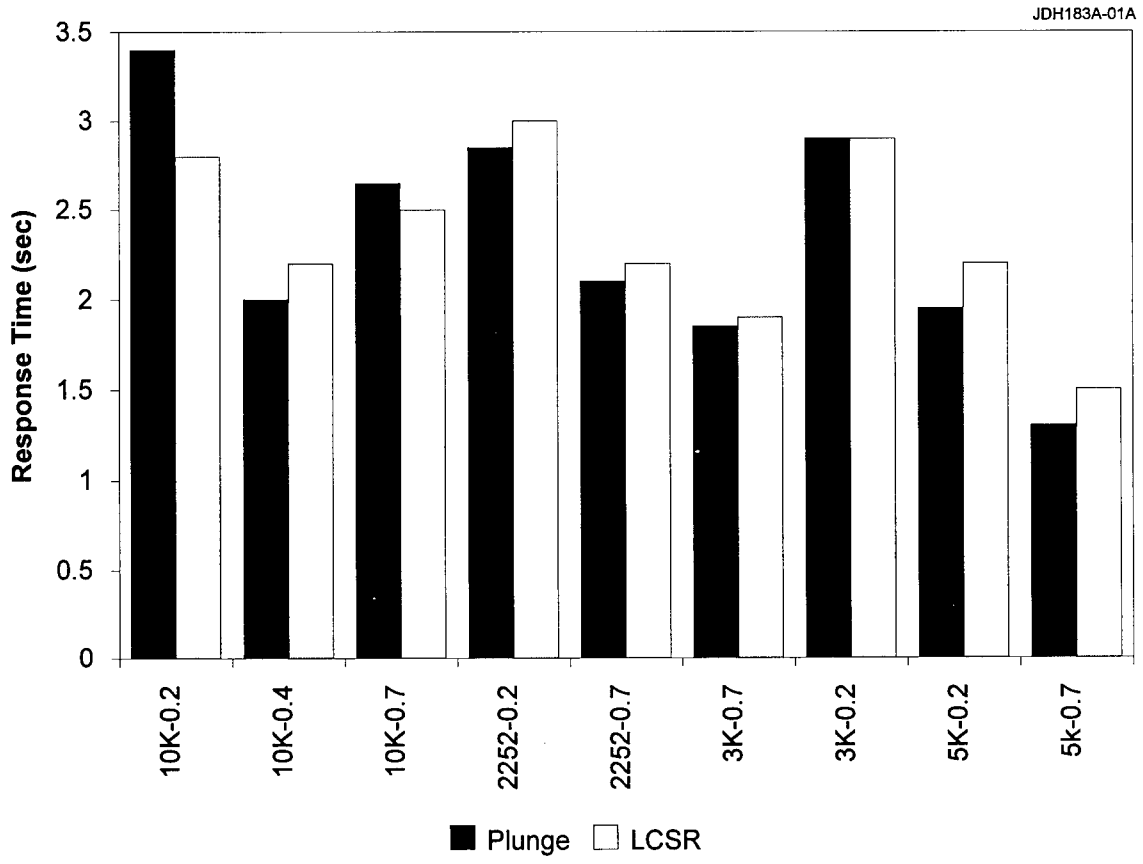

Figure 17.6 LCSR Validation Results for Thermistors

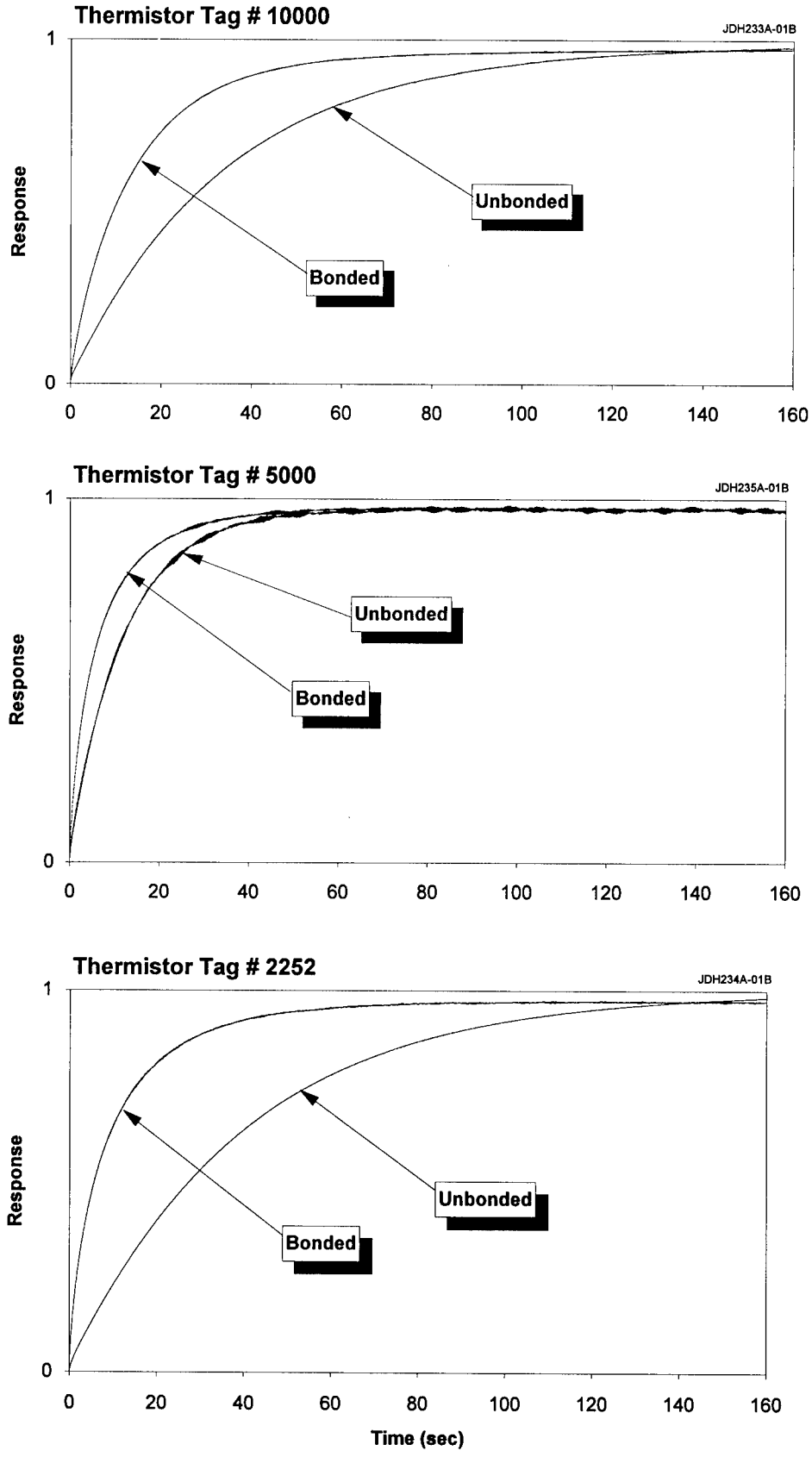

Figure 17.7 LCSR Transients for Three Thermistors in Bonded and Unbonded Conditions

18. IN-SITU DIAGNOSTICS OF THERMOCOUPLE PROBLEMS

The LCSR technique can be used for thermocouple diagnostics in addition to response time testing and detection of thermocouple bonding quality. For example, during the field measurements performed in this project, LCSR testing was able to identify secondary junctions in thermocouple circuits, and reveal thermocouples that were reverse-connected. These findings are described below.

18.1 Detection of Secondary Junction in SPIP Thermocouple

In July 1993, AMS performed a series of laboratory LCSR tests on twenty-seven thermocouples embedded in thirteen carbon-phenolic (FM5055) composite material specimens. The thermocouples were tested prior to firing of the composite specimens in the "Plasma-Arc Facility" at MSFC. Most of these thermocouples were small diameter (0.01"), Type K, sheathed or unsheathed sensors. Three of the thermocouples were unsheathed, Type S thermocouples made by SRI. The remaining thermocouples were made by Delta M and Thiokol. The results of the pre-firing installation tests of the thermocouple performed by AMS are shown in Figure 18.1. Note that one thermocouple, PA-9T, has a much larger installation index than the other thirty-eight thermocouples. A further analysis of the LCSR data on this thermocouple revealed a secondary junction in the thermocouple located several inches away from the thermocouple's measuring junction. A secondary junction in a thermocouple has the following effect on the LCSR test results. When an AC current is applied to heat the thermocouple for the LCSR test, the secondary junction also heats up. When the current is cut off, the secondary junction cools off as well as the measuring junction. Normally, the measuring junction is in a better heat transfer media than the secondary junction. Thus, the secondary junction cools off at a slower

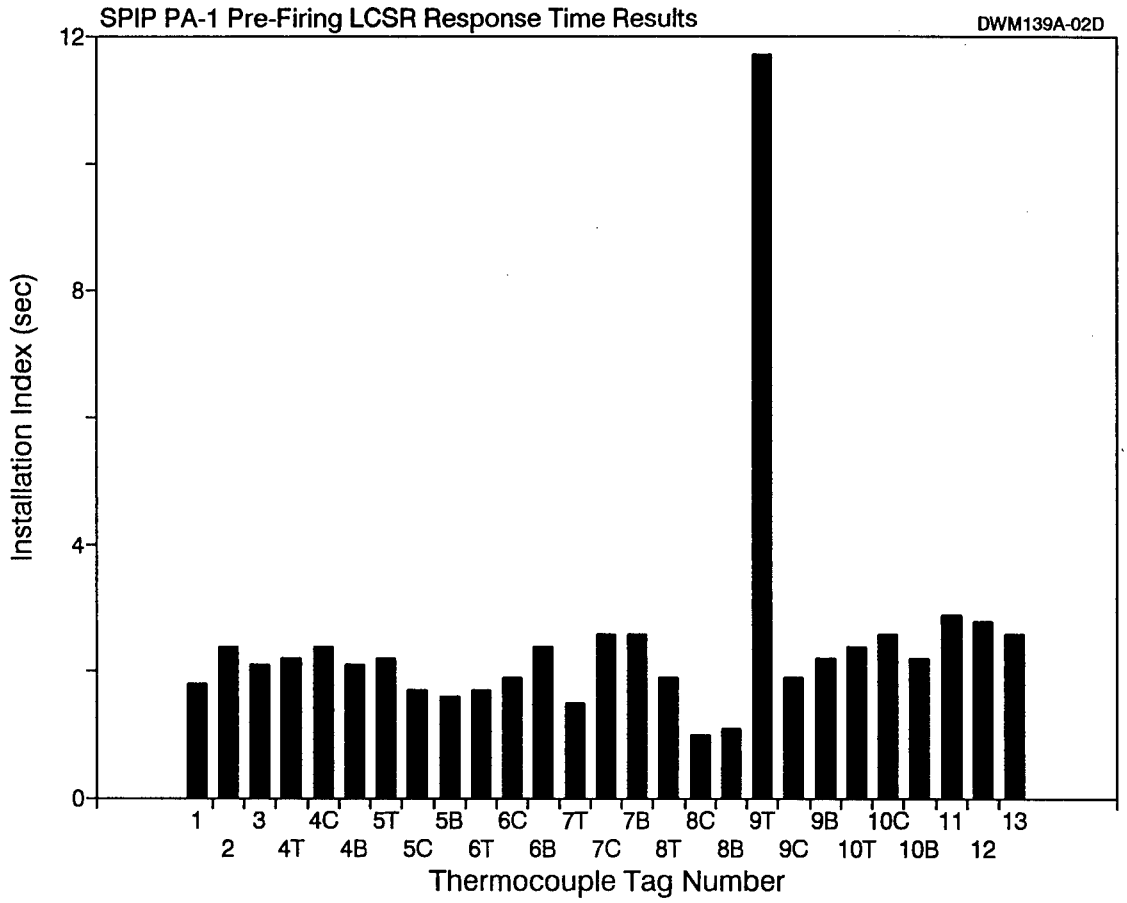

Figure 18.1 Results of Laboratory Testing of SPIP Thermocouples

rate than the measuring junction and dominates the LCSR transient. Figure 18.2 shows the LCSR transient for the thermocouple in question in comparison with two other thermocouples in the same block. Note that thermocouple #PA-9T takes longer to settle out than the other thermocouples. This is due to the slow cooling of the secondary junction.

18.2 Detection of Reverse-Connected Thermocouple

During LCSR testing of the instrumented 48-3 nozzle at MSFC, a thermocouple was found to have reverse leads. Figure 18.3 shows the LCSR transients for the reversed-connected thermocouple, as well as a normally connected thermocouple.

To remedy the situation, the thermocouple connections to the signal conditioning equipment were also reversed. This helped provide a normal temperature indication and the firing data from this thermocouple could be used just like the other normal thermocouples.

Reverse-connected thermocouples are a common occurrence because, when the thermocouple wires are bare, it is not possible to visually distinguish between the positive and negative legs. The LCSR method provides a simple means for remote testing of normal or reverse wiring of thermocouples.

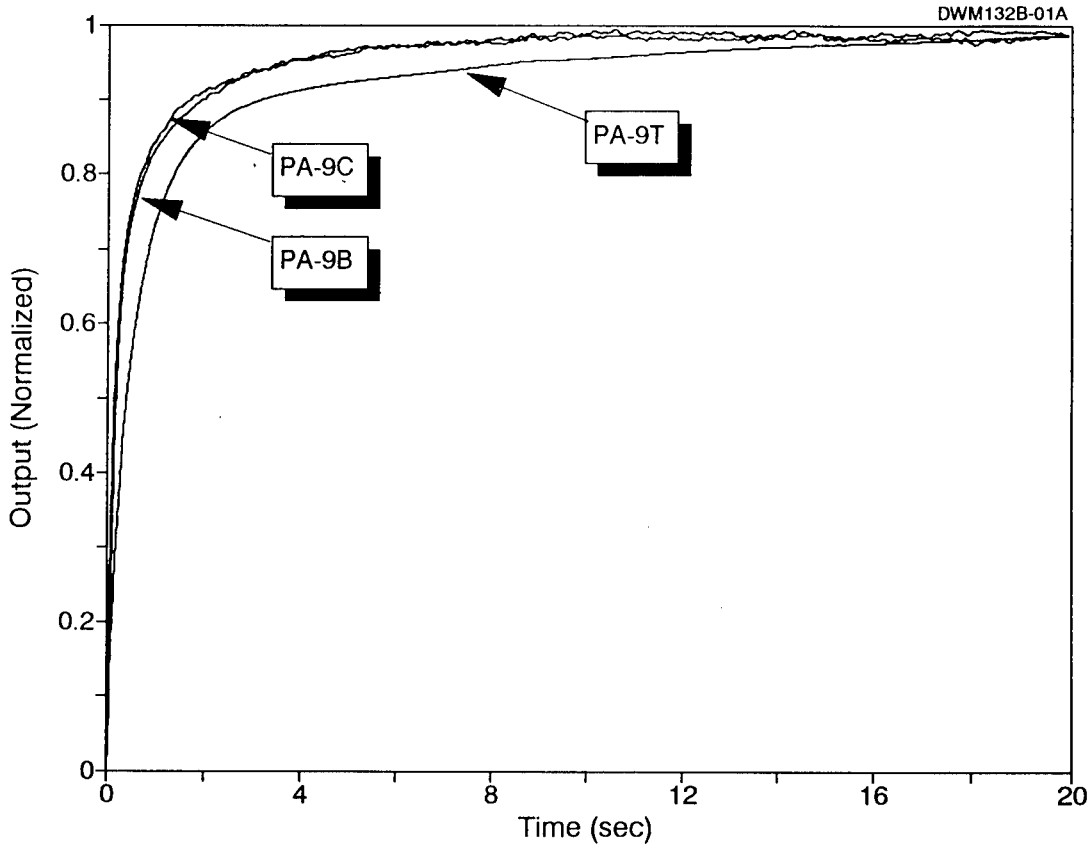

Figure 18.2 LCSR Transients for SPIP Thermocouples

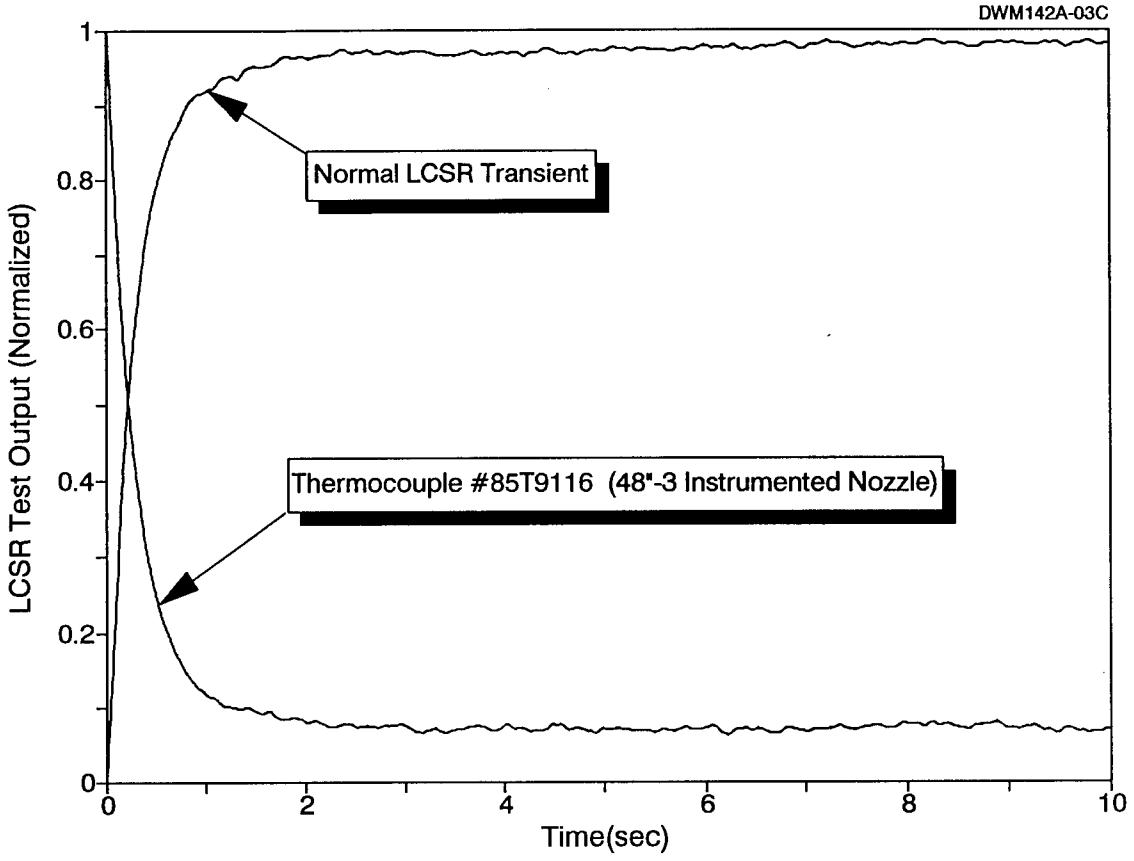

Figure 18.3 LCSR Transients for a Normally Connected and a Reverse-Connected Thermocouple

19. CONCLUSIONS

New equipment and techniques were successfully developed and validated to quantify the degree of bonding between a sensor and a solid material, and to identify the dynamic characteristics of the sensor. The sensors that were involved in this project included thermocouples, RTDs, strain gages, and thermistors. The conclusions from testing of each of these sensors are presented below.

19.1 Testing of Thermocouples

Testing the attachment of thermocouples to solid materials is important to NASA for validating the theoretical models and computer codes that are developed to describe the thermostructural behavior of composite materials for SRM nozzles and blast tube liners.

The LCSR method was successfully developed as a tool for verifying the attachment of thermocouples in solid materials as needed for this and other aerospace applications. Furthermore, a set of equipment and procedures were developed and delivered to NASA. The equipment is designed to enable NASA to perform thermocouple tests in-house.

19.2 Testing of RTDs

Testing the attachment of RTDs is important to NASA in the space shuttle program. Skin-mount RTDs are used on the fuel and oxidizer lines of the space shuttle to measure temperature as a means of detecting leaks through valves on the lines.

The LCSR test was successfully developed for verifying the attachment of skin-mount RTDs. As a result of this work, the foundation has been established for the design and construction of hardware, software, and procedures for in-situ testing of attachment of skin-mount RTDs in SSMEs.

19.3 Strain Gages

Strain gages are used in performance testing of SSMEs. As such, NASA was also interested in testing the attachment of strain gages to solid surfaces. Thus, the LCSR method was attempted for testing the installation of strain gages. Strain gages operate much like RTDs, and there were reasons to believe that the LCSR method would work on strain gages as effectively as on RTDs. This was proven to be the case. In particular, it was shown that, although the LCSR method can not be used to measure the response time of strain gages, it is a very successful method for testing the degree of bonding between a strain gage and a solid material.

19.4 Thermistors

Thermistors were not found to have been used in aerospace applications, probably due to their limited temperature range. Nevertheless, the LCSR method was applied to response time testing of thermistors to provide a complete picture on the applicability of this method for response time testing of the commonly-used industrial temperature sensors. The results showed that the test can successfully provide the response times of thermistors using the same equipment and procedures as for LCSR testing of RTDs.

19.5 Thermocouple Diagnostics

The LCSR method was found useful not only for thermocouple installation tests, but also for thermocouple diagnostics. In particular, the LCSR test was found to successfully identify thermocouple circuit problems such as secondary junctions and reverse leads.

19.6 High Temperature Measurements Using Thermocouples

The validity of the range extension technique was successfully demonstrated. This technique can be used to extend the temperature range of most conventional thermocouples. The method depends on the LCSR test to provide the response time of a thermocouple that is then used in combination with a measurement and extrapolation procedure to provide a means for accurate estimation of high temperatures.

REFERENCES

1. Carroll, R.M., Shepard, R.L., "Measurement of Transient Response of Thermocouples and Resistance Thermometers Using an In-Situ Method," Oak Ridge National Laboratory, Report Number ORNL/TM-4573, Oak Ridge, Tennessee, June 1977.

2. Hashemian, H.M., "Determination of Installed Thermocouple Response," U.S. Air Force, Arnold Engineering Development Center, Report Number AEDC-TR-86-46, December 1986.

3. Hashemian, H.M., "New Technology for Remote Testing of Response Time of Installed Thermocouples," United States Air Force, Arnold Engineering Development Center, Report Number AEDC-TR-91-26, Volume 1 - Background and General Details, January 1992.

4. Howard, J.L., Barthel, C.A., NASA/CR Final Report, "Improved Thermal Sensor for Measurement of Carbon-Phenolic Nozzle Materials During Hot Firing Development and Demonstration," Document No. HI-064F/1.2.9, Boeing Defense and Space Group, December 1994.

5. H.M. Hashemian, et al., "Long Term Performance and Aging Characteristics of Nuclear Plant Pressure Transmitters", U.S. Nuclear Regulatory Commission, Report Number NUREG/CR-5851, March 1993.

APPENDIX A

LCSR Theory and Derivation of Transformation Equations

LCSR THEORY AND DERIVATION OF TRANSFORMATION EQUATIONS

ABSTRACT

The Loop Current Step Response (LCSR) test can be used for remote measurement of response times of Resistance Temperature Detectors (RTDs) and thermocouples as installed in operating processes. The method provides the response of the sensor, accounting for most installation and process condition effects.

This appendix describes the LCSR theory for testing of RTDs and thermocouples in fluids. The LCSR method for testing the installation of sensors in solids basically follows the same procedure as the test in fluids. However, in testing the dynamic characteristics of sensors in solids, the interest is not as much in determining a response time as it is in distinguishing between a poor and a good bond. Nor does the LCSR transformation simply provide the sensor/solid response time.

The information that is contained in the body of this report shows that the LCSR method is successful in revealing the quality of bonding of a sensor to a solid material. To quantify the results of the LCSR test for this application, the LCSR transformation may be used with the understanding that the transformation was originally derived for LCSR testing of sensors in fluids, not solids. As such, instead of referring to LCSR results as response times or time constants, we have referred to them in this report as installation index to refer to the degree of bonding between a sensor and a solid.

1. INTRODUCTION

This appendix presents the details of the development and validation of the Loop Current Step Response (LCSR) method for in-situ measurement of response time of Resistance Temperature Detectors (RTDs) and thermocouples as installed in operating processes. The LCSR method has been validated and used for nearly 20 years for measurement of response times of safety system RTDs in nuclear power plants [1,2,3]. For thermocouples, the validation of the LCSR test was carried out by AMS nearly 10 years ago under a contract with the U.S. Air Force [4].

2. RESPONSE TIME TESTING METHODS

2.1 Plunge Test

The response time of a temperature sensor is classically measured in a laboratory environment using a method called the plunge test. In this test, the sensor is exposed to a sudden change in temperature and its output is recorded until it reaches steady state. The analysis of a plunge test to obtain the time constant of a sensor is simple. For example, if the sensor output transient is recorded on a strip chart recorder, the time constant is identified by measuring the time that corresponds to 63.2 percent of the final value (Fig. 1).

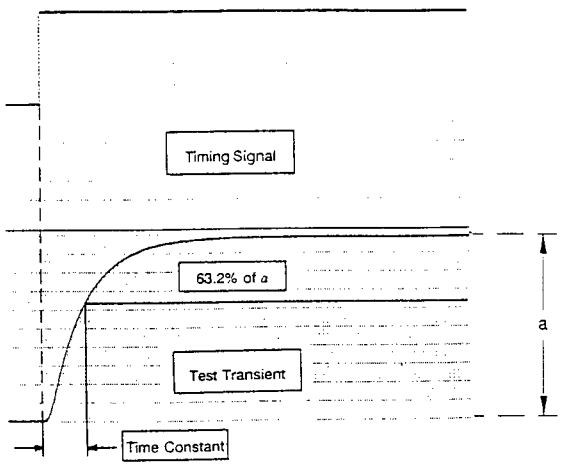

Figure 1. Determination of Temperature Sensor Time Constant from an Actual Plunge Test Transient.

It should be noted that although this definition of time constant is analytically valid only for a first order system, it is conventionally used for empirically establishing the response time of all temperature sensors regardless of the dynamic order. Therefore, all references to the terms "response time" or "time constant" in this appendix correspond to this definition regardless of the type or size of the sensor, the test condition, or the test method being used (whether it is the plunge or the LCSR test). It should be pointed out that the use of the term "time constant" in this appendix is not intended to imply that RTDs or thermocouples are necessarily representable by first order dynamics.

The time constant obtained by the plunge method is a relative index which should be accompanied by a description of the test conditions. This is important because the response time of temperature sensors is strongly dependent on the properties of the final medium in which they are plunged. The type of medium (air, water, etc.) and its velocity, temperature, and pressure must always be specified with the response time results. The fluid velocity is usually the most important factor followed by temperature and then pressure. These parameters affect the film heat transfer coefficient on the sensor surface which is related to the response time. Higher fluid velocities increase the film heat transfer coefficient on the surface of the sensor and reduce the response time. Temperature, however, has a mixed effect. On the one hand, temperature acts in the same manner as fluid velocity, i.e., it increases the film heat transfer coefficient and reduces the response time. On the other hand, high temperatures can affect the material properties inside the sensor and either increase or decrease the response time. Pressure does not usually affect the sensor response time except for its effect on the fluid properties that control the surface heat transfer coefficient. In addition to process effects, the response time of RTDs and thermocouples usually depends on installation, especially when the sensor is installed into a thermowell.

2.2 LCSR Test

Since the response time of a temperature sensor is strongly affected by installation and process conditions, laboratory measurements such as plunge tests in a reference condition cannot provide accurate information about the

"in-service" response time of the sensor. Therefore, an in-situ method that can be implemented at process operating conditions must be used. The LCSR method was developed to provide the in-situ response time testing capability that is needed to measure the in-service response times of RTDs and thermocouples.

The LCSR test procedure for RTDs and thermocouples is different even though the principle of the test is the same. For RTDs, the LCSR test is performed by connecting the RTD to one arm of a Wheatstone bridge and changing the bridge current from a few milliamperes to a level of about 40 to 80 milliamperes. The step change in current produces Joule heating in the RTD element and causes its resistance to increase in proportion to the RTD's ability to dissipate the heat to the environment. The transient change in RTD resistance produces a transient voltage signal at the output of the Wheatstone bridge which is referred to as the LCSR transient or the LCSR data for the RTD. This transient is then analyzed, as described in the following section on LCSR theory, to provide the time constant of the RTD under the conditions tested.

For thermocouples, the LCSR test is performed by heating the thermocouple internally by applying an electric current to its extension leads. The current is applied for a few seconds to raise the temperature of the thermocouple a few degrees above the ambient temperature. The current is then turned off and the thermocouple output is recorded as it cools to the ambient temperature. This output, which is referred to as the LCSR transient or LCSR data for the thermocouple, is predominantly due to the cooling of the thermocouple junction. The rate of the thermocouple cooling transient is proportional to its ability to dissipate the heat generated in its junction. Therefore, the LCSR data can be used with the analytical approach discussed in the following section to identify the response time of the thermocouple under the conditions tested.

The LCSR testing of thermocouples is performed using an AC current source to produce Joule heating. Since the electrical resistance of thermocouple circuits is small and distributed along the sensor, the heating current must be large enough to produce sufficient heating and provide a useful LCSR signal when the current is turned off. Depending on the size and length of the thermocouple and its extension wires, heating currents of approximately 0.3 to 3.0 amperes are usually used in LCSR testing of thermocouples as opposed to 40 to 80 milliamperes of DC current that are used in testing of RTDs. This is because in RTDs, the resistance of the circuit is much higher and predominantly concentrated at the RTD's sensing element.

3. LCSR THEORY

3.1 Background

The LCSR test is based on the principle that the output of a thermocouple or RTD to a step change in temperature induced inside the sensor can be converted to give the equivalent response for a step change in temperature outside the sensor. This is possible because the transfer function that represents the response to an external step change in temperature is related to that for an internal step change in temperature as follows:

$$G_{Plunge} = \frac{1}{(s-p_1)(s-p_2)\ldots} \tag{1}$$

$$G_{LCSR} = \frac{1}{(s-p_1)(s-p_2)\ldots}\,[(s-z_1)(s-z_2)\ldots] \tag{2}$$

Where G_{Plunge} represents the response that will be obtained in a plunge test and G_{LCSR} represents the response that will be obtained in a LCSR test. It is clear

that the plunge response is a subset of the LCSR response meaning that if the LCSR response is known, the p_1, p_2 , . . . will be known and can be used to obtain G_{Plunge}. The derivations that follow are carried out to show how to arrive at Eqs. (1) and (2).

3.2 Heat Transfer Analysis of a Temperature Sensor

The derivation of the LCSR and plunge test transfer functions given as G_{LCSR} and G_{Plunge} above are based on the assumption that the heat transfer between the sensor and the surrounding media is one dimensional (radial). With this assumption, the heat transfer between the sensing element in RTDs or the hot junction in thermocouples and the medium (fluid) surrounding the sensor may be represented by a lumped parameter network such as the one shown in Fig. 2. For this network, the transient heat transfer equation for node i is written as: (1)

$$mc \frac{dT_i}{dt} = \frac{1}{R_1}(T_{i-1} - T_i) - \frac{1}{R_2}(T_i - T_{i+1}) \quad (3)$$

where m and c are the mass and specific heat capacity of material in the node, and R_1 and R_2 are the heat transfer resistances between node i and the two adjacent nodes. Eq. (3) may be rewritten as:

$$\frac{dT_i}{dt} = a_{i,i-1} T_{i-1} - a_{i,i} T_i + a_{i,i+1} T_{i+1} \quad (4)$$

where

$$a_{i,i-1} = \frac{1}{mcR_1}$$

$$a_{i,i} = \frac{1}{mc}\left(\frac{1}{R_1} + \frac{1}{R_2}\right) \quad (5)$$

$$a_{i,i+1} = \frac{1}{mcR_2} .$$

AMS-DWG THC033A

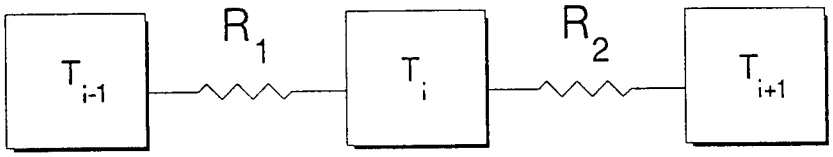

Figure 2. Lump Parameter Representation for LCSR Analysis.

The nodal equations may be applied to a series of nodes, starting with the node closest to the center $(i = 1)$ and ending with the node closest to the surface $(i = n)$:

$$\begin{aligned}
\frac{dT_1}{dt} &= -a_{11}\,T_1 + a_{12}\,T_2 \\
\frac{dT_2}{dt} &= a_{21}T_1 - a_{22}T_2 + a_{23}T_3 \\
\frac{dT_3}{dt} &= a_{32}T_2 - a_{33}T_3 + a_{34}T_4 \\
&\vdots \\
\frac{dT_n}{dt} &= a_{n,n-1}T_{n-1} - a_{n,n}T_n + a_{nF}T_F
\end{aligned} \tag{6}$$

where

T_i = temperature of the ith node (measured relative to the initial fluid temperature).

T_F = change of fluid temperature from its initial value.

These equations may be written in matrix form:

$$\frac{d\bar{x}}{dt} = A\bar{x} + \bar{f}\,T_F \tag{7}$$

where

(8)

$$\bar{x} = \begin{bmatrix} T_1 \\ T_2 \\ T_3 \\ . \\ . \\ . \\ T_n \end{bmatrix} \quad A = \begin{bmatrix} -a_{11} & a_{12} & 0 & 0 & 0 & 0 \\ a_{21} & -a_{22} & a_{23} & 0 & 0 & 0 \\ 0 & a_{32} & -a_{33} & a_{34} & 0 & 0 \\ 0 & . & . & . & . & . \\ 0 & . & . & . & . & . \\ 0 & . & . & . & . & . \\ 0 & . & . & . & a_{n,n-1} & -a_{n,n} \end{bmatrix} \quad \bar{f} = \begin{bmatrix} 0 \\ 0 \\ 0 \\ . \\ . \\ . \\ a_{nF} \end{bmatrix}$$

Laplace transformation of Eq. (7) gives:

$$[sI - A]\,\bar{x}(s) = \bar{f}\,T_F(s) + \bar{x}(t = 0). \tag{9}$$

The solution for the temperature at the central node, $x_1(s)$, is found by Cramer's rule:

$$T_1(s) = \frac{B(s)}{|sI-A|} \tag{10}$$

where

(11)

$$B(s) = \begin{bmatrix} T_1(0) & a_{12} & 0 & . & . & 0 \\ T_2(0) & (s+a_{22}) & -a_{23} & 0 & . & . \\ T_3(0) & -a_{32} & (s+a_{33}) & -a_{33} & . & . \\ . & . & . & . & . & . \\ . & . & . & . & . & 0 \\ . & . & . & . & . & 0 \\ [T_n(0) + a_n T_F(s)] & 0 & 0 & 0 & \ldots & -a_{n,n-1}(s+a_{n,n}) \end{bmatrix}$$

This Laplace transform is general for one-dimensional problems and its accuracy depends on the number of nodes used. Eq. (9) is solved below for two different initial conditions, one initial condition to correspond to the LCSR test and the other to correspond to the plunge test. In the LCSR test, the temperature in the center node of the sensing element is not ambient at time t = 0, while for the plunge test, the temperature at the center node is ambient at t = 0.

3.3 LCSR Equation

For the LCSR test, $\bar{x}(t = 0)$ is the initial temperature distribution, and it is a vector with all entries nonzero, meaning that the first column of $B(s)$ in the matrix of Eq. (11) has all nonzero entries.

Evaluation of the determinants, $B(s)$ and $|sI - A|$, in Eq. (10) gives:

$$G(s) = \frac{T_1(s)}{T_F(s)} = K \frac{(s - z_1)(s - z_2) \ldots (s - z_{n-1})}{(s - p_1)(s - p_2) \ldots (s - p_n)} \tag{12}$$

where each z_i is a zero (a number that causes $T_1(s)$ to equal zero), and p_i is a pole (a number that causes $T_1(s)$ to equal infinity) and K is a constant gain factor that can be set equal to unity to simplify the equation. The response $T_1(t)$ for a step change is obtained using the residue theorem (assuming all distant poles):

$$T_1(t) = \frac{(-z_1)(-z_2)\ldots(-z_{n-1})}{(-p_1)(-p_2)\ldots(-p_n)} + \frac{(p_1 - z_1)(p_1 - z_2)\ldots(p_1 - z_{n-1})}{(p_1 - p_2)(p_1 - p_3)\ldots(p_1 - p_n)} e^{p_1 t} + \frac{(p_2 - z_1)(p_2 - z_2)\ldots(p_2 - z_{n-1})}{(p_2 - p_1)(p_2 - p_3)\ldots(p_2 - p_n)} e^{p_2 t} + \ldots \tag{13}$$

This may be rewritten as

$$T(t) = A_0 + A_1 e^{p_1 t} + A_2 e^{p_2 t} + \ldots$$
$$A_0, A_1, A_2, \ldots = f(p_1, p_2, \ldots z_1, z_2, \ldots) . \quad (14)$$

Eq. (12) is referred to as the LCSR transfer function (G_{LCSR}) and Eq. (14) is referred to as the equation for the LCSR transient. If the data for a LCSR test is mathematically fit to Eq. (14), the values of $p_1, p_2, \ldots$ can be identified and used to construct the plunge test transient.

3.4 Plunge Test Equation

For a step perturbation of fluid temperature, $T_F(s)$ is nonzero, but $\bar{x}$ $(t = 0)$ has all zero entries because the initial temperature distribution is flat and equal to the initial fluid temperature. In this case, the first column of $B(s)$ contains all zeros, except for the last entry.

In this case, $B(s)$ from the matrix in Eq. (10) may be written as:

$$B(s) = \begin{bmatrix} 0 & a_{12} & 0 & . & . & . \\ 0 & (s+a_{22}) & -a_{23} & 0 & . & . \\ 0 & -a_{32} & (s+a_{33}) & -a_{34} & . & . \\ . & . & . & . & . & . \\ . & . & . & . & . & . \\ . & . & . & . & . & 0 \\ a_{nF} T_F(s) & 0 & 0 & 0 & . & -a_{n,n-1}(s+a_{n,n}) \end{bmatrix} \quad (15)$$

Using the Laplace expansion method for evaluation of the determinants, we obtain:

$$B(s) = a_{nF} T_F(s) (-1)^{n+1} \begin{bmatrix} -a_{12} & 0 & 0 & 0 & \ldots \\ (s+a_{22}) & -a_{23} & 0 & 0 & \ldots \\ -a_{32} & (s+a_{33}) & -a_{34} & 0 & \ldots \\ 0 & -a_{43} & (s+a_{44}) & -a_{45} & \ldots \\ . & . & . & . & \ldots \\ . & . & . & . & \ldots \\ . & . & . & . & \ldots \end{bmatrix} \quad (16)$$

This is a lower diagonal matrix, and its determinant is the product of the diagonals:

$$B(s) = a_{nF} T_F(s) (-1)^{n+1} (a_{12} a_{23} a_{34} \ldots) . \quad (17)$$

Therefore:

and the transfer function $\frac{T_1(s)}{T_F(s)}$ is:

$$T_1(s) = \frac{a_{nF} T_F(s)(-1)^{n+1}}{(s-p_1)(s-p_2)\ldots(s-p_n)} \tag{18}$$

$$G(s) = \frac{K}{(s-p_1)(s-p_2)\ldots(s-p_2)} \tag{19}$$

where K is a constant that can be set equal to unity to simplify the equation. By using the residue theorem, we obtain the following expression for the fluid temperature step change (Laplace transform of a unit step, i.e., $T_F(s) = \frac{1}{s}$) :

$$T_1(t) = \frac{1}{(-p_1)(-p_2)\cdots(-p_n)} + \frac{1}{p_1(p_1-p_2)(p_1-p_3)\cdots(p_1-p_n)} e^{p_1 t} + \frac{1}{p_2(p_2-p_1)(p_2-p_3)\cdots(p_2-p_3)} e^{p_2 t} + \ldots \tag{20}$$

This equation may be written as:

$$T_1(t) = B_0 + B_1 e^{p_1 t} + B_2 e^{p_2 t} + \ldots$$
$$B_0, B_1, B_2 \ldots = f(p_1, p_2, \ldots) \tag{21}$$

The following observations can be made about the fluid temperature step change (plunge) case:

1. The exponential terms $(p_1, p_2, \ldots)$ in Eq. (21) are the same as those of the LCSR equation given by Eq. (14). This is expected since the exponents depend only on the heat transfer resistances and heat capacities in the sensor, and these are the same for plunge and LCSR tests.

2. Unlike the LCSR Eq. (14), the coefficients that multiply the exponentials in Eq. (21) are determined by the values of the poles only and do not depend on zeros. Therefore, a knowledge of the poles alone is sufficient to determine both the coefficients and the exponentials of Eq. (21).

3.5 LCSR Transformation Procedure

The results of the derivations carried out above are used with the following procedure to convert the LCSR transient to give the equivalent plunge test transient:

1. Perform a LCSR test and sample the data with a computer.

2. Fit the LCSR data to the following equation and identify the p_i's. The A_i's do not have to be identified.

$$T(t) = A_0 + A_1 e^{p_1 t} + A_2 e^{p_2 t} + \ldots . \tag{22}$$

3. Substitute the p_i's identified in Eq. (22) into the plunge test equation (Eq. 20) to construct the plunge test response.

4. Use the transient identified in step 3 above to obtain the time

constant of the sensor by determining the time that it takes for the transient to reach 63.2 percent of its final steady state value.

3.6 Two-Dimensional Heat Transfer

The approach used above can be followed to analyze the thermocouple and RTD heat transfer based on a two dimensional model. The reader may consult Ref. (1) for a derivation of the two dimensional equation. The key results of the two dimensional analysis is that, unlike the one dimensional case, the step response results have zeros in the transfer function as well as poles. That is, the poles identified by the LCSR test are not all that is needed to construct the plunge test response. However, experience with typical industrial RTDs and thermocouples in typical installations has shown that the errors due to minor departures from one dimensional assumptions are often not significant.

4. LCSR VALIDATION

The validity of the LCSR test depends on two assumptions about the physical location of the sensing element in the sensing tip of the sensor. The two assumptions are:

1. The heat transfer between the sensor and its surrounding fluid must be one dimensional (radial).

2. The sensing element of the sensor must be located at the center of the sensor assembly or there must be little heat capacity between the sensing element and the centerline of the sensor assembly.

These assumptions must be satisfied for the heat transfer to and from the sensing element to be unidirectional and for the LCSR transient to be transformable to the plunge test transient. The only reliable and practical method to ensure that these assumptions are adequately satisfied and that the LCSR test is valid for the RTD or thermocouple is to perform experimental measurements. More specifically, each RTD or thermocouple design to be tested by the LCSR method must undergo an experimental laboratory validation to insure that the LCSR result is valid and accurate enough for the specific design. The validation should involve a plunge test followed by a LCSR test performed under the same test conditions on each RTD or thermocouple design to be validated. The LCSR data is then analyzed, as was described in the section entitled "LCSR Transformation Procedure", and the response time result is compared with that of the corresponding plunge test result to establish the validity and determine the accuracy of the LCSR method for the sensor design being validated.

For resistance temperature detectors (RTDs), the sensor is said to be testable by the LCSR method if the difference between its plunge test and LCSR test results is less than ±10 percent. For thermocouples, however, a difference of about ±20 percent is usually used as the threshold for expressing LCSR testability.(2) This is because thermocouples are more difficult to test with the LCSR method than RTDs.

4.1 Laboratory Validation Results for RTDs and Thermocouples

Tables I and II present typical validation results for representative RTDs and thermocouples tested in the laboratory in room temperature water at a flow velocity of 1 meter per second (m/s). The reasonable agreement between the plunge and the LCSR test results shown in these tables indicates that the sensors shown are in-situ testable by the LCSR method.

TABLE I

LCSR Validation Results for RTDs in Room Temperature Water at 1 m/s

RTD Number	Response Time (sec) Plunge	LCSR	Percent Difference
1	7.1	7.2	1.4
2	6.3	6.6	4.8
3	4.9	4.9	0.0
4	5.2	5.3	1.9
5	2.8	2.6	-7.1
6	3.1	3.1	0.0
7	0.38	0.42	10.5
8	4.8	4.5	-6.3
9	4.6	4.2	-8.7
10	2.0	2.1	5.0
11	3.5	3.4	-2.9
12	2.7	2.9	7.4
13	5.8	6.2	6.9

The above results include various models of RTDs manufactured by Conax, RdF, Rosemount and Weed.

TABLE II

LCSR Validation Results for Thermocouples in Room Temperature Water at 1 m/s

Thermocouple I.D. Number	Outside Diameter (mm)	Response Time (sec) Plunge	LCSR
	TYPE E		
44	6	1.9	1.6
27	5	1.9	1.8
29	3	1.4	1.3
43	2	0.3	0.4
	TYPE J		
46	6	1.8	1.5
36	5	1.4	1.1
38	3	1.8	1.4
40	2	0.4	0.4
	TYPE K		
4	6	2.7	2.7
7	5	2.7	2.4
9	3	0.7	0.6
13	2	0.3	0.2

The same type of results are listed in Tab. III from testing of thermocouples in room temperature air at a flow velocity of 14 m/s. Again, the agreement between the results of the two tests is reasonable in most cases, indicating that the LCSR method is valid for these thermocouples in air. The validation of the LCSR method for thermocouples in air is important because thermocouples are the most widely used temperature sensor for industrial temperature measurements in air and gases where RTDs can not usually be used due to the self heating problem inherent in RTDs.

TABLE III

LCSR Validation Results for Thermocouples in Room Temperature Air at 14 m/s

Thermocouple I.D. Number	Outside Diameter (mm)	Response Time (sec) Plunge	LCSR
	TYPE E		
51	Exposed Junction	1.1	0.8
43	2	3.9	4.5
29	3	10.6	12.1
27	5	17.1	22.3
44	6	23.9	32.6
	TYPE J		
52	Exposed Junction	1.3	1.2
40	2	3.2	3.8
38	3	9.9	12.1
36	5	17.5	21.3
46	6	24.9	35.9
	TYPE K		
22	Exposed Junction	0.5	0.3
13	2	3.7	3.9
9	3	10.0	11.3
7	5	17.1	23.0
4	6	25.2	29.7

Note that the thermocouple dimensions given in the tables included in this appendix are approximate values that were converted from English units and presented here in round numbers. Also note that the test results given for RTDs include various RTDs from four U.S. manufacturers and include both direct immersion and thermowell-mounted RTDs. The RTDs that have been validated for LCSR testability have mostly been of the types used in nuclear power plants. This is because of a requirement in the nuclear power industry for periodic measurement of response times of safety-related sensors to insure that aging degradation does not cause unacceptable dynamic performance. In addition to laboratory validation tests, nuclear plant RTDs have been validated for LCSR testability under simulated nuclear reactor conditions as described below.

4.2 Laboratory Validation Results for RTDs in Nuclear Power Plants

Because of the interest in response time testing of safety related RTDs in nuclear power reactors, the LCSR validation tests for RTDs were also performed in a test loop that simulated the water temperature, pressure, and flow that are found in typical pressurized water reactors.(3) Sample results of these tests are shown in Tab. IV for four RTDs of the types used in nuclear power plants. The results listed under plunge test in Tab. IV were actually obtained by sudden injection of cold water upstream of the RTD as installed in the test loop. A high speed reference thermocouple was attached to the tip of the RTD, and its output was used as the timing signal for the injection tests. The water in the test loop during the LCSR validation experiment was at a temperature of 280°C (536°F), a pressure of approximately 160 bars (2,320 psi), and a flow velocity of approximately 5 to 6 m/s (approximately 16 to 20 feet/second).

TABLE IV

Sample LCSR Validation Results for RTDs in Nuclear Power Plant Conditions

RTD Number	Time Constant (sec) Plunge	LCSR	Percent Difference
1	6.2	5.9	-4.8
2	4.1	3.7	-9.8
3	8.8	8.4	-4.5
4	0.14	0.13	-7.1

4.3 Validation Results for Thermocouples in Wind Tunnels

Due to the importance of thermocouple response time information in transient temperature measurements in flowing air and gases, particularly in aerospace applications, the validation of the LCSR method was also performed in subsonic and supersonic wind tunnels at ambient temperature[4]. The results of these tests are summarized in Tables V and VI. The good agreement between the plunge and LCSR results in these tables is indicative of the validity of the LCSR method for these thermocouples.

TABLE V

LCSR Validation Results for Thermocouples in Subsonic Wind Tunnel

Thermocouple I.D. Number	Response Time (sec) Plunge	LCSR
	27 m/sec ≈ 60 miles/hr	
14	1.4	1.2
15	0.7	0.8
16	1.7	1.5
22	0.4	0.5
29	8.0	9.1
40	2.5	4.4
	45 m/sec ≈ 100 miles/hr	
14	1.2	2.0
15	0.4	0.3
16	1.1	1.0
22	0.3	0.4
40	2.2	3.0
	55 m/sec ≈ 123 miles/hr	
29	6.0	6.3

In addition to demonstrating the validity of the LCSR method, the results in Table VI show how the response times of thermocouples are reduced from testing in air at 14 m/s to testing in the supersonic wind tunnel at Mach 2. The plunge test results shown under Mach 2 in Tab. VI are extrapolated from laboratory results using the formulas that provide response time estimates for high heat transfer coefficients based on measurements made in a laboratory in a fluid at moderate flow velocities[4].

TABLE VI

LCSR Validation Results for Thermocouple in Supersonic Wind Tunnel (Mach 2)

Thermocouple I.D. Number	Wire Outside Diameter (mm)	Response Time (sec) @ 14 m/sec	Response Time (sec) @ Mach 2	
		Plunge Test	Plunge*	LCSR
18	1.3	0.14	0.05	0.05
20	1.3	0.16	0.05	0.04
22	4.1	0.49	0.06	0.06
23	4.1	0.50	0.06	0.08

* Extrapolated from laboratory measurements.

5. ACCURACY OF LCSR TEST RESULTS

The results shown in Tables I through VI and other work completed by the authors and others have concluded that the LCSR method for RTDs can generally provide response time results with average accuracies of better than ±10 percent with respect to the true time constants obtained by the plunge test method. For thermocouples, however, due to difficulties in performing the tests, the accuracy of the LCSR results are not generally as good as those for RTDs. Based on the results of a comprehensive research and development project conducted over a three-year period, as reported in Ref. (4), the LCSR tests have been found to have an average accuracy of about ±20 percent for typical thermocouples tested in water or air at moderate temperature and flow conditions. It should be pointed out that accuracies of as good as 5 percent can sometimes be achieved in LCSR results for RTDs and thermocouples using carefully executed test procedures and by repeating the tests on the same sensor ten to twenty times and averaging the results for better statistical accuracy.

6. CONCLUSIONS

The Loop Current Step Response (LCSR) method has been validated and commercial equipment has been developed for in-situ measurement of response times of installed RTDs and thermocouples. The LCSR method accounts for the response time of the sensor itself, the thermowell (if one is used), and process conditions such as fluid temperature and velocity that can have an effect on response time.

The average accuracy of the LCSR method is about ± 10 percent for RTDs and about ±20 percent for thermocouples. Better LCSR accuracies can be achieved for both RTDs and thermocouples under suitable test conditions and with carefully executed test procedures and adequate test equipment. The LCSR method is useful in many applications involving transient temperature measurements with RTDs or thermocouples.

REFERENCES

1. Kerlin, T.W., "Analytical Methods for Interpreting In-Situ Measurements of Response Times in Thermocouples and Resistance Thermometers," Oak Ridge National Laboratory, Report Number ORNL/TM-4912, Oak Ridge, Tennessee (March 1976).

2. Hashemian, H.M., et al., "In-Situ Response Time Testing of Thermocouples", ISA Transactions, Volume 29, Number 4, pp. 97-104 (1990).

3. Hashemian, H.M., Jacquot, J.P., and Guerin, B., "Preliminary Report: Response Time Testing of Resistance Temperature Detectors (RTDs) in EDF Test Loop", Electricite de France, EDF Report Number HP/236/79/04 (January 1978).

4. Hashemian, H.M., "New Technology for Remote Testing of Response Time of Installed Thermocouples," U.S. Air Force, Arnold Engineering Development Center, Report Number AEDC-TR-91-26, Volume 1 (January 1992).

APPENDIX B

OPERATIONS MANUAL FOR DYNAMIC THERMOCOUPLE TEST EQUIPMENT

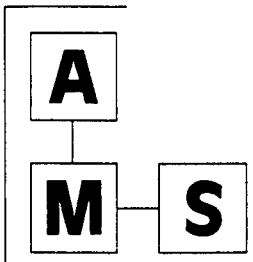

ANALYSIS AND MEASUREMENT SERVICES CORPORATION

AMS 9111 Cross Park Drive / Knoxville, TN 37923 USA

Manual #: NAS9601R0

OPERATIONS MANUAL FOR DYNAMIC THERMOCOUPLE TEST EQUIPMENT

Revision 0

January 1996

Telephone: (423) 691-1756 Fax: (423) 691-9344 E-mail: info@ams-corp.com

Manual #: NAS9601R0

PROPRIETARY NOTICE

This manual contains AMS proprietary information which shall be used only by the customer's own employees within the customer's organization for which this manual has been written. This manual shall not be reproduced in any form for use by any individual or organization outside of customer's facilities.

ANALYSIS AND
MEASUREMENT SERVICES
CORPORATION

AMS 9111 Cross Park Drive / Knoxville, TN 37923 USA

Manual #: NAS9601R0

Submitted By: Christopher N. Jones Date: 1/23/96

Reviewed By: Craig L. Shell Date: 1/23/96

Approved By: Dan D. Beverly Date: 01/23/96

Telephone: (423) 691-1756 Fax: (423) 691-9344 E-mail: info@ams-corp.com

1.0 INTRODUCTION

The AMS Model ETC-3 is an integrated instrument for performing Loop Current Step Response (LCSR) tests on thermocouples. The ETC-3 contains several desirable features for performing thermocouple tests using the LCSR method. Built-in signal conditioning amplifiers along with a mechanism that allows the current duration (heating time) to be manually adjusted based on the type, size, and installation configuration of each thermocouple are attributes of the ETC-3 dynamic thermocouple test unit.

The ETC-3 instrument includes the following components:

1. An AC power supply capable of supplying 0-60 VAC @ 5.0 amperes.
2. Analog current meter to avoid current overloading situations.
3. A set of adjustable medium and universal gain DC amplifiers.
4. Two position adjustable low-pass filter (5 Hz and 15 Hz) built into the medium gain DC amplifier and 60 Hz notch filter built into universal gain DC amplifier.
5. Adjustable current duration relay.

The LCSR raw data will be analyzed to provide both quantitative and qualitative information regarding the installation of the thermocouple. The analysis will be performed using computer-based software designed at AMS and introduced in section 5.0 of this manual. Figure 1.1 shows the necessary equipment setup to perform thermocouple installation testing featuring the AMS ETC-3 dynamic thermocouple test unit.

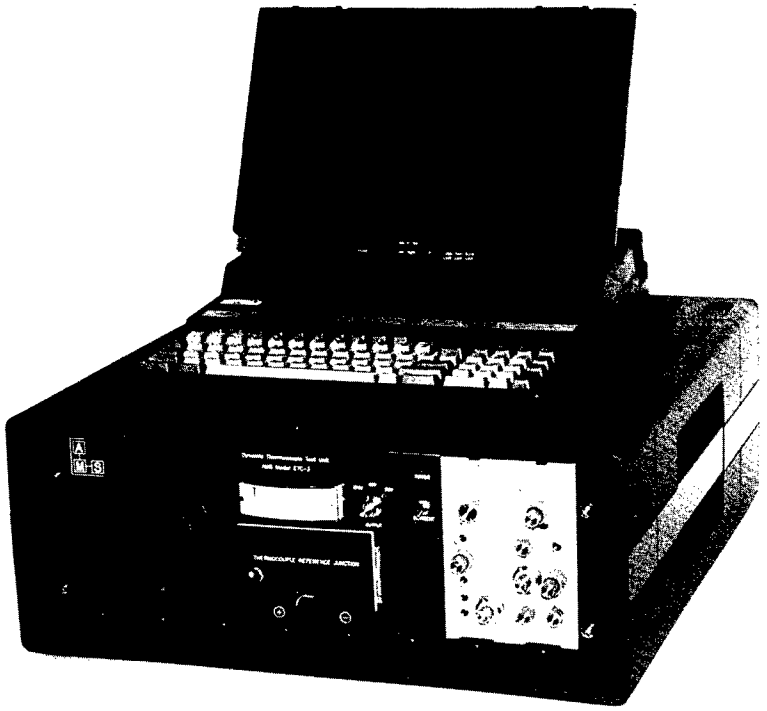

Figure 1.1 Test Setup Featuring The ETC-3 Thermocouple Test Unit

2.0 THERMOCOUPLE RESPONSE TIME TEST METHODS

The LCSR test is a method for measuring the response time of thermocouples. The advantage of this method over the traditional plunge test is that it permits in-situ testing of installed sensors. The plunge test requires that the sensor be removed from the process to be tested in a laboratory environment. An LCSR test on a thermocouple involves heating the sensor with a few amperes of AC current to induce a temperature rise in the sensing junction. A few seconds of heating generally provides a sufficient temperature rise within the thermocouple. The current is then discontinued and the resulting cooling transient of the thermocouple is amplified and recorded as the sensing junction returns to ambient temperature. This transient data may be analyzed using the software package provided by AMS to obtain the installation index of the sensor. Appendix A contains a description of the LCSR method. A detailed discussion is found in the final AMS report to NASA under contract number NAS8-40165.

3.0 DESCRIPTION OF TEST EQUIPMENT

3.1 ETC-3 Specifications

The AMS Model ETC-3 instrument is designed for LCSR testing of all sizes of insulated junction thermocouples. A photograph of the thermocouple installation test instrument (ETC-3) is shown in Figure 3.1. This instrument meets the following specifications:

Maximum output power: 0.3 KVA

Maximum output AC current: 5.0 amperes @ 60 Hz.

Maximum AC voltage: 0.5 of the line voltage (60 volts @ 60 Hz.)

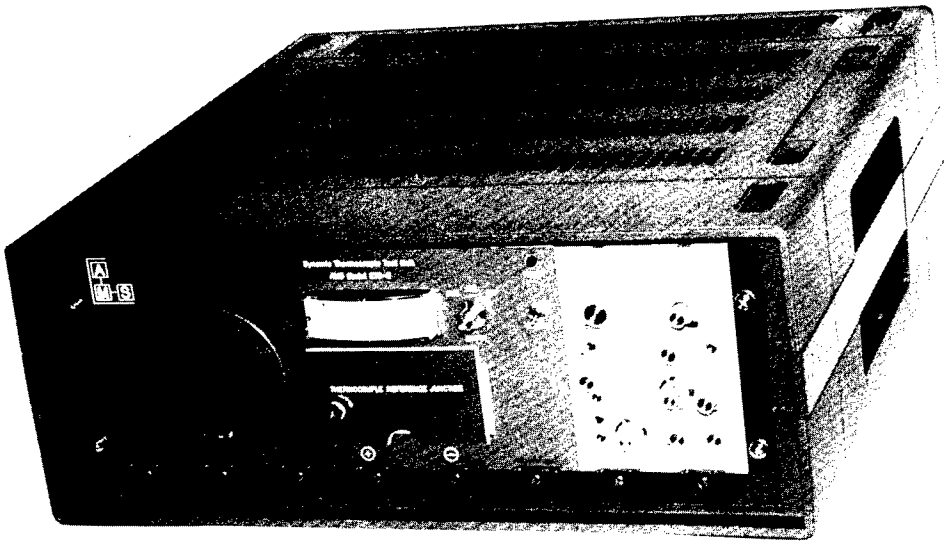

Figure 3.1 ETC-3 Dynamic Thermocouple (Response Time) Test Unit

Medium Amplifier Gain:
Minimum = 0.01
Maximum = 200

Universal Amplifier Gain:
Minimum = 0.2
Maximum = 100,000

Frequency Response:

Medium Gain Amplifier: Less than 3db down at 2KHz with filter off; flat to ± .5% from dc to 100Hz with filter off.

Universal Gain Amplifier: For low frequency and high frequency settings, amplifier output will be ±15% of the indicated frequency at 3db down with a rolloff of -6db/oct.

3.2 ETC-3 Operating Instructions

The AMS ETC-3 instrument operates from a single-phase 110 VAC power source with the neutral conductor at earth potential. The instrument has a 3-wire power cord with a 3-terminal polarized plug for connection to the power source and safety ground. The live conductor passes through a 3.0 Amp. fuse provided for over-current protection. The ground terminal of the plug is directly connected to the chassis.

The instrument is turned ON by a power switch on the rear panel (Figure 3.2). Also included on the rear panel are a power cord socket, fuse, current duration control, output ribbon connector, and digital multimeter hookup port.

A block diagram of the ETC-3 dynamic test instrument is shown in Figure 3.3. The function of the front panel components (Figure 3.4) are described below:

1. POWER: This LED lights when power switch is energized.

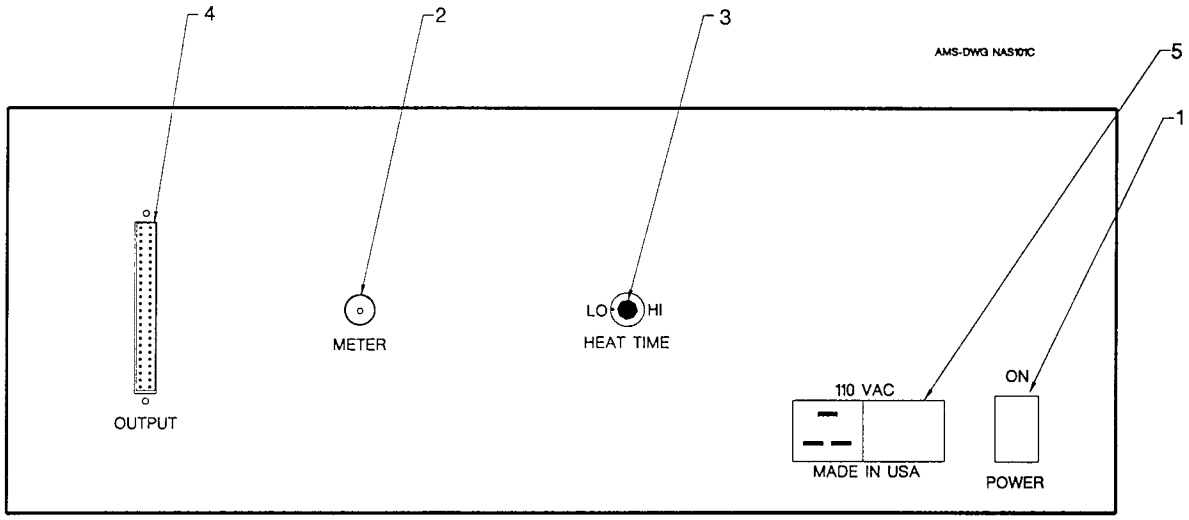

Figure 3.2 Rear Panel of ETC-3 Thermocouple Test Equipment

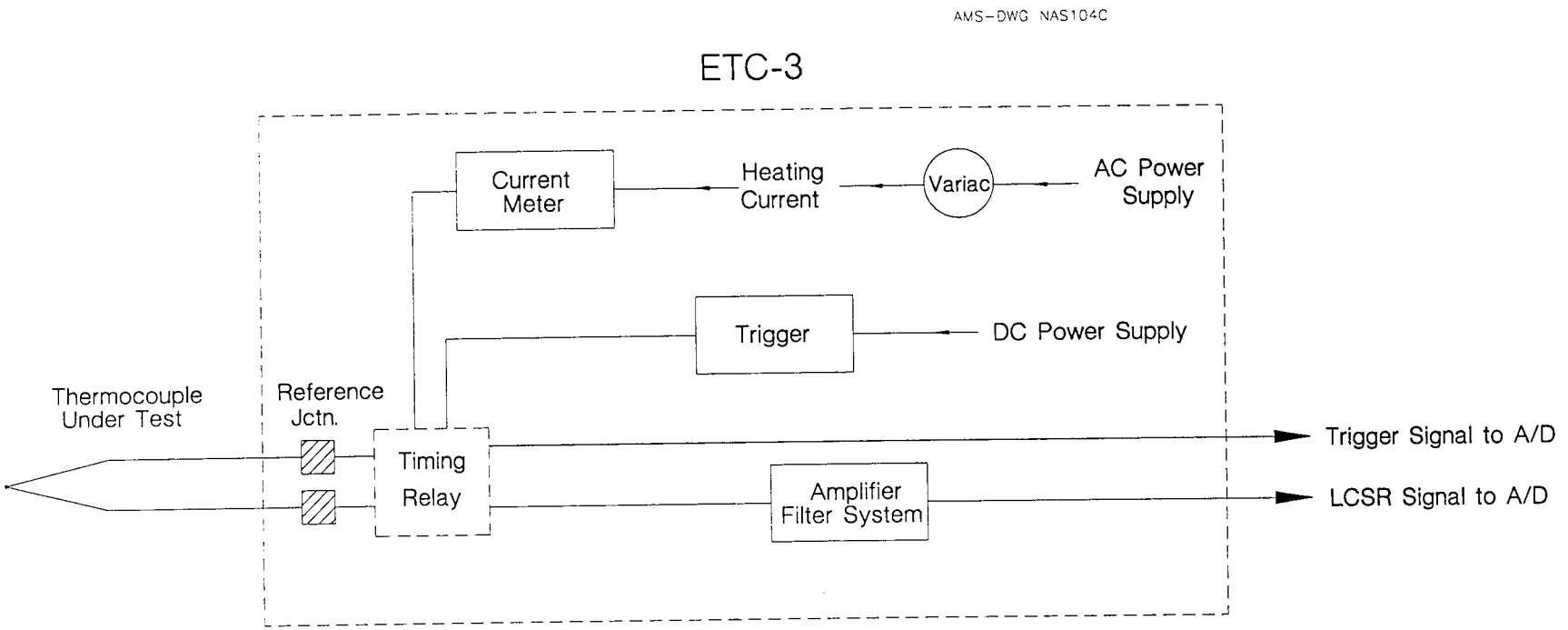

Figure 3.3 Diagram of ETC-3 Thermocouple Test Unit

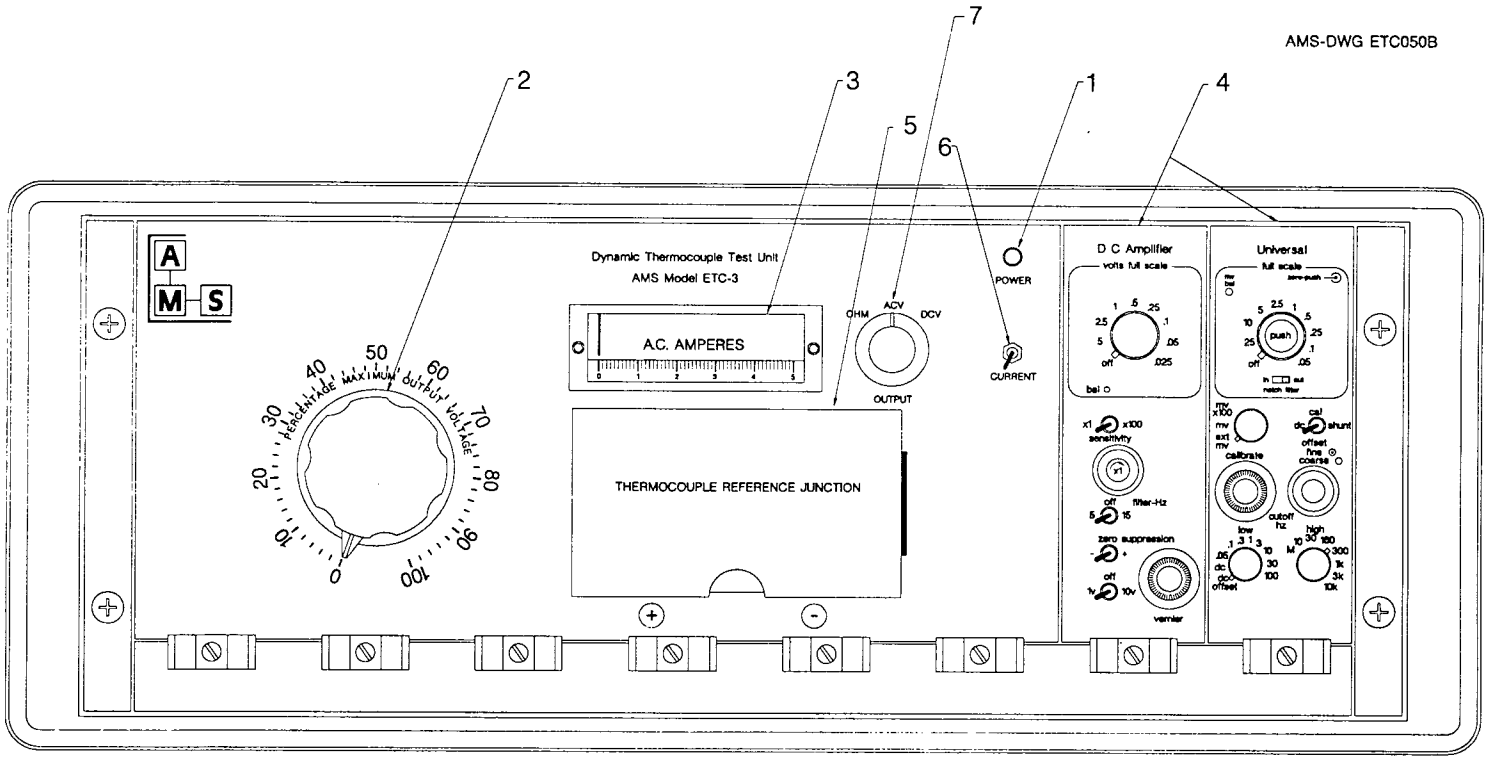

Figure 3.4 Front Panel of ETC-3 Thermocouple Test Equipment

2. VOLTAGE ADJUSTMENT: The voltage across the thermocouple is varied by turning the large voltage adjustment dial. This provides control for heating current to the thermocouple.

3. HEATING CURRENT METER: This meter indicates the value of AC current (in amperes) flowing through the thermocouple.

4. MEDIUM GAIN DC AMPLIFIER AND UNIVERSAL GAIN DC AMPLIFIER: Controls thermocouple output signal gain using the adjustment control knobs. Charts of signal amplification versus amplifier control setting for the Medium gain and Universal gain DC amplifiers are shown in Table 3.1 and Table 3.2, respectively. Medium gain amplifier includes 5 Hz and 15 Hz filter settings and universal gain amplifier includes a 60 Hz notch filter to limit high frequency noise associated with high amplifications.

5. THERMOCOUPLE REFERENCE JUNCTION: The thermocouple extension wire is connected to the copper block underneath a protective safety door. The negative thermocouple wire must be connected to the right-hand side terminal. **CAUTION - HIGH VOLTAGE:** High voltage is supplied to the copper blocks. To insure safety, connect the thermocouple with the main power switch in the OFF position and/or CURRENT switch in the DOWN position.

6. CURRENT: In the UP position, this switch allows for current to flow through the thermocouple during the heating stage.

7. OUTPUT: Selects type of output obtainable at the METER port (back panel). Selections include resistance (OHM), AC voltage (ACV), and DC voltage (DCV) used in heating current calculations and output display determination.

The function of the ETC-3 back panel components (Figure 3.2) are described below:

1. POWER SWITCH: ON/OFF switch that controls 110V power to ETC-3 thermocouple unit.

2. METER OUTPUT: Provides AC voltage and TC resistance readings for thermocouple current calculations. METER output is controlled via OUTPUT selection knob on the ETC-3 front panel (OHM, ACV, and DCV).

3. HEAT TIME CONTROL: Controls the current heating time (duration) of the thermocouple in test. Heating time is a function of thermocouple type, size, and installation environment. LO and HI settings allow heating time to be increased from 0 to 6.0 seconds. Maximum allowable heating time is approximately 10.0 seconds.

4. OUTPUT RIBBON CONNECTOR: Output terminal for control computer hookup.

5. POWER INPUT/FUSE: Input port for 110V power. Standard power cord connector with a fuse for internal component protection.

TABLE 3.1

MEDIUM GAIN AMPLIFIER

Dial Setting	Gain (x1 pos.)	Gain (x100 pos.)
5	1	0.01
2.5	2	0.02
1	5	0.05
0.5	10	0.1
0.25	20	0.2
0.1	50	0.5
0.05	100	1
0.025	200	2

TABLE 3.2

UNIVERSAL GAIN AMPLIFIER

Dial Setting	Gain (volts pos.)	Gain (mv pos.)
25	0.2	200
10	0.5	500
5	1	1,000
2.5	2	2,000
1	5	5,000
0.5	10	10,000
0.25	20	20,000
0.1	50	50,000
0.05	100	100,000

3.3 Control Computer

A Toshiba T3200 portable computer has been included as an accessory to the ETC-3 thermocouple test unit for thermocouple installation testing. The computer will be equipped with the necessary AMS data acquisition and analysis software (LCSR based) for determining the installation index of embedded thermocouples. Figure 3.5 shows a block diagram of a typical thermocouple test set-up utilizing the ETC-3 and Toshiba portable computer.

The T3200 operates with standard operating systems, such as MS-DOS®, which enables you to use various applications for word processing, spreadsheets, and data base management. The T3200 incorporates the following features and benefits:

- Microprocessor: An 80286-12 microprocessor operating an IBM PC AT-compatible BIOS ROM at 12 mHz with an 80287-8 math coprocessor.
- Disk Storage: An internal 3½" hard disk with 40Mb of fixed data storage and an internal double-sided, double density, 3½" diskette drive accommodating diskettes holding 1.44MB of information.
- Memory: One mega-byte of RAM including 640KB of standard RAM and 3 to 4KB of expanded memory.
- Expansion Slot: Two internal, IBM-compatible expansion slots - one full length 16 bit and one half length 8 bit.
- Plasma Screen: A high resolution, gas plasma display panel, composed of 720 horizontal and 400 vertical pixels, displays 25 lines of standard text 80 characters wide.

3.4 ETC-3 Limitations

In LCSR testing of thermocouples, four effects may interfere with the measurement of the sensor time constant. These are:

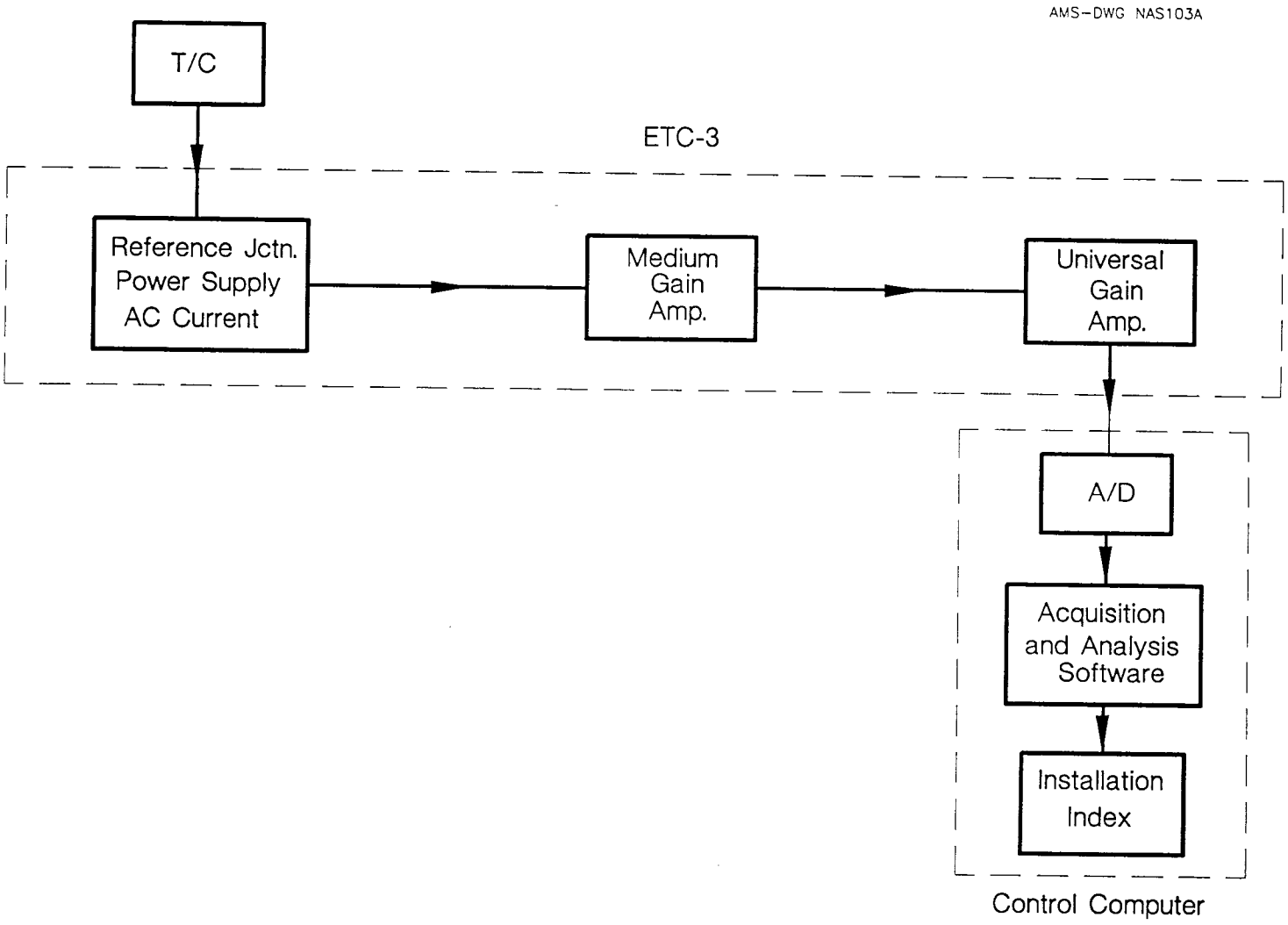

Figure 3.5 Diagram of Typical TC Test Set-Up Using the ETC-3 and Control Computer

1. Peltier Effect.
2. Magnetic Effects.
3. Resistance of extension wires.
4. High frequency electrical noise.

It is assumed that the user of this equipment is familiar with the Peltier and Magnetic Effects.

The AMS ETC-3 instrument eliminates the Peltier effect by using AC current for thermocouple heating. However, magnetic effects limit the use of this instrument to the following thermocouples:

1. Thermocouples without ferromagnetic wires.
2. Thermocouples with ferromagnetic wires, but operating above their Curie temperatures. (No magnetic effects are encountered above this temperature).
3. Thermocouples with ferromagnetic wires but a response time much greater than the relaxation time constant of the magnetic domains. (The relaxation time constant is typically around 50 ms).

The maximum current (I) available for heating a thermocouple with the ETC-3 test instrument is given by:

$$I = Vt / Rt$$

where Vt is the voltage across the thermocouple, and Rt is the sum of the thermocouple and lead wire resistances. Vt and Rt can be determined by setting the front panel selector to ACV and OHM, respectively, and monitoring the output at the METER port on the back panel of the ETC-3. A long extension wire limits the amount of current available for heating the thermocouple. This may result in a very small LCSR signal which may be difficult to monitor and analyze. This problem can be alleviated by reducing the length of the TC lead wires, using larger diameter lead

wires, or using external signal conditioning devices (amplifier and filter) to enhance the quality of the LCSR signal.

The LCSR signals from thermocouples are typically only a few tenths of a millivolt depending on the type of thermocouples being tested. Therefore high amplification of the TC signal is needed which, in turn, introduces high frequency noise in the acquired response data. A low pass filter (included in the medium gain amp.) and 60Hz notch filter (included in the universal gain amp.) can help over come this problem.

4.0 PERFORMING A THERMOCOUPLE TEST

4.1 Pre-Test Preparations

The following equipment is required for performing the LCSR tests:

1. AMS Model ETC-3 Thermocouple LCSR Test Instrument which includes filters and amplifiers.
2. Digital multimeter (DMM).
3. Spare TC or thermocouple checkout panel.
4. Data acquisition equipment (Control Computer).
5. Log Book with data sheets.

The ETC-3 is capable of applying hazardous voltages to the TC being tested. These voltages are also present on the front panel of the instrument. The user should exercise care in connecting the TC to the ETC-3. The user should also understand that misuse of the

equipment could partially damage the TCs being tested. Prior to plugging the unit to an AC power source, connect the thermocouple according to the instructions in the following section. Thermocouple connection to the instrument must be done with the main power OFF. If the thermocouple has a male of female connector, use a mating connector and extension wires (stranded) to connect the thermocouple to the instrument. Thermocouples with built-in extension wires and no connector may be connected directly to the instrument. Always keep the length of the extension wires as short as possible. Secure the thermocouple and extension wires in a manner to minimize vibration to avoid noise on the data.

A thermocouple checkout panel has been supplied to assist in equipment checkout. The checkout panel includes two 20 mil sheathed thermocouples arranged in an installed and uninstalled configuration as shown in Figure 4.1 Figure 4.2 shows the proper LCSR transient output acquired using the ETC-3 thermocouple test unit and thermocouple checkout panel.

4.2 Equipment Checkout Procedure

Prior to initial use or after extended periods of non-use, perform the functionality test addressed in Appendix B. This section gives the step-by-step instructions for performing a functional equipment checkout:

4.2.1 Set up the equipment as near as possible to the TC location. Figures 4.3 and 4.4 illustrate the equipment arrangement necessary for performing the following checkout procedure (printer is optional).

4.2.2 CAUTION: Prior to connecting power to the equipment, make sure that all power switches are OFF, and that the ETC-3 CURRENT switch is in the DOWN position.

4.2.3 Connect one of the checkout TCs (on the thermocouple checkout panel) to the reference junction (copper blocks) on the front panel of the ETC-3.

4.2.4 Close and latch protective safety door to conceal the TC reference junction. The ETC-3 will not operate until the safety door has been properly secured.

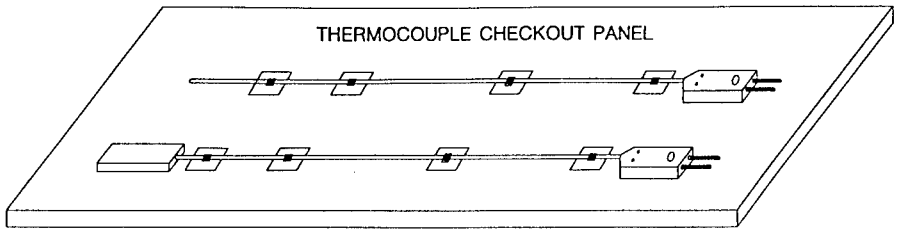

Figure 4.1 Thermocouple Checkout Panel Used in the Equipment Checkout Procedure

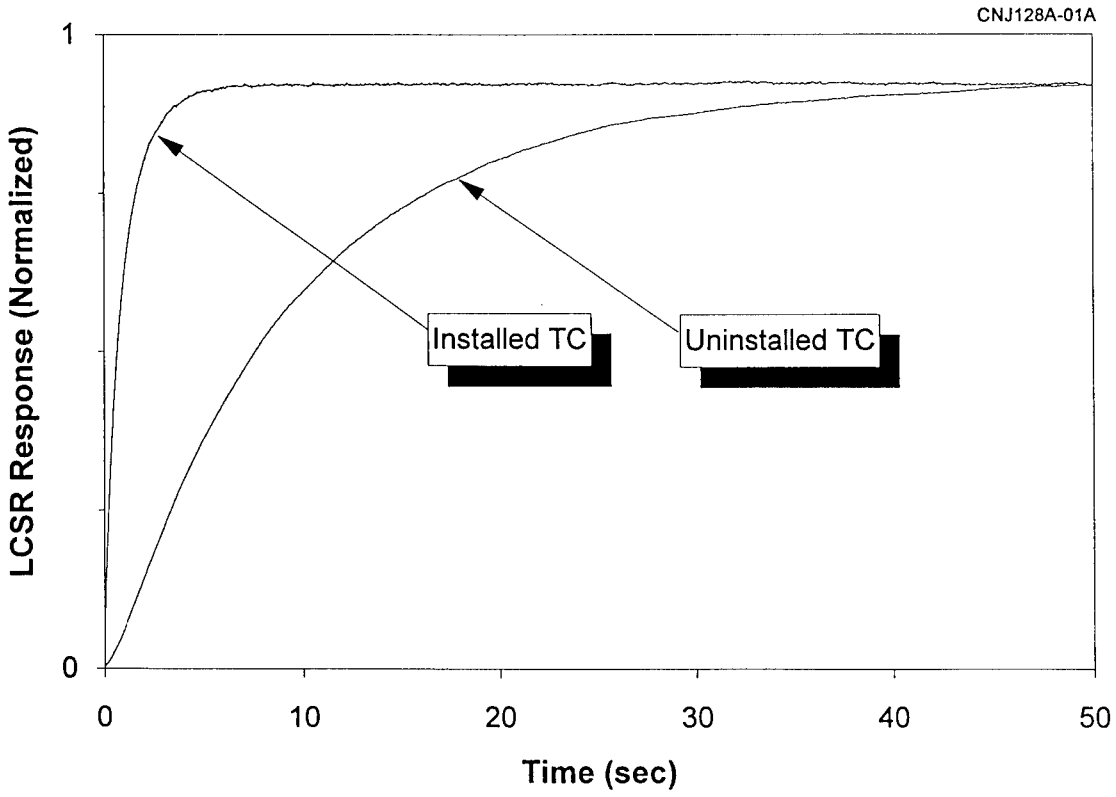

Figure 4.2 Typical Transient Output for Checkout Panel Thermocouples

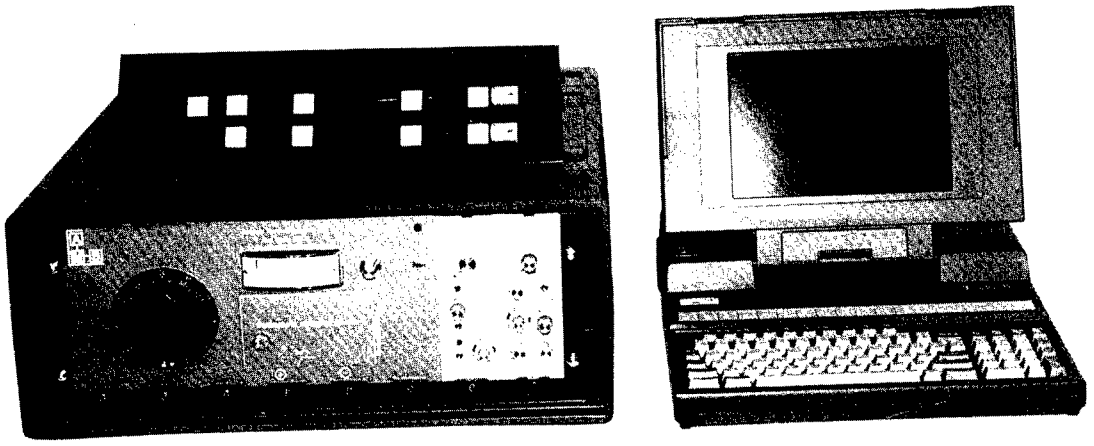

Figure 4.3 Equipment Needed for Pre-Test Checkout

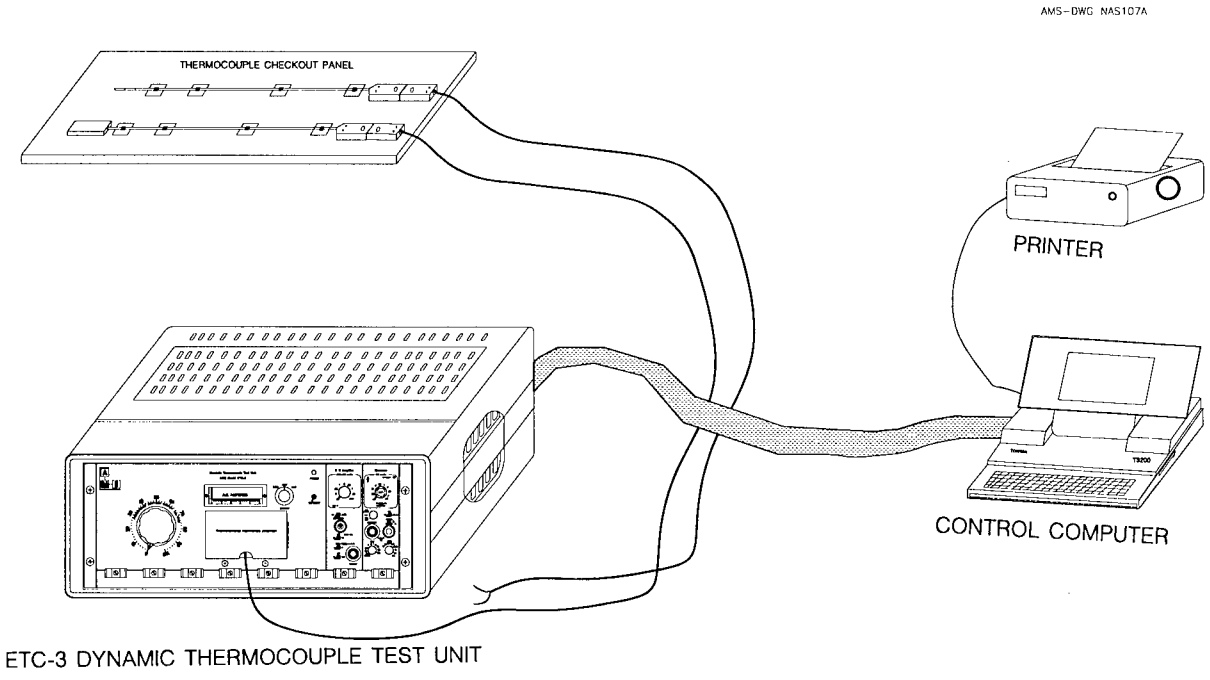

Figure 4.4 Equipment Setup for Pre-Test Checkout

4.2.5 Connect the equipment to a 110 VAC power source, turn POWER switch ON (back panel) and allow 15 minutes warm-up time.

4.2.6 Connect a DMM to the output of the ETC-3 (labeled METER on back panel).

4.2.7 Ensure that the ETC-3 VOLTAGE ADJUSTMENT is set to 0% (full counter clockwise).

4.2.8 Set OUTPUT control (front panel) to DC voltage (DCV).

4.2.9 Start LCSRTC thermocouple data acquisition software. Select oscilloscope (option O) to monitor thermocouple voltage output.

4.2.10 Figure 4.5 shows the initial amplifier setup for the checkout panel thermocouples. Amplifier gains will vary according to the checkout thermocouple that is being tested. For the provided checkout panel, the installed thermocouple requires a medium gain setting of .25 and universal gain setting of .5, while the uninstalled thermocouple requires gains of .5 and 1.0 for the medium and universal gain DC amplifiers, respectively. More gain is required for the installed checkout thermocouple because of its ability to dissipate energy (into host material) much more rapidly than the uninstalled (bare) thermocouple.

4.2.11 Set Heating Time control (back panel) to desired amount for check-out TC (approximately 2 seconds).

4.2.12 Adjust amplifier gain, offset, and filter settings, as necessary, to obtain a correctly scaled transient for the data acquisition software (approximately 9.0 DC volts out).

4.2.13 Set the CURRENT switch on the ETC-3 to the UP position.

4.2.14 Set the CURRENT switch to the DOWN position after the TC heating is complete. Wait for the TC to return to ambient temperature.

4.2.15 Incrementally increase the VOLTAGE ADJUSTMENT to achieve a full-scale thermocouple transient. Observe the heating current ammeter on the ETC-3 front panel to avoid excessive current levels.

4.2.16 Re-adjust amplifier gain and offset (if needed) to obtain a correctly scaled transient for the data acquisition software.

4.2.17 Repeat 4.2.13 to 4.2.16 as necessary to obtain a properly scaled transient.

4.2.18 Choose Option 2 of the LCSRTC acquisition software to acquire thermocouple output data. Set acquisition parameters for proper ΔT and number of samples (40 msec and 1500 points, respectively for checkout panel TCs).

4.2.19 Set the CURRENT switch to the UP position. Press [Enter] to begin sampling data. Current will be applied for desired duration as determined in step 4.2.11.

AMS-DWG NAS102B

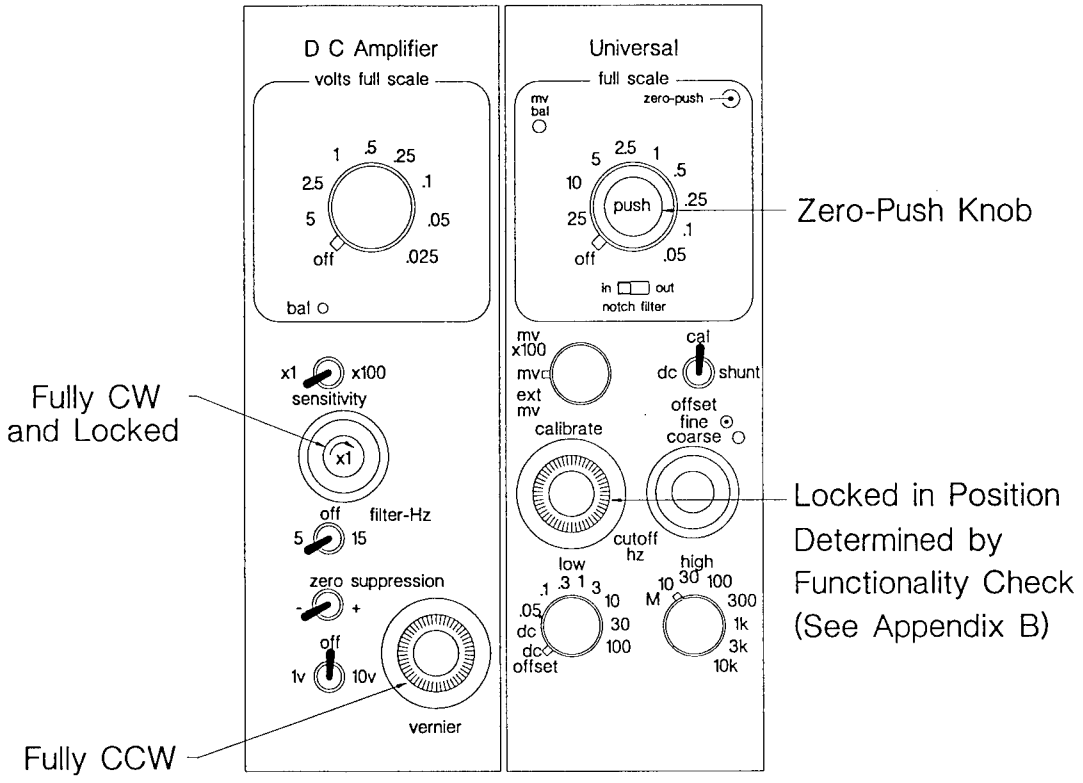

Figure 4.5 Gain, Offset, and Filter Settings for Medium and Universal DC Amplifiers

4.2.20 Observe the complete cooling transient on the computer screen. Set the CURRENT switch to the DOWN position after acquisition is complete.

4.2.21 View the complete TC transient data (Option 4) and save the data (Option 3) to a data file.

4.2.22 Repeat 4.2.19 to 4.2.21 as necessary to obtain a properly scaled transient. Some re-adjustment in amplifier gain may be necessary as checkout proceeds.

4.2.23 Ensure that the CURRENT switch is in the DOWN position.

4.2.24 Turn the VOLTAGE ADJUSTMENT to 0% (full counter clockwise).

4.2.25 Disconnect the checkout TC from the ETC-3.

Acceptance Criteria

The output obtained at step 4.2.20 must be a reasonably clean (free of excessive high and low frequency noise) exponential transient.

4.3 Thermocouple LCSR Test Procedure

The purpose of this procedure is to give detailed instructions for in-situ response time testing of thermocouples (TCs) using the LCSR method. In-situ testing allows the installed sensor to be tested remotely while it is exposed to normal operating conditions and without interference to the process operation. This procedure is based on using the AMS model ETC-3 thermocouple test instrument along with a data acquisition control computer. The user of this procedure is assumed to be familiar with LCSR methods.

The LCSR test must be performed at steady state conditions. That is, the process temperature, must be as constant as possible during the LCSR test. The inherent random fluctuations of these parameters may be tolerated but should be minimized by:

1. Using sufficient heating current in the LCSR test to improve the signal to noise ratio.

2. Using sufficient heating time to obtain proper signal to noise ratio.

3. Taking more than one data set on each sensor, then using an averaging technique to smooth the data. Depending on the amount and magnitude of the fluctuations, from 5 to 10 data sets are usually sufficient for this averaging.

The following is the complete thermocouple LCSR test procedure:

4.3.1 Perform the pre-testing procedure and equipment checkout procedure outlined in the above sections. Do not connect a TC to the ETC-3 unless the procedure in Section 4.2 is satisfactorily completed and the acceptance criteria are met. Proper operation of the ETC-3 must be assured before any connection to a TC is made.

4.3.2 Ensure that the ETC-3 VOLTAGE ADJUSTMENT is set to 0% (Full counterclockwise) and that the CURRENT switch is set to the DOWN position.

4.3.3 Connect the TC to be tested to the reference junction on the front panel of the ETC-3.

4.3.4 Close and latch the protective safety door to conceal the TC reference junction. The ETC-3 will not operate until the safety door has been properly secured.

4.3.5 Set OUTPUT knob (front panel) to OHM position. Measure the thermocouple loop resistance (at METER port on back panel) and record the value on the attached data sheet along with the other information requested in data sheet.

4.3.6 Set OUTPUT knob (front panel) to DCV.

4.3.7 Start LCSRTC thermocouple data acquisition software. Select oscilloscope (option O) to monitor thermocouple voltage output.

4.3.8 Adjust medium and universal amplifier gain, off-set and filter as necessary to obtain a correctly scaled signal for the data acquisition software (approximately 9.0 volts (DC) out). The type and installation of the TCs will determine the amount of amplifier gain that is necessary to achieve a proper TC signal.

4.3.9 Set the desired heating time using the HEAT TIME control on back panel.

4.3.10 Set the CURRENT switch on the ETC-3 to the UP position.

4.3.11 Set the CURRENT switch to the DOWN position after the TC heating is complete. Wait for the TC to return to ambient temperature.

4.3.12 Incrementally increase the VOLTAGE ADJUSTMENT to achieve a full-scale thermocouple transient. Observe the heating current ammeter on the ETC-3 front panel to avoid excessive current levels.

4.3.13 Re-adjust amplifier gain and offset (if needed) to obtain a correctly scaled transient for the data acquisition software.

4.3.14 Repeat 4.3.10 to 4.3.13 as necessary to obtain a properly scaled transient.

4.3.15 Record appropriate data on the attached data sheet.

4.3.16 Escape [ESC] from oscilloscope mode of LCSRTC software and choose software option 2 to acquire thermocouple output data. Set the acquisition parameters for proper ΔT, number of samples, and file storage location.

4.3.17 Set the CURRENT switch to the UP position. Press [Enter] to begin data acquisition using LCSRTC. Wait for the desired heating time (set in step 4.3.9).

4.3.18 Ensure that the data acquisition equipment is recording the TC cooling transient. Set the CURRENT switch to the DOWN position after acquisition is completed.

4.3.19 View the data using Options menu selection 4.

4.3.20 Save the data (if acceptable) using Options menu selection 5.

4.3.21 Repeat 4.2.17 and 4.2.20 as necessary to obtain the desired number of LCSR transients. Allow the thermocouple to properly cool to ambient temperature before initiating each sampling iteration. Slight adjustments in the current of the TC signal gain may be necessary as each testing iteration proceeds.

4.3.22 Stop the data acquisition equipment.

4.3.23 Record appropriate data on the attached data sheet and sign the data sheet.

4.3.24 Turn the VOLTAGE ADJUSTMENT to 0% (full counterclockwise).

4.3.25 Ensure that the CURRENT switch is in the DOWN position.

4.3.26 If desired, the data can be processed and averaged by selecting software option 6.

4.3.27 Disconnect the TC from the ETC-3.

Acceptance Criteria

The output obtained at step 4.3.18 must be reasonably clean (free of excessive high and low frequency noise) exponential transient.

4.3.28 Repeat 4.3.2 to 4.3.27 for each TC to be tested.

THERMOCOUPLE LCSR DATA SHEET

Date _____ Time _____

Plant _____

Sensor ID _____ Manufacturer _____

Model # _____

Type: ___ E ___ J ___ K ___ T _____ Other

Wire Length _____ Wire Diameter (Gage) _____

Junction Type: _____ Exposed Junction _____ Sheathed (Insulated Junction) _____ Sheathed (Grounded Junction)

Thermocouple Loop Resistance _____ (Ohms)

Installation Remarks: _____

_____

_____

_____

Process Flow _____

Conditions: Temperature _____

Service _____

Remarks _____

_____

Test Conditions:

Heating Current _____ (Amps) Heating Time _____ (Sec)

Output Voltage _____ (Volts)

Filter Setting(s) _____

Amplifier Gain(s) _____

Data Recording:

Disk ID _____ File Names: _____ To _____

Delta T _____ Number of Samples _____

Remarks: _____

_____

_____

_____

Signature

4.4 Analysis of Thermocouple Data

The analysis of acquired thermocouple transient data using AMS-designed software, LCSRTC10, provides the user with a quantitative installation value (installation index), as well as a qualitative visual comparison for complete thermocouple attachment determination. Multiple TC transient data files can be loaded and simultaneously viewed, on-screen, for a complete qualitative comparison. Figure 4.2 shows a qualitative comparison of TC transient data for the checkout panel thermocouples. A distinct difference can be observed in the data for an installed and uninstalled thermocouple as the installed thermocouple has a more rapid response. A numerical value called an installation index is also provided to the user for a quantitative comparison of thermocouple installation quality. An increasing installation index value is indicative of an increase in the degree of TC installation degradation (poorer installation) and a slower response time.

5. THERMOCOUPLE TEST SOFTWARE

Thermocouple test data acquisition and analysis is performed by AMS software LCSRTC10 in association with the ETC-3 and Toshiba T3200 control computer. LCSRTC10 is a DOS-based program that provides data processing, display, and analysis capabilities. The software provides a qualitative display as well as a quantitative value (installation index) enabling researchers to make important determinations with regard to sensor installation.

5.1 Program Installation

The thermocouple software can be installed on the control computer by manually copying the files from the installation disk to the hard drive.

Manual Installation:

1. Power up the control computer with the installation disk NOT inserted in the floppy drive.

2. The program is pre-installed on the system provided. If the software needs to be reinstalled for any reason, type from the DOS prompt "A:install". This will create a directory call "LCSRTC" on the C: drive and copy the software into this directory. If the software is being installed on a computer other than the one provided be sure the computer has a 286 or better processor and a math coprocessor. If the thermocouple software has been properly installed, the control program can be started simply by typing **C:\LCSRTC\LCSRTC**.

5.2 General Operation

The LCSRTC10 software utilizes a menu-driven interface that provides data acquisition, data analysis, and data visualization functions. Menus can be initiated or halted by using [Enter] or [Esc], respectively.

5.3 Options Menu

The Options menu is the main menu of the LCSRTC software. Each program function is accessed through the options menu. There are nine Options menu items with each having additional sub-menus: Oscilloscope, Erase Data File, Acquire Data, Store Data on Disk, Plot Data to Screen, DOS Shell, Process Data, A/D Test, and Exit.

5.3.1 O - Oscilloscope

This sub-menu initiates the oscilloscope screen that is used for initial acquisition parameter and equipment setup. The oscilloscope mode monitors thermocouple DC output voltages.

5.3.2 1 - Erase Data File

This sub-menu prompts the user for a file name (AAA0000) to be erased from the current working directory. To replace a previously created data file, the old file must first be erased. "Z" [Enter] will return the user to the Options menu.

5.3.3 2 - Acquire Data

This option allows the user to acquire data associated with the transient output of a thermocouple. Current sampling information (Actual Delta T, Number of Points Sampled, and Total Sampling Time) and data directory information are automatically displayed. Additional options are available within the Acquire Data menu and include the following:

1. To Begin Sampling - Initiate acquisition of thermocouple transient output data and create the appropriate data file (.DAT).

2. To Change Parameters - Allows sampling parameters to be adjusted according to various thermocouple installation configuration and environmental factors.

3. To Return to Menu - Return the user to the Options menu.

5.3.4 3 - Store Data on Disk

After successfully acquiring an LCSR transient, the data may be saved to disk with this option. The filename should be three letters followed by four numbers, for example "NAS0001." If files are numbered sequentially in this manner they may be more easily grouped when the data is being processed.

5.3.5 4 - Plot Data to Screen

Using this option, the user can review previously acquired data.

5.3.6 5 - DOS Shell

This allows the user to execute system commands without exiting the software. Typing "exit" will return the user to the Options menu.

5.3.7 6 - Process Data

After data has been acquired and saved, it may be analyzed, compared to other data, and printed using this option. There are two file selection options available to the user: 1) selection according to a sequentially ordered range of filenames, or 2) independent filename selection. Once the filenames are properly selected, these processing options are presented:

1. Create "T"ext Files - Text files are intended to provide a means of representing the data via spreadsheet analysis.

2. Create "A"veraged Files - Multiple files may be averaged to reduce the effect of noise and promote repeatability in thermocouple testing.

3. "G"raph Files - The graph option allows for visual inspection of thermocouple transient output and allows the user to overlay multiple data files.

There are also options to "C"ontinue processing additional files or "R"eturn to the Options menu. The processing option automatically normalizes the transient so that the data starts at 0 and ends at 90% of the maximum value. If the data was acquired using different sampling frequencies, the averaging routine will interpolate the data with the lower frequency and store the results at the highest frequency of the data runs being averaged. The printing option allows printing to an HP LaserJet, Diconix 300 and 180si printer, or other compatible printer.

5.3.8 7 - A/D Test

This option is used to verify the calibration (see Procedure ETC9601R0) of the analog to digital converter (A/D) using a continuous display of the raw A/D output in counts. The A/D is configured by AMS in a 0-10 volts range before shipment. The A/D is 12-bit, so the output will be 0-4095 for a 0-10 volt signal.

5.3.9 8 - Exit

Exit the program.

6. ETC-3 FUNCTIONALITY CHECK

In order to insure the ETC-3 test equipment is correctly functioning, a functionality check should be performed prior to initial use or after periods of limited operation. This check should be performed annually. The ETC-3 functionality check should be performed in accordance with Appendix B of this manual.

7. QUALITY ASSURANCE

All equipment manufactured by AMS is constructed under the AMS Quality Assurance Program. Each piece of equipment is thoroughly checked for proper operation of the hardware and software. This involves, but is not limited to, checking for proper operation of the ETC-3 Dynamic Thermocouple Test Unit components.

A functionality report is filed at AMS for each unit prior to shipment. This instrument should undergo the functionality checkout described in Section 6 at least once every year either by the customer or by AMS.

APPENDIX A

Description of LCSR Test

LCSR TESTING OF THERMOCOUPLES

LCSR testing of thermocouples is based on internal heating of the thermocouple by applying an electrical current to its extension leads. The current is applied for a few seconds and then turned off. This heats the thermocouple junction several degrees above its ambient temperature. When the current is stopped, the thermocouple output is monitored as the junction cools to the ambient temperature. The rate of this cooling depends on the response time of the thermocouple and how well the thermocouple is attached to the material whose temperature is being monitored. For thermocouples that are attached to or embedded in a solid material, the LCSR cooling rate is dominated by the bonding between the thermocouple and the solid material.

An AC power supply is used to heat the thermocouple with a current of 1 to 3 amperes depending on the resistance of the thermocouple circuit. The heating current is applied for 5 to 15 seconds depending on the conditions in which the thermocouple is tested. Following this heating period, the AC current is switched off and the thermocouple output is recorded immediately after the cessation of the heating current. The output is recorded until it reaches steady state indicating that the thermocouple junction has returned to the ambient temperature. The thermocouple cooling transient is then analyzed to obtain the dynamic response of the thermocouple under the installation conditions tested. The following publications may be consulted for more details:

Hashemian, H.M., "Determination of Installed Thermocouple Response." U.S. Air Force, Arnold Engineering Development Center, Report Number AEDC-TR-86-46, (December 1986).

Hashemian, H.M., "New Technology for Remote Testing of Response Time of Installed Thermocouples." United States Air Force, Arnold Engineering Development Center, Report Number AEDC-TR-91-26, Volume 1 - Background and General Details, (January 1992).

Hashemian, H.M., et al., "Improved Temperature Measurement in Composite Material for Aerospace Applications." National Aeronautics and Space Administration, Marshall Space Flight Center, Contract Number NA58-39814, MSFC, AL, (July 1993).

Hashemian, H.M., and Petersen, K.M., "Loop Current Step Response Method For In-Place Measurement of Response Time of Installed RTDs and Thermocouples." Published by American Institute of Physics, Seventh International Symposium on Temperature, Volume Six, pp. 1151-1156, Toronto, Canada, (May 1992).

Hashemian, H.M., et al., "In-Situ Response Time Testing of Thermocouples." ISA Transactions, Volume 29, Number 4, pp. 97-104, (1990).

Hashemian, H.M., Petersen, K.M., "In-Situ Test Gauge Thermocouple Performance, Part 1." Intech, Vol. 40, No. 1, pp. 30, (January 1993).

Hashemian, H.M., Petersen, K.M., "In-Situ Test Gauge Thermocouple Performance, Part 2." Intech, Vol. 40, No. 6, pp. 31, (June 1993).

APPENDIX B

ETC-3 Functionality Procedure

ANALYSIS AND
MEASUREMENT SERVICES
CORPORATION

AMS 9111 Cross Park Drive / Knoxville, TN 37923 USA

Procedure # ETC9601R0

ETC-3 FUNCTIONALITY PROCEDURE

Revision 0

JANUARY 1996

Telephone: (423) 691-1756 Fax: (423) 691-9344 E-mail: info@ams-corp.com

PROPRIETARY NOTICE

ANALYSIS AND
MEASUREMENT SERVICES
CORPORATION

AMS 9111 Cross Park Drive / Knoxville, TN 37923 USA

Procedure # ETC9601R0

Prepared By: Lucy S. Shull Date: 1/19/96

Reviewed By: Christopher N. Jones Date: 1/19/96

Approved By: Dan D. Beverly Date: 01/19/96

Telephone: (423) 691-1756 Fax: (423) 691-9344 E-mail: info@ams-corp.com

1. INTRODUCTION

This procedure contains the steps necessary to perform a functionality check of the AMS model ETC-3 thermocouple test instrument. The functionality check is to be performed, at a minimum, on an annual basis by properly trained and qualified personnel. Personnel performing this procedure shall be familiar with the operation of the ETC-3. In addition any repair or replacement of parts also necessitates a check of the functionality of the ETC-3.

WARNING: WHILE PERFORMING THE FUNCTIONAL CHECK PROCEDURE THE VOLTAGE OUTPUT KNOB (LOCATED ON THE ETC-3 FRONT PANEL) SHOULD BE IN THE FULLY COUNTER CLOCKWISE POSITION, THE REFERENCE JUNCTION DOOR OPEN AND THE CURRENT SWITCH IN THE DOWN POSITION. SEE AMS MANUAL # NAS9601R0 FOR DIAGRAMS OF COMPONENT LOCATIONS.

2. EQUIPMENT REQUIRED

The following equipment is necessary to perform a functionality check of the ETC-3.

1. Two calibrated DMMs. The calibration should be current and traceable to NIST.
2. D.C. power supply.

3. FUNCTIONALITY TEST

3.1 ETC-3 Amplifier Adjustment

The ETC-3 amplifier adjustment involves applying a short to the input (reference junction) of the equipment and adjusting the amplifier balance to null any offset that may have occurred.

3.1.1 Apply a short to the thermocouple input (reference junction) on the front of the ETC-3.

3.1.2 Turn equipment on and allow to warm up for 5 minutes.

3.1.3 Configure the amplifiers per Figure 3.1.

3.1.4 Connect a one calibrated DMM to the meter jack on the rear of the ETC-3.

3.1.5 Place the output selector knob (on the front of the ETC-3) in the DC position.

3.1.6 Push the Zero-Push knob on the universal amplifier to the LOCKED-IN position.

3.1.7 Adjust the balance (mv bal) on the universal amplifier to obtain an output voltage as close as possible to zero.

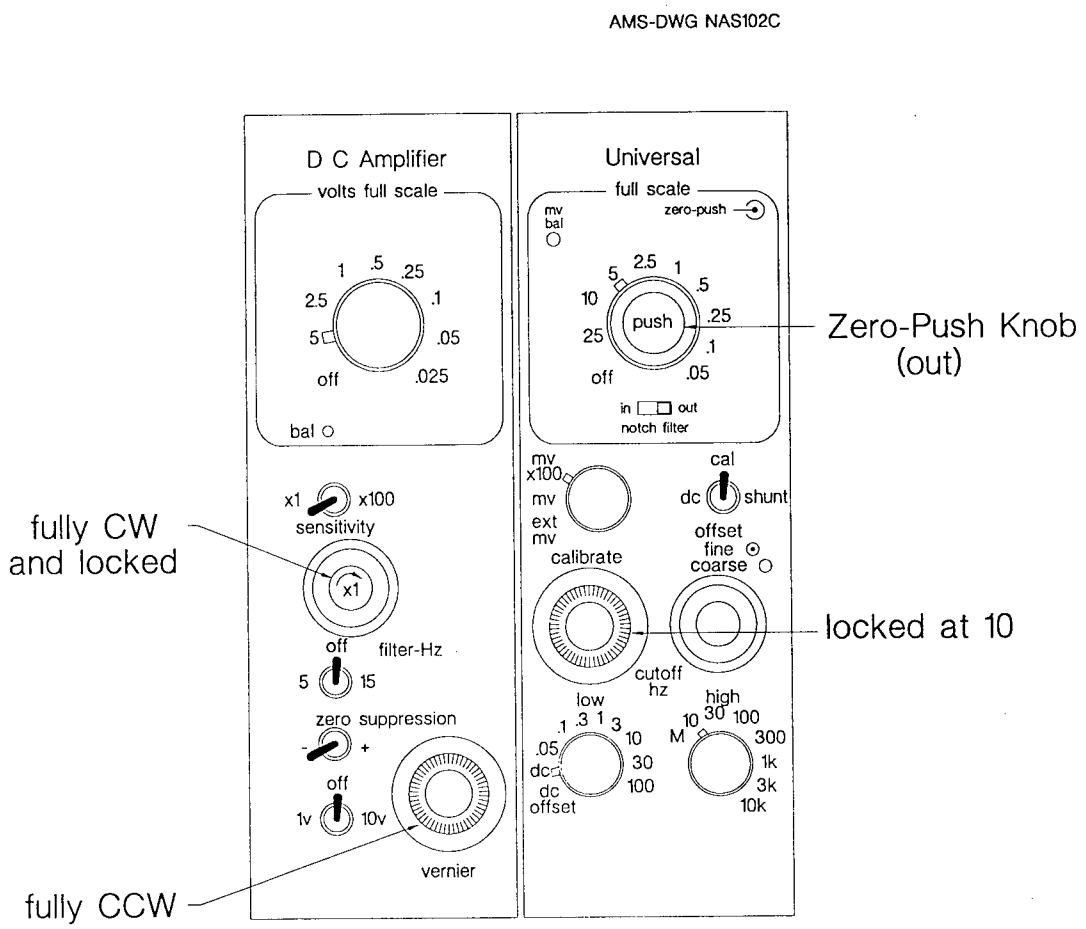

Figure 3.1 Amplifier Configuration

3.1.8 Push the Zero-Push knob on the universal amplifier to the OUT Position.

3.1.9 Adjust the balance (bal) on the medium gain amplifier to obtain an output voltage as close as possible to zero.

3.1.10 Disconnect the short from the thermocouple input (reference junction).

3.1.11 Connect a power supply to the thermocouple input (reference junction) and the second DMM.

NOTE: The polarity must be reversed when connecting to the reference junction (eg. power supply volt (+) to reference junction (-)).

3.1.12 Adjust the power supply to approximately 1.00 VDC.

3.1.13 Adjust the calibrate knob on the front of the Universal amplifier until the voltmeter connected to the meter jack (rear of ETC-3) is matched to the voltage from the power supply. Lock the knob in place.

3.2 System Voltage Check

The system voltage check involves the comparison of the input voltage, which is measured using a calibrated DMM, with the indicated counts from the A/D. This is used to verify that the voltages applied to the system are properly acquired by the A/D.

3.2.1 The amplifiers should be adjusted as outlined in 3.1 above.

3.2.2 Connect a variable DC power supply to the thermocouple input (reference junction).

3.2.3 Execute LCSRTC on the control computer. Enter option number 8 (A/D Test).

3.2.4 Apply known voltages of 2,5,8 VDC.

NOTE: The polarity must be reversed when connecting to the reference junction (eg. power supply volt (+) to reference junction (-)).

3.2.5 Record the measured voltage.

3.2.6 Record the actual measured number of counts (voltage) indicated by the computer (A/D) for the applied voltage. A sample data sheet is provided following the A/D voltage check section.

3.2.7 Compute the theoretical number of counts from the measured voltage using the following equation.

$$\underset{(counts)}{Output} = \left(\frac{4095}{10}\right) [Measured\ Voltage]$$

3.2.8 Compute the difference between actual A/D counts and the theoretical number of counts.

$$Difference = [Actual\ Measured] - [Theoretical\ Value]$$

3.2.9 Repeat steps 3.2.4 through 3.2.8 for each applied voltage.

Acceptance Criteria: **The absolute difference between the actual A/D and theoretical number of counts must be less than or equal to 10 counts at each measured voltage. If the acceptance criteria is not met, refer to the manufacturers calibration procedure for adjusting the amplifiers and/or A/D.**

SYSTEM VOLTAGE CHECK DATA SHEET

Model # ETC-3 Serial # 960155101

Voltmeter Measured Input Voltage (volts)	Theoretical Output (counts)	Measured A/D Output (counts)	Difference (counts)

Signature _____ Date _____

ETC9601R0

APPENDIX C

SMALL DIAMETER THERMOCOUPLES MANUFACTURED BY DELTA M CORPORATION

Small Diameter Thermocouples Manufactured by Delta M Corporation

A majority of the thermocouples used in the Solid Propulsion Integrity Program (SPIP) are small diameter, sheathed, insulated junction thermocouples (type "K") manufactured by Delta M Corporation (Figures C.1 and C.2). These thermocouples were selected for the SPIP to provide researchers with a small, fast response temperature gage to record measurements inside test specimens of composite material during sharp thermal transients. In addition, the sheathed thermocouple design provides certain advantages over the unsheathed types, such as elimination of secondary junctions caused by thermocouple leads that touch. This appendix provides the results of a study performed to understand some of the techniques used in the manufacture of these thermocouples in preparation for Loop Current Step Response (LCSR) field tests at Southern Research Institute (SRI) and Marshall Space Flight Center (MSFC). This information was obtained during a site visit to the Delta M manufacturing facilities in Oak Ridge Tennessee.

1. Failure Mechanisms in Small Diameter Thermocouples

Many of the production techniques used in the manufacture of Delta M thermocouples were developed in the early 1980's during tests performed in large, out-of-reactor, thermal-hydraulic test facilities at the Oak Ridge National Laboratory (ORNL), and later at the Delta M manufacturing facilities. The need for small, reliable thermocouples (type "K"), capable of measuring high temperatures during sharp thermal transients necessitated many advancements in existing thermocouple manufacturing techniques. Use of existing thermocouples at the ORNL facilities had resulted in premature failure of a large percentage of the thermocouples (up to 100%) during exposure to high steady-state temperatures and thermal cycling. An investigation indicated four main mechanisms for the failures [1]:

1. Thermoelement Grain Size
2. Differential Thermal Expansion
3. Oxidation
4. Residual Cold Work in the Thermoelements

Each of these mechanisms are described below:

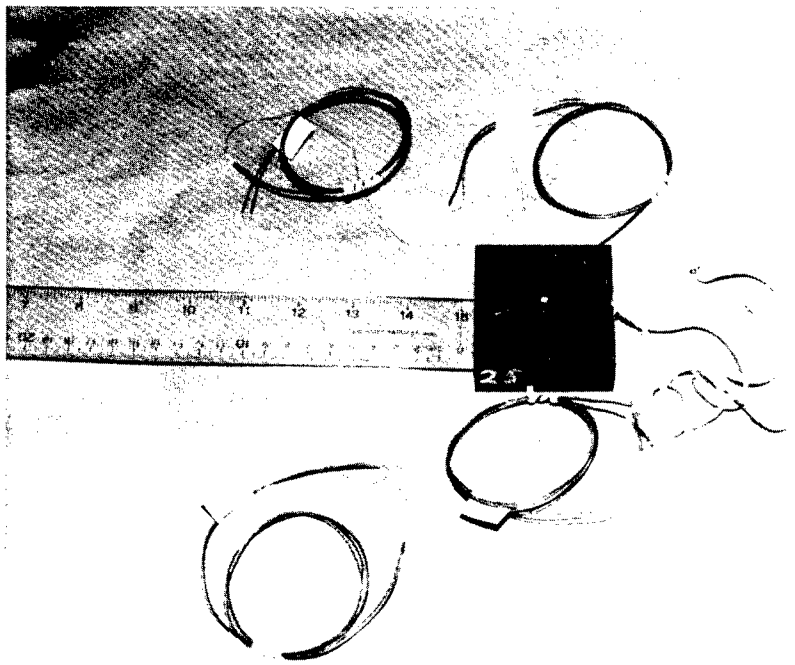

Figure C.1 Photograph of Small Diameter Thermocouples Used in The Solid Propulsion Integrity Program (SPIP).

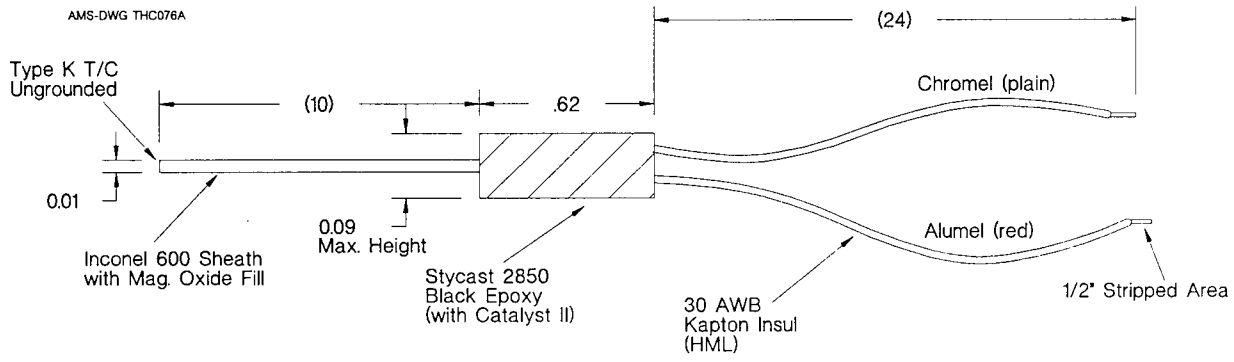

Figure C.2 Diagram of Small Diameter Delta M Thermocouple (HTT3-U-010-I600-10"-K-MgO-K). Reproduced From Delta M Drawing ELS-500. All dimensions are in inches.

Thermoelement Grain Size

In general, small diameter insulated junction thermocouples are manufactured using a recursive drawing-annealing procedure. The thermocouple elements are assembled in a sheath, with the insulation material (usually magnesium oxide) packed around the elements. The assembly is then pulled (drawn) through a series of progressively smaller dies in order to reduce the overall diameter of the thermocouple. As the assembly is drawn, the diameters of the thermoelements within the sheath are also reduced. In the case of the 0.3mm thermocouples shown in Figure C.1, the thermoelement diameters are reduced to approximately 0.03mm. When the microstructures of the components are examined, the diameter of the thermoelements can consist of a single grain (essentially a single crystal), and in some cases result in grain boundaries extending the full diameter of a thermoelement (Figure C.3). At high temperatures, grain boundaries create an area within the thermoelement that is significantly weaker than the grains themselves, and result in "weak links" in the structure of the thermoelement. Any stress induced in the thermocouple (such as that caused by vibration, thermal expansion, or shock) may cause the thermocouple to fail.

Differential Thermal Expansion

Differential thermal expansion can occur in thermocouples during exposure to high temperature. Since each component of a thermocouple (sheath, thermoelements and insulation) have their own linear expansion coefficient ($\propto$), significant stresses can be induced within the thermocouple under certain conditions. Figure C.4 illustrates the relation between linear expansion and temperature for components used in the construction of a type "K" thermocouple. The linear expansion coefficients for type "S" thermoelements are also shown. Two different sheath materials are illustrated: Inconel 600™ and 304 stainless steel. As seen in this figure, there is a significant (0.2 to 0.3%) difference between the thermal expansion coefficients of the stainless steel and the Inconel 600™ (in addition to the Chromel and Alumel) at about 1000°C. If a thermocouple is constructed of materials with large differences in linear expansion coefficients, relatively large amounts of stress can be induced in the thermoelements at high temperatures since each component will expand differently. To illustrate these effects, the following example is given based on approximated values for linear expansion coefficients for a type "K" thermocouple[2]:

Initial Temperature: 25°C
Final Temperature: 300°C
Initial Thermocouple Length: 25cm
Average Thermal Expansion Coefficients (C^{-1}):

Stainless Steel	19.1 E- 6
Alumel	13.0 E-6
Chromel	16.2 E-6

$$L = \propto L_o (t_f - t_o) \qquad (C.1)$$

AMS-DWG THC083A

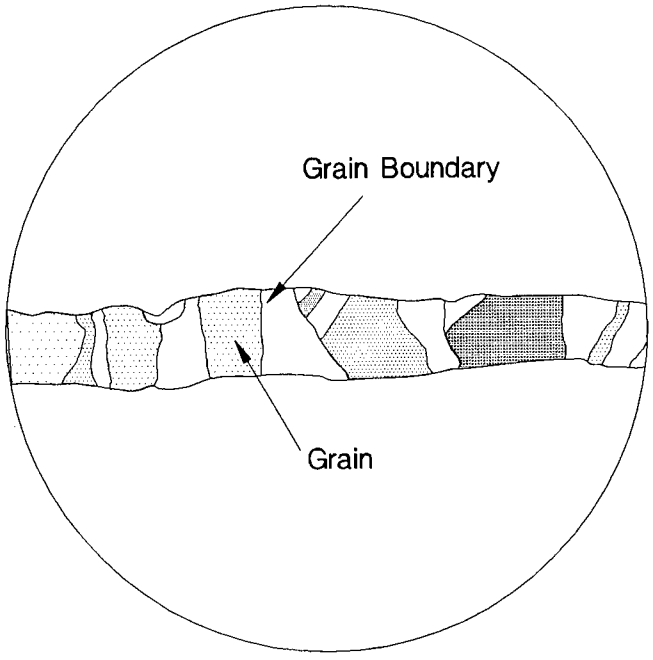

Figure C.3 Illustration of Grain Size and Grain Boundary in Relation To Diameter of Thermoelement.

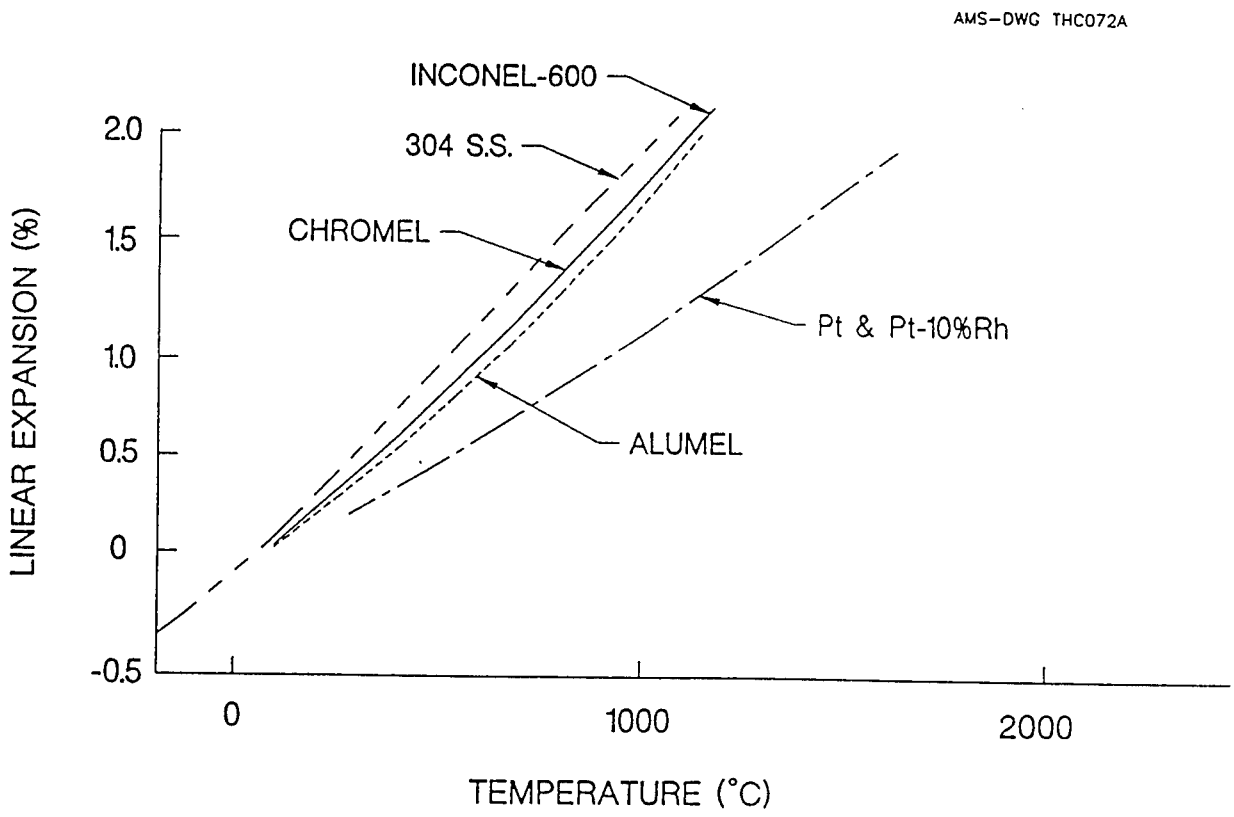

Figure C.4 Differences in Linear Expansion as a Function of Temperature For Materials Used in Type K and S Thermocouples.

where L is the change in length of the component
α is the linear expansion coefficient
L_0 is the initial length of the component
t_1 is the final temperature
t_0 is the initial temperature

For this case the change in length for each component of the thermocouple is:

$L_{\text{Stainless Steel}} =$ 0.13cm
$L_{\text{Alumel}} =$ 0.09cm
$L_{\text{Chromel}} =$ 0.11cm

As seen in this example, the stainless steel sheath will expand the most, resulting in stretching of the Chromel and Alumel thermoelements. However, if the Inconel 600™ is used as a sheath material, the stresses within the thermoelement will be reduced since the linear expansion closely approximates that of both the Chromel and Alumel thermoelements.

Oxidation

A third factor discovered in the examination of failures of small diameter thermocouples was the presence of oxidation in the type "K" thermoelements. If the amount of oxygen and moisture in the thermocouple is high, oxides can form in both the Chromel and Alumel elements, resulting in embrittlement and early failure. This effect becomes aggravated when the thermocouples are operated in the 815 to 1038°C range[3]. To prevent this from occurring, there must be a minimum of oxygen, moisture, and hydroxides or oxides in the thermocouple insulation.

Residual Cold Work In Thermocouples

After manufacture, a small amount of cold work or pre-strain can remain in the thermoelements of type "K" thermocouples. The effects of this cold work are two-fold:

- The cold work will change the value of the Seebeck coefficient of the thermoelements and therefore cause the thermocouple to deviate from standard thermocouple calibration curves. If the thermoelements are heated to a temperature above the recrystallization temperature, the thermocouple will be annealed, relieving the cold work and further changing the Seebeck coefficient.

- Exposure of the thermocouple to temperatures above the recrystallization temperature will cause relatively large increases in the grain size. This can result in grain boundaries extending the full diameter of a thermoelement and therefore create areas within the microstructure where fracture of the thermoelements can occur.

In order to manufacture a thermocouple with the optimum material properties, and a microstructure free of cold work or oxidation, a detailed fabrication process was developed. This process is described in the following section.

2. Manufacturing Practices for Delta M Thermocouples

Many of the details concerning the manufacture of Delta M thermocouples are proprietary in nature, but the following outline provides a general description of the steps used in manufacture of the type "K" design. A block diagram of the process is shown in Figure C.5.

1. Sheath material (Inconel 600™ tubing) is obtained and magnesium oxide insulation material is inserted into the tubing. Thermocouple leads are then installed into the insulation, taking precautions not to contaminate the thermoelements.

2. The tip of the tubing is then swaged in order to compress the first 3 to 5 cm. of the sheath, forming a tapered tip. Swaging is a procedure which is often used to reduce the cross-sectional area of rods and tubing and is performed by rotating a series of hammers around the material at high speed (Figure C.6). This compacts the magnesium oxide insulation material within the sheath and allows drawing of the assembly through a die as described in the next step.

3. The swaged portion of the sheath is drawn through a die, reducing the overall O.D. of the thermocouple sheath and thermoelements by approximately 10%. This process induces a moderate amount of cold work in all components of the thermocouple.

4. To relieve the cold work in the thermocouple materials and permit further drawing, a recovery-anneal process is performed on the thermocouple. The temperature and duration of the annealing process have been perfected over several years to insure that microstructure grain size refinement takes place. The optimum final condition is a microstructure with small grain size and free of impurities. An illustration of the changes which occur in the materials during the drawing-annealing process are shown in Figure C.7.

5. The procedure of swaging, drawing and annealing is repeated until a thermocouple sheath with the desired outside diameter is obtained.

6. A small amount of magnesium oxide insulation material (equal to about one or two diameters) is removed from the tip of the thermocouple to gain access to the enclosed thermocouple leads.

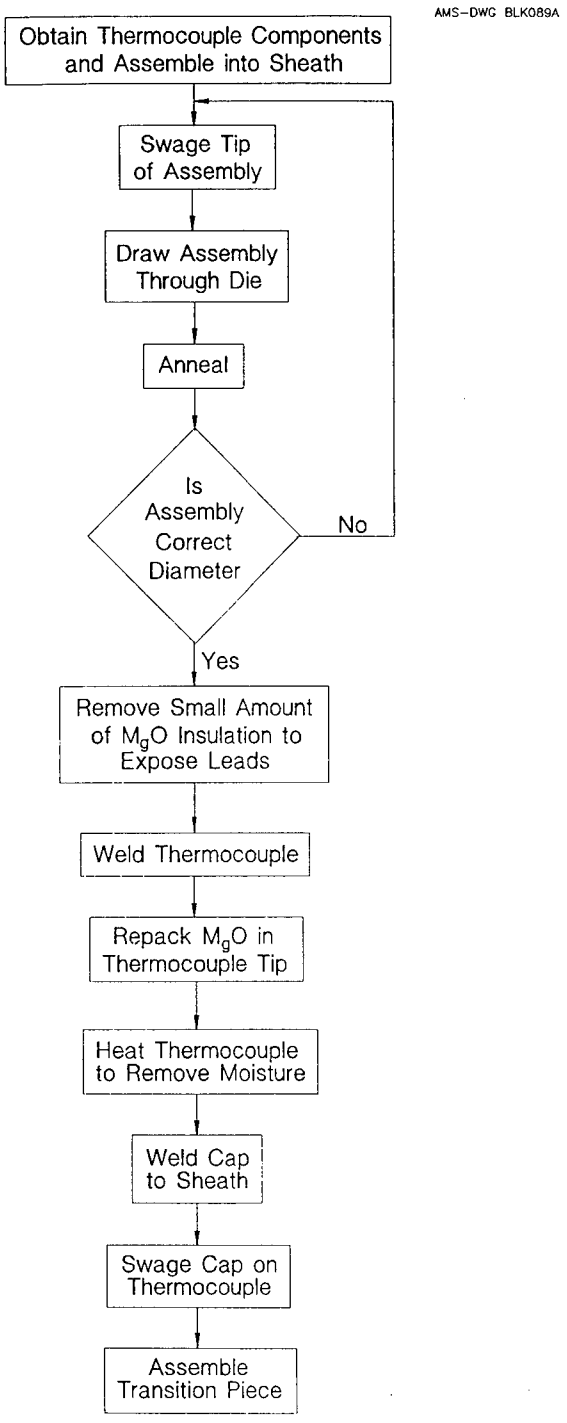

Figure C.5 Manufacturing Processes Used in Construction of Delta M Thermocouples

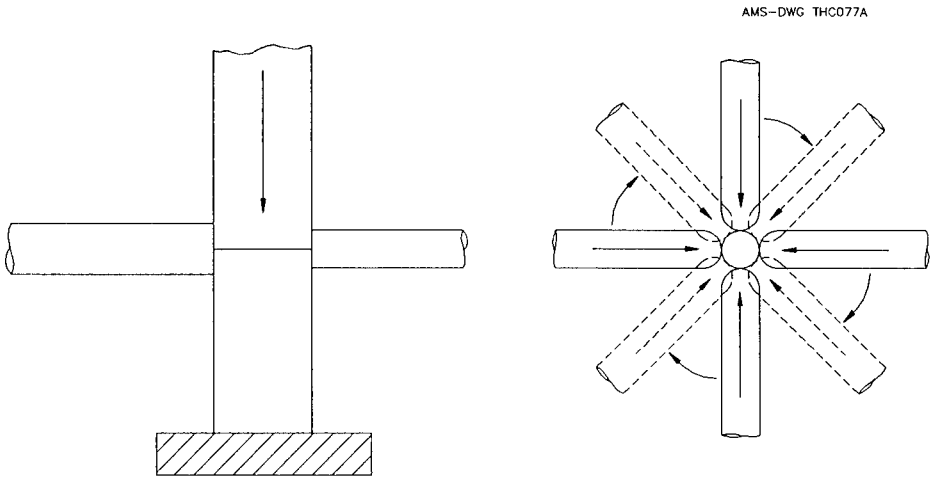

Figure C.6 Illustration of Swaging of Tubing

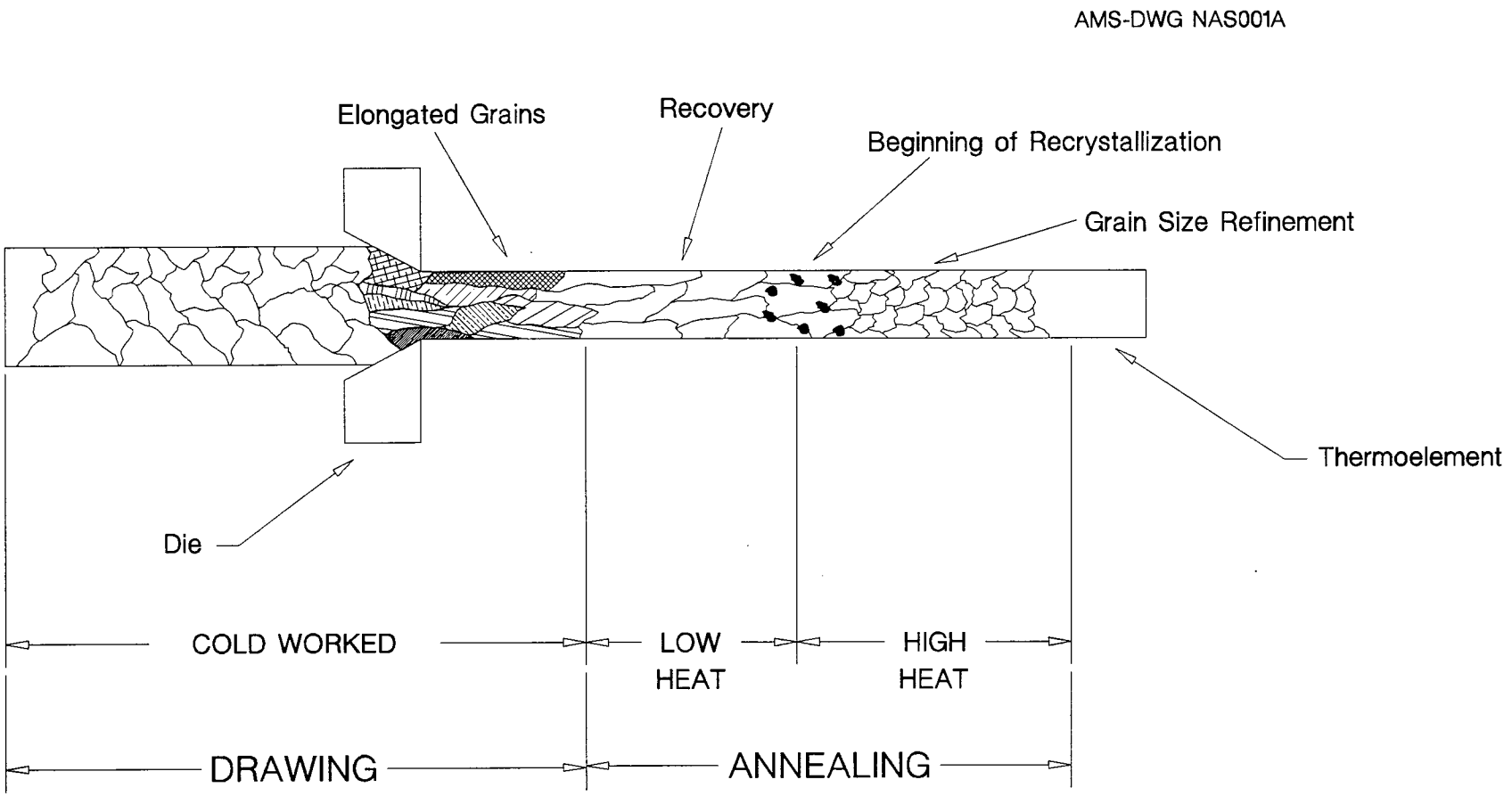

Figure C.7 Changes In Thermocouple Materials During the Drawing-Annealing Process

7. The thermocouple is welded under a microscope, and magnesium oxide insulation is re-packed around the thermocouple.

8. The thermocouple is heated to remove any moisture which penetrated the internals of the thermocouple during manufacture.

9. A cap is welded to the tip and then swaged to ensure the welded portion of the thermocouple is the same diameter as the remaining portion of the sheath.

10. The thermocouple leads are then assembled in a transition piece to allow easy use of the thermocouple.

The entire assembly process is shown schematically in Figure C.8.

References:

1. McCulloch, R.W.; Clift, J.H, "Lifetime Improvement of Small-diameter Sheathed Thermocouples for Use in High-temperature and Thermal Transient Operations," American Institute of Physics, 1982.

2. Anderson, R.L.; Ludwig, R.L., "Failure of Sheathed Thermocouples Due to Thermal Cycling," American Institute of Physics, 1982

3. Spooner, N.F. and Thomas, J.M., "Longer Life for Chromel-Alumel Thermocouples," Met. Prog. (November 1955).

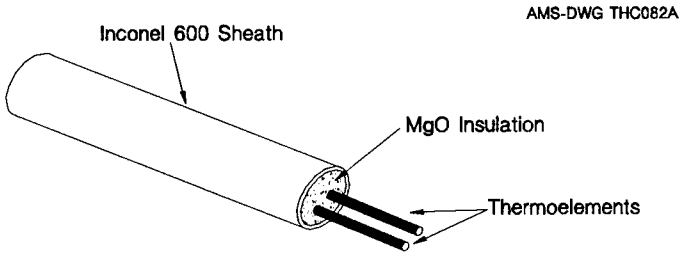

Thermocouple Reduction:

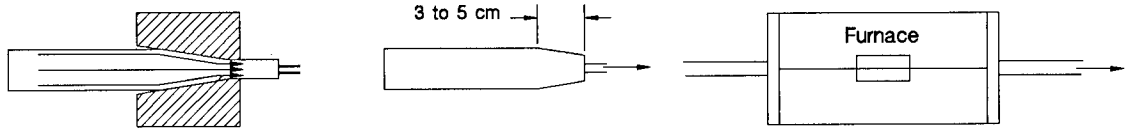

Final Assembly:

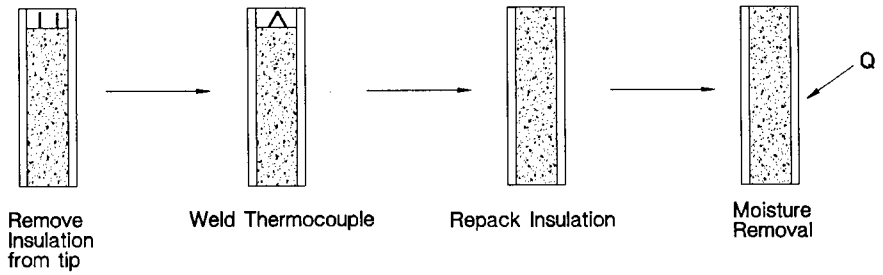

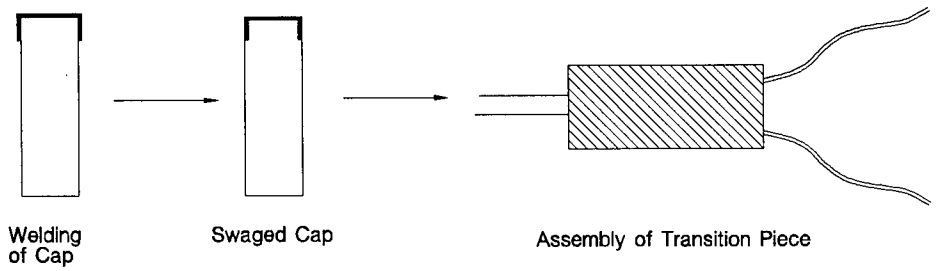

Figure C.8 Schematic Diagram of the Manufacturing Processes For Delta M Thermocouples.

APPENDIX D

REPORT OF LABORATORY TESTING OF THIOKOL BLOCKS

ANALYSIS AND
MEASUREMENT SERVICES
CORPORATION

AMS 9111 CROSS PARK DRIVE / KNOXVILLE, TN 37923 USA (615) 691-1756

NASA9405R0

THE INSTALLATION INTEGRITY TESTING OF EMBEDDED THERMOCOUPLES FOR SOLID PROPULSION INTEGRITY PROGRAM

Revision 0

December 1994

Prepared By

Analysis and Measurement Services Corporation
AMS 9111 Cross Park Drive
Knoxville, TN 37923
Phone: 615-691-1756
Fax: 615-691-9344

Prepared For

Elizabeth Emory
Hercules Aerospace Company
P.O. Box 98
Magna, Utah 84044
Phone: 801-251-5077

PREFACE

AMS is conducting a comprehensive research project for NASA Marshall Space Flight Center (MSFC) to develop equipment and techniques for testing the installation integrity of thermocouples, strain gages, and other sensors installed on solid surfaces or embedded in solid materials. As a part of this project, AMS has conducted tests on thermocouples that are assembled by Hercules for MSFC. This report summarizes the results of the AMS tests for Hercules.

TABLE OF CONTENTS

1. INTRODUCTION

Analysis and Measurement Services Corporation (AMS) performed thermocouple installation testing on the Solid Propulsion Integrity Program (SPIP) 94 Analog Test Matrix carbon-phenolic specimens. A total of forty-two specimens were tested at the AMS laboratories during an eight month period from March 1994 through October 1994. Each specimen contained one to six embedded thermocouples. In addition, two evaluation blocks were tested. The evaluation blocks were used to determine the optimal placement of the thermocouples in a test matrix. The thermocouples were installed in the test specimens in either a probe or a Cured-In-Place (CIP) configuration. After completion of installation integrity testing at AMS, thirty-eight of the specimens were shipped to the Southern Research Institute (SRI) in Birmingham, Alabama for additional testing on the Nozzle Ablative Simulation (NAS) Apparatus and the remaining six specimens were shipped to Marshall Space Flight Center (MSFC) for further testing in the Plasma Arc Facility.

The purpose of the testing at AMS was to provide Loop Current Step Response (LCSR) results to assist in the evaluation of the analog temperature transient data taken during the testing of Solid Rocket Motor (SRM) nozzle material at SRI and Marshall Space Flight Center. The LCSR tests concentrated on evaluating the differences in the dynamic response characteristics of each thermocouple as installed in the carbon-phenolic test specimens prior to the ablative testing. In addition, the LCSR data provides useful information for evaluating the two different installation arrangements used. It has been shown in laboratory tests performed at AMS that inadequate or poorly installed thermocouples can be detected by comparing the LCSR responses. A poor installation will result in a slower response time due to differences in the heat transfer properties of the area immediately surrounding the thermocouple.

2. BACKGROUND

The accuracy of transient temperature measurements with thermocouples is highly dependent on the response time of the thermocouples in the specific media (water, air, solids, etc.) in which they are installed. It has been shown that the response characteristics of thermocouples that are installed in solid materials, such as those used in the SPIP Test Matrix, depend strongly on the bonding between the thermocouple and the solid material. As documented in several papers and in the report of a recent research project performed by AMS for NASA [1,2,3], the LCSR test method can be used to evaluate the installation of thermocouples embedded in solid materials.

The LCSR test involves applying an electrical current to the thermocouple leads. This current results in Joule heating of the measuring junction, bringing it to an elevated temperature, several degrees above the ambient temperature. The heating current is then terminated, and the output from the thermocouple is monitored as it cools back to the ambient temperature. This cooling transient contains inherent information about the dynamic response characteristics of the thermocouple in the particular environment in which it is installed. The LCSR transients in this report are shown in terms of the averaged LCSR transient for each thermocouple. Note that the LCSR tests for each thermocouple were repeated several times as necessary to compensate for temperature fluctuations and noise that are usually encountered due to high amplifier gains that must be used. The individual LCSR transients were then averaged together for each thermocouple to provide a smooth LCSR data set to facilitate the analysis. The transients shown in this report have been normalized so that the they can be easily intercompared.

3. RESULTS

From March 1994 through October 1994, AMS performed a series of LCSR tests on forty-four instrumented test specimens. Table 1 lists all the thermocouples tested and the installation integrity test results. The results are expressed in terms of a transient delay which are referred to in this project as the installation index. The installation index corresponds to the quality of a thermocouple attachment as opposed to an in-situ response time. As shown in Table 1, several thermocouples were not testable because they were "open" when they arrived at AMS. Each specimen contained between one to six 0.010" diameter type-K thermocouples, manufactured by Delta M Corporation of Oak Ridge, Tennessee, for a total of 204 sensors. Figures 1A through 1D are drawings of the test matrices for all of the specimens tested. This test matrix shows two different installation methods for the thermocouples tested. In the first method, the thermocouples were inserted into a 0.365" - 0.375" diameter, machined, cylindrical plug. These plugs were then installed into a corresponding hole bored into the test material specimen block. This is referred to as a probe type installation (Figure 2). In the second type of installation, the thermocouples were Cured-In-Place (CIP) in the test material specimen block. A drawing of a typical CIP installation is shown in Figure 3.

3.1 LCSR Results

The LCSR installation index results found in Table 1 were calculated by applying three independent algorithms to the LCSR data. The results from these three methods were then averaged to determine a final installation index. The thermocouple results were then grouped according to the installation type and a statistical analysis was applied to each group of LCSR installation integrity indices to flag any significant outliers. Figures 4 and 5 show histograms

TABLE 1
Listing of SPIP 94 Matrix Thermocouples Tested

Item	Tag #	Block	Installation Type	Installation Index (sec)
1	1	1	CIP	0.99
2	4	2	CIP	0.99
3	2	3	CIP	1.02
4	3	4	CIP	0.86
5	83	4	CIP	0.96
6	51	5	CIP	0.85
* 7	53	5	CIP	N/A
8	55	5	CIP	0.75
9	56	6	CIP	0.73
10	57	6	CIP	1.06
11	58	6	CIP	0.95
12	17	7	PLUG	0.46
13	59	7	CIP	0.90
14	20	8	PLUG	0.37
15	60	8	CIP	0.85
16	79	9	CIP	0.68
17	202	9	PLUG	0.82
18	78	10	CIP	0.61
19	201	10	PLUG	0.40
20	76	11	CIP	0.68
21	205	11	PLUG	0.40
22	82	12	CIP	1.32
23	203	12	PLUG	0.55
24	21	14	CIP	1.13
25	84	14	CIP	0.93
26	85	14	CIP	0.97
27	146	14	PLUG	0.64
28	147	14	PLUG	0.50
29	150	14	PLUG	0.43
30	5	15	CIP	1.29
31	16	15	CIP	1.22
32	80	15	CIP	1.03
33	148	15	PLUG	0.75
34	149	15	PLUG	0.46
35	179	15	PLUG	0.75
36	144	16	PLUG	0.44
37	145	16	PLUG	0.56
38	178	16	PLUG	1.22
39	242	16	CIP	1.39
40	243	16	CIP	1.39

* Open Circuit

CONTINUED ON THE NEXT PAGE

TABLE 1
(Continued)
Listing of SPIP 94 Matrix Thermocouples Tested

Item	Tag #	Block	Installation Type	Installation Index (sec)
41	244	16	CIP	1.38
42	22	17	PLUG	0.34
43	23	17	PLUG	0.43
44	24	17	PLUG	0.38
45	225	17	CIP	0.99
46	226	17	CIP	1.30
* 47	228	17	CIP	N/A
48	156	18	PLUG	0.86
49	196	18	PLUG	1.00
50	197	18	PLUG	1.12
51	231	18	CIP	1.24
52	234	18	CIP	1.03
53	235	18	CIP	1.38
54	25	19	PLUG	0.37
55	164	19	PLUG	0.76
56	165	19	PLUG	0.75
57	221	19	CIP	0.93
58	223	19	CIP	0.84
59	227	19	CIP	1.03
60	198	20	PLUG	0.41
61	199	20	PLUG	0.56
62	200	20	PLUG	0.57
63	237	20	CIP	1.40
64	239	20	CIP	0.80
65	240	20	CIP	0.86
66	157	21	PLUG	0.39
67	158	21	PLUG	0.40
68	160	21	PLUG	0.38
69	204	21	CIP	1.03
70	229	21	CIP	1.25
71	230	21	CIP	0.87
72	212	24	CIP	1.37
73	217	24	CIP	1.11
* 74	224	24	CIP	N/A
75	209	25	CIP	1.48
* 76	210	25	CIP	N/A
* 77	211	25	CIP	N/A
78	99	26	CIP	0.83

* Open Circuit

CONTINUED ON THE NEXT PAGE

TABLE 1
(Continued)

Listing of SPIP 94 Matrix Thermocouples Tested

Item	Tag #	Block	Installation Type	Installation Index (sec)
79	I	26	CIP	0.86
80	J	26	CIP	0.80
81	91	27	CIP	0.89
82	98	27	CIP	0.70
83	K	27	CIP	0.75
84	161	28	PLUG	0.69
85	162	28	PLUG	0.71
86	163	28	PLUG	0.80
87	207	28	CIP	0.73
88	214	28	CIP	0.79
89	216	28	CIP	0.81
90	166	29	PLUG	0.37
91	167	29	PLUG	0.43
92	168	29	PLUG	0.42
93	208	29	CIP	0.44
94	213	29	CIP	0.44
95	215	29	CIP	0.39
96	95	30	CIP	0.49
97	131	30	PLUG	0.38
98	132	30	PLUG	0.34
99	133	30	PLUG	0.38
100	L	30	CIP	0.28
101	M	30	CIP	0.47
102	88	31	CIP	0.43
103	120	31	PLUG	0.39
104	134	31	PLUG	0.39
105	135	31	PLUG	0.40
106	N	31	CIP	0.43
107	O	31	CIP	0.43
108	96	34	CIP	0.89
* 109	D	34	CIP	N/A
110	E	34	CIP	0.70
111	A	35	CIP	0.77
112	B	35	CIP	0.87
113	C	35	CIP	0.77
114	87	36	CIP	0.77
115	G	36	CIP	0.78
116	H	36	CIP	0.80
117	89	37	CIP	0.85

* Open Circuit

CONTINUED ON THE NEXT PAGE

TABLE 1
(Continued)
Listing of SPIP 94 Matrix Thermocouples Tested

Item	Tag #	Block	Installation Type	Installation Index (sec)
118	92	37	CIP	0.83
119	F	37	CIP	0.79
** 120	186	38	CIP	0.64
121	187	38	CIP	1.54
122	189	38	CIP	1.37
123	252	38	PLUG	0.61
124	253	38	PLUG	1.18
125	255	38	PLUG	0.79
126	153	39	CIP	1.18
127	154	39	CIP	1.40
128	176	39	CIP	1.29
129	254	39	PLUG	1.11
130	259	39	PLUG	0.78
131	260	39	PLUG	0.84
132	185	40	CIP	1.51
** 133	190	40	CIP	0.64
134	193	40	CIP	1.39
135	248	40	PLUG	0.44
136	249	40	PLUG	0.93
137	251	40	PLUG	0.76
138	191	41	CIP	1.36
139	192	41	CIP	1.29
140	194	41	CIP	1.40
141	246	41	PLUG	0.77
142	247	41	PLUG	0.41
143	250	41	PLUG	0.50
144	182	42	CIP	0.95
145	188	42	CIP	0.90
146	195	42	CIP	0.91
147	177	43	CIP	0.85
148	181	43	CIP	0.96
149	183	43	CIP	0.93
150	271	44	PLUG	0.81
151	276	44	PLUG	1.49
152	279	44	PLUG	1.33
153	121	45	PLUG	1.09
154	122	45	PLUG	1.33
155	278	45	PLUG	1.03
156	128	46	PLUG	0.62

** Low IR

CONTINUED ON THE NEXT PAGE

TABLE 1
(Continued)
Listing of SPIP 94 Matrix Thermocouples Tested

Item	Tag #	Block	Installation Type	Installation Index (sec)
157	130	46	PLUG	1.01
158	280	46	PLUG	0.56
159	126	47	PLUG	0.66
160	127	47	PLUG	0.55
161	277	47	PLUG	0.84
* 162	13	53	CIP	N/A
163	18	53	CIP	0.93
164	26	53	CIP	0.87
165	27	53	CIP	0.78
166	28	53	CIP	0.83
167	29	53	CIP	0.86
168	30	53	CIP	0.87
169	31	53	CIP	0.77
170	32	53	CIP	1.24
171	33	53	CIP	0.85
172	34	53	CIP	0.80
* 173	35	53	CIP	N/A
174	36	53	CIP	0.90
* 175	37	53	CIP	N/A
176	38	53	CIP	1.20
* 177	39	53	CIP	N/A
178	40	53	CIP	0.99
* 179	41	53	CIP	N/A
180	42	53	CIP	0.94
* 181	43	53	CIP	N/A
182	44	53	CIP	0.85
* 183	45	53	CIP	N/A
184	46	53	CIP	0.80
185	47	53	CIP	1.04
186	48	53	CIP	0.85
187	49	53	CIP	0.89
* 188	50	53	CIP	N/A
189	6	54	CIP	1.20
190	7	54	CIP	1.00
191	9	54	CIP	1.00
192	14	54	CIP	0.96
193	15	54	CIP	1.01
194	61	54	CIP	0.85
195	62	54	CIP	0.86

* Open Circuit

CONTINUED ON THE NEXT PAGE

TABLE 1
(Continued)

Listing of SPIP 94 Matrix Thermocouples Tested

Item	Tag #	Block	Installation Type	Installation Index (sec)
196	63	54	CIP	1.06
197	64	54	CIP	1.26
198	66	54	CIP	1.12
199	67	54	CIP	0.98
200	68	54	CIP	0.88
201	69	54	CIP	1.12
202	71	54	CIP	0.91
** 203	72	54	CIP	0.93
204	74	54	CIP	0.92

** Low IR

SPIP 94 ANALOG TEST MATRIX

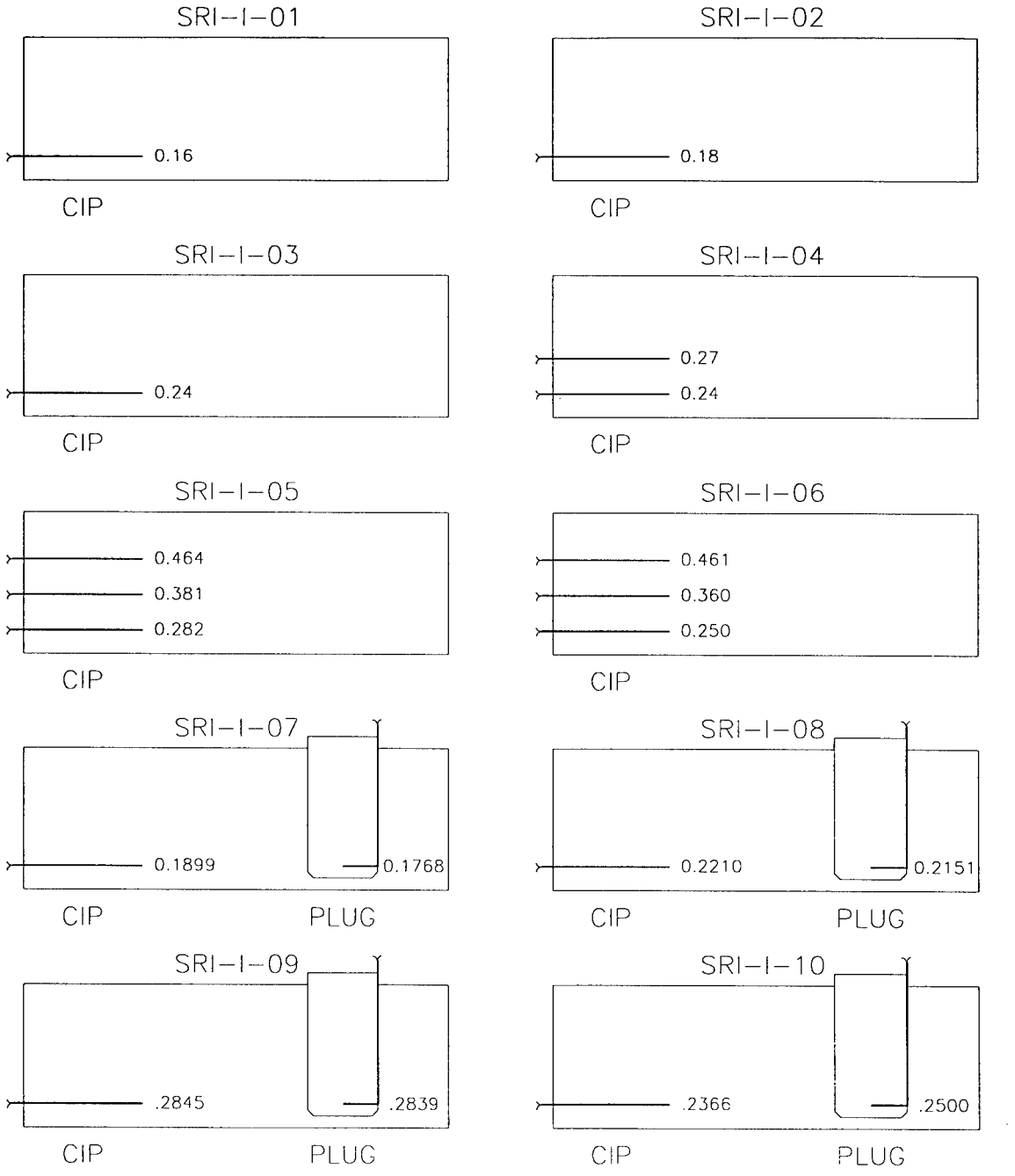

*Note: All dimensions are inches from flame surface.

Figure 1A Layout of SPIP 94 Analog Test Matrix

SPIP 94 ANALOG TEST MATRIX

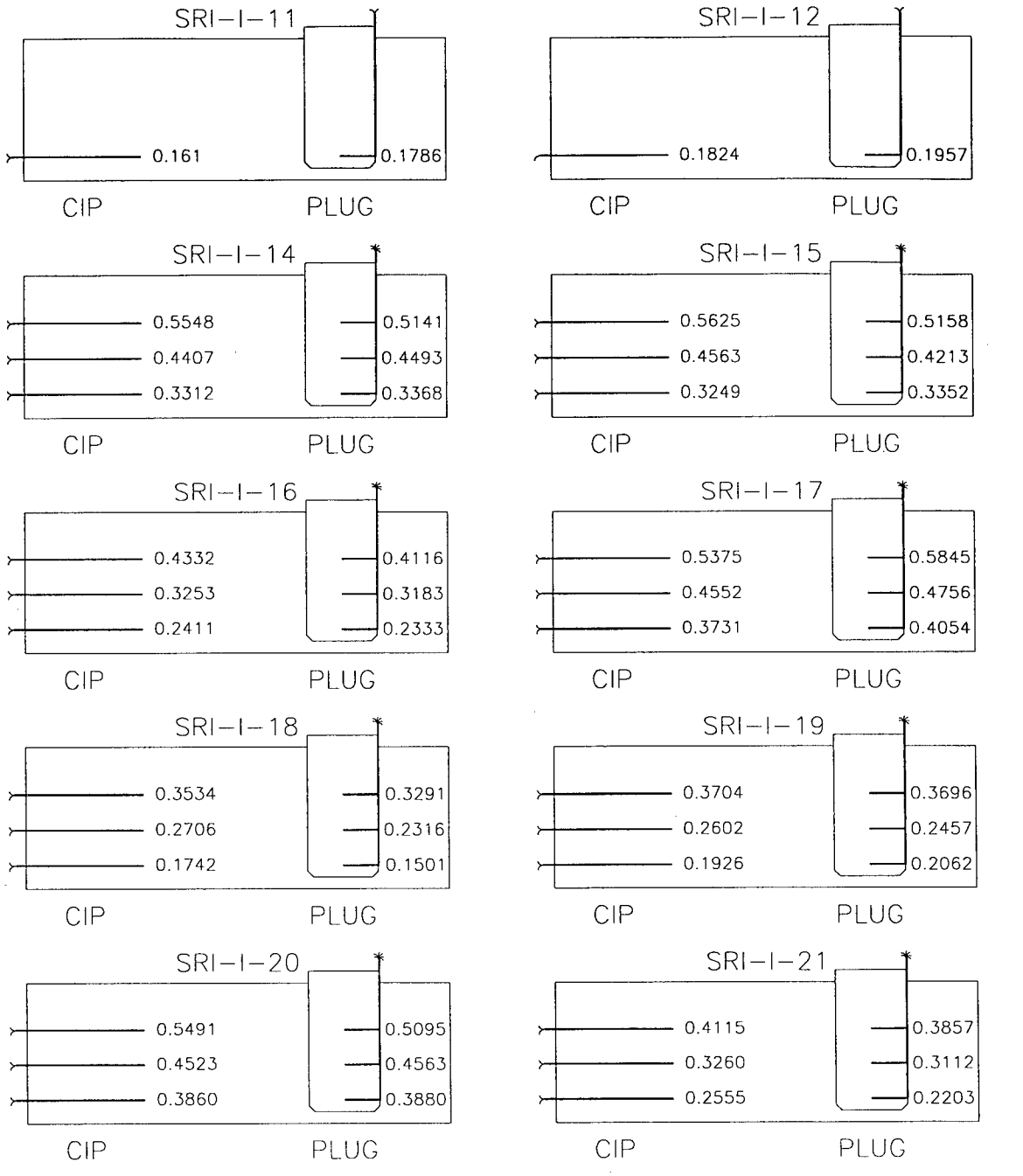

*Note: All dimensions are inches from flame surface.

Figure 1B Layout of SPIP 94 Analog Test Matrix

SPIP 94 ANALOG TEST MATRIX

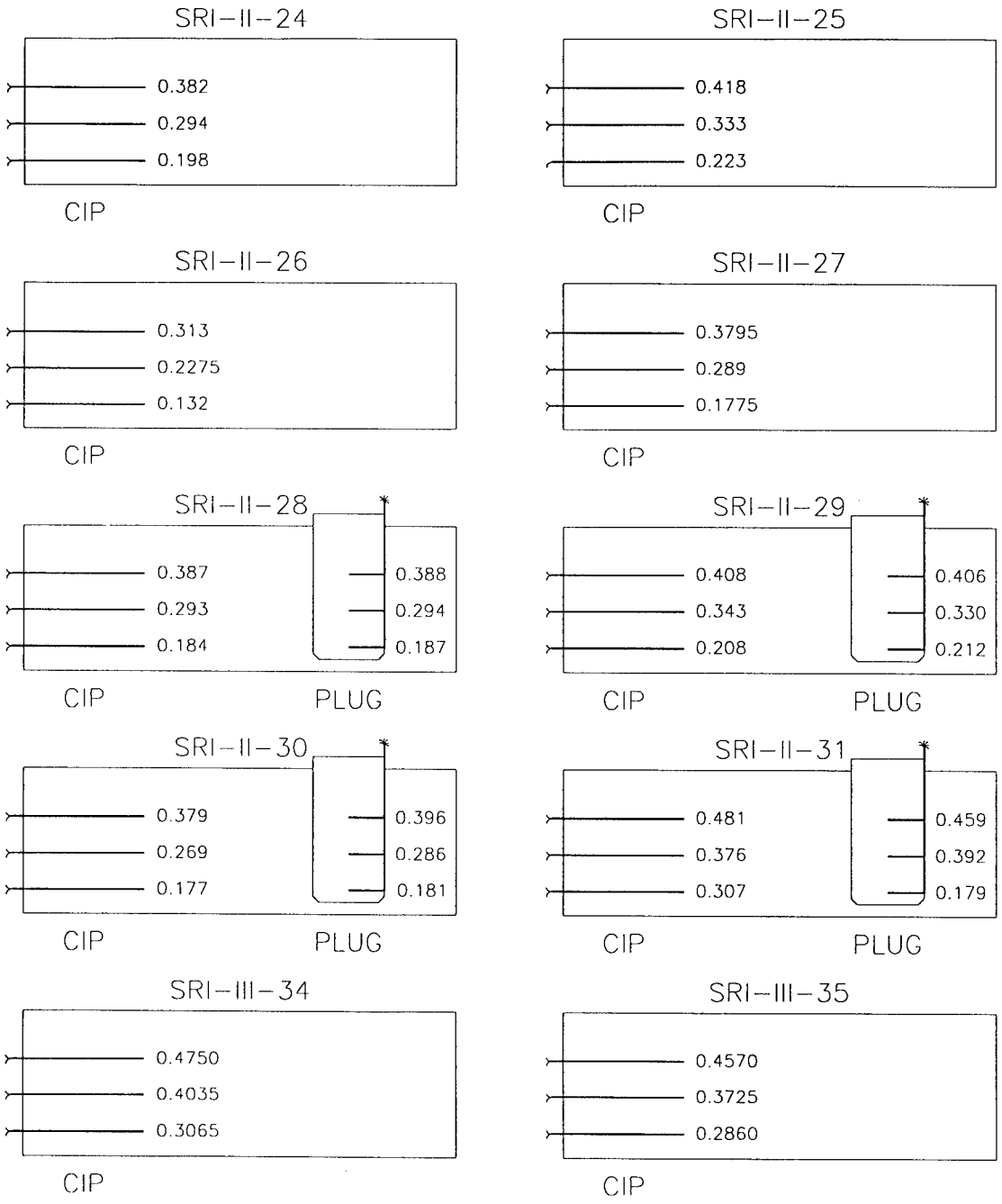

*Note: All dimensions are inches from flame surface.

Figure 1C Layout of SPIP 94 Analog Test Matrix

SPIP 94 ANALOG TEST MATRIX

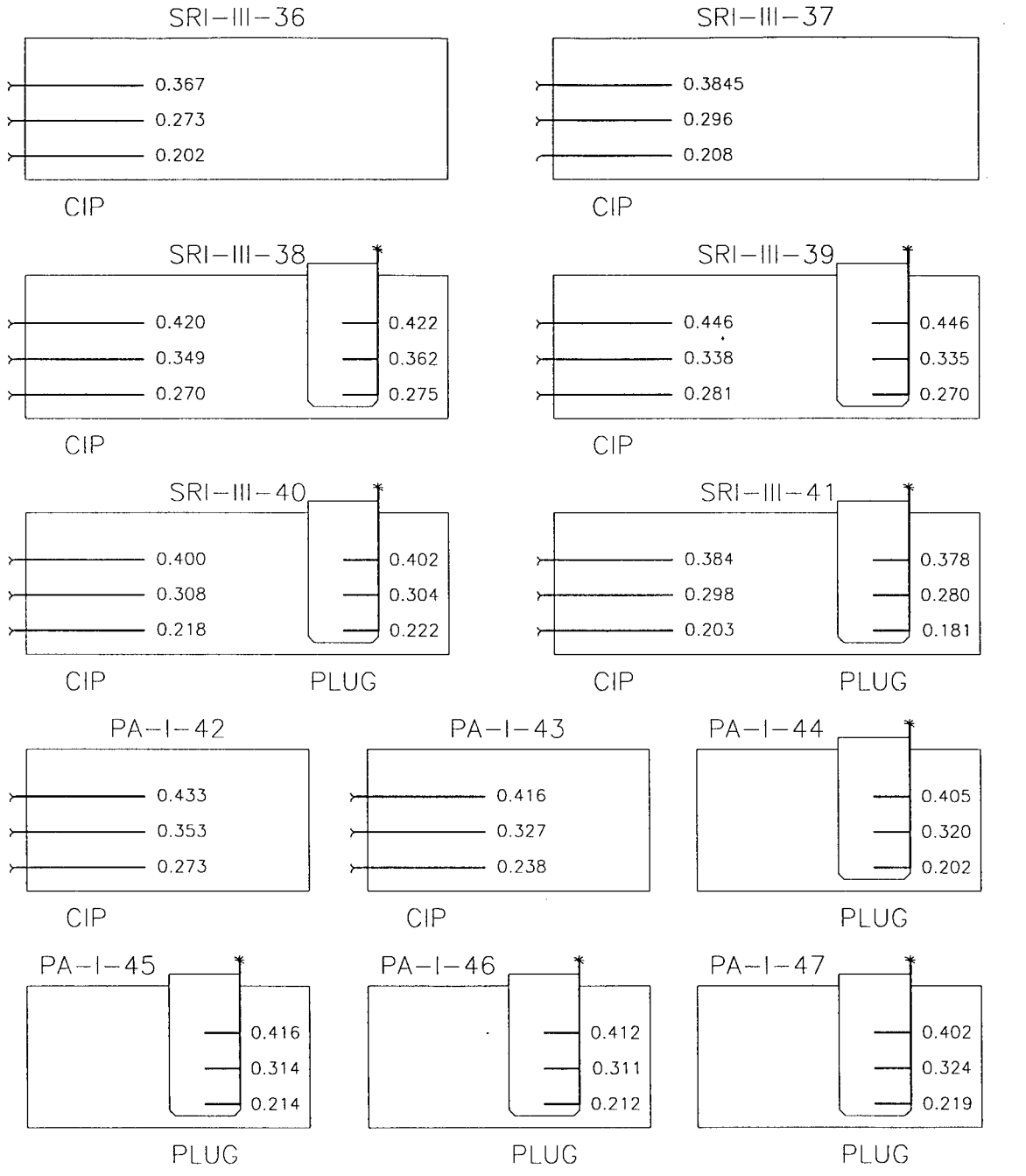

*Note: All dimensions are inches from flame surface.

Figure 1D Layout of SPIP 94 Analog Test Matrix

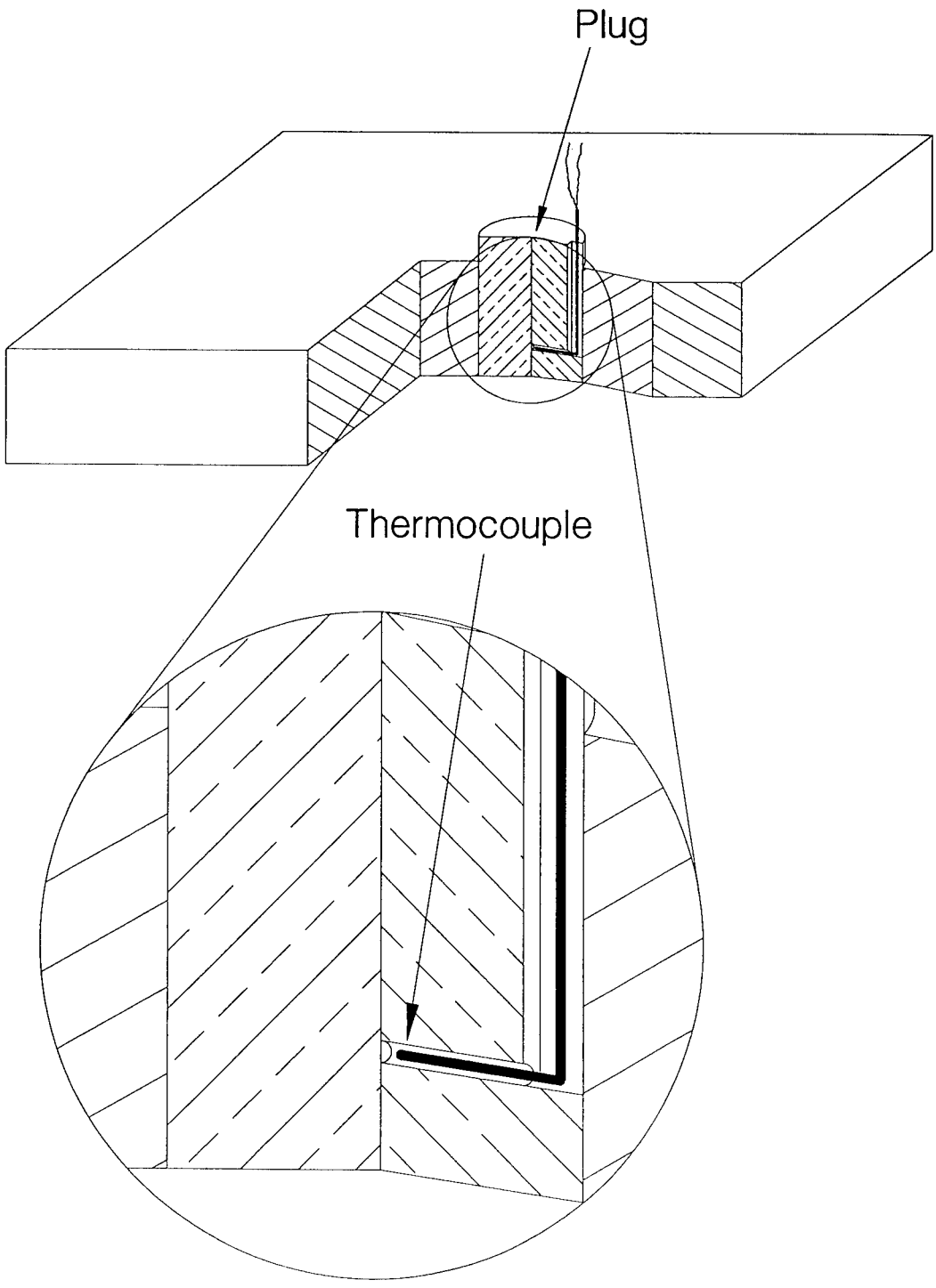

Figure 2 Carbon-Phenolic Probe Installation

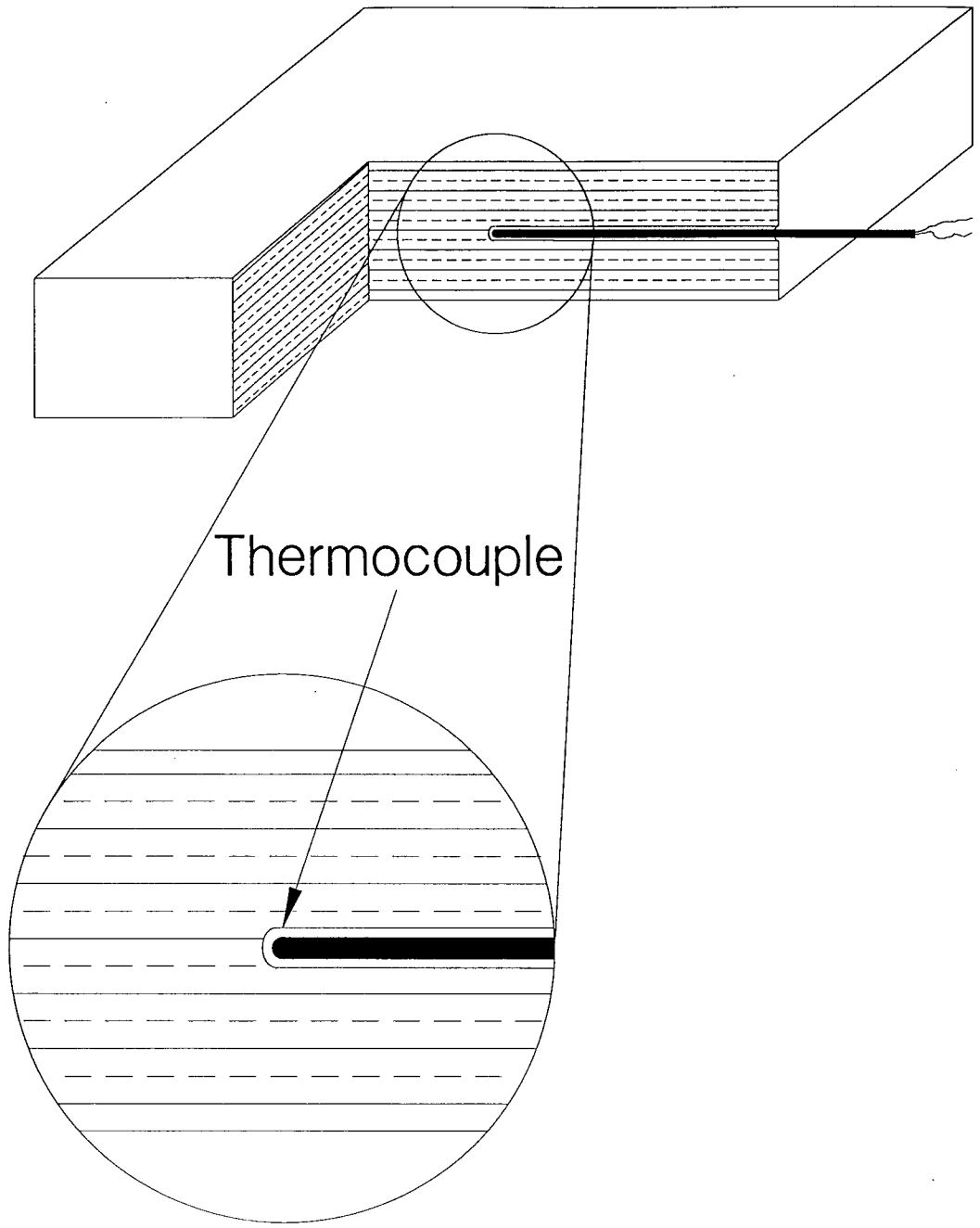

Figure 3 Carbon-Phenolic Cured-In-Place Installation

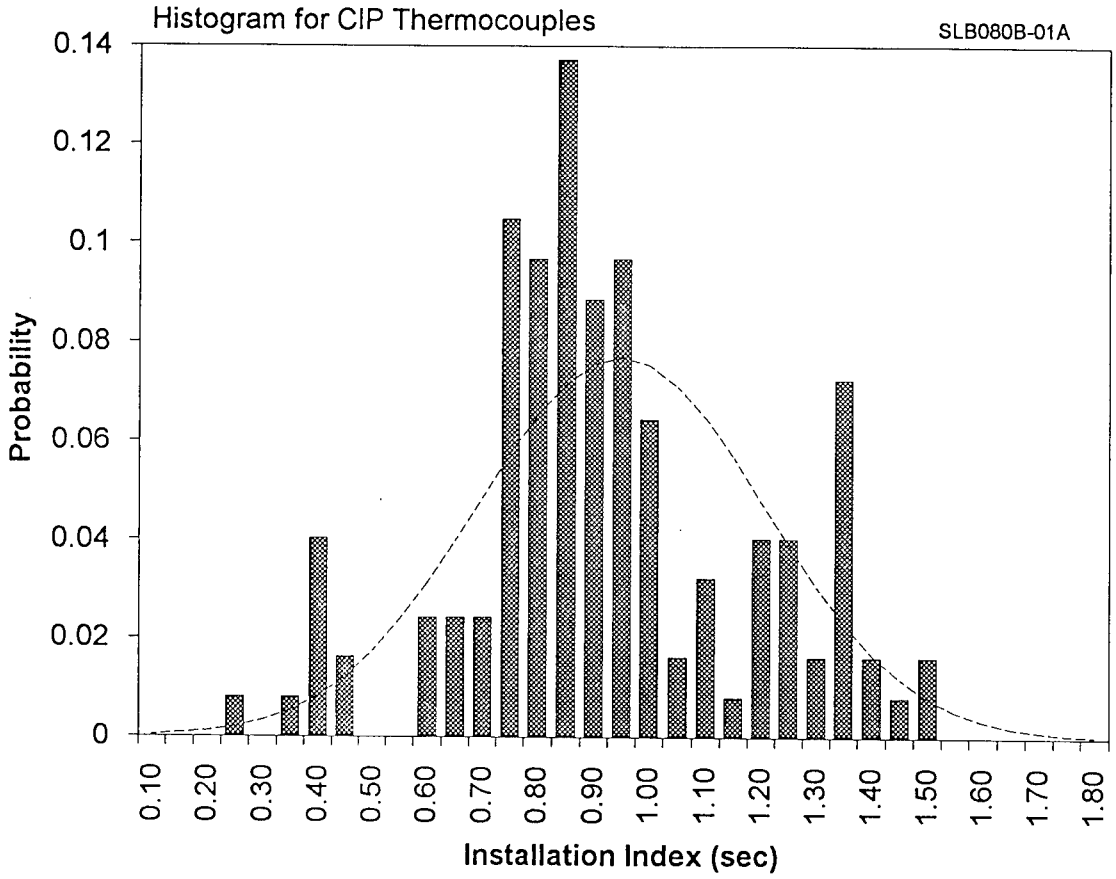

Figure 4 Histogram of Installation Indices for CIP Thermocouples

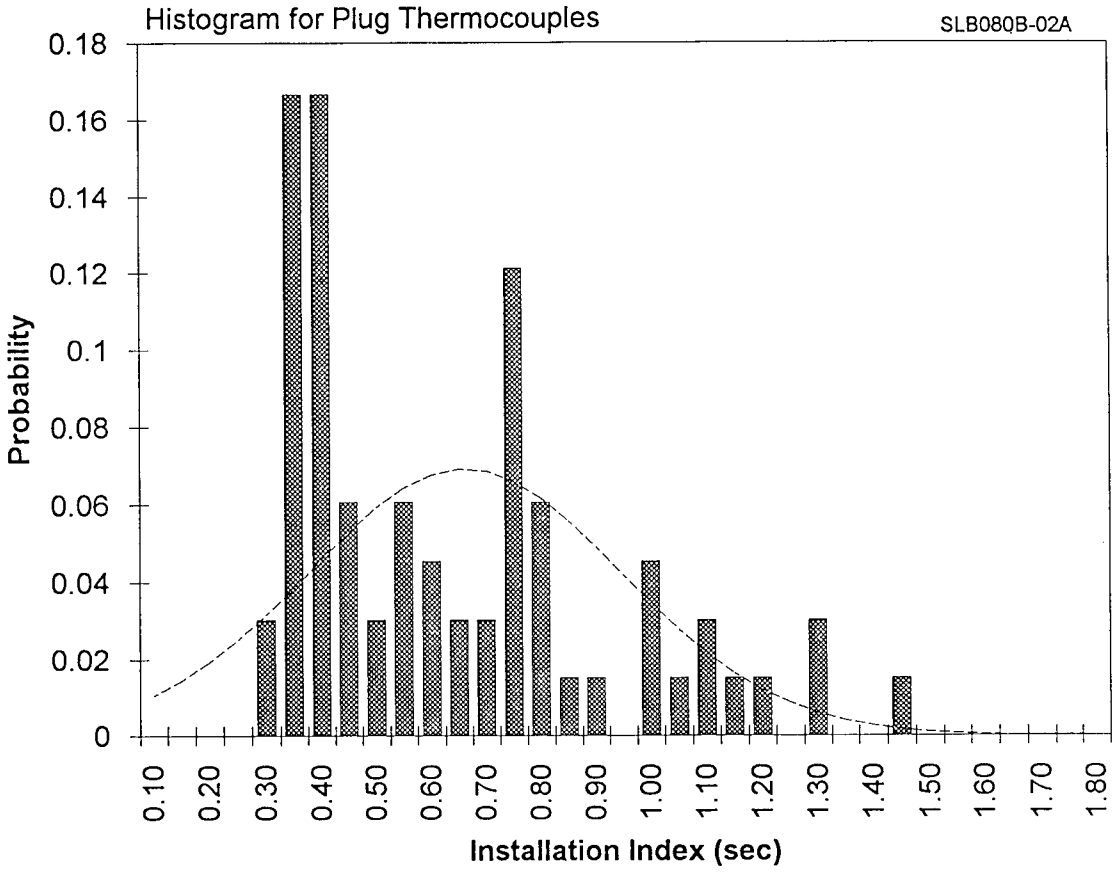

Figure 5 Histogram of Installation Indices for Probe Thermocouples

along with standard gaussian distributions for the two types of installations evaluated. It can be seen from these figures that the CIP installation (Figure 4) demonstrated a more gaussian behavior than the probe installation. The skewed data shown in Figure 5 for the probe installations may be due to the mechanical processes involved in the detailed machining and manual insertion of the thermocouples.

The thermocouples in each installation type were then classified into three types (I, II, III) to represent three classifications of installation integrity. The best installations, or those with the fastest responses, were identified as Class I, and Class III contained the slowest thermocouples. Class I and III thermocouples were those with installation indices greater than one standard deviation from the mean. Those thermocouples which had LCSR installation indices less than one standard deviation from the mean were grouped into Class II. Class II contained 68% of the thermocouples tested. Additional statistical analyses were applied to determine if any of the thermocouples were gross outliers. An outlier was defined as any thermocouple whose installation index fell outside of a two standard deviation band around the mean. These outliers are thermocouples that seem to have either very good or very poor installation.

All CIP thermocouples tested are listed in Table 2 and are grouped by their installation integrity class (I, II or III). The three distinct groups listed in Table 2 represent the varying quality of the installation. The results for the CIP installations are shown in a graphical form in Figures 6 and 7. The CIP installed thermocouples that were determined to be outliers are listed in Table 3. As seen in this table, sensors L and 215 had a very good installation and thermocouples 185, 187 and 209 had a poor installation in reference to the other CIP thermocouples. Figures 8 through 10 show the LCSR transients for the outliers listed in Table 3 versus class I, II and III LCSR transients.

TABLE 2

Listing of Cured-In-Place Thermocouple Classifications

Item	Tag #	Block	Installation Index (sec)	Classification
1	L	30	0.28	I
2	215	29	0.39	I
3	N	31	0.43	I
4	O	31	0.43	I
5	88	31	0.43	I
6	213	29	0.44	I
7	208	29	0.44	I
8	M	30	0.47	I
9	95	30	0.49	I
10	78	10	0.61	I
11	186	38	0.64	I
12	190	40	0.64	I
13	79	9	0.68	I
14	76	11	0.68	I
15	98	27	0.70	II
16	E	34	0.70	II
17	207	28	0.73	II
18	56	6	0.73	II
19	K	27	0.75	II
20	55	5	0.75	II
21	A	35	0.77	II
22	C	35	0.77	II
23	31	53	0.77	II
24	87	36	0.77	II
25	27	53	0.78	II
26	G	36	0.78	II
27	F	37	0.79	II
28	214	28	0.79	II
29	46	53	0.80	II

CONTINUED ON NEXT PAGE

TABLE 2
(Continued)

Listing of Cured-In-Place Thermocouple Classifications

Item	Tag #	Block	Installation Index (sec)	Classification
30	239	20	0.80	II
31	J	26	0.80	II
32	H	36	0.80	II
34	34	53	0.80	II
35	216	28	0.81	II
36	99	26	0.83	II
37	92	37	0.83	II
38	28	53	0.83	II
39	223	19	0.84	II
40	61	54	0.85	II
41	89	37	0.85	II
42	177	43	0.85	II
43	33	53	0.85	II
44	48	53	0.85	II
45	60	8	0.85	II
46	51	5	0.85	II
47	44	53	0.85	II
48	3	4	0.86	II
49	I	26	0.86	II
50	240	20	0.86	II
51	62	54	0.86	II
52	29	53	0.86	II
53	B	35	0.87	II
54	230	21	0.87	II
55	26	53	0.87	II
56	30	53	0.87	II
57	68	54	0.88	II
58	91	27	0.89	II
59	96	34	0.89	II
60	49	53	0.89	II

CONTINUED ON NEXT PAGE

TABLE 2
(Continued)

Listing of Cured-In-Place Thermocouple Classifications

Item	Tag #	Block	Installation Index (sec)	Classification
61	59	7	0.90	II
62	36	53	0.90	II
63	188	42	0.90	II
64	195	42	0.91	II
65	71	54	0.91	II
66	74	54	0.92	II
67	72	54	0.93	II
68	84	14	0.93	II
69	221	19	0.93	II
70	183	43	0.93	II
71	18	53	0.93	II
72	42	53	0.94	II
73	182	42	0.95	II
74	58	6	0.95	II
75	181	43	0.96	II
76	83	4	0.96	II
77	14	54	0.96	II
78	85	14	0.97	II
79	67	54	0.98	II
80	1	1	0.99	II
81	40	53	0.99	II
82	225	17	0.99	II
83	4	2	0.99	II
84	9	54	1.00	II
85	7	54	1.00	II
86	15	54	1.01	II
87	2	3	1.02	II
88	227	19	1.03	II
89	204	21	1.03	II
90	80	15	1.03	II
91	234	18	1.03	II

CONTINUED ON NEXT PAGE

TABLE 2
(Continued)

Listing of Cured-In-Place Thermocouple Classifications

Item	Tag #	Block	Installation Index (sec)	Classification
92	47	53	1.04	II
93	57	6	1.06	II
94	63	54	1.06	II
95	217	24	1.11	II
96	69	54	1.12	II
97	66	54	1.12	II
98	21	14	1.13	II
99	153	39	1.18	II
100	38	53	1.20	II
101	6	54	1.20	II
102	16	15	1.22	III
103	32	53	1.24	III
104	231	18	1.24	III
105	229	21	1.25	III
106	64	54	1.26	III
107	5	15	1.29	III
108	176	39	1.29	III
109	192	41	1.29	III
110	226	17	1.30	III
111	82	12	1.32	III
112	191	41	1.36	III
113	189	38	1.37	III
114	212	24	1.37	III
115	235	18	1.38	III
116	244	16	1.38	III
117	243	16	1.39	III
118	193	40	1.39	III
119	242	16	1.39	III

CONTINUED ON NEXT PAGE

TABLE 2
(Continued)

Listing of Cured-In-Place Thermocouple Classifications

Item	Tag #	Block	Installation Index (sec)	Classification
120	237	20	1.40	III
121	154	39	1.40	III
122	194	41	1.40	III
123	209	25	1.48	III
123	185	40	1.51	III
125	187	38	1.54	III

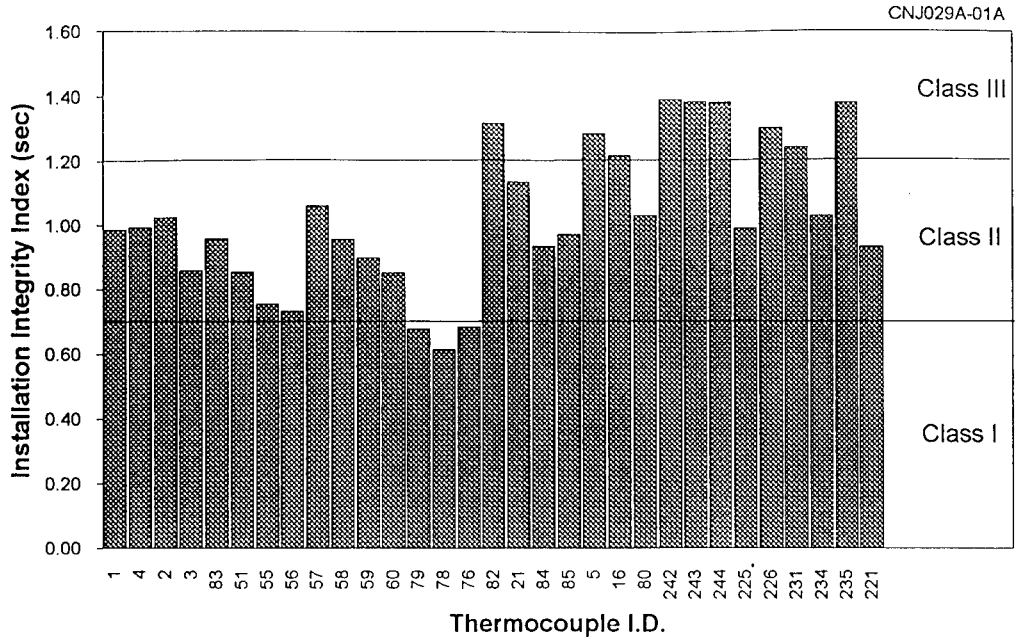

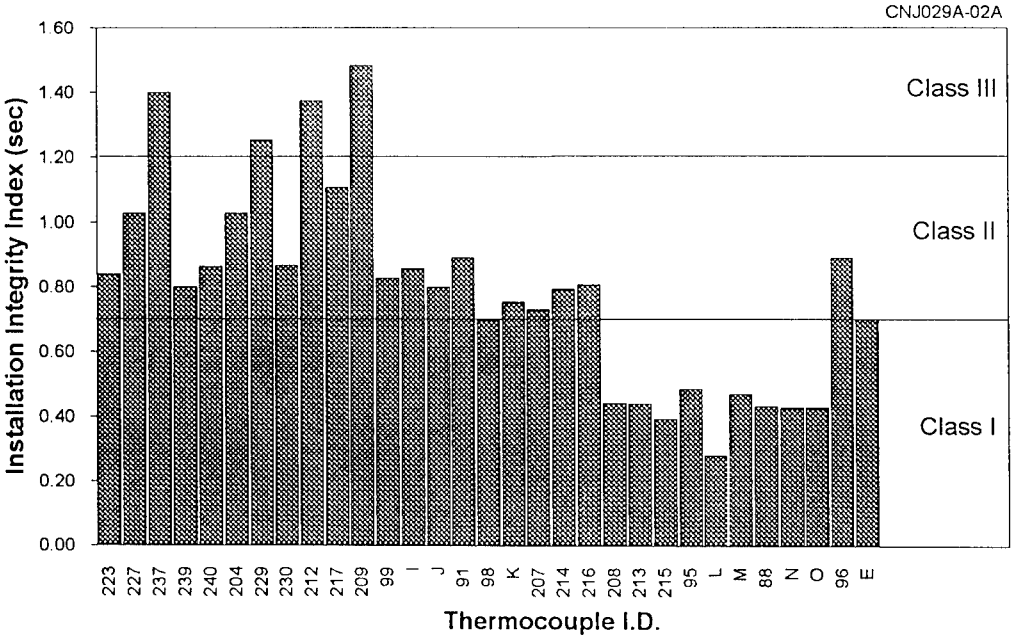

Figure 6 Installation Classifications for CIP Thermocouples

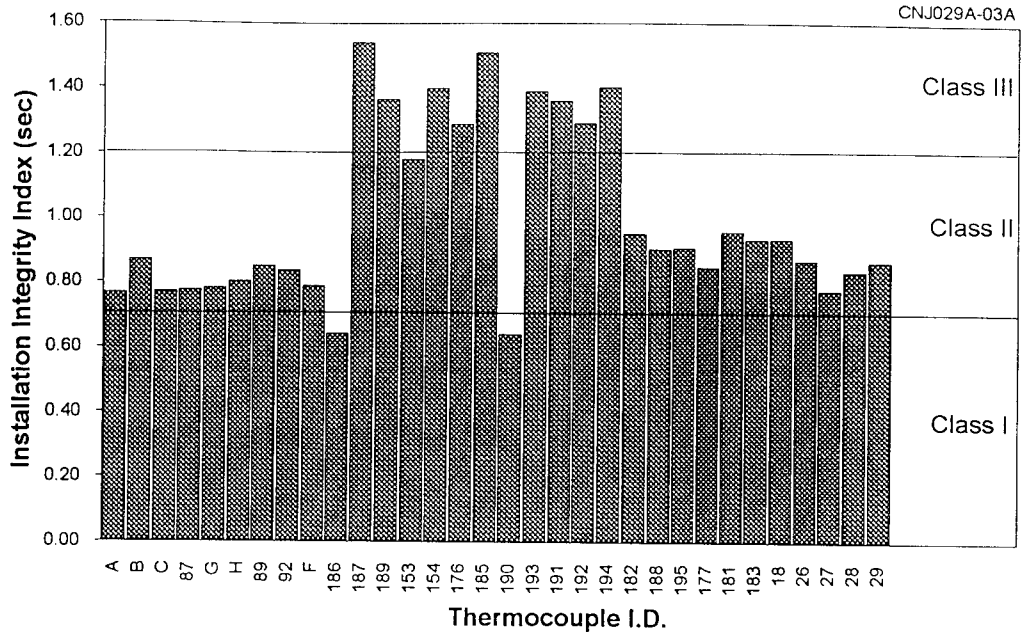

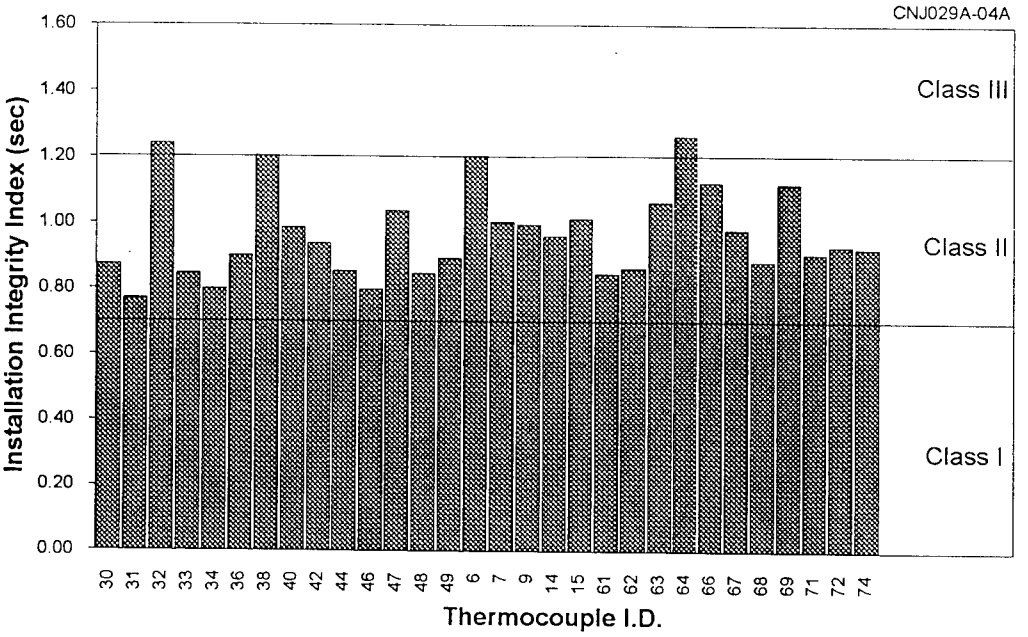

Figure 7 Installation Classifications for CIP Thermocouples

TABLE 3

Listing Of Cured-In-Place Outliers

ITEM	TAG #	BLOCK	INSTALLATION INDEX
1	L	30	0.28
2	215	29	0.39
3	209	25	1.48
4	185	40	1.51
5	187	38	1.54

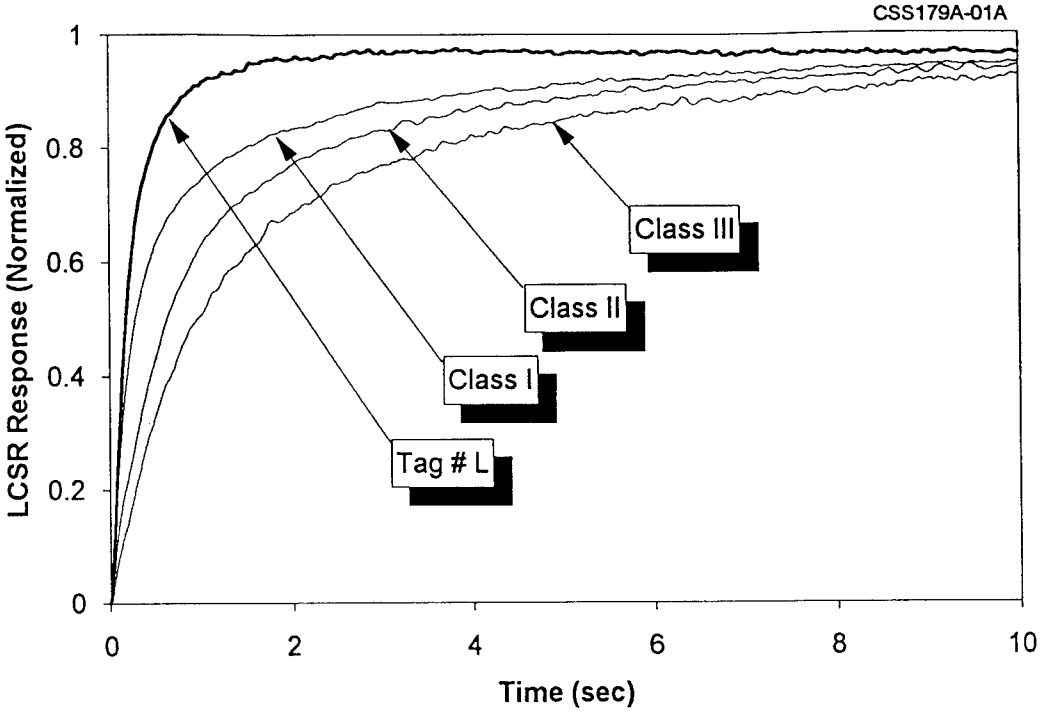

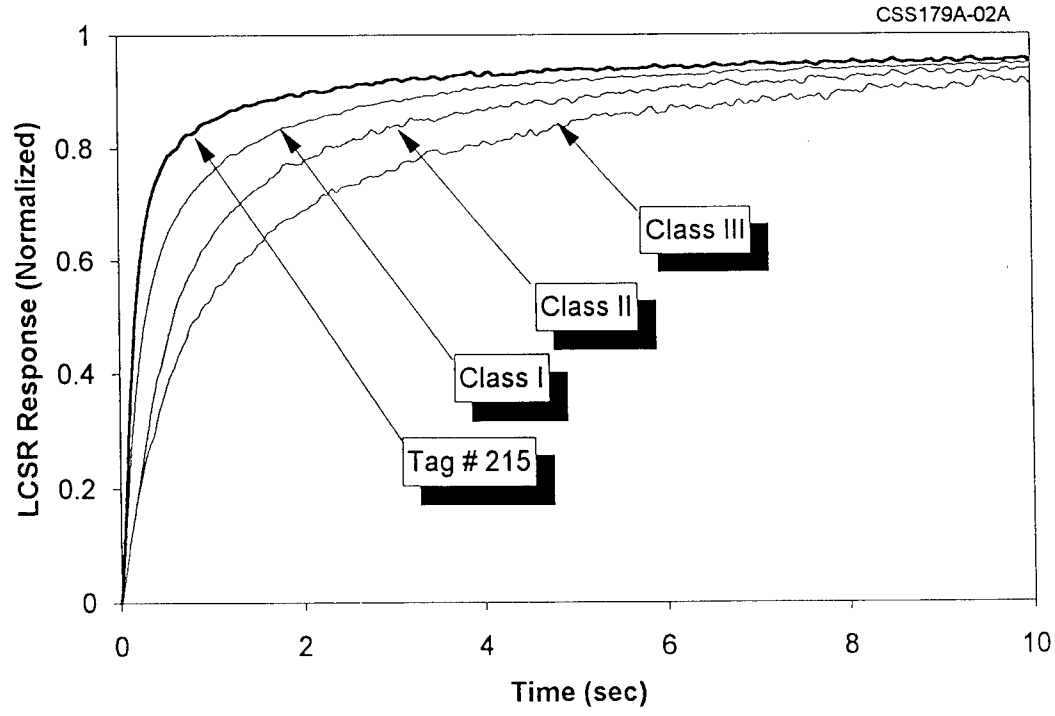

Figure 8 Identified Outliers for CIP Installations

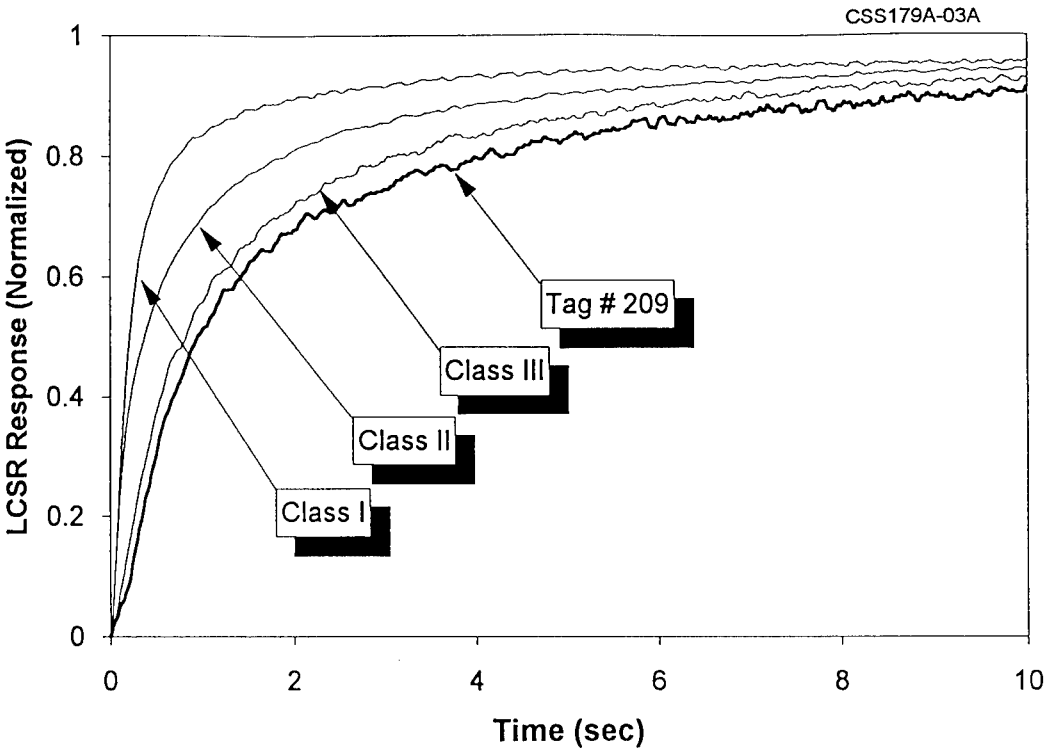

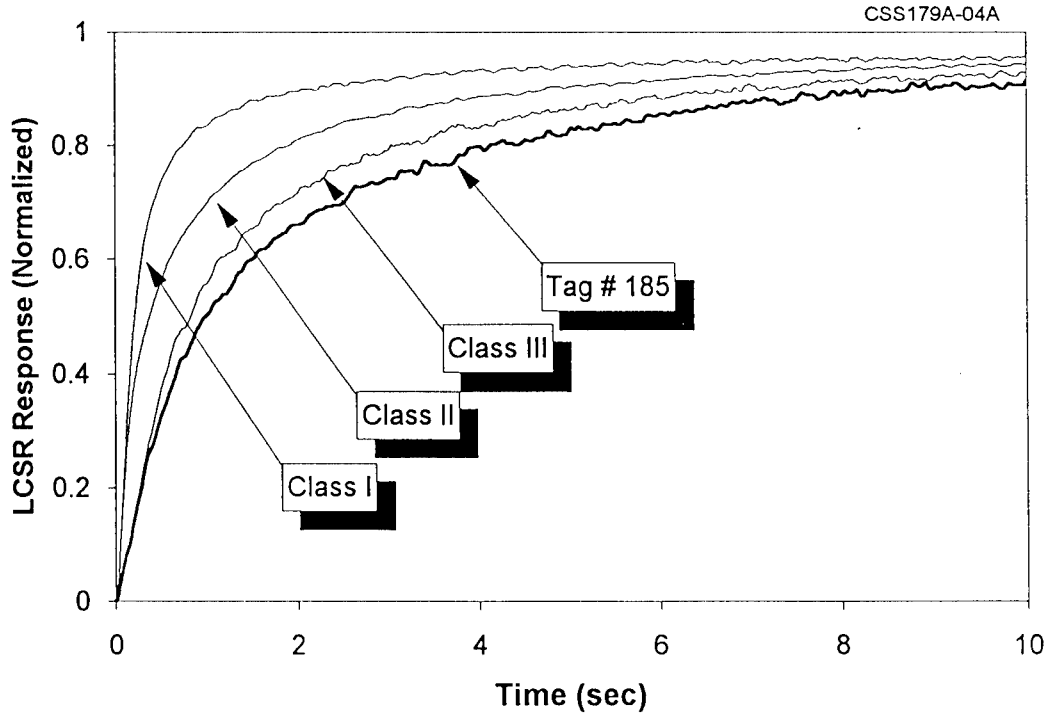

Figure 9 Identified Outliers for CIP Installations

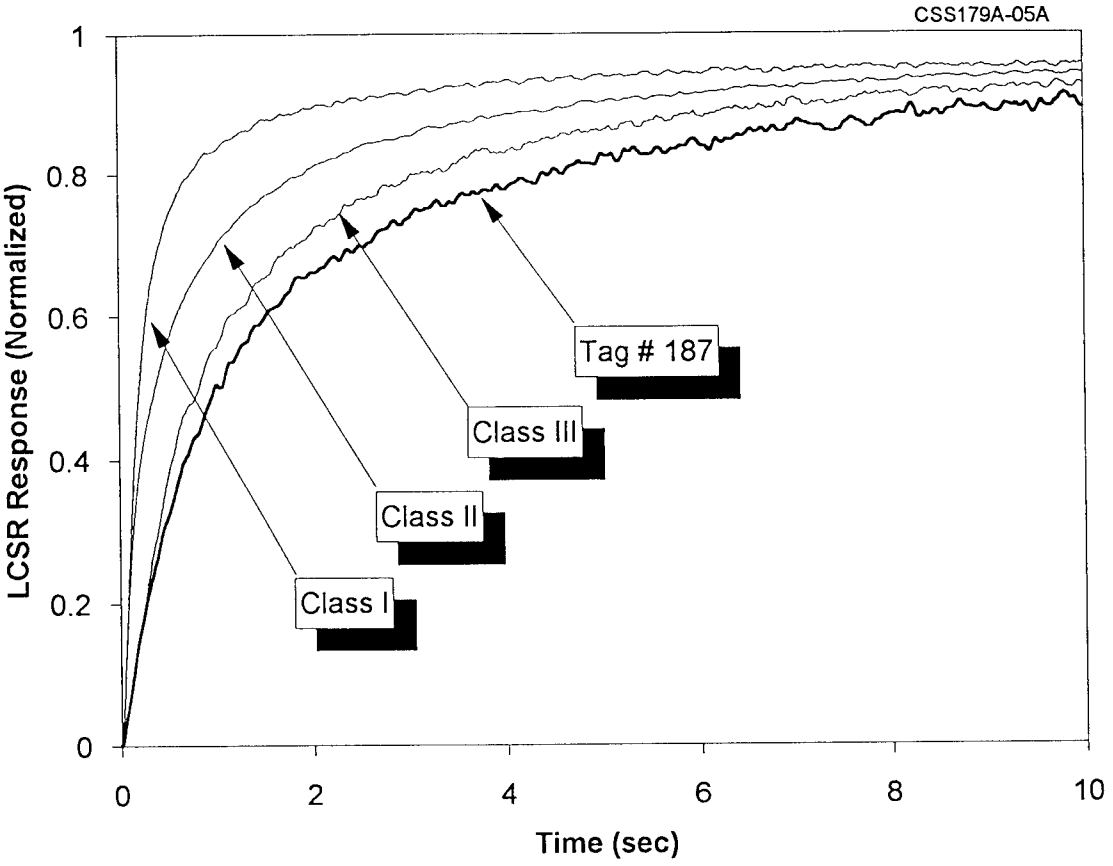

Figure 10 Identified Outliers for CIP Installations

Table 4 lists all the thermocouples with probe-type installation grouped according to their classification. Figure 11 shows the results for the probe installed thermocouples graphically. The outliers for the probe installation type thermocouples are listed in Table 5. Figures 12 and 13 show the LCSR transients for the outliers listed in Table 5 versus typical class I, II and III LCSR transients. Figure 14 shows the transients for the three CIP sensors in block 38. Among these three sensors, tag #186 responded differently than the other two sensors. This could be attributed to a low insulation resistance (IR). Low insulation resistance was verified by taking actual insulation resistance measurements on sensor 186.

3.2 LCSR Versus Analog Results

After the LCSR testing at AMS, the carbon-phenolic specimens were sent to either SRI or the Marshall Space Flight Center Plasma Arc facilities for firing. The firing tests consisted of heating one side of the specimen and acquiring data from the sensors on the front and back surfaces as well as the sensors embedded in the material. This data was subsequently analyzed by AMS to see if a correlation existed between the analog results and the LCSR results could be determined.

In the analog data, several blocks exhibited an unusual phenomenon in that a sensor far away from the firing surface would respond quicker than a sensor close to the firing surface. Two examples of this behavior are shown in Figure 15. Note that only the sensors in question are shown in these figures. The remaining sensors in the block were removed in order to highlight the phenomenon. This behavior was seen in nine of the test specimens on fourteen different occasions as listed in Table 6. After identifying this behavior, the LCSR results were evaluated for each of the occurrences. The results showed that for eight of the fourteen cases, the sensor which responded faster had a smaller installation integrity index than the sensor that was closer to the firing surface.

TABLE 4

Listing of Probe Installed Thermocouple Classifications

Item	Tag #	Block	Installation Index (sec)	Classification
1	132	30	0.34	I
2	22	17	0.34	I
3	166	29	0.37	II
4	20	8	0.37	II
5	25	19	0.37	II
6	133	30	0.38	II
7	24	17	0.38	II
8	160	21	0.38	II
9	131	30	0.38	II
10	120	31	0.39	II
11	134	31	0.39	II
12	157	21	0.39	II
13	158	21	0.40	II
14	135	31	0.40	II
15	201	10	0.40	II
16	205	11	0.40	II
17	135	31	0.40	II
18	198	20	0.41	II
19	247	41	0.41	II
20	168	29	0.42	II
21	150	14	0.43	II
22	23	17	0.43	II
23	167	29	0.43	II
24	144	16	0.44	II
25	248	40	0.44	II
26	149	15	0.46	II
27	17	7	0.46	II
28	147	14	0.50	II
29	250	41	0.50	II
30	203	12	0.55	II
31	127	47	0.55	II
32	145	16	0.56	II
33	199	20	0.56	II
34	280	46	0.56	II

CONTINUED ON NEXT PAGE

TABLE 4
(Continued)

Listing of Probe Installed Thermocouple Classifications

Item	Tag #	Block	Installation Index (sec)	Classification
35	252	38	0.61	II
36	128	46	0.62	II
37	146	14	0.64	II
38	126	47	0.66	II
39	161	28	0.69	II
40	162	28	0.71	II
41	179	15	0.75	II
42	148	15	0.75	II
43	165	19	0.75	II
44	164	19	0.76	II
45	251	40	0.76	II
46	246	41	0.77	II
47	259	39	0.78	II
48	255	38	0.79	II
49	163	28	0.80	II
50	271	44	0.81	II
51	202	9	0.82	II
52	260	39	0.84	II
53	277	47	0.84	II
54	156	18	0.86	II
55	249	40	0.93	II
56	196	18	1.00	III
57	130	46	1.01	III
58	278	45	1.03	III
59	121	45	1.09	III
60	254	39	1.11	III
61	197	18	1.12	III
62	253	38	1.18	III
63	178	16	1.22	III
64	279	44	1.33	III
65	122	45	1.33	III
66	276	44	1.49	III

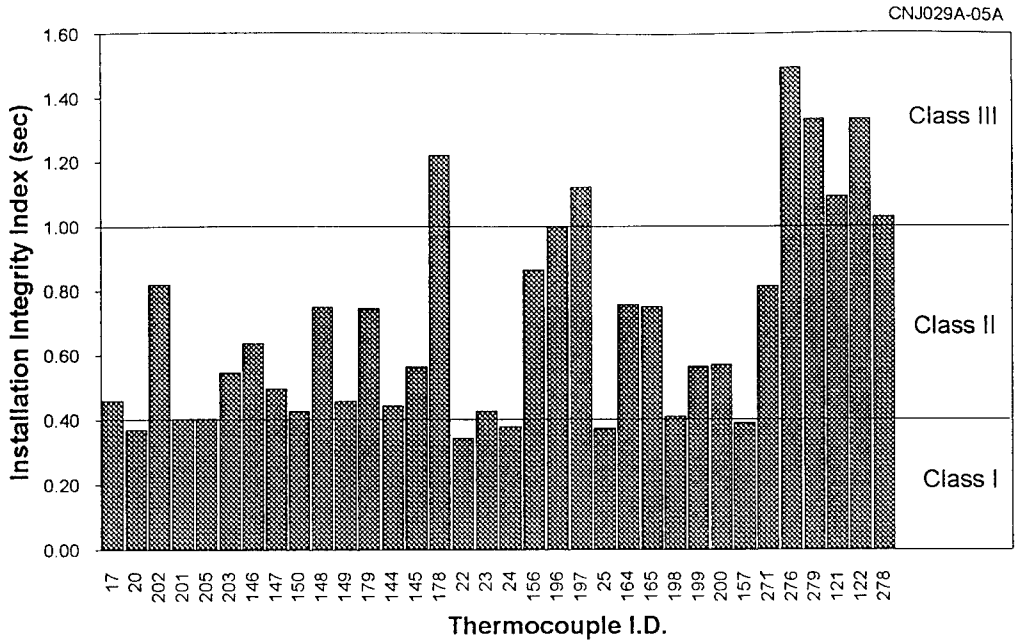

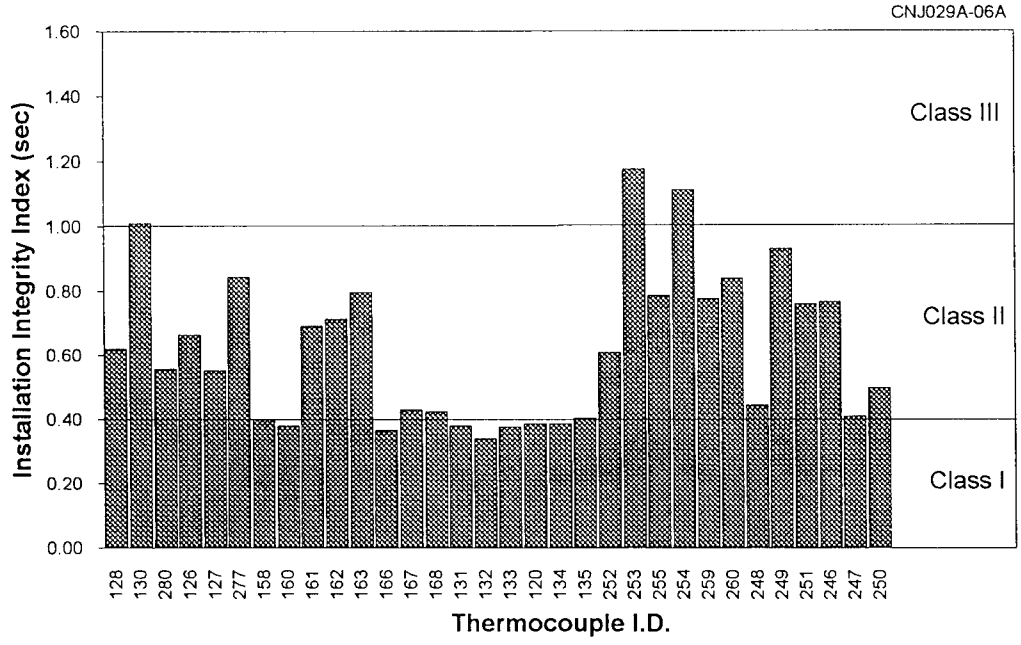

Figure 11 Installation Classification for Probe Thermocouples

TABLE 5

Listing of Probe Outliers

Item	Tag #	Block	Installation Index (sec)
1	122	45	1.33
2	279	44	1.33
3	276	44	1.49

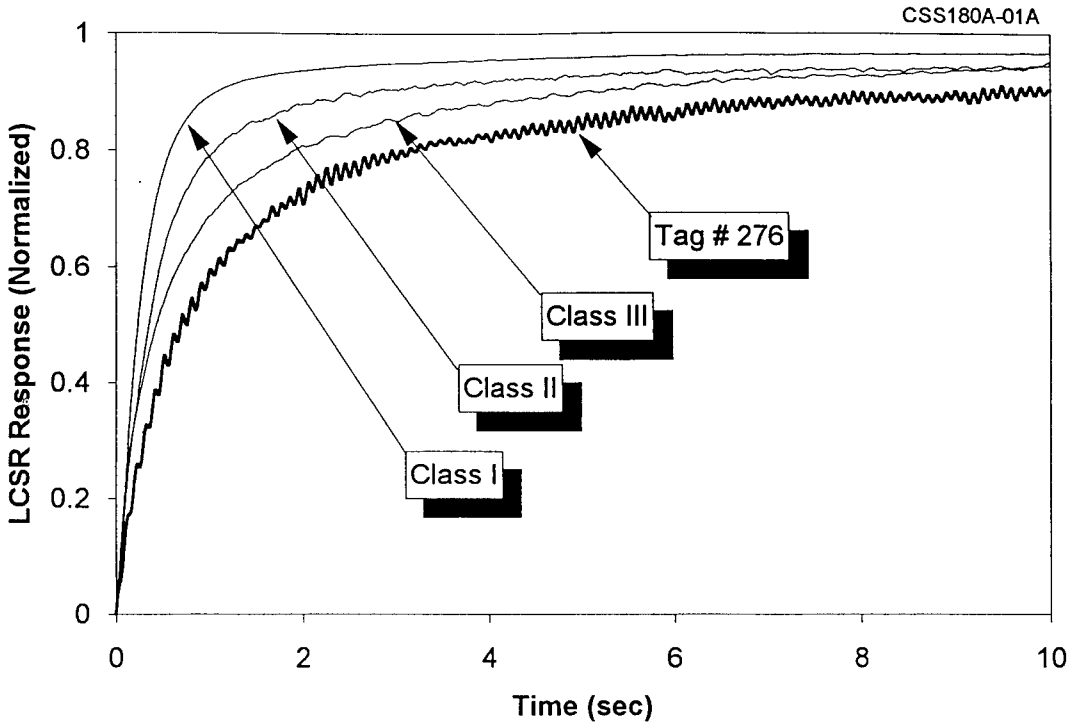

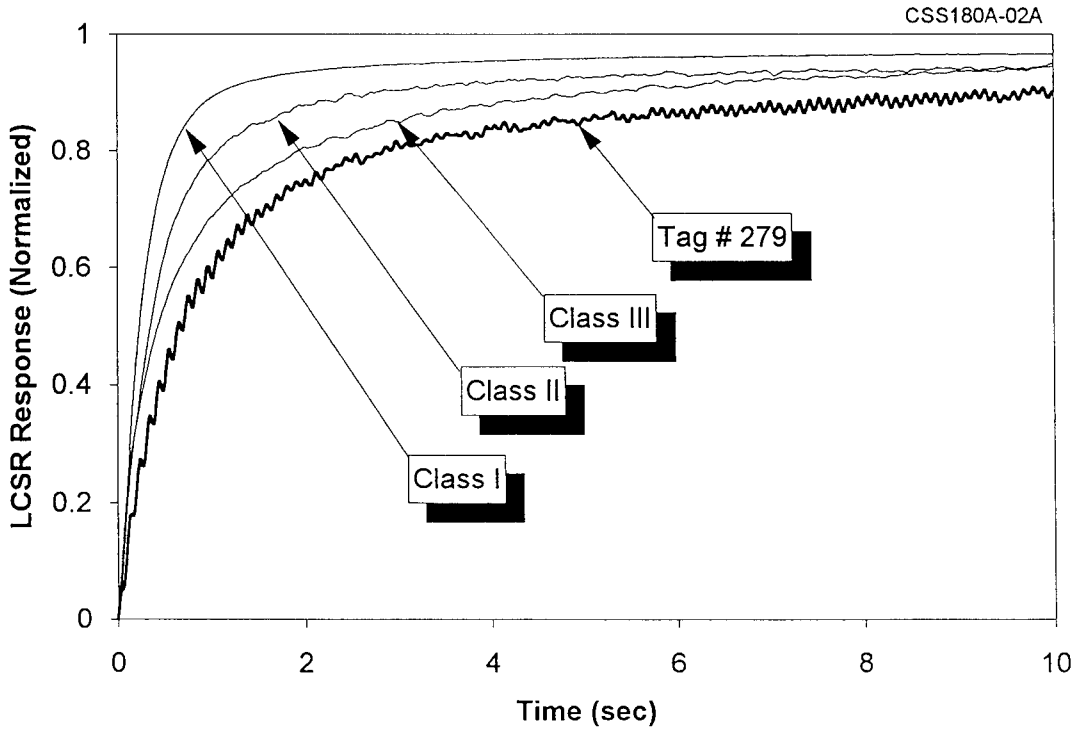

Figure 12 Identified Outliers for Probe Installations

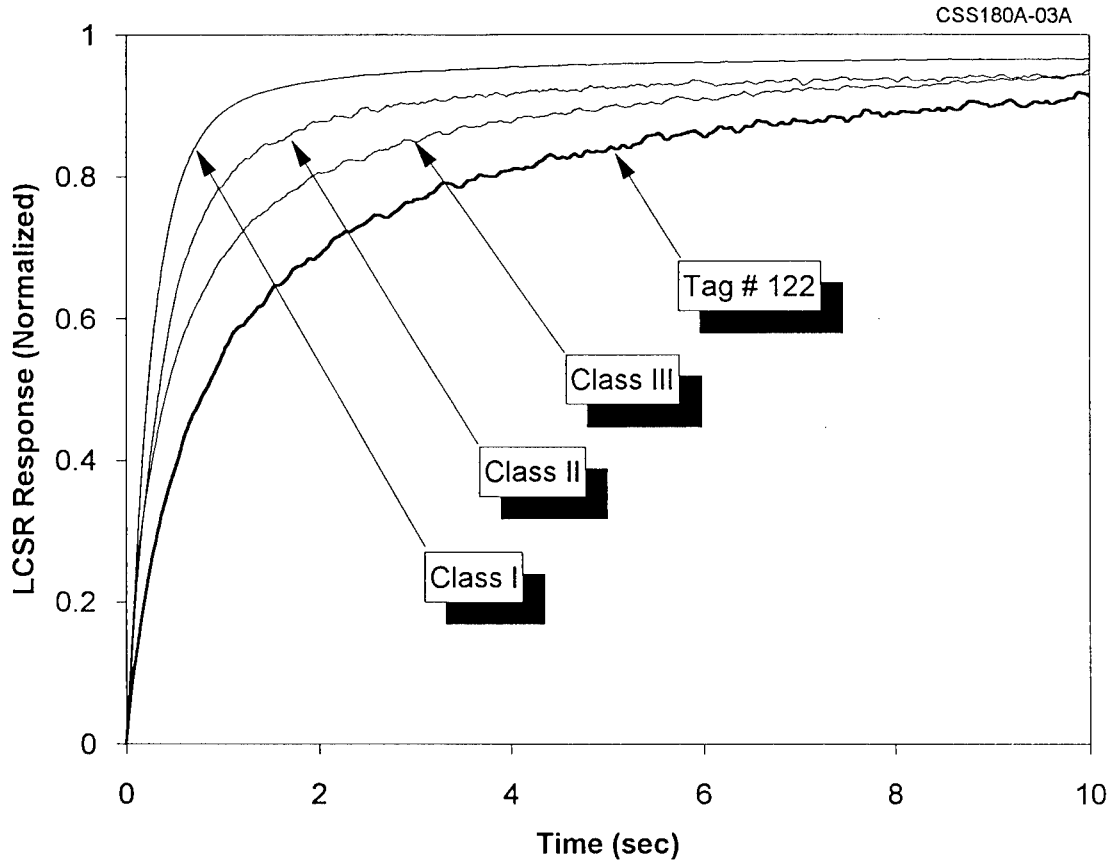

Figure 13 Identified Outliers for Probe Installations

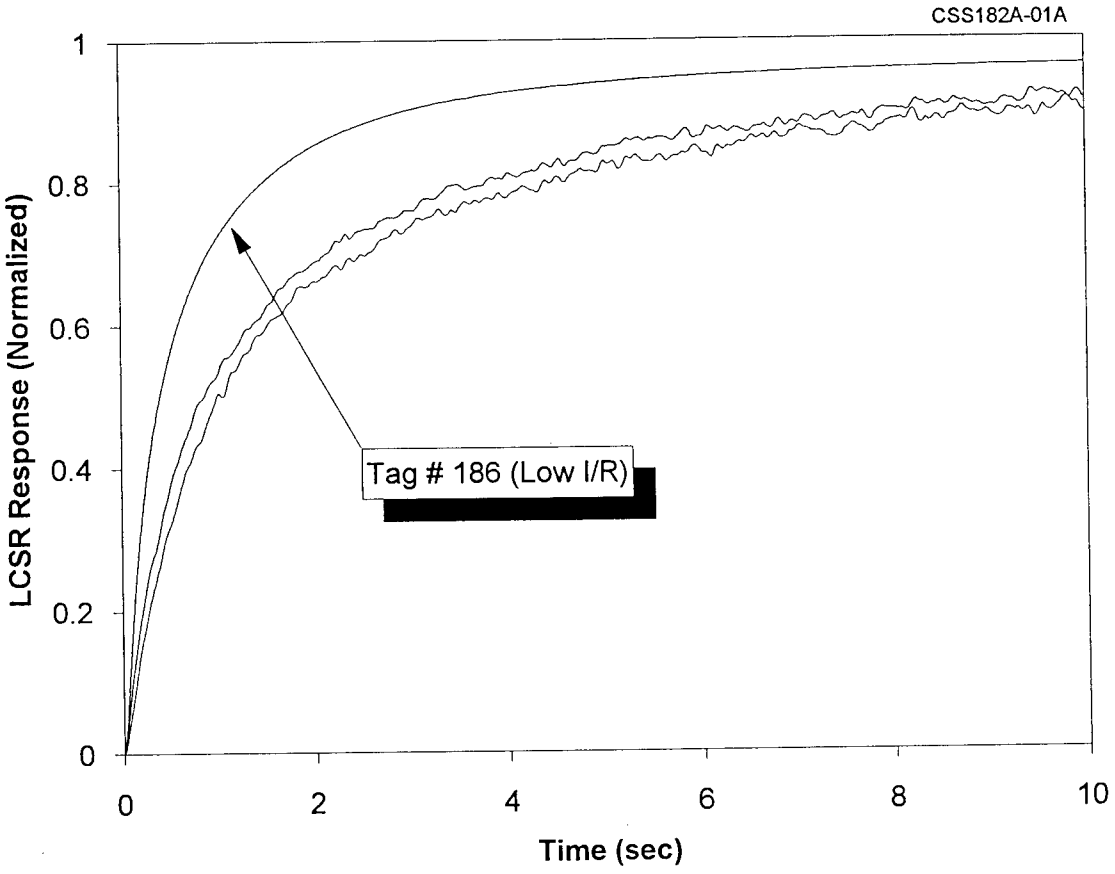

Figure 14 LCSR Transient for a Thermocouple with Low Insulation Resistance in Sample SRI-III-38

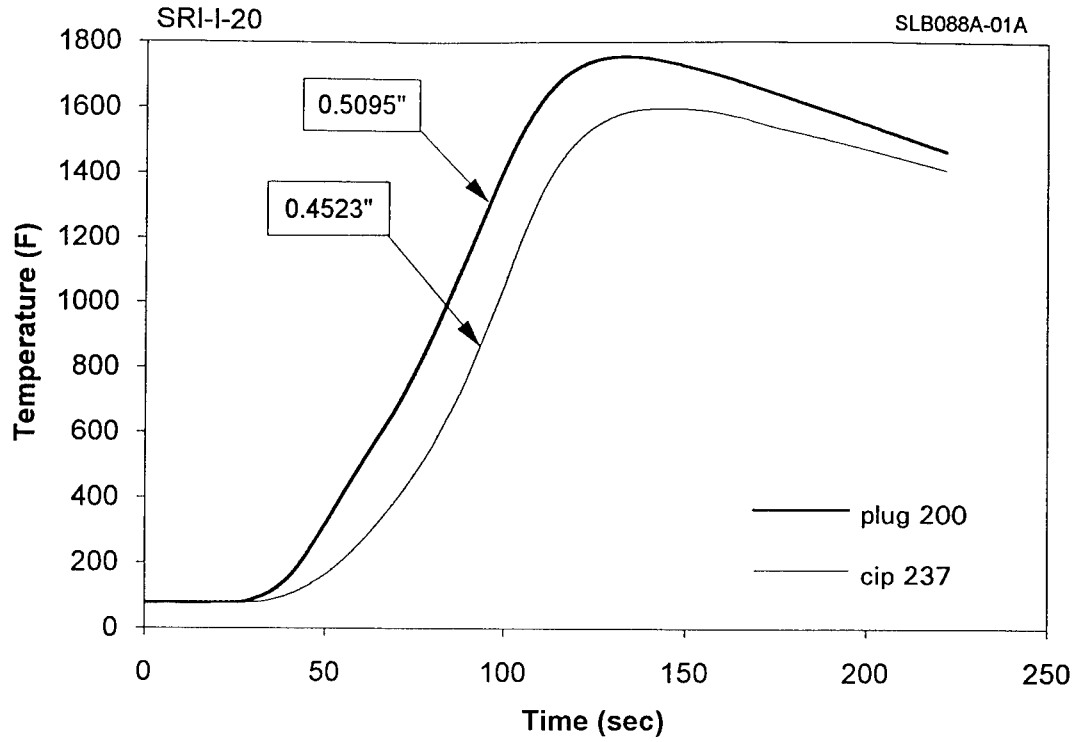

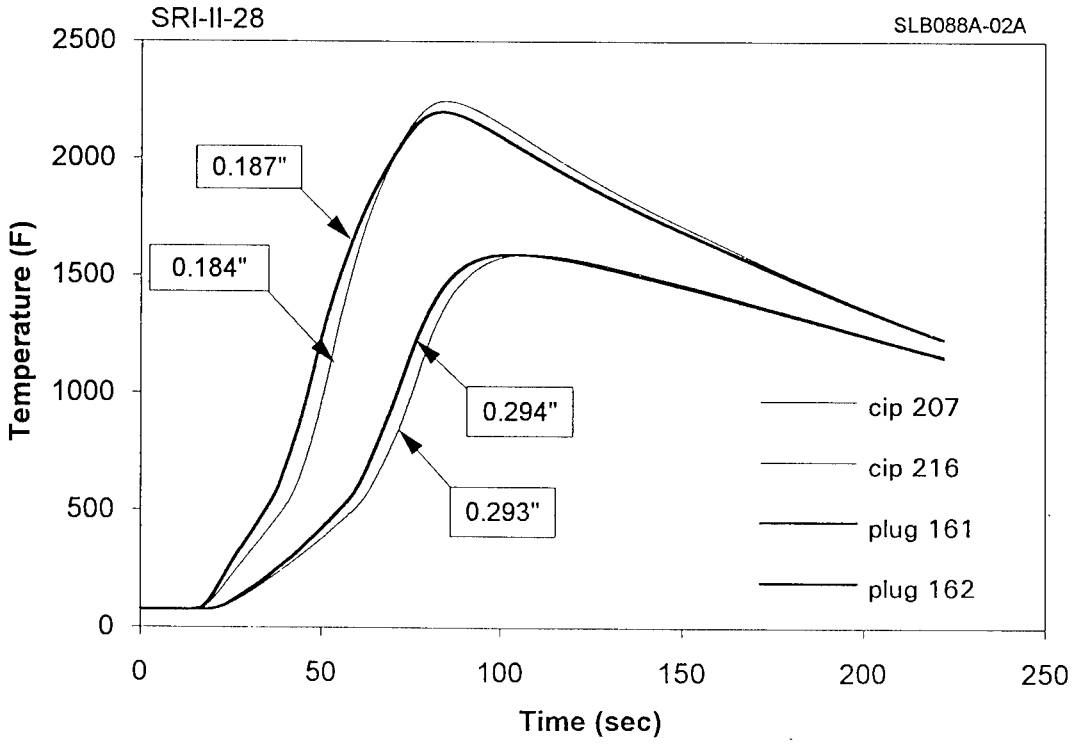

Figure 15 Example of Abnormal Behavior in SRI Analog Data

TABLE 6

Thermocouple Analog Data Comparisons

Item	Block	Thermocouples Compared
1	7	17,59
2	8	20, 9
3	14	85, 146
4	17	22, 225
5	18	231, 196
6	18	234, 156
7	18	235, 197
8	20	200, 237
9	28	161, 216
10	28	162, 207
11	28	163, 214
12	40	190, 251
13	41	191, 246
14	41	192, 247

Of the remaining six cases, a case by case analysis was used to evaluate why the sensors responded differently. In the first case, the sensor was found to have a low insulation resistance and therefore the LCSR transient was significantly different from the transients of the other sensors of the same installation (Figure 16). The next three cases all occurred in block number 18. This block was found to have very similar transients for the CIP sensors and the plug sensors (Figure 17), where the CIP and plug transients are usually very different (Figure 18). The remaining two cases seem to follow the typical CIP and plug type transients. The dynamic response of the last two sensors may have been influenced by factors other than the installation.

4. CONCLUSIONS

LCSR transients for measuring the installation integrity of embedded thermocouples were evaluated for 204 thermocouples and the following conclusions were made:

1. Fourteen of the 204 thermocouples were received "open" and were therefore not testable.
2. Three thermocouples had very low insulation resistances.
3. Eight thermocouples were identified as outliers from an attachment standpoint.
4. The Cured-In-Place thermocouples demonstrated a better gaussian distribution when compared to the probe installations.
5. Of the fourteen inconsistencies identified using the analog data, 12 were detectable by using LCSR.

Based on the findings presented in this report, the LCSR test is an effective tool for verifying the attachment of thermocouples in solid material.

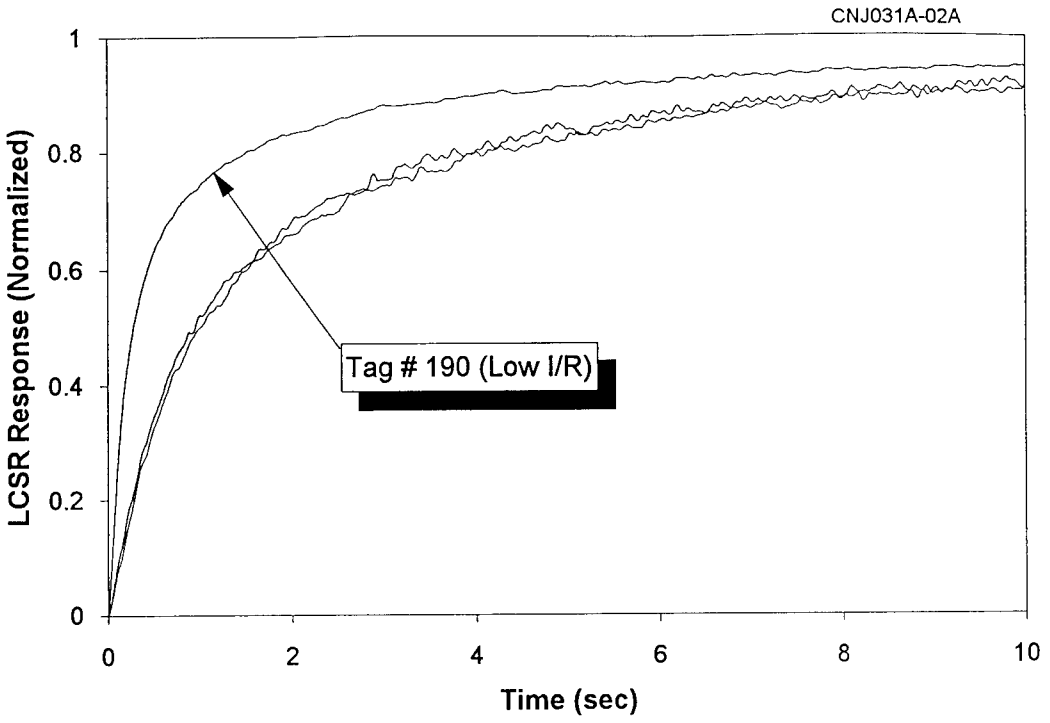

Figure 16 LCSR Transient for a Thermocouple with Low Insulation Resistance in Sample SRI-III-40

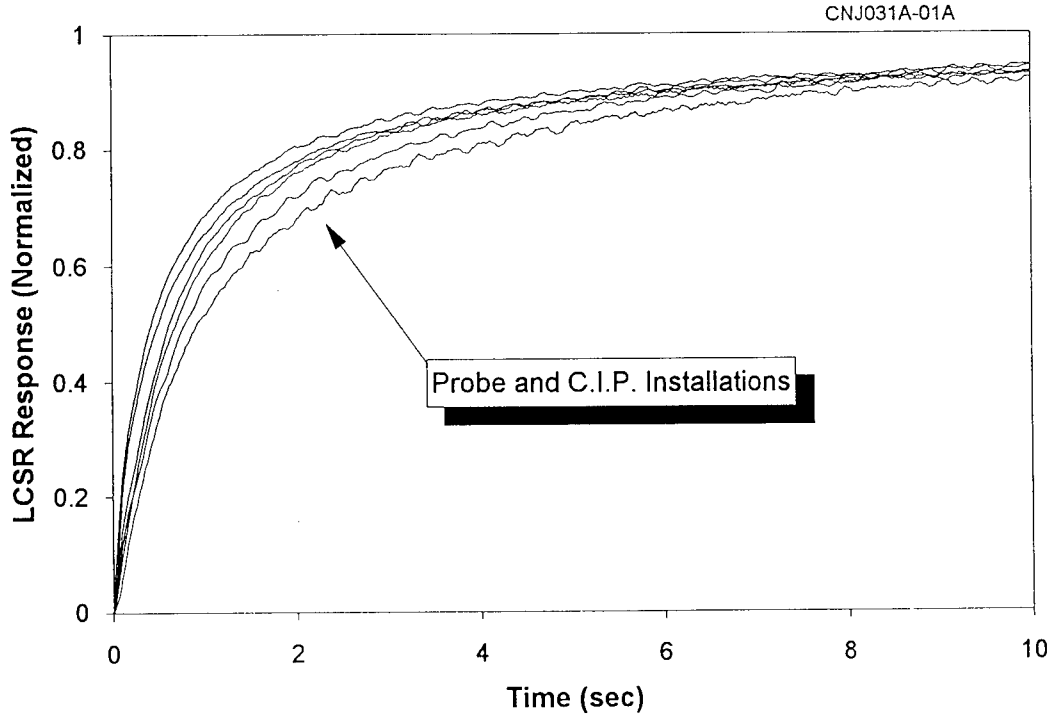

Figure 17 Abnormal LCSR Transients for Probe Thermocouples in Sample SRI-I-18

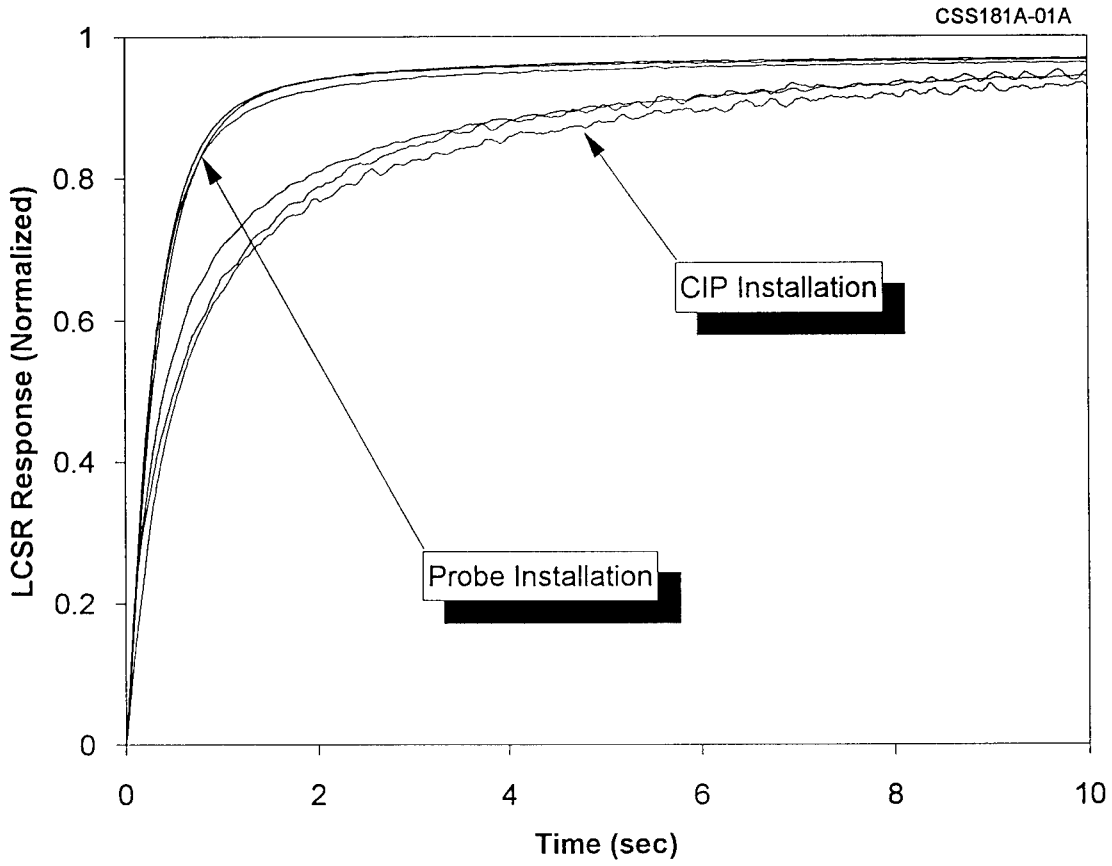

Figure 18 Normal LCSR Transients for Probe and CIP Thermocouples

REFERENCES

1. Hashemian, H.M., Mitchell, D.W., Shell, C.S., and Farmer, J.P., "Improved Temperature Measurement in Composite Material for Aerospace Applications," AMS Report #NASA9306R0, prepared for NASA, Marshall Space Flight Center, July 1993.

2. Hashemian, H.M., "New Technology for Testing the Installation Integrity of Thermocouples in Composite Materials for SRM Nozzles," presented at ISA 40th International Instrumentation Symposium, Baltimore, MD, May 1994.

3. Hashemian, H.M., Mitchell, D.W. and Petersen, K.M., "New Technology for Testing the Attachment of Sensors in Composite Materials for SRM Nozzles," presented at 1995 JANNAF RNTS Meeting, Seattle, Washington, November 1994.

APPENDIX E

TESTING OF BLAST TUBE LINER MATERIAL

ANALYSIS AND
MEASUREMENT SERVICES
CORPORATION

AMS 9111 CROSS PARK DRIVE / KNOXVILLE, TN 37923 USA (615) 691-1756

Report #: NASA9402R0

RESULTS FROM INSTALLATION INTEGRITY TESTING OF EMBEDDED THERMOCOUPLES FOR THE REDESIGNED SOLID ROCKET MOTOR BLAST TUBE LINER

Revision 0

August 1994

Prepared For

Lon Stevens
Thiokol/MSFC OPR OFC
BLDG 4712 Apollo Road Room B301D
Marshall Space Flight Center, Alabama 35812

1. INTRODUCTION

Analysis and Measurement Services Corporation (AMS) performed a series of installation integrity tests on several thermocouples embedded in the Redesigned Solid Rocket Motor (RSRM) blast tube liner. The tests were performed at the George C. Marshall Flight Center (MSFC) in March and April 1994. The testing consisted of pre and post-curing tests. During the pre-curing tests, eleven Erosion Monitoring Thermocouple Array (EMTA) gages, each containing six thermocouples, were tested. Post-curing tests consisted of ten of the pre-cured EMTA gages and four additional gages for a total of 84 thermocouples.

The thermocouple testing at MSFC was performed using the Loop Current Step Response (LCSR) method. The purpose of this testing was to provide LCSR results to assist in the evaluation of the transient temperature data taken during firing of the instrumented blast tube. The pre-cure LCSR test results were also used to determine which gages would be cured into the blast tube liner.

The LCSR tests concentrated on evaluating the differences in the response characteristics of each thermocouple prior to firing the blast tube. In addition, the LCSR data provides useful information for evaluating the effects of the curing process on the sensors responses. It has been shown in laboratory tests performed at AMS that inadequate or poorly installed thermocouples can be detected by noticeable differences in the LCSR response. A poor installation will result in a slower response time due to differences in the heat transfer properties of the area immediately surrounding the thermocouple. The data presented in this report are in terms of normalized LCSR transients for all thermocouples tested.

2. BACKGROUND

The accuracy of transient temperature measurements with thermocouples is highly dependent on the response time of the thermocouples in the specific media (water, air, solids, etc.) in which they are installed. It has been shown, during laboratory research performed by AMS, that the response characteristics of thermocouples that are installed in solid materials, such as those used in the RSRM, depend strongly on the bonding between the thermocouple and the solid material (i.e., the installation integrity). As documented in the results of a recent research project performed by AMS for NASA, the LCSR test method can be used to assist in evaluating the installation of thermocouples embedded in solid materials.

The LCSR test involves applying an electrical current through the thermocouple leads. This current results in Joule heating of the measuring junction to an elevated temperature, several degrees above the ambient temperature. The heating current is then terminated, and the output from the thermocouple is monitored as it cools back to the ambient temperature. This cooling transient contains inherent information about the response of the thermocouple in the particular environment in which it is installed.

3. RESULTS

On March 9-11, 1994, AMS performed a series of LCSR tests on eleven instrumented EMTA gages embedded in the RSRM blast tube liner. These gages were constructed from four different composite materials: 5066 (carbon-phenolic), 5067 (carbon-phenolic), AsNBR (asbestos filled rubber) and CFEPDM (carbon filled rubber). Each gage contained six thermocouples cured

into the material that were to be used for transient temperature measurements during the firing. Figure 1 is an illustration of the EMTA gages prior to curing them into the blast tube liner. All thermocouples tested in each gage were small diameter (0.005"), type K, bare thermocouples manufactured by Thiokol Corporation.

On April 18-21, 1994, AMS performed additional LCSR tests after the EMTA gages were cured into the blast tube liner of the RSRM, referred to as the post-cure tests. A total of fourteen gages, with six thermocouples each, were post-cure tested for a total of 84 thermocouples. Ten of the fourteen gages were also tested prior to curing them into the blast tube liner. This provided a set of comparison data that could be used to represent the effects of the curing process on the installation integrity of the thermocouples. Figure 2 is an illustration of the configuration of the gages that are cured into the blast tube liner material. Figure 3 is an illustration of the RSRM blast tube.

3.1 PRE-CURE TESTING

Table 1 is a listing of the pre-cure thermocouples tested. Note that a low insulation resistance (I/R) was noted for thermocouple tag number #2 in gage #28. The insulation resistance was measured between the thermocouple leads and the stainless steel tube which encased the thermocouple leads (see Figure 1). The CFEPDM material, used in gage #28, is electrically conductive, therefore, the bare thermocouple junctions are covered with "M Bond 610", a commonly used epoxy, before they are cured into the gage assembly in order to provide electrical insulation. The low I/R seen in this thermocouple could be due to an insufficient amount of epoxy around the junction resulting in increased conductivity between the junction and the stainless steel tube. I/R tests were also performed on all CFEPDM gages, even those that were not LCSR tested. Thermocouple #4 in gage #40 was also found to have a low I/R. As a result, both gage #28 and gage #40 were not cured into the blast tube liner.

AMS-DWG NAS008B

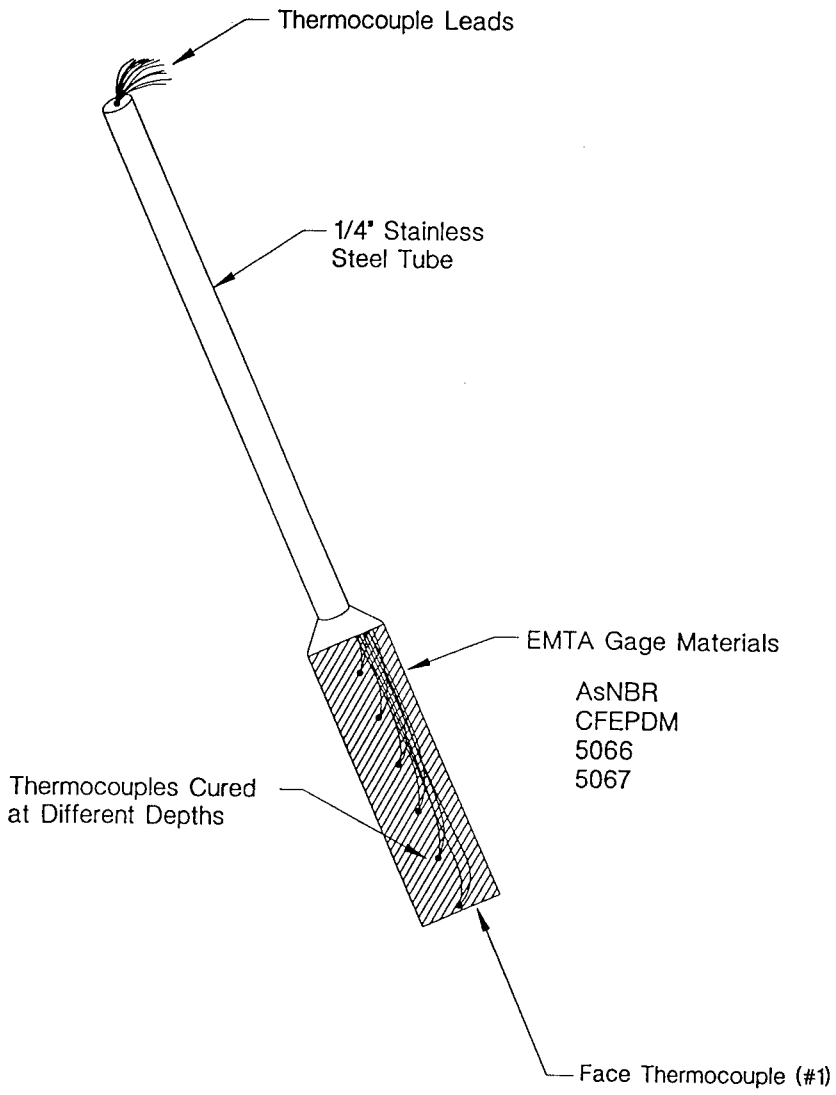

Figure 1. Erosion Monitoring Thermocouple Array Gage Prior to Curing

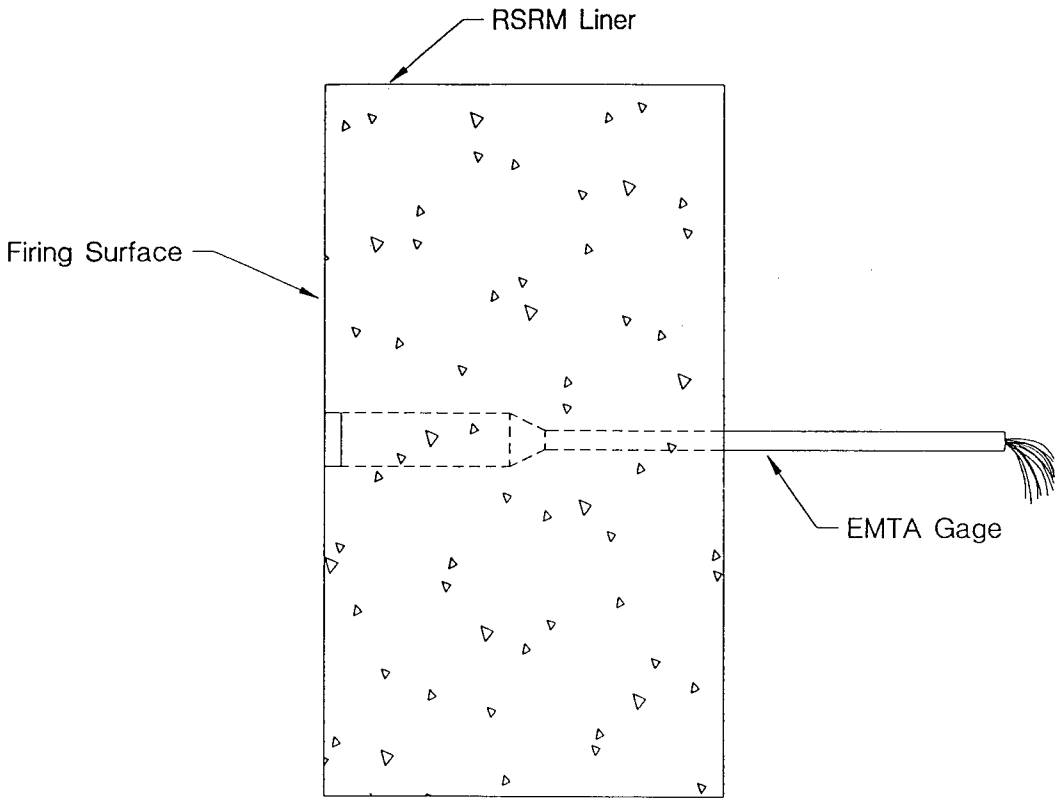

Figure 2. Erosion Monitoring Thermocouple Array Gage After Being Cured into Blast Tube

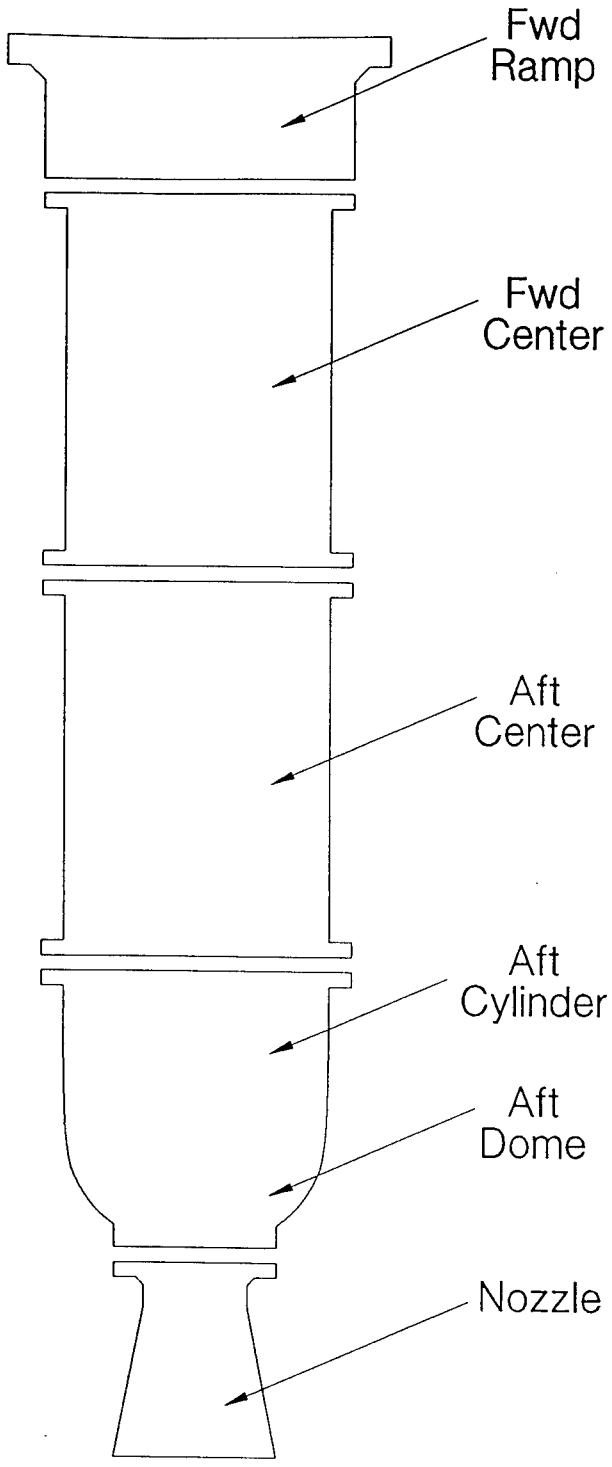

Figure 3. Redesigned Solid Rocket Motor Blast Tube

TABLE 1

Listing of Pre-Cured Thermocouples Tested in the Redesigned Solid Rocket Motor Liner at Marshall Space Flight Center

Item #	Gage #	TC Number	Material
1	21	1	5066
2	21	2	5066
3	21	3	5066
4	21	4	5066
5	21	5	5066
6	21	6	5066
7	25	1	5066
8	25	2	5066
9	25	3	5066
10	25	4	5066
11	25	5	5066
12	25	6	5066
13	26	1	5066
14	26	2	5066
15	26	3	5066
16	26	4	5066
17	26	5	5066
18	26	6	5066
19	29	1	5066
20	29	2	5066
21	29	3	5066
22	29	4	5066
23	29	5	5066
24	29	6	5066

CONTINUED NEXT PAGE

TABLE 1 (Continued) Listing of Pre-Cured Thermocouples Tested in the Redesigned Solid Rocket Motor Liner at Marshall Space Flight Center			
Item #	Gage #	TC Number	Material
25	22	1	5067
26	22	2	5067
27	22	3	5067
28	22	4	5067
29	22	5	5067
30	22	6	5067
31	23	1	5067
32	23	2	5067
33	23	3	5067
34	23	4	5067
35	23	5	5067
36	23	6	5067
37	31	1	AsNBR
38	31	2	AsNBR
39	31	3	AsNBR
40	31	4	AsNBR
41	31	5	AsNBR
42	31	6	AsNBR
43	32	1	AsNBR
44	32	2	AsNBR
45	32	3	AsNBR
46	32	4	AsNBR
47	32	5	AsNBR
48	32	6	AsNBR

CONTINUED NEXT PAGE

TABLE 1 (Continued) Listing of Pre-Cured Thermocouples Tested in the Redesigned Solid Rocket Motor Liner at Marshall Space Flight Center			
Item #	Gage #	TC Number	Material
49	28	1	CFEPDM
* 50	28	2	CFEPDM
51	28	3	CFEPDM
52	28	4	CFEPDM
53	28	5	CFEPDM
54	28	6	CFEPDM
55	34	1	CFEPDM
56	34	2	CFEPDM
57	34	3	CFEPDM
58	34	4	CFEPDM
59	34	5	CFEPDM
60	34	6	CFEPDM
61	37	1	CFEPDM
62	37	2	CFEPDM
63	37	3	CFEPDM
64	37	4	CFEPDM
65	37	5	CFEPDM
66	37	6	CFEPDM

* Low Insulation Resistance

The averaged, and normalized, LCSR transients are shown in Figures 4 to 7. These figures have been grouped according to gage material type. The averaged transients represent the average of five to ten individual transients taken for each thermocouple. In seven of the eleven gages (gage #'s 22,23,25,29,31,32,37), thermocouple #1 showed a slight response difference with respect to the other 5 thermocouples in the gage. Thermocouple #1 is the face thermocouple (Figure 1). Gage #26 also showed a slight difference for thermocouple #'s 4 and 5.

3.2 POST-CURE TESTING

Table 2 is a listing of the post-cured thermocouples tested. Note that three thermocouples were defective due to open circuits in the thermocouple leads. In addition to the open circuits, thermocouple #4 in gage #34, located at AFT Dome 270° had a low I/R reading. This gage was pre-cure tested and did not have a low resistance reading before being cured into the blast tube liner. The averaged LCSR transients for the post-cure tests are shown in Figures 8 to 11. The transients are grouped according to their location in the blast tube liner. The post-cure testing revealed eight of the fourteen gages (gage #'s 25,31,37,30,20,29,27,24) with slight response differences with respect to the other 5 thermocouples in the gage. Of these eight gages, six (gage #'s 25,31,37,29,30,20) of the outlier's were identified as thermocouple #1. Four (gage #'s 25,31,37,29) of the six, thermocouple #1 outlier's gages, were also identified as having a slight response difference in the pre-cure testing. The other two gages (#'s 30,20) were not pre-cure tested.

3.3 PRE-CURE VS POST-CURE

Ten of the eleven instrumented gages tested before being cured into the blast tube liner were also post-cure tested. Gage #28, originally planned for installation into the AFT Dome CYL 270°

5066 Material - Before Cure

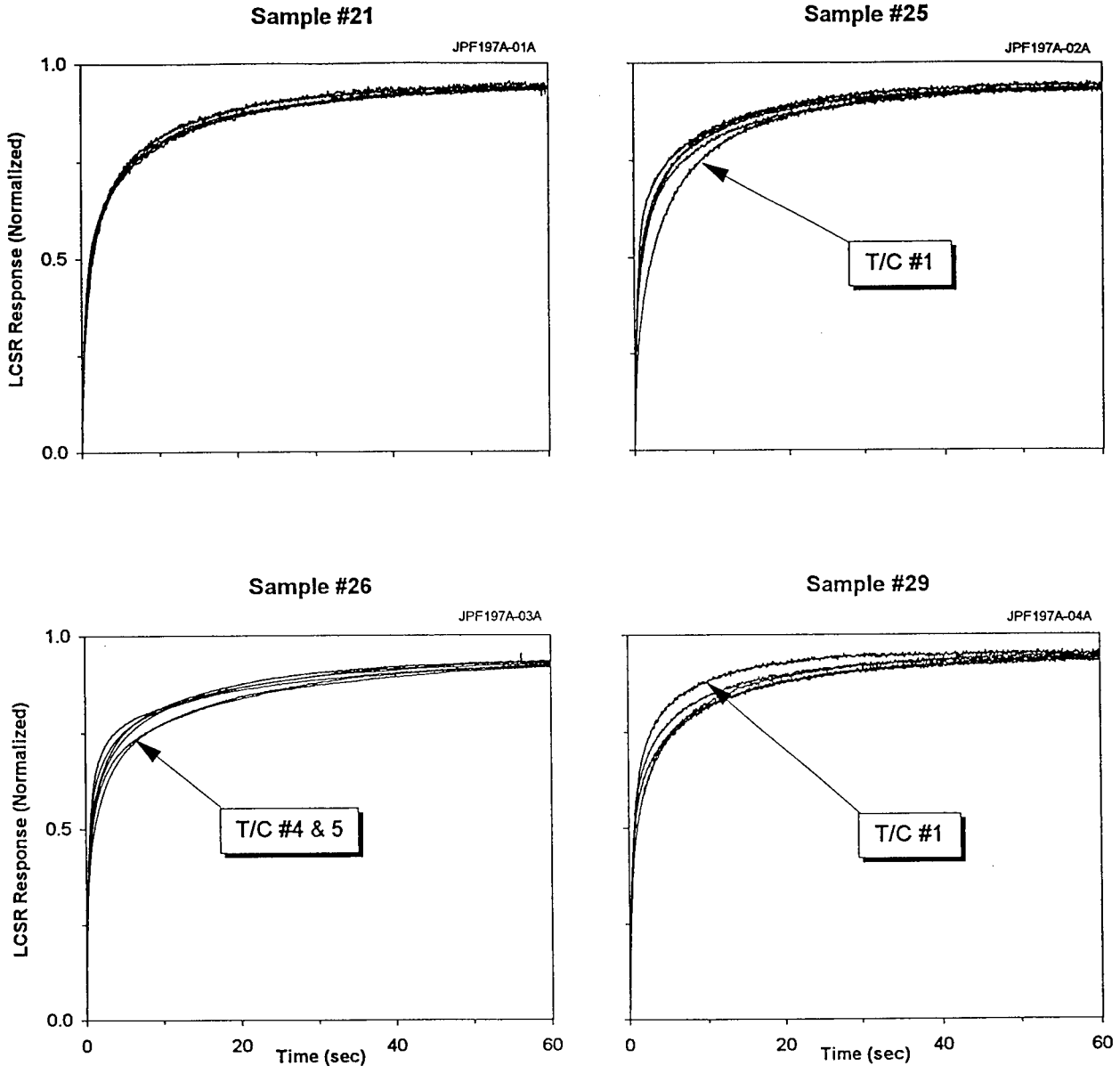

Figure 4. LCSR Transients for EMTA Gages in 5066 Material

5067 Material - Before Cure

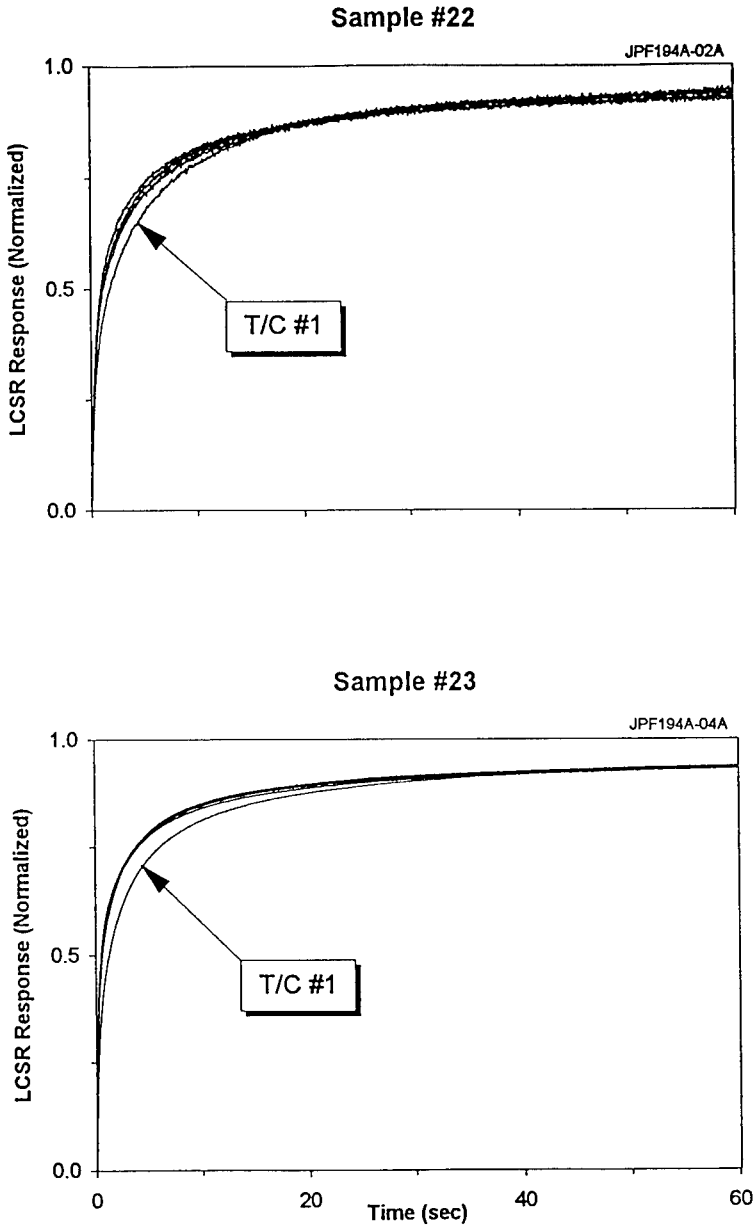

Figure 5. LCSR Transients for EMTA Gages in 5067 Material

AsNBR Material - Before Cure

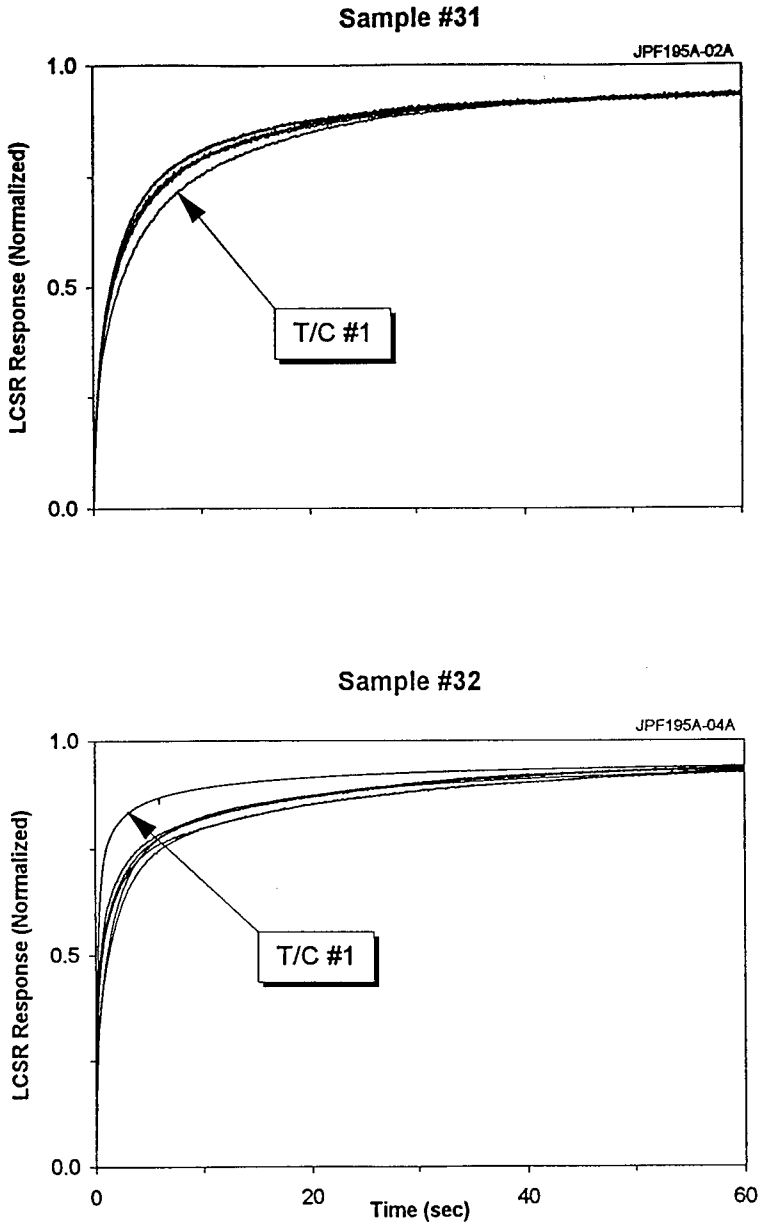

Figure 6. LCSR Transients for EMTA Gages in AsNBR Material

CFEPDM Material - Before Cure

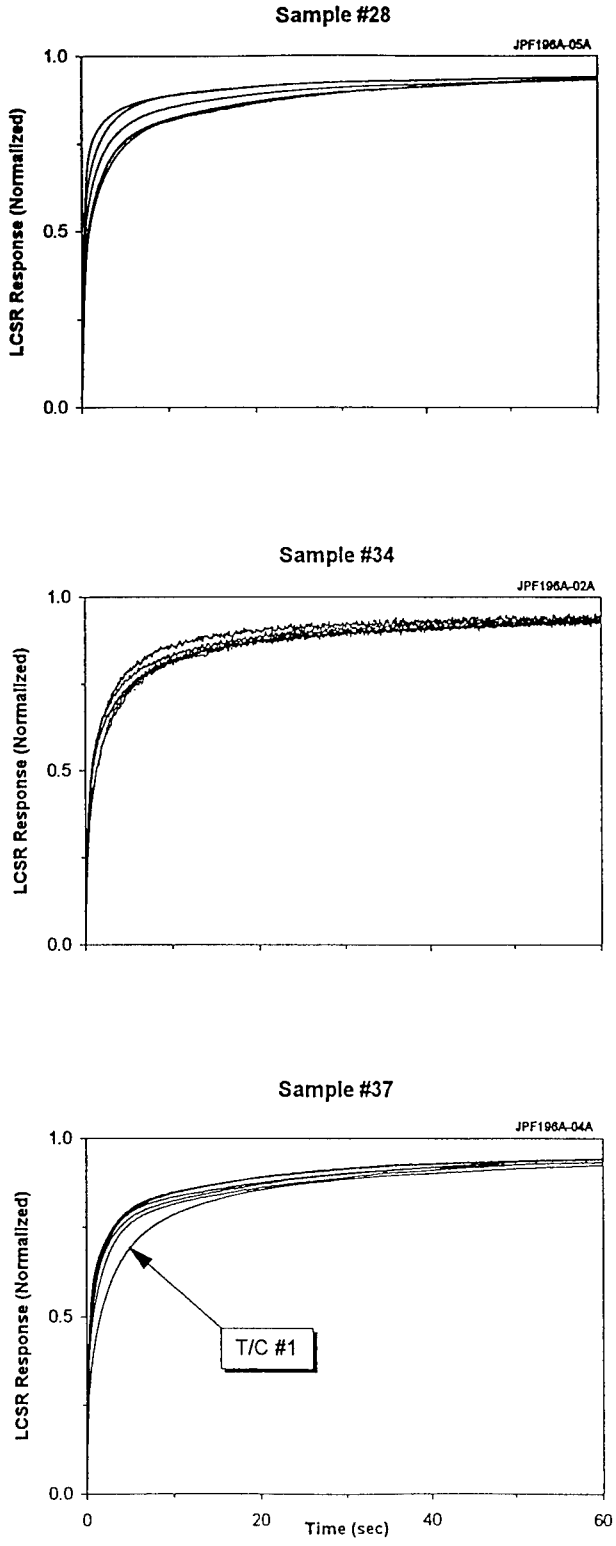

Figure 7. LCSR Transients for EMTA Gages in CFEPDM Material

TABLE 2
Listing of Post-Cured Thermocouples Tested in the Redesigned Solid Rocket Motor Liner at Marshall Space Flight Center

Item #	Gage #	Location	TC #	Material
**1	32	AFT Center 0°	1	AsNBR
2	32	AFT Center 0°	2	AsNBR
3	32	AFT Center 0°	3	AsNBR
4	32	AFT Center 0°	4	AsNBR
5	32	AFT Center 0°	5	AsNBR
6	32	AFT Center 0°	6	AsNBR
7	26	AFT Center 90°	1	5066
8	26	AFT Center 90°	2	5066
9	26	AFT Center 90°	3	5066
10	26	AFT Center 90°	4	5066
11	26	AFT Center 90°	5	5066
12	26	AFT Center 90°	6	5066
13	25	AFT Center 180°	1	5066
14	25	AFT Center 180°	2	5066
15	25	AFT Center 180°	3	5066
16	25	AFT Center 180°	4	5066
17	25	AFT Center 180°	5	5066
18	25	AFT Center 180°	6	5066
19	31	AFT Center 270°	1	AsNBR
20	31	AFT Center 270°	2	AsNBR
21	31	AFT Center 270°	3	AsNBR
22	31	AFT Center 270°	4	AsNBR
23	31	AFT Center 270°	5	AsNBR
24	31	AFT Center 270°	6	AsNBR

** Open Circuit

CONTINUED NEXT PAGE

TABLE 2 (Continued)
Listing of Post-Cured Thermocouples Tested in the Redesigned Solid Rocket Motor Liner at Marshall Space Flight Center

Item #	Gage #	Location	TC #	Material
25	27	AFT Dome CYL. 0°	1	AsNBR
26	27	AFT Dome CYL. 0°	2	AsNBR
27	27	AFT Dome CYL. 0°	3	AsNBR
28	27	AFT Dome CYL. 0°	4	AsNBR
29	27	AFT Dome CYL. 0°	5	AsNBR
30	27	AFT Dome CYL. 0°	6	AsNBR
31	22	AFT Dome CYL. 90°	1	5067
32	22	AFT Dome CYL. 90°	2	5067
33	22	AFT Dome CYL. 90°	3	5067
34	22	AFT Dome CYL. 90°	4	5067
35	22	AFT Dome CYL. 90°	5	5067
36	22	AFT Dome CYL. 90°	6	5067
37	21	AFT Dome CYL. 180°	1	5066
38	21	AFT Dome CYL. 180°	2	5066
39	21	AFT Dome CYL. 180°	3	5066
40	21	AFT Dome CYL. 180°	4	5066
41	21	AFT Dome CYL. 180°	5	5066
42	21	AFT Dome CYL. 180°	6	5066
43	37	AFT Dome CYL. 270°	1	CFEPDM
44	37	AFT Dome CYL. 270°	2	CFEPDM
45	37	AFT Dome CYL. 270°	3	CFEPDM
46	37	AFT Dome CYL. 270°	4	CFEPDM
47	37	AFT Dome CYL. 270°	5	CFEPDM
48	37	AFT Dome CYL. 270°	6	CFEPDM

CONTINUED NEXT PAGE

TABLE 2 (Continued)
Listing of Post-Cured Thermocouples Tested In the Redesigned Solid Rocket Motor Liner at Marshall Space Flight Center

Item #	Gage #	Location	TC #	Material
49	30	FWD Ramp 90°	1	5066
50	30	FWD Ramp 90°	2	5066
**51	30	FWD Ramp 90°	3	5066
52	30	FWD Ramp 90°	4	5066
53	30	FWD Ramp 90°	5	5066
**54	30	FWD Ramp 90°	6	5066
55	29	FWD Ramp 270°	1	5066
56	29	FWD Ramp 270°	2	5066
57	29	FWD Ramp 270°	3	5066
58	29	FWD Ramp 270°	4	5066
59	29	FWD Ramp 270°	5	5066
60	29	FWD Ramp 270°	6	5066
61	24	AFT Dome 0°	1	AsNBR
62	24	AFT Dome 0°	2	AsNBR
63	24	AFT Dome 0°	3	AsNBR
64	24	AFT Dome 0°	4	AsNBR
65	24	AFT Dome 0°	5	AsNBR
66	24	AFT Dome 0°	6	AsNBR
67	23	AFT Dome 90°	1	5067
68	23	AFT Dome 90°	2	5067
69	23	AFT Dome 90°	3	5067
70	23	AFT Dome 90°	4	5067
71	23	AFT Dome 90°	5	5067
72	23	AFT Dome 90°	6	5067

CONTINUED NEXT PAGE

** Open Circuit

TABLE 2 (Continued) Listing of Post-Cured Thermocouples Tested In the Redesigned Solid Rocket Motor Liner at Marshall Space Flight Center				
Item #	**Gage #**	**Location**	**TC #**	**Material**
73	20	AFT Dome 180°	1	5066
74	20	AFT Dome 180°	2	5066
75	20	AFT Dome 180°	3	5066
76	20	AFT Dome 180°	4	5066
77	20	AFT Dome 180°	5	5066
78	20	AFT Dome 180°	6	5066
79	34	AFT Dome 270°	1	CFEPDM
80	34	AFT Dome 270°	2	CFEPDM
81	34	AFT Dome 270°	3	CFEPDM
* 82	34	AFT Dome 270°	4	CFEPDM
83	34	AFT Dome 270°	5	CFEPDM
84	34	AFT Dome 270°	6	CFEPDM

* Low Insulation Resistance

AFT Center - Post Cure

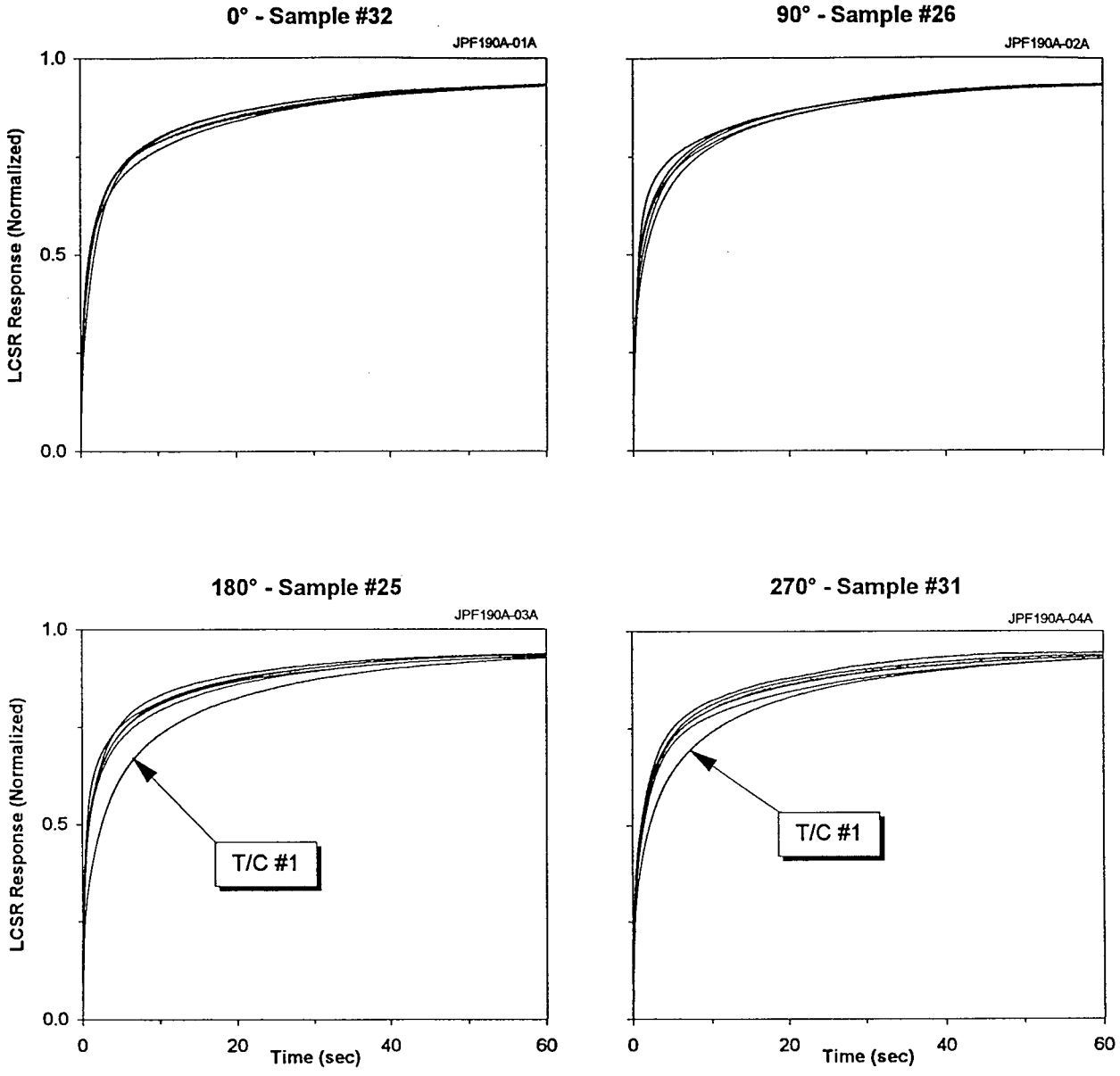

Figure 8. LCSR Transients for EMTA Gages at AFT Center Position in Blast Tube

AFT Dome CYL. - Post Cure

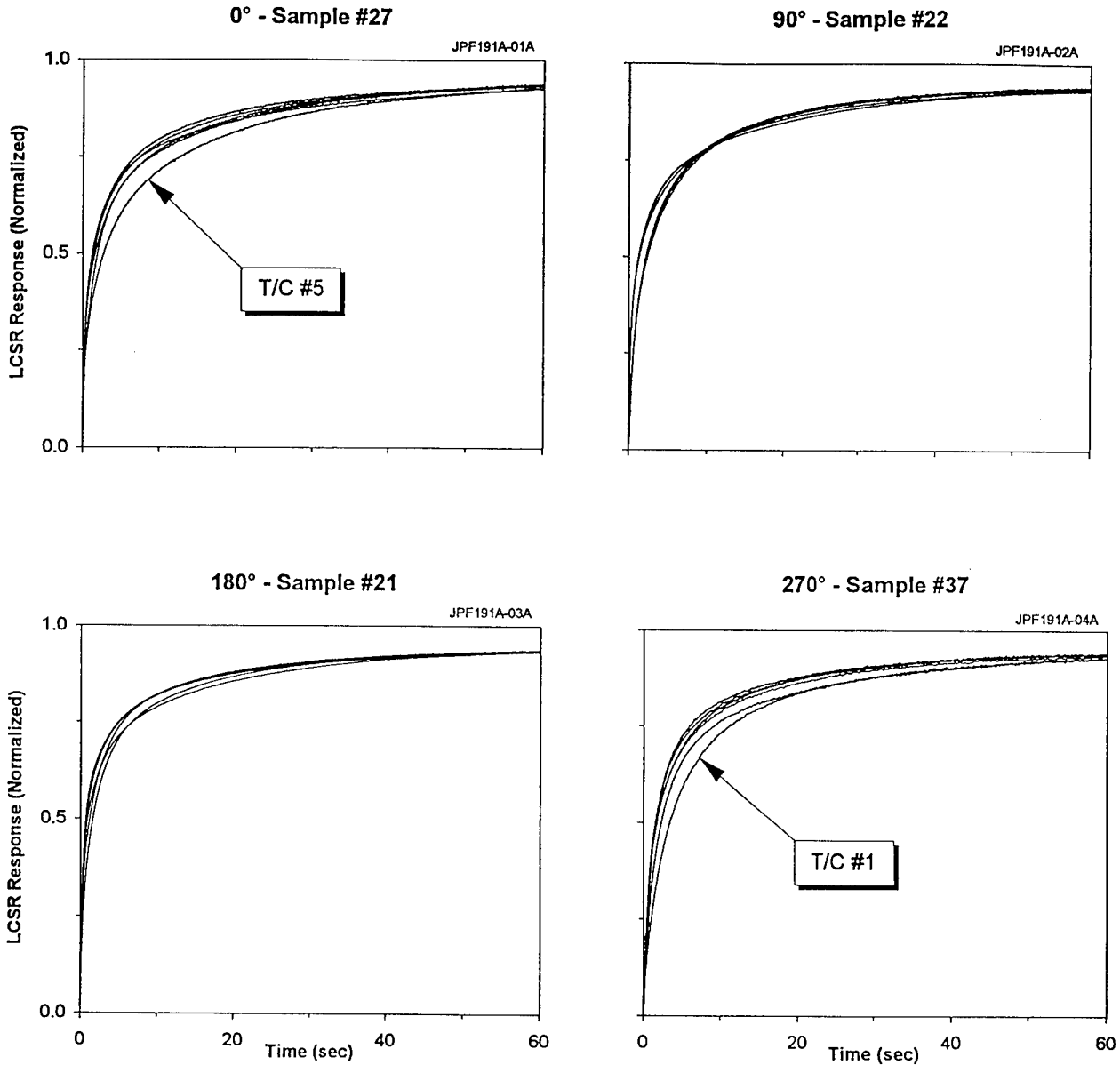

Figure 9. LCSR Transients for EMTA Gages at AFT Dome Cyl. Position in Blast Tube

FWD Ramp - Post Cure

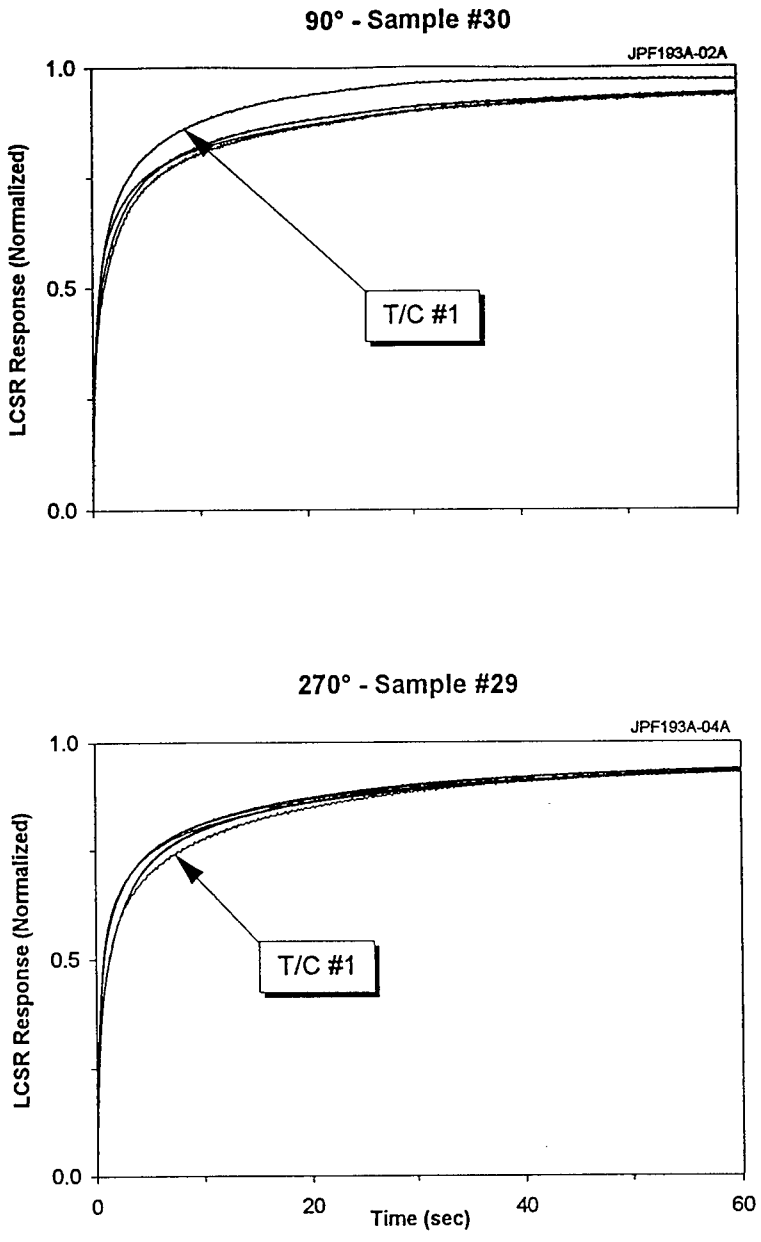

Figure 10. LCSR Transients for EMTA Gages at FWD Ramp Position in Blast Tube

AFT Dome - Post Cure

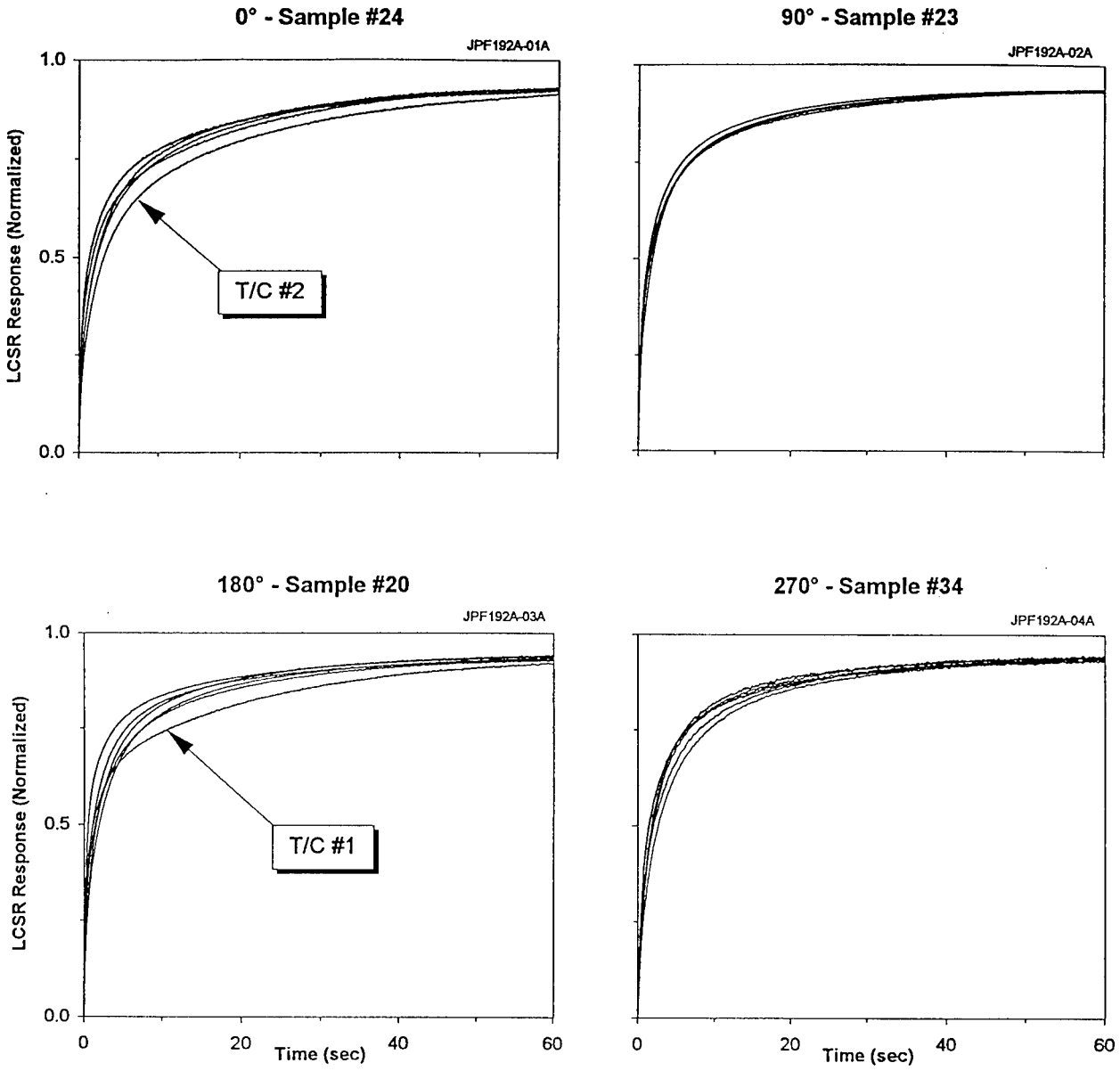

Figure 11. LCSR Transients for EMTA Gages at AFT Dome Position in Blast Tube

location was not cured into the liner. It was replaced with gage #37. This change was implemented because of the low I/R reading detected during the pre-cure tests for thermocouple (tag number #2) in gage #28. Figures 12 to 21 show comparisons between the pre-cure and post-cure LCSR transients grouped according to the gage location in the blast tube. As seen in these figures, most of the thermocouples had a slightly slower response after curing compared to the pre-cure tests. In two locations (Aft Center 270° and the Aft Dome Cyl 180°), the post-cure transients were faster than the pre-cure transients.

4. CONCLUSIONS

A series of LCSR tests were performed on several thermocouples embedded in the Redesigned Solid Rocket Motor blast tube liner. The purpose of the tests was to evaluate the installation integrity of the thermocouples. This testing consisted of pre and post-curing tests. During the pre-curing tests, eleven Erosion Monitoring Thermocouple Array (EMTA) gages, each containing six thermocouples, were tested. The pre-cure testing revealed low insulation resistances for thermocouple #2 in gage 28 and thermocouple #4 in gage 40. As a result, both gage #28 and gage #40 were not cured into the blast tube liner. Post-curing tests consisted of the ten of the pre-cured EMTA gages and four additional gages for a total of 84 thermocouples. Post-cure testing also revealed low insulation resistance for thermocouple #1 in gage 32. Open circuits were identified during the tests in thermocouple #1 in gage 32, thermocouple #3 in gage 30 and thermocouple #6 in gage 30 during the post-cure testing. Thermocouple #1 (face thermocouple) in each of the assemblies generally had a slight response difference with respect to the other thermocouples in the gage. The response differences occurred in seven of the eleven gages in the pre-cure tests and in six of the fourteen gages in the post-cure LCSR testing. Overall, there was no indications of any significant change in response that could be attributed to the curing process.

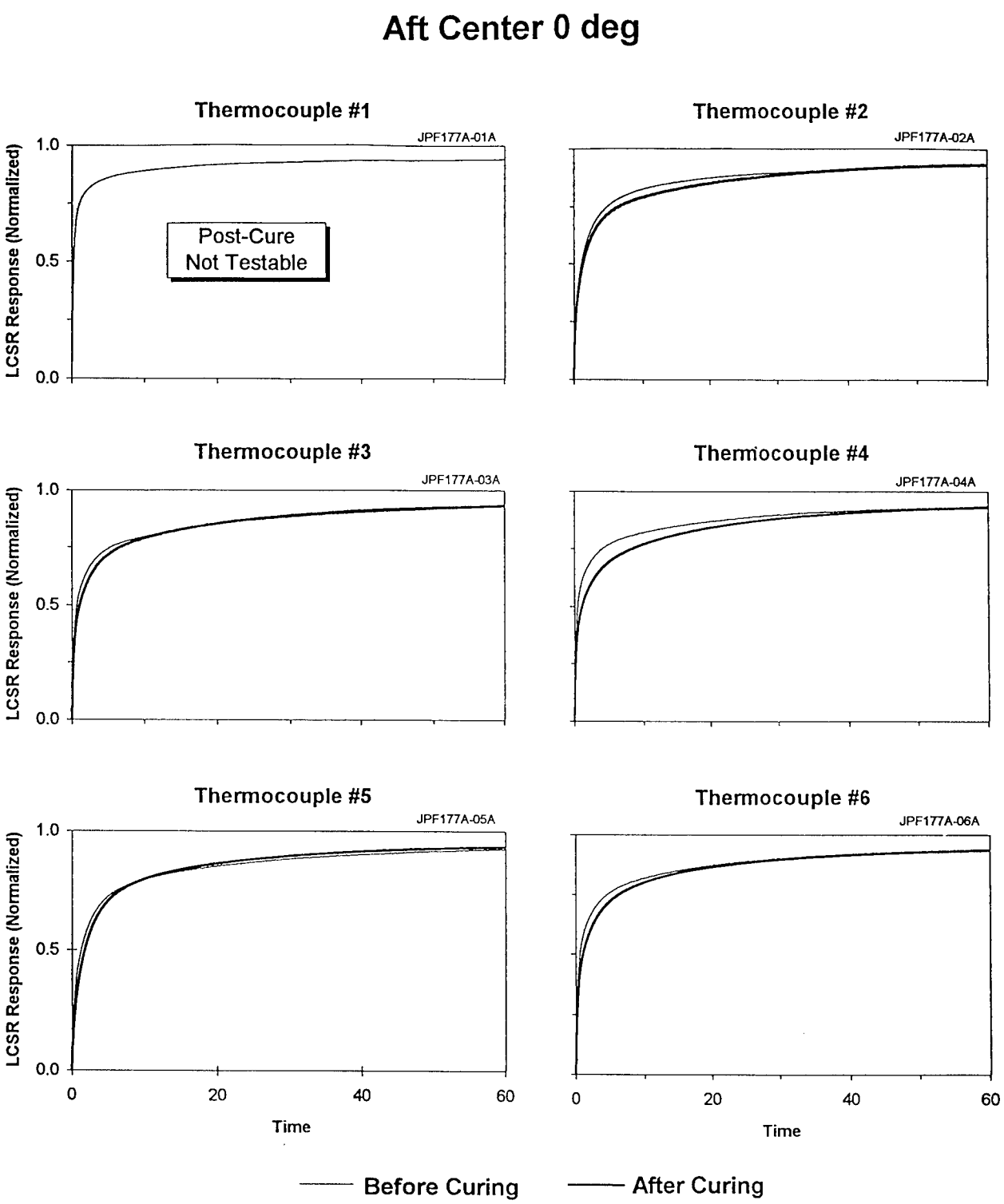

Figure 12. Before and After Curing Comparisons for Gage #32

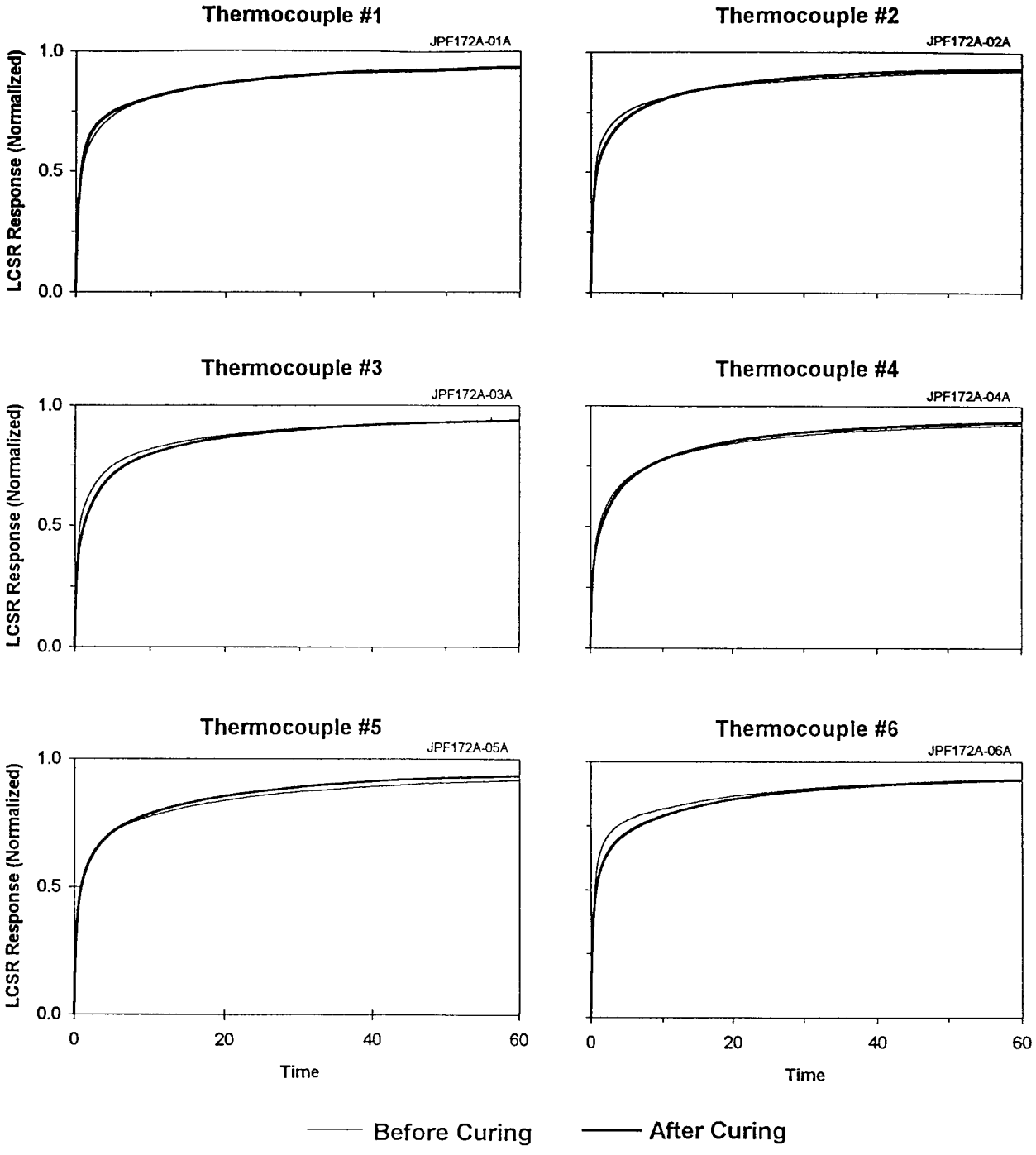

Figure 13. Before and After Curing Comparisons for Gage #26

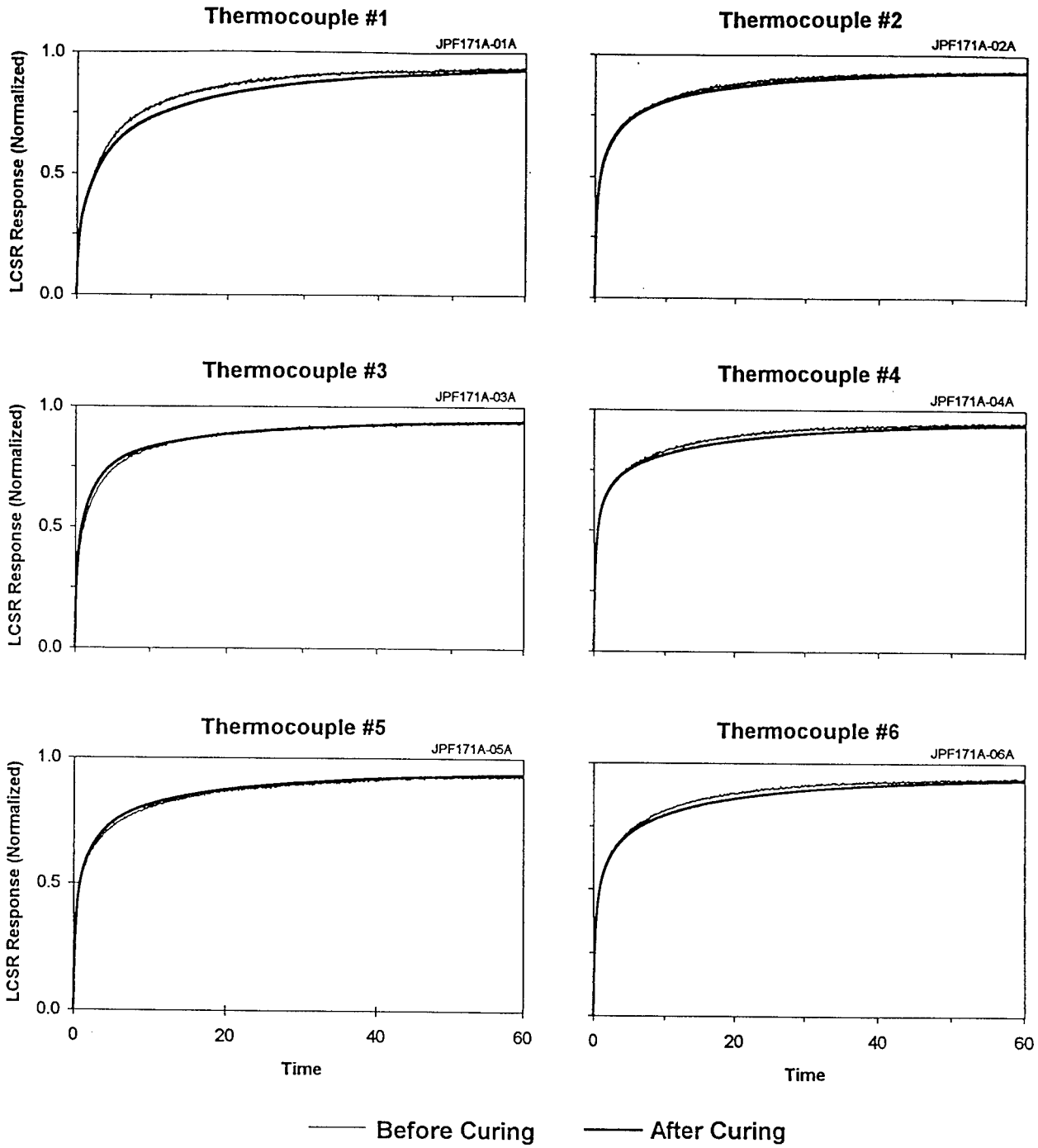

Figure 14. Before and After Curing Comparisons for Gage #25

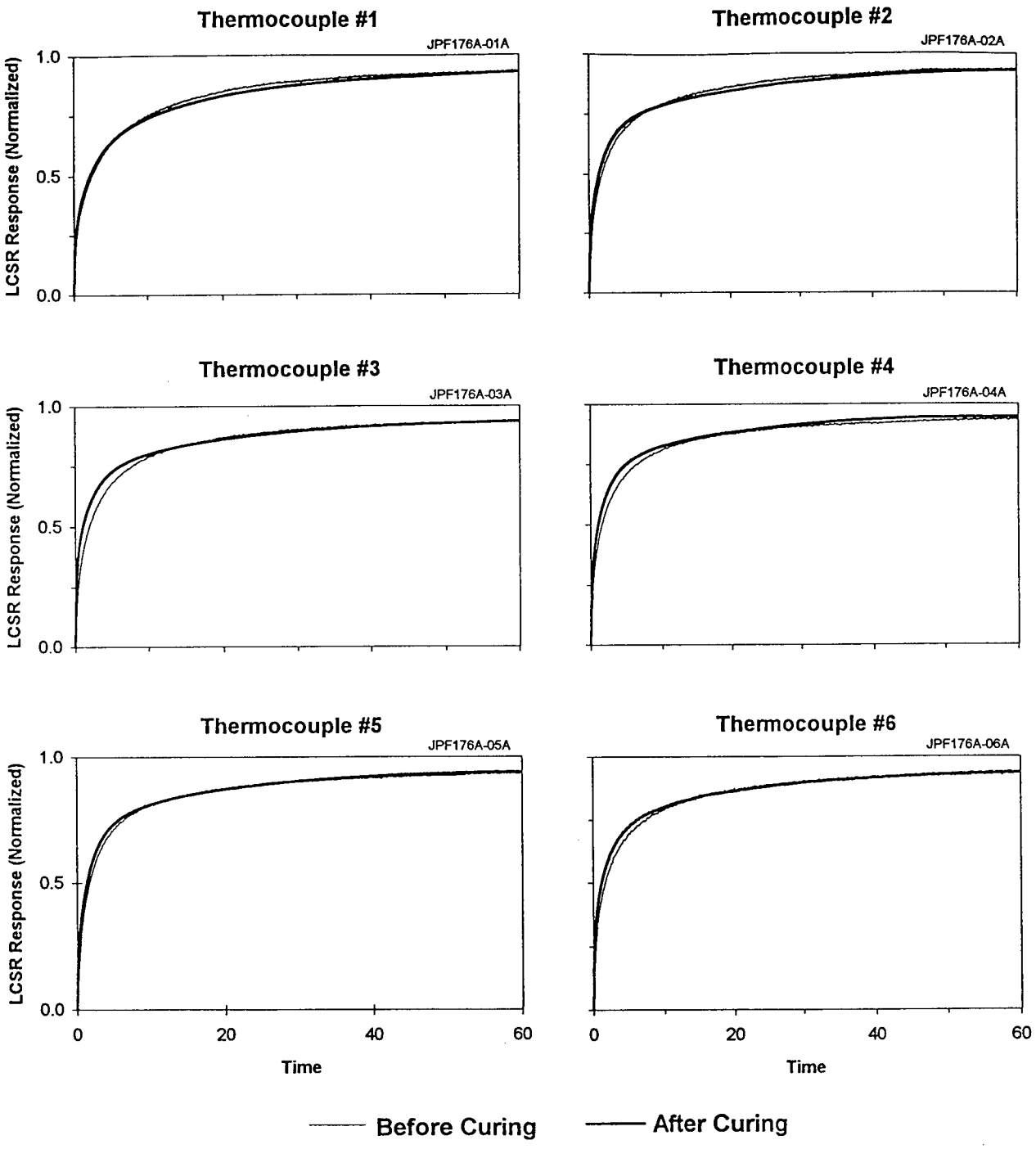

Figure 15. Before and After Curing Comparisons for Gage #31

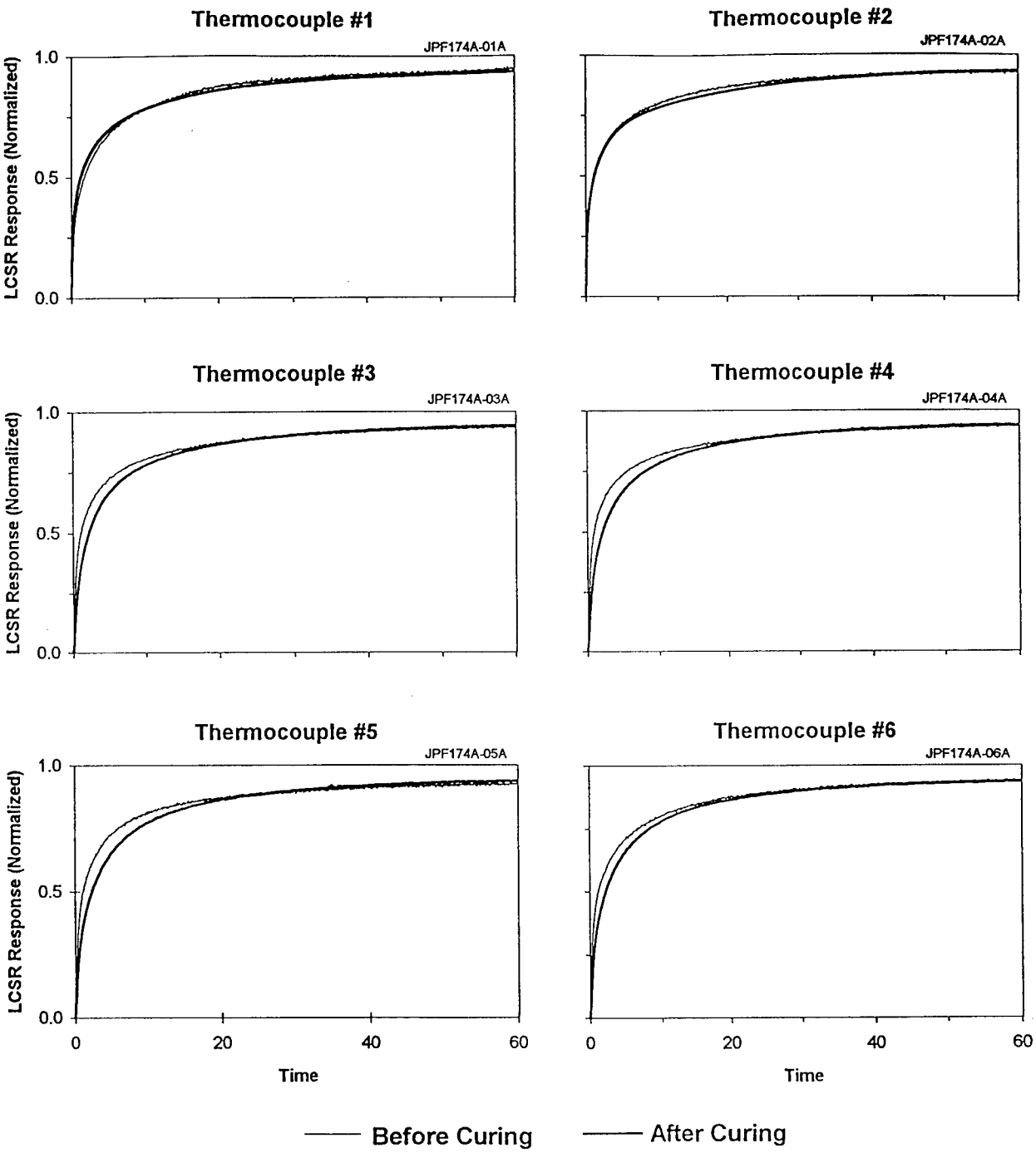

Figure 16. Before and After Curing Comparisons for Gage #22

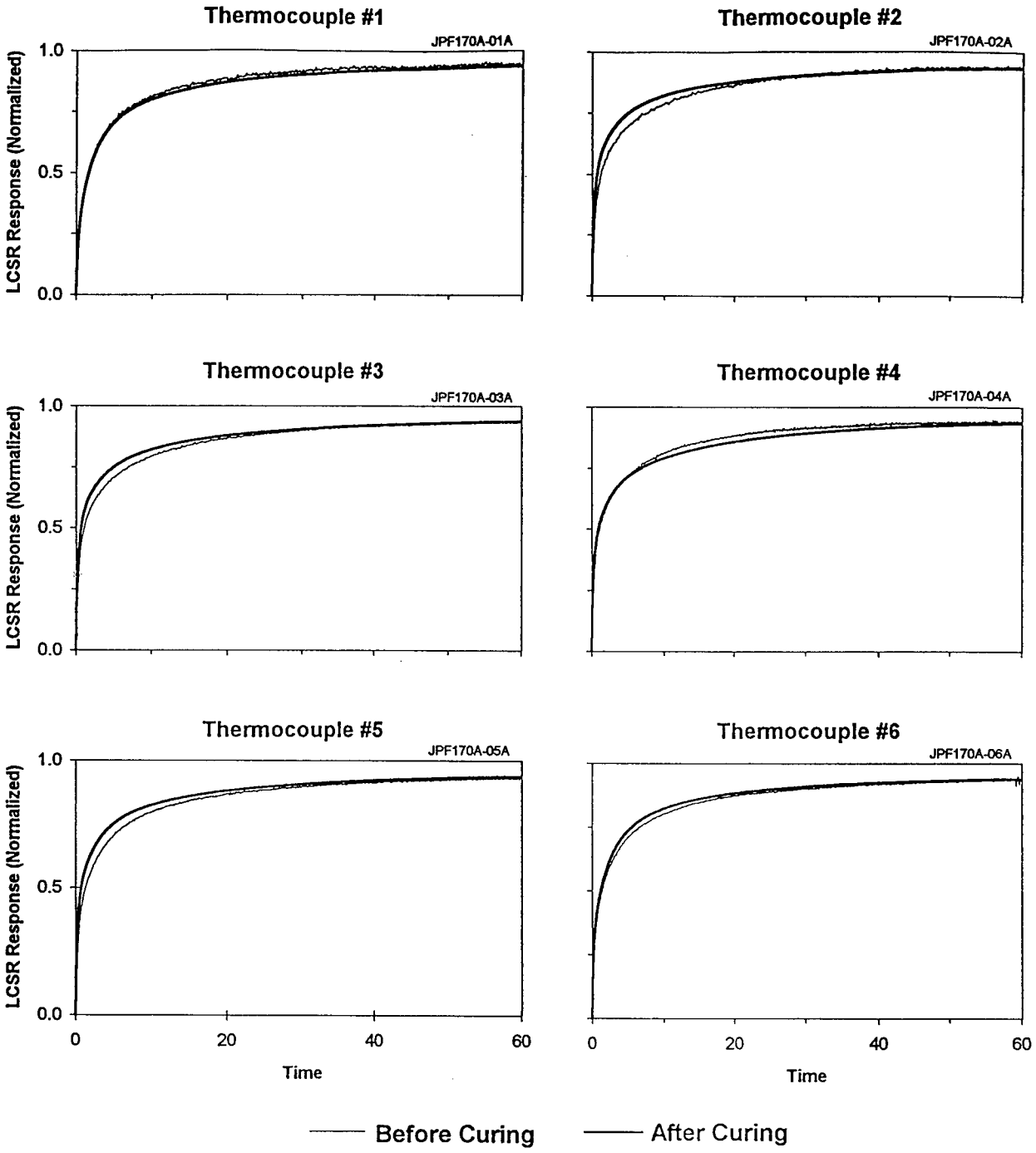

Figure 17. Before and After Curing Comparisons for Gage #21

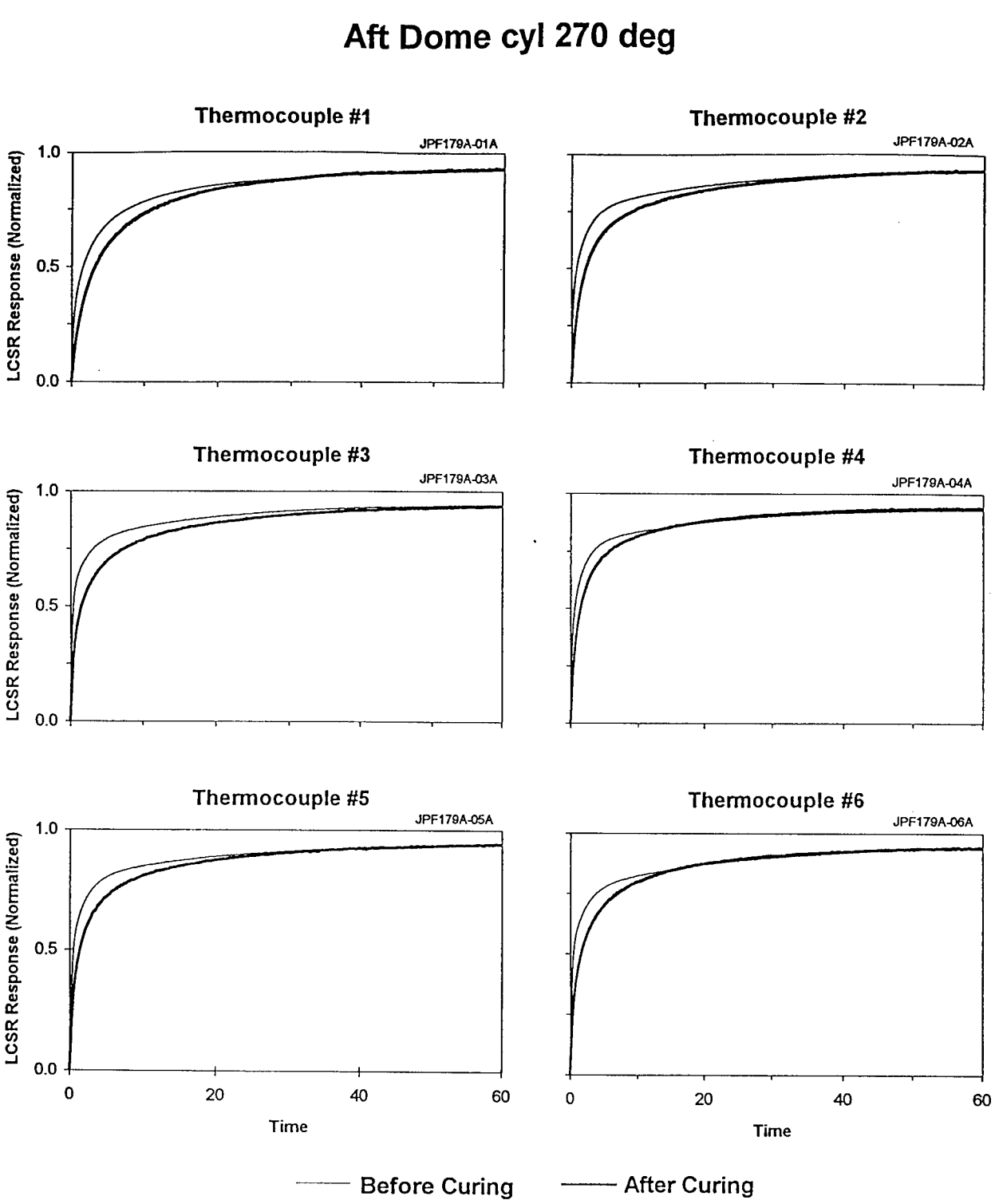

Figure 18. Before and After Curing Comparisons for Gage #37

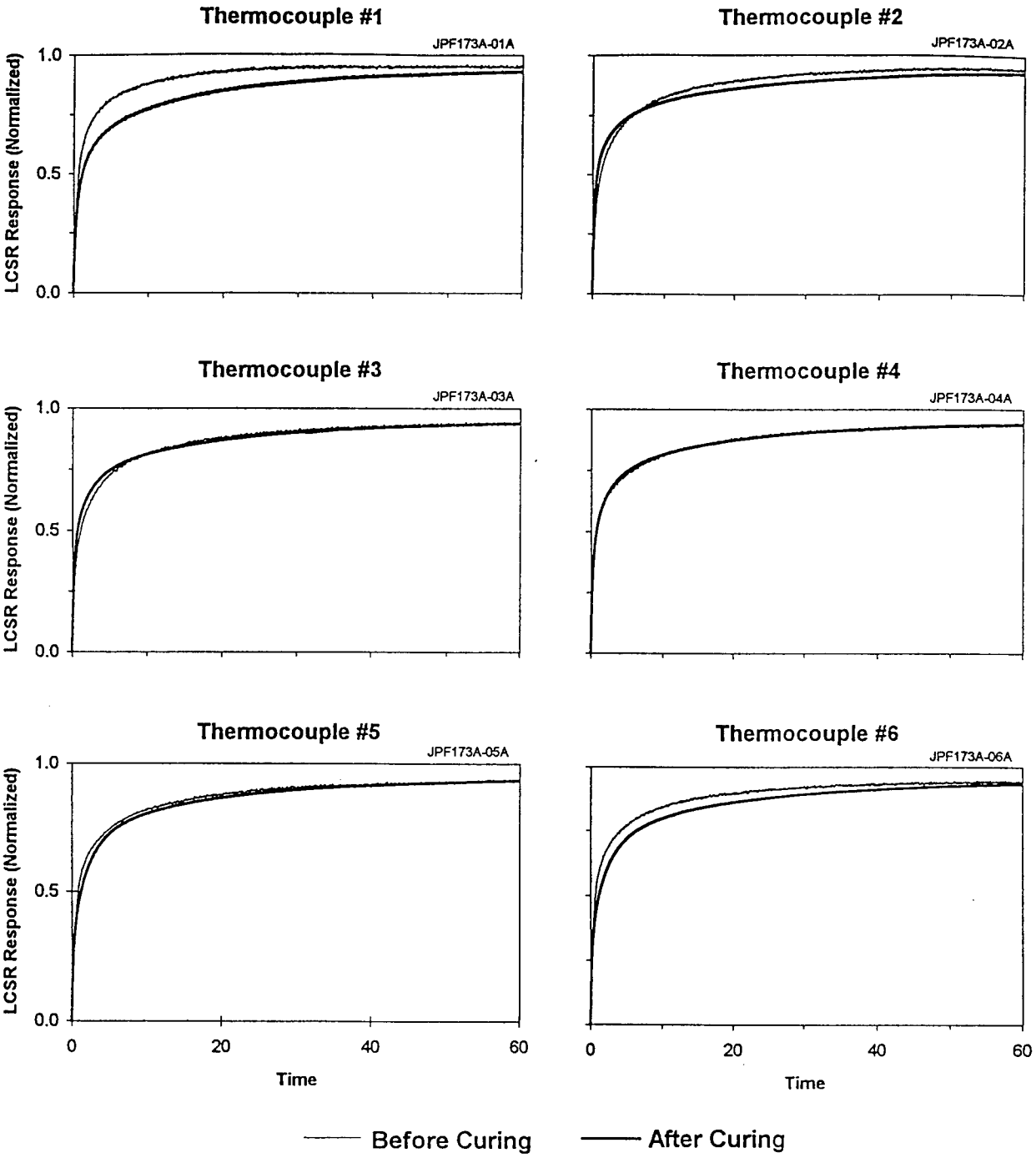

Figure 19. Before and After Comparisons for Gage #29

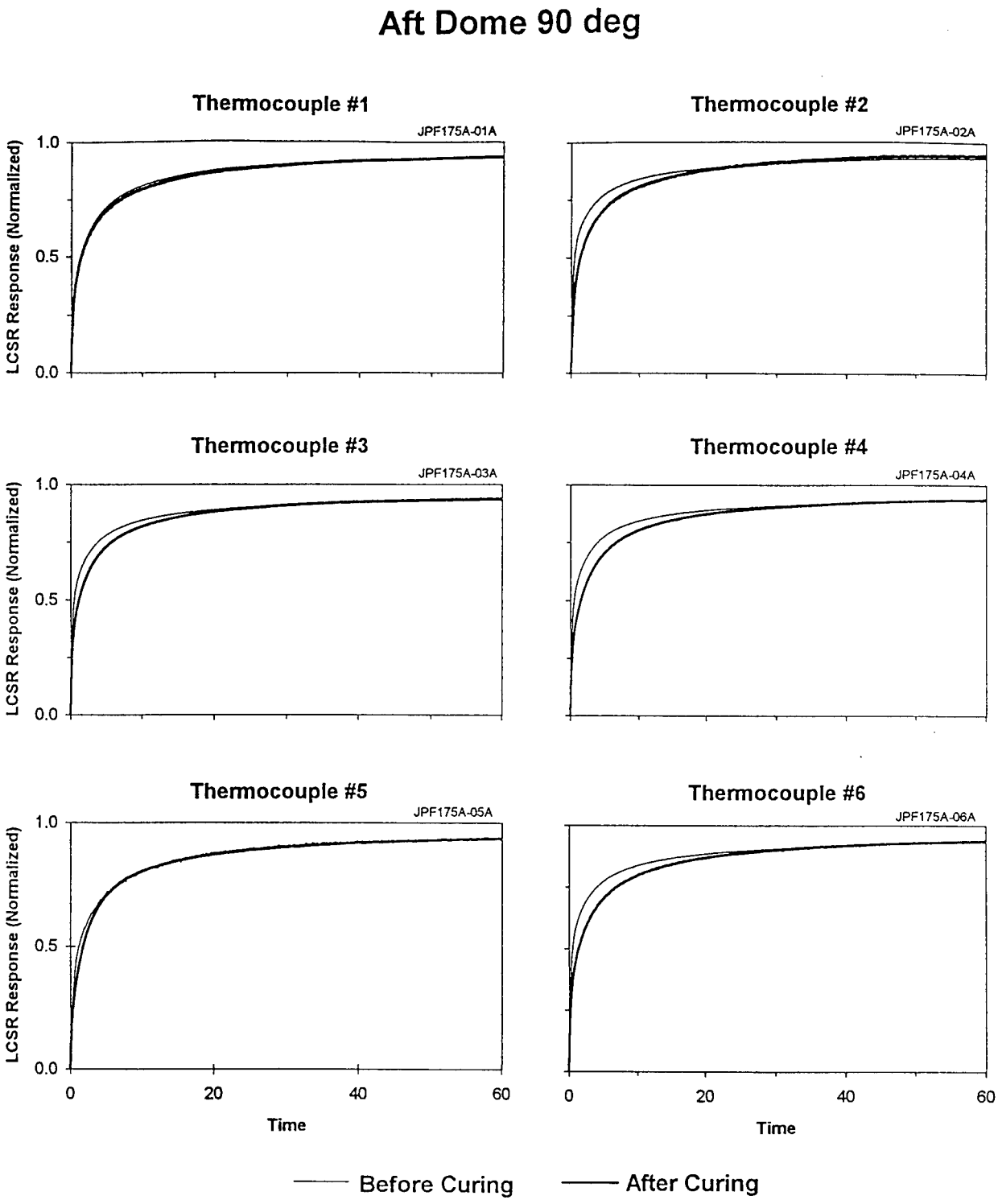

Figure 20. Before and After Comparisons for Gage #23

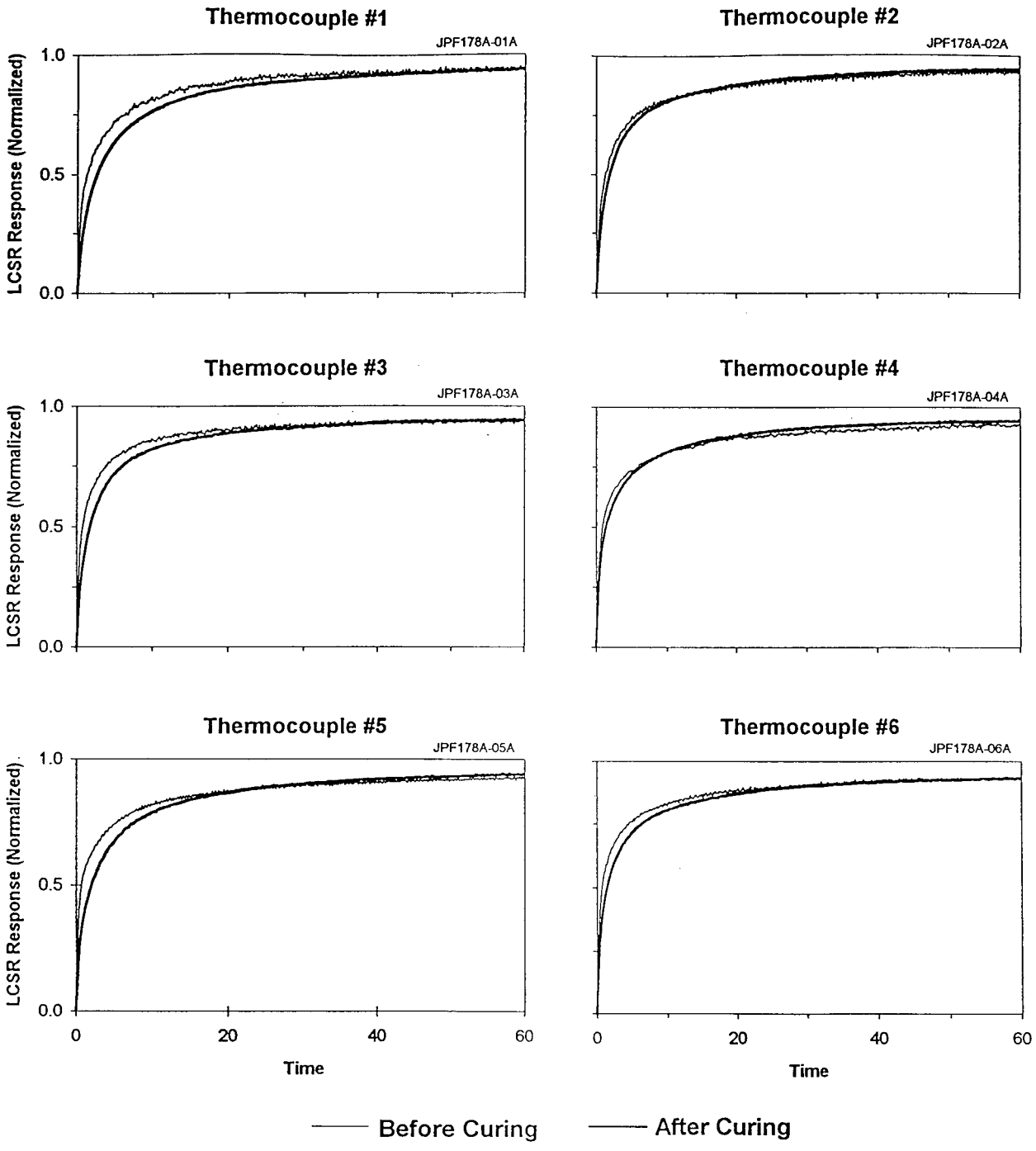

Figure 21. Before and After Curing Comparisons for Gage #34

APPENDIX F

SURVEY OF AEROSPACE INDUSTRY ON ADHESIVES AND BONDING PRACTICES

SURVEY RESULTS

This appendix provides a summary of an informal survey of the aerospace industry to identify sensor adhesives and bonding practices.

A listing of those who responded to the survey are given in Table F.1, followed by a summary of the results of the survey in Table F.2.

TABLE F.1

SURVEY PARTICIPANTS
Boeing Aircraft Jim Wallace 206-655-2972
Cotronics Corp. Barry Reznik, Pres 718-646-7996
Entran Devices Bob Levy 1-800-635-0650
HITEC (Mass) Douglas A. Unkel President (508) 692-4793
Micro-Measurements Group (SC) Tom Rummage 205-830-2832
NASA Lewis Research Ctr (CL) Dr. Jih Lei 216-433-3922
NASA - Marshall Bob Burns 205-544-2556
Thiokol/Huntsville Lon Stevens 205-544-6146
Thiokol/Utah John Shipley 801-863-6945
University of TN Scott Liter 974-6751

TABLE F.2

SUMMARY OF SURVEY RESULTS				
Question 1	**Questions 2**	**Question 3**	**Question 4**	**Question 5**
What type of adhesive bonding is performed in your company?	**What commercially available adhesives does your company use?**	**Do you follow a specific adhesive bonding procedure? If yes, are there special or unique procedures you use?**	**Have you encountered any problems with adhesive bonding in the past? If yes, please describe the situation.**	**Under your particular bonding conditions, what adhesive works best (please describe)?**
None	Market various adhesives including ceramic adhesives	Yes. 1) Roughen surface 2) Mix and apply adhesive 3) Embed Sensors 4) Tape leads to hold in place 5) Apply excess material to fully coat sensors 6) Cure if required	Yes Vibration in engine components cause bonds to degrade	903 Green works best in aircraft engines and is used by Pratt Whitney in engine components. Easy pre-mixed.
Mainly bonding of strain gages to various aircraft structural elements	We have experimented with most and find Omega's adhesive to work well	Yes Surface preparation is very important. Acetone is a good substance for surface preparation. It is very important to apply the initial layer quite thin, attach the sensor, and apply further adhesive on top of the sensor.	Not Many Most of our applications are moderate temperature, low vibrations environments. A special task team of 5 individuals does all Boeing's bonding to maintain consistency in the bonding procedure	Under ambient and cooler temperature, Omega 200 Epoxy adhesive is very good. It doesn't get brittle in subzero temperatures reached as the aircraft gains altitude. High temperature adhesives become brittle at lower temps. Easy to mix air tight packages.
Stain gages and accelerometers	Depends on the application. Sometimes Omega adhesives or micro-measurements and M-Bond series. Depends on the sensor and conditions in which it will be used	Yes In-house procedures are followed to allow for proper surface preparation and cleaning prior to bonding and a bonding procedure specifies curing rates, etc.	Yes Most bonding problems with Entran gages have to do with improper surface preparation or poor bonding technique of the small size gages.	M-Bond series
Strain gages (high temp) Thermocouples (turbine applications)	Rokide sprayed aluminum oxide with a nickel aluminide base coat	Yes All bonding is performed by HITEC with in-house procedure	Yes Rokide is very hard to spray to a consistent thickness and if the thickness is not thick enough or too thick, it can cause problems in the output. These gages are not as easy to bond as the foil type gages	Rokide ($A1_2 0_3$)

TABLE F.2 (cont.)

Question 1	Questions 2	Question 3	Question 4	Question 5
What type of adhesive bonding is performed in your company?	**What commercially available adhesives does your company use?**	**Do you follow a specific adhesive bonding procedure? If yes, are there special or unique procedures you use?**	**Have you encountered any problems with adhesive bonding in the past? If yes, please describe the situation.**	**Under your particular bonding conditions, what adhesive works best (please describe)?**
Strain Gauges and Transducers	1) MBond-200/Gen Purpose 2) AE-10-resist moisture 3) AE-15 - Similar to AE-10 and used in critical Applications 4) 610 - Wide temp range 5) 600 - similar to 610 but faster reacting 6) 43-B-temp & moisture & chemical resistant Special Purpose Adhesives 1) GA-2 - Rough Surface 2) GA-61 - Similar to GA-2 bur more viscows 3) GA-100 - Ceramic cement used with special design high temp strain gages 4) A-12 - high elongation adhesive 5) 300 - Polyester adhesive used when low temp curing is required 6) 450 - high performance epoxy for high-temp transducer applications	Yes Each epoxy has a special procedure on how to apply cement, each application is different and surface prep and current type will change	Unbonding 1. high elongation which breaks bond 2. pour surface preparation 3. impact loading	Yes Each epoxy has a special procedure on how to apply cement, each application is different and surface prep and current type will change
Bond T/Cs using ceramic adhesives and pastes	ZYP coatings, ORPAC, and Sauereisen #10	Yes Inject cements with hypodermic needles	Yes Adhesive bonds fail at elevated heating rates and temperatures	Like RS1000 because it is the easiest and most convenient to use

TABLE F.2 (cont.)

Question 1	Question 2	Question 3	Question 4	Question 5
What type of adhesive bonding is performed in your company?	**What commercially available adhesives does your company use on the market?**	**Do you follow a specific adhesive bonding procedure? If yes, are there special or unique procedures you use?**	**Have you encountered any problems with adhesive bonding in the past? If yes, please describe the situation.**	**Under your particular bonding conditions, what adhesive works best (describe)?**
Bond T/Cs into carbon phenolic	EA934 Havoflex 117A	Yes Develop procedures based on manufacturers specifications. Thin down adhesive with solvents, use vacuum technology and accelerate cure with very high temps.	Yes Need to avoid voids and air gaps	Without question for very high temps, the Havoflex has superior thermal and electrical properties. Use it to bond and protect components in high temp environments in Hybrid rocket engines
T/C, Pressure Sensors, and Semi-conductor strain gauges	Strain gages: Micro-Measurements M-Bond 610 and 200 T/Cs: HISOL EA 945, 934	Flow manufacturer's specs / outlined by engineering Seldom go out on your own	Yes Contamination of silicones, problems in curing, and using old batches of adhesive	M-Bond 610 for strain gages is preferred. M-Bond 200 does not always stick to surface.
Strain gages, PRTS, and thermocouples are bonded to various SSME locations	Silver-filled epoxy: Eccobond 56C and Catalyst 9 by Emnerson and Cummings Polyeurothane - Crest 810	Yes Rosemont bonding procedure using acetone surface preparation and fiberglass backing soaked with polyeurothane coating	Yes PRTs become debonded and unable to detect this until the coating is removed	Eccobond 56C
High Temp Sensors: Strain gages, thermocouples, heat flux sensors	Very temperature dependent	Low Temp - Mfr's specs High Temp - Unique Techniques: French Braid - (strain gages) Plasma Spray - Aluminum Sputtering - Very High Temp Application	Temperature compatibility - sensor peels off substrate	Varies with temperature. Cannot be specific.

APPENDIX G

BONDING TECHNIQUES FOR RTDs AND STRAIN GAGES

APPENDIX G

1. BONDING TECHNIQUES FOR SURFACE MOUNTED RTDs AND STRAIN GAGES

1.1 RTD Bonding

A. Required Material

1) Adhesive (or cement) conducive to bonding and sensor operational environment
2) Adhesive tape with high electrical and thermal resistance
3) Polyurethane adhesive coating (where applicable)
4) Glass woven fabric (where applicable)
5) Acetone,denatured alcohol, or isopropyl alcohol
6) Protective rubber gloves
7) Lint-free cloth wipes
8) Commercial heat gun (for accelerating cures)
9) Glass containers and mixing spatula
10) Standard medicine dropper
11) Steel wool or other abrasive metal polish
12) Sand paper of appropriate grit for wet sanding
13) Plastic film
14) LCSR/SHI equipment
15) Volt/Ohm meter and megohmmeter

B. Application Environment

The temperature of the bonding environment should be in the range of 50-150 degrees F. All mounting surfaces should be entirely free of moisture during the bonding procedure.

C. Preliminary Test

Using a Volt/Ohm meter, measure the resistance between PRT lead wires. The readings should be within manufacturer resistance specifications. Test the insulation resistance (IR) of the PRT to be sure the IR value is within manufacturers specifications. Reject gages that do not adhere to these specifications.

D. Preliminary Preparation

Clean (polish) mounting area to bright finish with steel wool. Wearing gloves, wet sand the mounting area. Wipe bonding area, unidirectionally, with lint-free cloths that have been dampened with Acetone until there is no evidence of stain on the cloth. Flush the bonding area and rinse the PRT head and sheath with Acetone or equivalent.

E. Adhesive Preparation

Using a clean non-porous flat surface and clean mixing spatula, thoroughly mix epoxy adhesive or cement while following specified manufacturers mixing instructions or those instructions that have proven effective in the past. Care must be taken to mix the materials as specified and to note the effective product usage date and pot life of each material.

F. Mounting

Gently form the PRT sheath wire to fit the contours of the part it is to be mounted upon. This fit will provide a relaxed contact between the sensor and the mounting surface. Do not bend the sheath wire within .25" of the PRT sensing head. Position the sensor over the center of the prepared bonding area and tape the sensor wires with adhesive tape. Thoroughly wet (with prepared adhesive or cement) the sensing surface of the PRT and the corresponding mounting surface. The coating on each should be approximately .006"-.020" in thickness. Gently press the sensor end to seat it firmly into place and remove all excess epoxy or cement from the edges of the sensor with a mixing spatula. A small amount of excess is acceptable. Apply a plastic film cover over the sensor to hold it in place and ensure a free-release surface and moisture barrier. Allow time for the cement or epoxy to cure according to manufacturer specifications. Accelerated cure times are acceptable when following manufacturer schedules.

G. Polyurethane Application

This process must be carried out over a temperature range of 50-150 degrees F in a moisture free environment. Clean the cured epoxy (cement) area including a 1" margin around the sensor using Acetone and a cloth soaked in Acetone. Steel wool can be used to restore the surface to a bright finish. Allow 15 minutes (minimum) to dry. Examine the bonding area for any visual evidence of sensor debonding. Apply the LCSR and SHI tests as a nonvisual means of detecting bonding quality. Reject sensors that fail either visual, LCSR, or SHI test criteria for proper bonding.

Examine the components that make up the polyurethane adhesive for inconsistencies as specified by the manufacturer. Mix polyurethane per manufacturer specifications in a well ventilated area and examine mixture for proper consistency. Apply a thin, even coat of polyurethane over the sensor and mounting area. Be sure sensor is fully covered. Place a small section of glass weave fabric over the polyurethane coated surfaces. Be sure the glass weave fabric becomes totally saturated. Remove all folds and air pockets from the glass fabric so it conforms to the sensor surface. Remove all excess polyurethane. Allow the polyurethane to cure according to manufacturer's specifications. Visually inspect for debonding. Apply the LCSR/SHI test to determine concealed debonding that is not detectable by visual means. Reject any sensor bond that can be detected visually or by LCSR/SHI tests.

All hazardous materials and processes should be handled within the safety provisions set forth by the manufacturer and the particular safety specifications of the user facilities. Questions regarding safety matters should be referred to the manufacturer of the material in question. Before work begins, remove all existing strain gages on the test component.

2. STRAIN GAGE BONDING

A. Required Material

1) Adhesive (or cement) conducive to bonding and sensor operational environment
2) Adhesive tape with high electrical and thermal resistance
3) 180 grit open-meshed non-clogging sanding fabric
4) Deionized water
5) Acetone,denatured alcohol, or isopropyl alcohol
6) Protective gloves
7) Lint-free cloth solvent wipes
8) Commercial heat gun (for accelerating cures)
9) Surface conditioner
10) Cotton-tipped applicators
11) Clean tissue or gauze
12) Neutralizer
13) Mylar tape or polyamide tape
14) I.D. tags
15) Teflon sheet
16) 3/32" thick silicone foam rubber pad
17) Clamp
18) Heat shrink mylar tape
19) Borescope (if available)
20) Volt/Ohm meter and megohmmeter
21) Overlay gage coating
22) LCSR/SHI equipment

B. Application Environment

The temperature of the bonding environment should be in the range of 50-150 degrees F. All mounting surfaces should be entirely free of moisture during the bonding procedure.

C. Preliminary Preparation

Wipe bonding surface with acetone, denatured alcohol, or isopropyl alcohol to remove surface contamination. The solvent wipe shall include the area approximately 4" to 6" on all sides of the installation area. Air dry for 15 minutes at ambient conditions. Do not expose solvent or vapors to open flame or heat

source. The bonding area shall be abraded in a cross-hatched fashion with the specified sanding fabric in order to remove materials on the bonding area that would prevent good bonding. Pitting, protrusions, scratches and other such imperfections must be removed by grinding, filing or other suitable methods. Spray the bonding area with deionized water to obtain a completely wetted surface. Apply surface conditioner (where applicable) and scrub with cotton-tipped applicators until a clean tip is no longer discolored by scrubbing. Keep the surface constantly wet with the conditioner until cleaning is completed. Wipe the cleaned area with a single unidirectional stroke of a clean tissue or gauze. With an additional clean tissue, make a single stroke in the opposite direction. Never wipe back and forth. Apply a surface prep neutralizer to a tissue until completed saturated. Apply the neutralizer to the bonding area and scrub with cotton-tipped applicators. Wipe the area dry with single unidirectional tissue strokes.

D. Adhesive Preparation/Application

Mix the adhesive according to manufacturer suggested procedures. Mixing of a spare amount of adhesive is recommended to prevent unexpected delays during strain gage installation.

Bonding of strain gages and terminal strips should take place within 45 minutes after surface preparation. Place the strain gage on high temperature mylar tape or polyamide tape. Temporary ID tags should be applied to gage lead wires. Coat the gage and terminal mounting surface with a thin layer of adhesive. Do not allow the adhesive applicator to touch the tape mastic which holds the preassembled gage in place. Let the adhesive air dry 10 to 15 minutes. Position the gage/terminal until it is tacked down. Use additional mylar tape, if necessary, with tape/adhesive contact kept to a minimum. Apply a thin piece of teflon

followed by a 3/32" thick silicone foam rubber pad over the gage/terminal area. Apply sufficient pressure using a clamp to ensure an intimate cure between the strain gage and the substrate. Wrap with heat shrink mylar tape and apply a heat gun for shrinking. Cure adhesive in accordance with manufacturer's curing schedules.

E. Gage/Bond Inspection

Visually inspect the bonded gage. 10X or 40X magnification should be used if available. Adhesive must be evident along the entire periphery of the gage. Apply the LCSR/SHI test to ensure that no air bubbles, voids, or contaminates are present in regions where they cannot be visually detected. A borescope can also be used for verification (if one is available). Using a volt/ohm meter and a megohmmeter, verify that the resistance between each leg as well as the insulation resistance are within manufacturer's specifications.

F. Overcoat Application

Apply two coats of strain gage coating using a fine brush. The first coat shall be a thin, brush applied layer over the bonded gage/terminal assemblies. The overcoat should extend around the gage/terminal periphery. Allow two hours minimum for air drying of the first coat. The second coat should be applied evenly with a brush, fully covering the area previously coated. No visible voids should be present.

TTB – OPERATION INSTRUCTIONS	TECH	INSPECTION	
		CONT.	NASA

TTB–SOP–I–006
STRAIN GAGE INSTALLATION

DATE: MAY 1, 1992

WRITTEN BY: Howard A. SooHoo 5/29/92
HOWARD A. SOOHOO
INSTRUMENTATION ENGINEER
NASA/EP75

APPROVED BY: Van A. Blankenship 5/29/92
VAN BLANKENSHIP
INSTRUMENTATION TEAM LEADER
NASA/EP75

NOTES:

1. This stand operating procedure is to specify a uniform method for strain gage installation at the Technology Test Bed (TTB) Test Facility.
2. This procedure shall be followed for all strain gage installations for test operations at the TTB Test Facility.
3. The Test Stand Instrumentation Engineer shall be responsible for patching to be used and for providing wiring/list measuring programs with necessary calibration and set–up.
4. This procedure conforms to Rockwell specification RL01033 steps 3.3.2.1 thru 3.3.2.4.4.

GENERAL NOTES:

1. Heavy oxides may be removed with abrasive mats.
2. Hands shall be free of creams and lotions during strain gage installation.
3. All abrading shall be kept to a minimum to assure maximum pump house life.
4. The last three wipes shall be wiped in one direction only. Change pads after each wipe.

PAGE COMPLETE:
DATE _____ QC _____

TTB – OPERATION INSTRUCTIONS	TECH	INSPECTION	
		CONT.	NASA

PROCEDURE:

Before any work begins, remove any existing strain gages on the test component.

Step 1.0
Adhesive Preparation
Mix M-Bond 610 by allowing both resin and curing to come to ambient temperature. Pour contents of bottle labeled 'Curing Agent' into bottle labled 'Resin' using disposable plastic funnel. Tighten brush cap and shake vigorously for 10 seconds minimum. Mark bottle with date in space provided on label. Allow adhesive to atand for one hour minimum. mixed adhesive has a pot life of six weeks maximum when stored at room temperature. Adhesive containing particulate matter shall not be used. Allow air bubbles to rise to the surface and dissipate before using.

NOTES:

1. Since the mixing operations can take a few hours, it is advisable to mix a spare bottle to help prevent unexpected delays during strain gage installation.
2. Mixed M-Bond 610 should be allowed to come to ambient temperature prior to use.

Time Step 1.0 started _____ hours.

* Time Finished _____ hours.
* Minimum one hour from Step 1.0.

Step 2.0
Surface Preparation

Step 2.1
Solvent Degreasing
Prepare the surface to be bonded by wiping with acetone conforming to O-A-051 or isopropyl alcohol conforming to TT-I-735 to remove surface contamination. The solvent wipe shall include the area approximately 4" to 6" on all sides of the installation area in order to minimize the chance of recontamination in subsequent operations. Air dry 15 minutes at ambient conditions.

PAGE COMPLETE:
DATE _____ QC _____

TTB – OPERATION INSTRUCTIONS	TECH	INSPECTION	
		CONT.	NASA

******** Caution ********
Do not expose solvent or vapors to open flame or heat source. Use in well ventilated area.

Step 2.2
Surface Abrasion
The bonding area shall be abraded in a cross-hatched fashion with 180 grit open-meshed non-clogging sanding fabric in order to remove materials on the bonding area that would prevent good bonding. Repeat Step 2.1

Step 2.3
Water Break-free Surface
(To be performed only at engineers request)
Spray bonding area with deionized water to verify a water break-free surface (completely wetted surface) is obtained.

NOTE:
Heat treatment may be used if water break-free surface cannot be obtained, heat area to cure temperature as specified in Step 8.0 and hold for approximately 1/2 hour. Cool and repeat Step 2.1 and Step 2.3 cycle as required until water break-free surface is obtained.

Step 2.4
Surface Conditioning
Repeatedly apply M-Prep Conditioner 'A' to the bonding surface and scrub with cotton-tipped applicators until a clean tip is no longer discolored by scrubbing. During this process, the surface shall be kept constantly wet with Conditioner 'A' until the cleaning is completed. Cleaning solutions should never be allowed to dry on the surface. When clean the surface shall be dried by wiping the cleaned area with a single slow stroke of a clean tissue or gauze. The stroke shall begin inside the cleaned area to avoid dragging contaminants in from the boundary of the area. Then, with a fresh clean tissue or gauze, a single stroke is made in the opposite direction. The clean tissue or gauze shall never be wiped back and forth, since this may redeposit contaminants on the cleaned surface.

PAGE COMPLETE:
DATE _____ QC _____

TTB – OPERATION INSTRUCTIONS	TECH	INSPECTION	
		CONT.	NASA
Step 2.5 Neutralizing Apply a liberal amount of M-Prep Neutrilizer 5 to saturate a clean tissue. Apply to the gaging area and scrub with a cotton-tipped applicator. Wipe the area dry with single, slow passes of clean tissue or gauze. Use a fresh piece of tissue or gauze for each additional pass required to dry the area. The stroke shall begin inside the cleaned area to avoid dragging contaminants in from the boundary area. Then with a fresh clean tissue or gauze, a single stroke is made in the opposite direction. The clean tissue or gauze shall never be wiped back and forth, since this may redeposit contaminants on the cleaned surface. Step 2.6 Bonding Bonding of strain gages and terminal strips shall take place within 45 minutes maximum of cleaning as specified in Step 2.5 or the surface preparation steps of Step 2.0 thru 2.5 shall be repeated. Step 3.0 Gage Preparation Place strain gage/terminal (bond surface away from tape) on high temperature mylar tape or polyimide tape. Strain gage should have lead wires already soldered to tabs at this point. Step 4.0 Terminal Bonding (To be performed only at engineers request) Prepare bonding surface by performing steps 1.00 thru 2.6 of this procedure. NOTES: 1. Temporary I.D. tags may be used on gage lead wires. 2. Step 5.0 thru 7.0 shall be completed within four hours. Step 5.0 Adhesive Application Coat gage/terminal mounting surface and pump mounting surface with a thin layer of M-Bond 610 adhesive. Do not allow the adhesive applicator to touch the tape mastic which holds the pre-assembled gage assembly in place. Let the adhesive air dry 10 to 15 minutes.			

PAGE COMPLETE:
DATE _____ QC _____

TTB – OPERATION INSTRUCTIONS	TECH	INSPECTION	
		CONT.	NASA

Step 6.0
Gage Positioning
Place the gage/terminal assembly in its position. Use only enough pressure to allow the assembly to be tacked down. Hold in place with additional mylar or polyimide tape if neccessary, but the tape contact with the adhesive should be kept to a minimum.

Step 7.0
Application of Pressure
Cover the bonded strain gage assembly with a thin piece of teflon sheet which may be anchored down with high temperature myalr or polyimide tape. Use an approximately 3/32 thick silicone foam rubber pad (such as the silicone gum pad provided by Micro Measurements) to cover an area slightly larger than the gage/terminal areas. Sufficient pressure (clamping) can be applied to ensure intimate contact between the strain gage and the substrate during cure by wrapping the assembly with unsupported, self–adhering silicone rubber tape or by wrapping with heat shrink mylar tape and shrinking with a heat gun, or with a suitable clamping fixture.

NOTES:
1. Use of silicone pad and teflon sheet is optional.
2. Metal flex ducting may be used with heat gun to increase performance.

******** Caution ********
Never maintain the heat gun air flow directly onto the strain gage. Protect heat–sensitive hardware in the vicinity of the bonding area by shielding with aluminum foil or by removing sensitive item.

Step 8.0
Curing of adhesive
The bonded assembly shall be cured at 265°F +/–15°F for at least 2 1/2 hours. Slowly raise substrate temperature to the cure temperature range for the specified time. Heat can be applied to the assembly using heat guns as long as the substrate temperature is monitored by the use of thermo–couple and the heat flow is never maintained directly onto the strain gage.

PAGE COMPLETE:
DATE _____ QC _____

TTB – OPERATION INSTRUCTIONS	TECH	INSPECTION	
		CONT.	NASA

Step 8.1
Start Time
Enter time on buy–off sheets.

Step 8.2
End Time
Enter time on buy–off sheets.

Step 9.0
Removal of Tape
Substrate must be below 150°F before removing pressure (clamp) from assembly. Slowly remove the gum pad and then slowly remove the tape and the teflon sheet.

Step 10.0
Visual Inspection
Visually inspect strain gage bonds at 10X to 40X magnification (if accessable to magnification) and verify that an adhesive is present all around the periphery of the gage. Verify that there is adhesion at the gage edges and ensure that no air bubbles, voids, contaminates, or particulates are present in the adhesive under the gage. Verify gage and terminal location to drawing requirements.

NOTE:
A borescope may be used for verification.

Step 11.0
Resistance Test
Using a volt/ohm meter, measure the resistance between each leg of gage. Gage should read between 340 to 360 ohms. Record on buy–off sheet.

CCN _____ D/D _____

Step 12.0
Insulation Resistance Test
Using a Megohmmeter, measure insulation resistance between gage and test component. Test voltage should not exceed 1000 volts +/–2.5 VDC and should read a minimum of 1000 megohms for 5 to 600 seconds. Record on buy–off sheet.

CCN _____ D/D _____

PAGE COMPLETE:
DATE _____ QC _____

TTB – OPERATION INSTRUCTIONS	TECH	INSPECTION	
		CONT.	NASA
Step 13.0 Application of Gage/Terminal Overcoat Step 13.1 Cleaning Wipe overcoating area with a cotton swab moistened with isopropyl alcohol (TT-I-735) or 1,1,1-trichloroethane (O-T-620 or RB0210-021). Step 13.2 Drying of Overcoat Area Remove moisture from the strain gage prior to over-coating by gently drying the strain gage with a heat gun. Do not maintain air flow from heat gun directly on the gage. Do not apply heat for more than 10 minutes. Step 13.3 Overcoat Application M-Coat 'A' Two coats of M-Coat 'A' shall be applied. The first coat shall be a thin, brush applied layer over the bonded gage/terminal assemblies. Care shall be taken to insure M-Coat 'A' is brushed under the lead wires. Overcoat shall extend around the gage/terminal periphery. Allow two hours minimum for air drying of first overcoat. The second coat shall be applied evenly by brush, fully covering the area previously coated. No visible voids shall be present. Bottles of M-Coat 'A' which contain gelatinous or particulate matter shall not be used. Step 14.0 Upon completion of gage installation, put all gages back on line, Splice to appropriate drag-on cables indicated by MSID number or MID number.			

PAGE COMPLETE:
DATE _____ QC _____

REPORT DOCUMENTATION PAGE

Form Approved
OMB No. 0704-0188

1. AGENCY USE ONLY (Leave Blank)	2. REPORT DATE	3. REPORT TYPE AND DATES COVERED
	May 1996	Contractor Report (Final)

4. TITLE AND SUBTITLE

New Instrumentation Technologies for Testing the Bonding of Sensors to Solid Materials

5. FUNDING NUMBERS

NAS8-40165

6. AUTHOR(S)

H.M. Hashemian, C.S. Shell, and C.N. Jones

7. PERFORMING ORGANIZATION NAME(S) AND ADDRESS(ES)

Analysis and Measurement Services Corporation
AMS 9111 Cross Park Drive
Knoxville, TN 37923

8. PERFORMING ORGANIZATON REPORT NUMBERS

M-811

9. SPONSORING/MONITORING AGENCY NAME(S) AND ADDRESS(ES)

George C. Marshall Space Flight Center
Marshall Space Flight Center, Alabama 35812

10. SPONSORING/MONITORING AGENCY REPORT NUMBER

NASA CR-4744

11. SUPPLEMENTARY NOTES

Technical Monitor: Robert Burns, Information and Electronic Systems Laboratory, Science and Engineering Directorate

12a. DISTRIBUTION/AVAILABILITY STATEMENT

Unclassified-Unlimited

Subject category 35

12b. DISTRIBUTION CODE

13. ABSTRACT *(Maximum 200 words)*

This report presents the results of a comprehensive research and development project that was conducted over a three-year period to develop new technologies for testing the attachment of sensors to solid materials for the following NASA applications: 1) testing the performance of composites that are used for the lining of solid rocket motor nozzles, 2) testing the bonding of surface-mounted platinum resistance thermometers that are used on fuel and oxidizer lines of the space shuttle to detect valve leaks by monitoring temperature, 3) testing the attachment of strain gages that are used in testing the performance of space shuttle main engines, and 4) testing the thermocouples that are used for determining the performance of blast tube liner material in solid rocket boosters.

14. SUBJECT TERMS

Thermocouples, Strain Gages, RTDs, Bonding, Model Validation, SRM Nozzel, Composite Material, Space Shuttle, Response Time Testing

15. NUMBER OF PAGES

403

16. PRICE CODE

A18

17. SECURITY CLASSIFICATION	18. SECURITY CLASSIFICATION OF THIS PAGE	19. SECURITY CLASSIFICATION OF ABSTRACT	20. LIMITATION OF ABSTRACT
Unclassified	Unclassified	Unclassified	Unlimited

NSN 7540 - 01 - 280 - 5500

☆U.S. GOVERNMENT PRINTING OFFICE—1996—733-109/40034

Standard Form 298 (Rev 2-89)
Prescribed by ANSI Std. 239-18

National Aeronautics and
Space Administration
Code JTT
Washington, DC
20546–0001

Official Business
Penalty for Private Use, $300

Postmaster: If Undeliverable (Section 158 Postal Manual), Do Not Return